Screening of actinobacteria for novel antimalarial compounds

Daniel John Watson

(WTSDAN003)

Submitted to the University of Cape Town
In fulfilment of the requirement for the degree:
PhD Clinical Pharmacology

Faculty of Health Sciences

UNIVERSITY OF CAPE TOWN

February 2020

Supervisor: A/Prof Lubbe Wiesner
Co-supervisor: Dr Paul Meyers

DECLARATION

It is herewith declared that the work represented in this dissertation/thesis is the independent work of the undersigned (except where acknowledgements indicate otherwise) and has not been submitted at any other University for a degree. In addition, copyright of this thesis is hereby ceded in favour of the University of Cape Town.

Signed by candidate

15/7/2020

Date

Acknowledgements

This thesis is dedicated to my friends and family who gave me the opportunities and support that allowed me to fulfil my dream.

Firstly, I would like to thank the NRF and UCT for funding me through my MSc and PhD. Without it, none of this would have been possible.

To my supervisor Prof Lubbe Wiesner, thank you for providing me with the opportunity to pursue my interests and passions. Your faith in me and this project kept me going even when I was not sure I could.

To my co-supervisor Dr Paul Meyers, thank you for your patience and wisdom. Thank you for helping me learn from my endless mistakes in the lab and while writing. Your voice of reason lead me through more than a few trying times.

A special thanks to Prof Peter Smith who taught me to turn a loss into a win and whose wisdom and encouragement meant more than I could ever show.

Thank you to my colleagues and friends at the Division of Pharmacology: Alicia, Alek, Anton, Dale, Virgil, Sumaya, Jill, Lloyd, Lizahn, Devasha, Katie, Lucas, and many more, for their help and encouragement. It was a pleasure to work with you all.

A special thank you to Dr Joel Rindelaub and Dr Bruno Sacchetto Paulo for helping me with article access and my questions. They really helped turn the project around at crucial stages.

Thank you to my colleagues in the Department of Chemistry and Molecular and Cell Biology: Kojo Acquah, Dr Godwin Dziworn, Diana Melis, Sam and Adeebah, for their help with data acquisition and analysis.

Thank you to my friends: Bianca, Brad, Chad, Jess, Simone, Rudi, Hanneke, Callen, Kim, John, James, my DnD crew, and the TrueKrav and X wing community, for their support, interest and dealing with me during the good times and bad times.

Thank you to my partner Hannah, for her constant love and support, and making me the happiest man in the world.

Finally, thank you to my family: Carmen, George and Simon. Without your guidance, unconditional love and faith this never would have happened. I don't know what I would do without any of you and I love you all.

"Success is not final, failure is not fatal: it is the courage to continue that counts" Winston Churchill

Abstract

The success of our first-line antimalarial treatments is threatened by increased drug resistance in *Plasmodium* parasites. This makes the development of novel drugs critical to combat malaria. Historically, natural products have been an excellent source of novel antimalarial compounds and thus are an ideal place to search for potential drugs. Filamentous members of the bacterial phylum, *Actinobacteria*, are well-known antibiotic producers, but their antimalarial potential has not been well investigated. This makes these actinobacteria a potentially valuable source of novel antimalarial compounds.

To evaluate the antimalarial potential of the filamentous actinobacteria, uncharacterized environmental actinobacterial strains from the Meyers laboratory culture collection, as well as the type strains of new actinobacterial species identified and characterized in the Meyers laboratory, were screened for antiplasmodial activity against drug-sensitive *Plasmodium falciparum*, NF54. Liquid cultures were extracted using the mid-polar solvent, ethyl acetate, with the aim of discovering drug-like molecules that can be administered orally. Thirty-one strains of actinobacteria belonging to eight genera (*Actinomadura, Amycolatopsis, Gordonia, Kribbella, Micromonospora, Nocardia*, *Nonomuraea*, and *Streptomyces*) were screened revealing fourteen active strains. Eight strains were identified for further study as the displayed antiplasmodial efficacy matching predefined criteria. Of these eight candidates, *Streptomyces* strain PR3 was selected, as it showed excellent antiplasmodial efficacy, no cytotoxicity against Chinese Hamster Ovary (CHO) or liver HepG2 cell lines, no haemotoxicity, and was easy to culture.

Bioassay-guided fractionation of the crude extracts of strain PR3, supported by high-resolution mass spectrometry (HRMS) and nuclear magnetic resonance (NMR) analysis, was conducted to isolate and identify the compounds responsible for the antiplasmodial activity. During purification by solid phase extraction (SPE), a novel class of compounds was isolated. The structure of these compounds was elucidated by HRMS and NMR analysis and determined to be a series of crown ethers with a methylated backbone. These methylated crown ethers (MCE) were not produced by strain PR3, but by the cyclization of polypropylene glycol (PPG) oligomers from Amberlite® XAD-16N 20–60 mesh resin under aqueous conditions. The MCEs displayed weak antiplasmodial activity against *P. falciparum* NF54, without cytotoxicity against the Chinese Hamster Ovary, HepG2 cell lines, nor human erythrocytes. To the author's

knowledge, the MCEs are novel compounds, and this is the first time the cyclization of PPG oligomers into crown ethers has been reported.

As the MCEs were not responsible for strain PR3's potent antiplasmodial activity, further study was conducted. Using the Global Natural Product Social molecular networking (GNPS) workflow, genome mining, and NMR analysis, it was revealed that the cyclodepsipeptides, valinomycin, montanastatin, and nine other novel analogues were responsible for the high antiplasmodial activity detected. A review of the literature revealed that the structure of four of these analogues had been predicted, based on MS/MS and the biosynthesis of valinomycin. Using the same described biosynthetic logic and MS/MS analysis, two new cyclodepsipeptides, compounds 1054 and 1068, were elucidated. Unfortunately, chromatographic systems developed were unable to purify the cyclodepsipeptides, and individual evaluation of their antiplasmodial efficacy and host selectivity was not possible.

The fraction containing the cyclodepsipeptides exhibited strong antiplasmodial activity against the drug-sensitive, NF54 and multidrug-resistant K1, strains of *P. falciparum*. No cytotoxicity was displayed against the CHO cell line and no haemotoxicity was seen against human erythrocytes. Moderate toxicity was exhibited against the liver HepG2 cell line; however, the selectivity index of the cyclodepsipeptides suggested that they are selectively targeting the *Plasmodium* parasites. Overall, these results are positive, and further study of the individual cyclodepsipeptides is warranted.

During the investigation, discrepancies were noticed between different fractions in terms of antiplasmodial activity. These fractions contained both the MCEs and, cyclodepsipeptides along with a range of impurities, yet they displayed potent antiplasmodial activity. Further study suggested that combination of the MCEs and cyclodepsipeptides elicits a synergistic response and improves antiplasmodial efficacy. This was determined independently using two models, the fixed-ratio isobologram method and the CompuSyn programme based on the mass-action law principle. The workflow developed during this investigation demonstrates how new technologies can be used to dereplicate and elucidate bioactive natural products. This workflow can be utilized to continue this research and identify new natural products that can combat malaria.

List of Abbreviations

ACT	Artemisinin based Combination Therapy
APAD	3-acetyl pyridine
BCCM	Belgian Co-Ordinated Collection of Microorganisms
BGC	Biosynthetic Gene Cluster
bp	base pairs
CCC	counter current chromatography
CE	collision energy
CHO	Chinese Hamster Ovary
CI	combination index
CM	complete medium
COSY	correlation spectroscopy
CSP	circumsporozoite protein
CZ	Czapek Solution Agar
DDT	dichloro-diphenyl-trichloroethane
DHA	dihydroartemisinin
DHFR	dihydrofolate reductase
DHPS	dihydropteroate synthetase
DMEM	Dulbecos Modified Eagles Medium
DMSO	dimethyl sulfoxide
DNDi	Drugs for Neglected Disease initiative
DSMZ #553	German Culture Collection medium #553

EtAc	ethyl acetate
FCS	foetal calf serum
FDA	Food and Drug Administration
FIC_{50}	fractional IC_{50}
FT-IR	Fourier Transform Infrared Radiation
GC	gas chromatography
GDP	gross domestic product
GIT	gastrointestinal tract
GMEP	Global Malaria Eradication Programme
GNPS	Global Natural Product Social Molecular Networking
Hiv	α-hydroxyisovaleric acid
HM	Hacène's Medium
HMBC	heteronuclear multiple-bond coherence
HPLC	high performance liquid chromatography
HRMS	high-resolution mass spectrometry
HTS	high throughput screening
IC_{50}	half maximal inhibitory concentration
IDA	information-dependent acquisition
IPT	intermittent preventative treatment
IR	infrared radiation
IRS	indoor residual spraying
ISP-2	International *Streptomyces* Project medium 2
ITN	insecticide treated nets
JCM #61	Japan Collection of Microorganisms #61

KEGG	Kyoto Encyclopedia of Genes and Genomes
K13	Kelch 13
Lac	lactic acid
LC	liquid chromatography
LEDC	less economically developed country
Leu/Ile	leucine/isoleucine
m/z	mass/charge ratio
MCE	methylated crown ether
MDA	mass drug administration
MeOH	methanol
MMV	Medicines for Malaria Venture
MR4	Malaria Research and Reference Reagent Resource
MS/MS	tandem mass spectrometry
MSI	Metabolomics Standards Initiative
MTT	3-(4,5-dimethylthiazol-2-yl)-2,5-diphenyl tetrazolium bromide
NBT	nitro blue tetrazolium
NCBI	National Centre for Biotechnology Information
NMR	nuclear magnetic resonance
NP	normal phase
NRPS	non-ribosomal peptide synthetase
P	partition coefficient
PBS	phosphate buffered saline
PEG	polyethylene glycol
PfCRT	*P. falciparum* chloroquine resistance transporter

PfEMP1	*P. falciparum* erythrocyte membrane protein 1
pLDH	parasite lactate dehydrogenase
Ppant	4′-phosphopantetheine
PPG	polypropylene glycol
psi	pounds per square inch
QTOF	quadrupole time of flight
rcf	relative centrifugal force
RI	resistance index
RP	reverse phase
SERCaP	Single Exposure Radical Cure and Prophylaxis
ΣFIC	sum of the fractional IC_{50}'s
SI	selectivity index
SIM	single ion monitoring
SMC	seasonal malaria chemoprevention
SP	sulfadoxine-pyrimethamine
SPE	solid-phase extraction
TOF	time of flight
Tris	tris(hydroxymethyl)aminomethane
UPLC	ultra-performance liquid chromatography
USA	United States of America
UV-Vis	ultraviolet-visible light
Val	valine
var	variable
WGS	whole-genome sequencing

Contents

List of Figures

List of Tables

1 Literature Review

1.1 Malaria

1.1.1 Background

Malaria is a life-threatening, infectious disease that threatens 50% of the world's population (Vinet and Zhedanov, 2010). In 2018, malaria was estimated to be responsible for 228 million new infections and 405 000 deaths (World Health Organization, 2019). The vast majority of these deaths, 93% (404 550), occurred in African countries. Tragically, children are the most vulnerable, with 61% (266 000) of fatalities attributed to children below the age of 5. Malaria occurs in tropical and subtropical locations (Figure 1.1) and is localised to regions of high temperatures, heavy rainfall, high humidity, and the presence of the *Anopheles* mosquito vector (Centers for Disease Control and Prevention, 2015). Malaria in humans can be caused by five parasites of the *Plasmodium* genus (World Health Organization, 2018). These are *Plasmodium falciparum*, *Plasmodium vivax*, *Plasmodium malariae*, *Plasmodium ovale*, and *Plasmodium knowlesi*. Of these five species, *P. falciparum* causes most infections and deaths and is thus the main target of drug therapies. *P. falciparum* infection is the most prevalent in Africa and South East Asia, while *P. vivax* infection is the most prevalent in Central and South America (World Health Organization, 2018).

P. vivax can replicate and spread at lower temperatures and thus is more widespread than *P. falciparum* (UNICEF/WHO, 2015). Despite this, *P. vivax* infects fewer people, especially in Africa where most of the population do not produce the protein required by *P. vivax* to enter the erythrocyte. This protein is coded for by the Duffy gene, which is absent in many African populations (UNICEF/WHO, 2015).

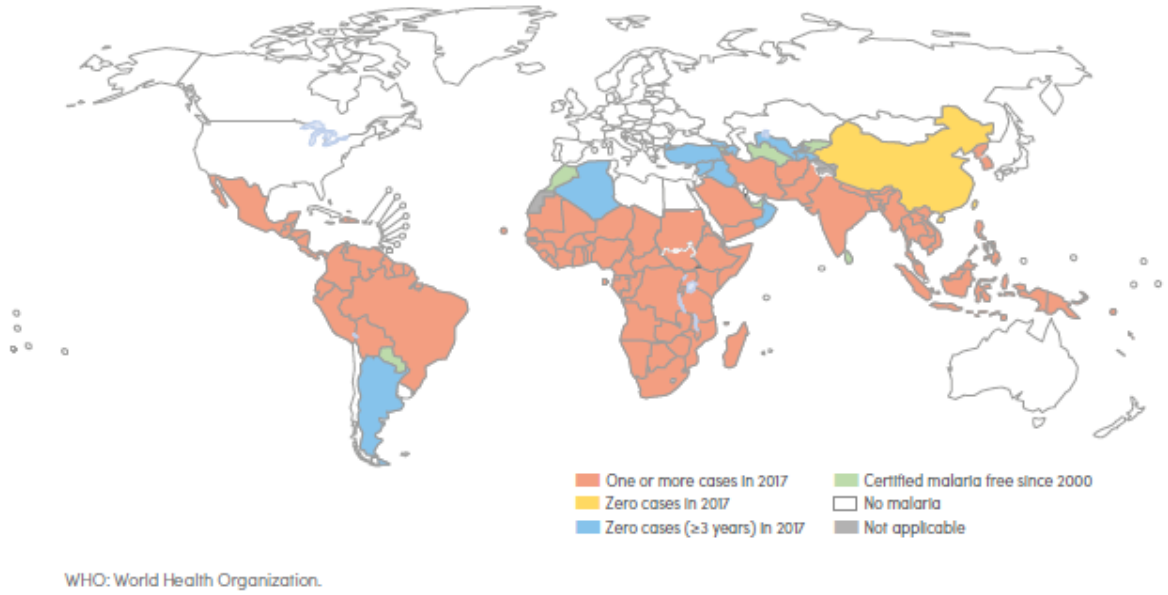

Figure 1.1: Global distribution of malaria in 2017 (World Health Organization, 2018).

1.1.2 Lifecycle

The *Plasmodium* parasites have a complex, multistage lifecycle as illustrated in Figure 1.2. This lifecycle involves two hosts: humans and the female *Anopheles* mosquito. There are more than 400 species belonging to the *Anopheles* genus, but only 30 of these are capable of transmitting malaria (UNICEF/WHO, 2015). During a blood meal, an infected mosquito infects the human host with sporozoites clustered in its salivary glands (Cowman *et al.*, 2016). These travel through the bloodstream to the liver and infect hepatocytes by a method known as traversal. Once inside the hepatocyte, the sporozoites develop into merozoites over 3–12 days, depending on the *Plasmodium* species (Sturm, 2006). Merozoites leave the hepatocytes by budding off in vesicles known as merosomes and travel into the bloodstream via the hepatic circulation. Merozoites infect erythrocytes and form immature trophozoites, known as the ring stage, as their developing genome is ring shaped (Boddey and Cowman, 2013). Over a 48-hour period, immature trophozoites mature and undergo cell division in a process known as schizogony. During schizogony, multinucleated schizonts replicate into dozens of merozoites which lyse the erythrocyte and are released into the bloodstream. These merozoites then infect

erythrocytes, and the process is repeated. The lysis of erythrocytes by merozoites leads to the release of toxins and wastes (Kayser *et al.*, 2002). This leads to the activation of macrophages and the release of cytokines and chemokines, which generate an immune response. This process induces the three classic symptoms of malaria; fever, chills, and sweating. The lysis of erythrocytes decreases red blood cell count, which contributes to lethargy, headaches, and anaemia - among other symptoms.

During infection, large scale molecular remodelling of the erythrocyte occurs to allow continued development of the parasite (Boddey and Cowman, 2013). During this process, the highly-differentiated erythrocyte is converted into a system that allows the parasite to develop, scavenge host nutrients, and evade host immune responses. A massive array of proteins are produced and exported through the parasite, into the erythrocyte and onto the erythrocytic membrane. Remodelling creates an extra-parasitic transport network that can transport resources, wastes, and protein complexes to specific locations. Remodelling increases the permeability of the infected erythrocytes' membranes, improving the transport network. During remodelling in *P. falciparum*-infected erythrocytes, *P. falciparum* erythrocyte membrane protein 1 (PfEMP1) is expressed (Smith *et al.*, 1995). PfEMP1 is responsible for cytoadherence between infected erythrocytes and other cells. The PfEMP1 protein family is expressed by approximately 60 variable (*var*) genes per haploid parasite genome, and each displays monoallelic expression (Scherf *et al.*, 1998). This generates a highly-variable array of surface antigens, enabling the parasite to evade the host immune response.

Cytoadherence allows sequestration of the parasite-infected cells, which avoids passage through the spleen and thus, destruction by splenic macrophages (Boddey and Cowman, 2013). Cytoadherence also leads to reduced blood flow in infected areas, reducing the parasite's exposure to immune cells. This sequestration is an important part of *P. falciparum* pathology. Mass clotting can occur in vital areas which can lead to respiratory and renal failure, and to a major symptom of *P. falciparum* infection, cerebral malaria.

In cerebral malaria, cytoadherence in the capillaries, in and surrounding the brain, can reduce blood flow and lead to strokes. If the capillaries rupture, brain oedema and neurological impairment can ensue.

P. falciparum-infected cells can also preferentially adhere to the placenta making pregnant women extremely vulnerable to the disease (Greenwood, 2010). Malaria infection in pregnant

women can lead to maternal anaemia, child growth retardation, placental infections, low birth weights, and, in the worst cases, maternal and neonatal mortalities (Mosha *et al.*, 2014).

During the next stage of infection, a proportion of merozoites develop into sexual gametocytes instead of schizonts, in the erythrocyte. These immature gametocytes do not lyse the erythrocyte, but instead mature before the next stage (Cowman *et al.*, 2016). In the case of *P. falciparum*, gametocytes take 11 days to mature and sequester in the bone marrow to avoid clearance and immune responses (Joice *et al.*, 2014). The exact cause of this developmental switch to gametocyte formation is still uncertain, however, it has been linked to high parasitaemia and exposure to certain drugs, such a chloroquine (Cowman *et al.*, 2016). After the gametocytes mature, they return to the bloodstream and are taken up when a mosquito feeds on the infected human host.

When in the midgut lumen of the mosquito, female gametocytes are fertilised by male gametocytes to form an ookinete (Aly *et al*., 2009). The ookinete moves to the basal lumina in the midgut and develops into an oocyst. Finally, the oocyst develops into sporozoites, which infect the salivary glands of the mosquito and the cycle repeats.

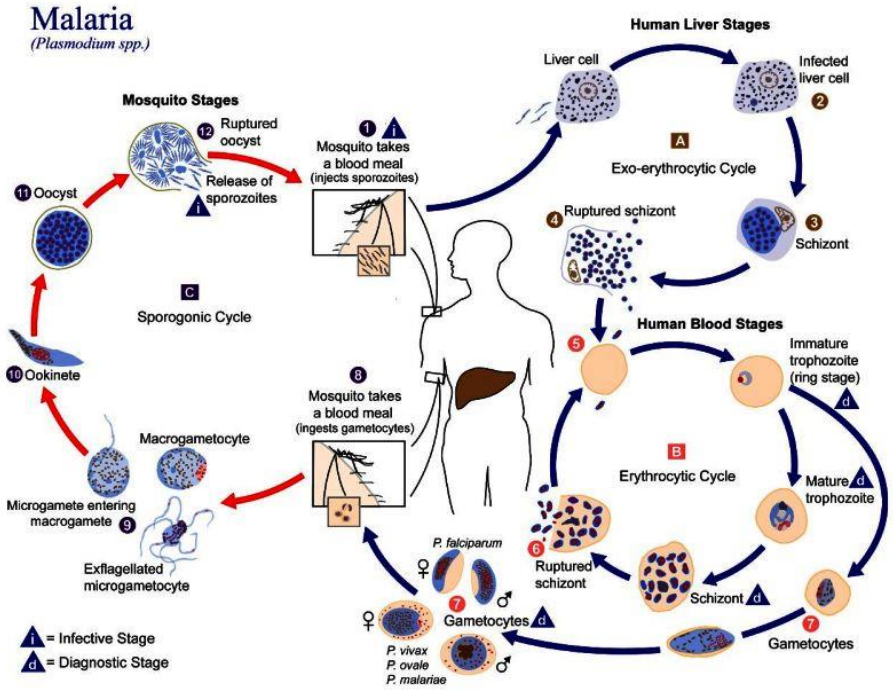

Figure 1.2: Summary of the lifecycle of *P. falciparum* in the human and *Anopheles* hosts (Beck, 2006).

1.1.3 Economic Burden

Malaria has a very clear social impact due to the high global mortalities, but the disease also causes a great economic burden. A long-term study found that between 1960 and 1995, countries with malaria had a mean growth in income per capita of 0.4%, while countries without malaria had a mean growth in income per capita of 2.3% (Gallup and Sachs, 2001). A decrease in the malaria incidence of 10% was seen to lead to an increase of 0.3% in economic growth. Over 25 years, this was predicted to be equal to half the per capita gross domestic product (GDP) of a less economically developed country (LEDC). Malaria not only slows economic growth, but poverty potentiates the disease itself. As discussed previously, malaria occurs in tropical and subtropical regions, which are also the poorest areas in the world. At the household level, poorer-quality housing can make families more vulnerable to infection by mosquitoes (Teklehaimanot and Paola Mejia, 2008). Peak malaria incidence times often overlap with harvest periods, leading to food insecurity and loss of income if working family members are infected. Poorer families often lack access to medical facilities or are unable to afford preventive measures such as mosquito nets. Lack of education can slow the uptake of prevention schemes and recognition of malaria symptoms. At the national scale, this burden becomes even greater. Infected patients drain resources and are unable to work, leading to a loss of capital. International investors are discouraged from investing in malaria-afflicted countries due to increased labour costs and health risks. Government funding is prioritized to combat malaria instead of being invested in developing infrastructure. The poorest suffer the most, and it is very difficult to escape the cycle of disease and poverty that is created. This is one of the reasons why Africa, the poorest continent, carries the bulk of the global malaria burden.

1.2 Prevention and Treatment of Malaria

1.2.1 History

Malaria causes a severe socio-economic burden, although there has been much success in reducing this burden over the past decades. Current incidence and mortality figures represent a decrease in the impact of malaria (World Health Organization, 2018). For example, in 2000,

malaria caused approximately 262 million new infections and 839 000 deaths, compared to the 219 million new infections and 435 000 deaths in 2017. This success can be attributed to the development of healthcare infrastructures, the use of insecticides to control the *Anopheles* vector, prophylaxis to prevent infection, and first-line antimalarial drugs to treat infections.

This success has been hard-earned and the result of many failures and tough lessons. The greatest example of this was the Global Malaria Eradication Programme (GMEP) launched in 1955 (Nájera *et al.*, 2011). This was the first large scale programme that focused on combating malaria long term and on a global scale. The GMEP focused on eradication techniques over control methods. The main methods used were intensive spraying of the pesticide, dichloro-diphenyl-trichloroethane (DDT), indoors and outdoors to kill mosquitoes and the mass drug administration (MDA) of chloroquine to infected patients. The GMEP closed 14 years later, after much criticism and a list of failures, but overall it should be seen as a success. It successfully eradicated malaria in various regions, such as the United States of America and Eastern Europe and reduced the burden of the disease in many others.

The GMEP was, however, unable to eradicate malaria in the areas that carried the highest burden, particularly in Africa. The single-minded focus on using DDT for the eradication of mosquitoes and the MDA of chloroquine ended up being the downfall of the GMEP (D'Alessandro and Buttiens, 2001; Nájera *et al.*, 2011). Chloroquine resistance was propagated due to its extensive use in monotherapy. Furthermore, early signs of chloroquine resistance in Southeast Asia were ignored, as it was believed that DDT use would halt the transmission of the *Plasmodium* parasites. DDT resistance in mosquitoes accelerated, health care infrastructure was not developed, malaria research stalled, and traditional control measures - such as draining marshes, were no longer implemented (Nájera *et al.*, 2011). This allowed these high-burden areas to persist. When eradication programmes were removed, a resurgence of malaria was seen, including in areas, such as Sri-Lanka and Madagascar, which were believed to have been cleared of the disease (Greenwood *et al.*, 2008). The GMEP proved that, in order to combat malaria, a diverse set of methods are required, at a large scale, over a very long time period. It also showed the risks of using drugs in monotherapy on such a large scale.

Today, malaria is combatted with three techniques. These are: halting transmission with control measures, preventing infection with prophylaxis and treating infections with a combination of antimalarial drugs. To better facilitate these methods, health service infrastructure needs to be developed, malaria research encouraged, and surveillance systems put in place. Much was

learned from the GMEP and the goals remained the same, despite its failures and setbacks. This has contributed to the subsequent success in combatting the disease. However, there is still much work to be done and major problems to be faced.

1.2.2 Vector Control

Vector control refers to reducing or eliminating *Anopheles* vector populations and protecting human populations from mosquito bites (UNICEF/WHO, 2015). The bulk of the success against malaria can be attributed to vector control (Raghavendra *et al.*, 2011). One of the most effective methods of vector control is the use of insecticide-treated nets (ITNs). ITNs protect people while they sleep, which is when they are the most vulnerable, and the *Anopheles* mosquito is the most active. ITNs are also useful in protecting sedentary people, such as pregnant women, the elderly, the sick, and young children, who are all extremely vulnerable to malaria. ITNs have been shown to reduce malaria incidence by 50% and mortality of under 5 year olds by 17% (Lengeler, 2004). The insecticides used on ITNs all belong to the pyrethroid family, as they have low mammalian toxicity, long lasting residual effects and are highly effective against mosquitoes (Raghavendra *et al.*, 2011).

Indoor residual spraying (IRS) is another effective vector control measure. Insecticides are sprayed in residential and working areas to kill mosquitoes and provide residual protection (Raghavendra *et al.*, 2011). It is estimated that ITNs and IRS prevented 517 million cases of malaria between 2000 and 2015 (Sherrard-Smith *et al.*, 2018). Carbamates and organophosphates, as well as pyrethroids, are used in IRS (Ranson and Lissenden, 2016).

New biological controls are being investigated, such as the use of members of *Wolbachia*, a genus of intracellular pathogenic symbiotic bacteria, to sterilize mosquito populations. Infection of mosquitoes by *Wolbachia* can cause cytoplasmic instability and sterilization (Bian *et al.*, 2013). However, *Wolbachi*a was only recently shown to be able to infect *Anopheles* species, and its use has only been implemented on a limited scale. Biological impact, resistance, and effectiveness across the relevant malaria-carrying *Anopheles* species still need to be investigated.

While vector control is very effective, it does still face several challenges. Distribution, implementation and education around ITNs and IRS is lacking, which is slowing progress

(World Health Organization, 2018). Of greater concern is insecticide resistance development in mosquitoes. Decades of use has led to resistance in *Anopheles* mosquitoes to all the major insecticides (Ranson and Lissenden, 2016).

In Africa, there is complete pyrethroid resistance in malaria vectors, which threatens to neutralize the use of ITNs. Resistance to DDT, carbamates, and organophosphates is also emerging and spreading. Areas that rely heavily on ITNs are especially vulnerable, as there is such a limited number of insecticides available with similar properties. For example, carbamates and organophosphates share the same mechanism of action, which make them susceptible to cross resistance. The current strategy implemented by the WHO is to continue using ITNs, as the nets create an effective physical barrier (Ranson and Lissenden, 2016; World Health Organization, 2018). Rotating the use of insecticides every season is one way to slow the development of insecticide resistance, however, novel insecticides are required to continue vector-control programmes. Signs are appearing that insecticide resistance is impacting control programmes, but the exact extent is still not understood (Ranson and Lissenden, 2016).

1.2.3 Chemoprevention

Chemoprevention or prophylaxis involves maintaining levels of antimalarial drugs in the host's blood to suppress malaria infection (UNICEF/WHO, 2015). This is particularly useful in protecting vulnerable populations and is recommended by the WHO for children under the age of five and pregnant women (World Health Organization, 2018). These treatments can either involve intermittent preventative treatment (IPT), which is the periodic administration of an antimalarial compound, or seasonal malaria chemoprevention (SMC), where treatment is only administered during high-risk periods (i.e. during the rainy season). These treatments have been shown to reduce low birth weight cases, maternal anaemia, and neonatal mortalities. The WHO-recommended antimalarial drugs for IPT are the folate synthesis inhibiting sulfadoxine-pyrimethamine (SP) combination (section 1.2.5.2). For SMC, amodiaquine is recommended, and a combination of SP and amodiaquine is recommended for young children.

1.2.4 Vaccines

Despite decades of research, there are currently no commercial vaccines available for malaria (Ajua *et al.*, 2015). An effective vaccine would be the ultimate control measure, as it would provide long term and complete protection. Due to the multistage lifecycle and diverse biology of the *Plasmodium* parasites, developing a vaccine is a complex challenge. The most successful candidate is the RTS,S/AS01 vaccine, which is comprised of hepatitis B surface antigens fused to a fragment of the circumsporozoite protein (CSP) of *P. falciparum* (Mahmoudi and Keshavarz, 2017). The RTS,S/AS01 vaccine stimulates antibody generation specific to CSP, an antigen found on sporozoites and liver schizonts. After successful Phase II clinical trials, the vaccine moved into Phase III trials involving 15 000 African children, aged 5–17 months (Greenwood and Doumbo, 2016). The trial revealed that the RTS,S/AS01 vaccine provided a vaccine efficacy of only approximately 30%. While most vaccines provide at least 70–80% vaccine efficacy, considering the complex nature of malaria this is a positive result (Greenwood and Doumbo, 2016; Mahmoudi and Keshavarz, 2017). Even partial coverage could help the control of the disease, and further work is being done to develop an improved version of the RTS,S/AS01 vaccine (Cowman *et al.*, 2016).

1.2.5 Antimalarial Drugs: Past and Present

1.2.5.1 Quinolines

One of the oldest antimalarials used is quinine, a quinoline isolated from the bark of the *Cinchona calisaya* tree in South America in the 1600s (Hobbs and Duffy, 2011). Although quinine is an effective antimalarial in its own right, its adverse side effects (hearing loss, vomiting, hypotension, abdominal pain to name a few) and the difficulty of producing large quantities hindered its use (Achan *et al.*, 2011).

Quinine was later synthesised and derivatised into the class of compounds known as the 4-aminoquinolines. This drug class includes chloroquine, lumefantrine, mefloquine, and amodiaquine. Of these, chloroquine is the most widely used (Figure 1.3). Chloroquine was the first drug to be administered on a global scale when it was administered in the GMEP (section 1.2.1). (D'Alessandro and Buttiens, 2001).

Chloroquine was considered the gold standard of antimalarials due to its high efficacy, low cost, and low toxicity (Fidock *et al.*, 2000). During infection of the erythrocyte, the *Plasmodium* parasites degrade haemoglobin into haem and globin. Haem is toxic and is converted into non-toxic hemozoin, inside the digestive vacuole. The globin is metabolized into peptides which provide nutrients and are used in biosynthesis (Combrinck *et al.*, 2013). Chloroquine has been shown to exert its cytotoxicity by interfering with the conversion of haem to hemozoin in the digestive vacuole. This leads to the accumulation of toxic haem and the death of the parasite.

Chloroquine is no longer effective due to the emergence of wide-spread resistance (Greenwood *et al.*, 2008). The proposed mechanism of resistance states that a mutation in the *P. falciparum* chloroquine resistance transporter (PfCRT), a proton pump in the membrane of the digestive vacuole, effluxes charged chloroquine out of the digestive vacuole (Fidock *et al.*, 2000). By removing chloroquine from its site of action, it is unable to exert its cytotoxic mode of action. Chloroquine resistance emerged almost simultaneously in Brazil, Venezuela, and Colombia in 1960 and independently in Myanmar, Cambodia, and Vietnam in 1961 (D'Alessandro and Buttiens, 2001). The exact causes are still unknown but, as discussed previously, the GMEP exacerbated resistance development. Soon afterwards, chloroquine resistance spread globally and is now seen in almost all malaria-endemic countries. Due to this, alternative antimalarials have been employed.

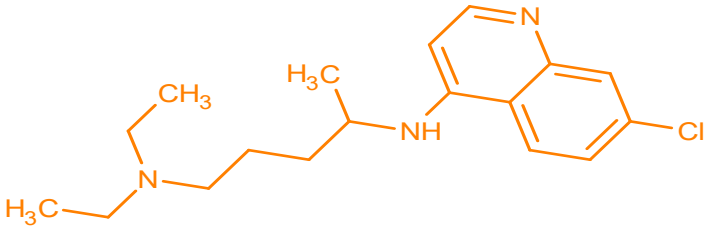

Figure 1.3: Molecular structure of chloroquine (Chemicalize).

1.2.5.2 Sulfadoxine-Pyrimethamine

The combination of drugs sulfadoxine-pyrimethamine (SP) saw increased use as chloroquine resistance became more prominent in the 1960s and is still used in chemoprevention programmes today (Figures 1.4 and 1.5) (D'Alessandro and Buttiens, 2001; World Health Organization, 2018). SP has a long elimination half-life and good efficacy against the *Plasmodium* parasites, which is why it provides successful chemoprevention treatment (Nzila *et al.*, 2000).

Sulfadoxine inhibits *para*-amino benzoic acid conversion to folic acid by binding to dihydropteroate synthetase (DHPS) (Sarmah *et al.*, 2017). Folic acid is essential for parasite replication. Pyrimethamine inhibits the dihydrofolate reductase (DHFR) enzyme complex, which is responsible for the production of purines and pyrimidines required for DNA synthesis before cell division. Both act as competitive inhibitors of the enzyme substrates (Muller and Hyde, 2010). The two drugs are extremely effective in combination, as *Plasmodium* parasites can scavenge dihydrofolate, which reduces the inhibitory effect of pyrimethamine. DHPS is only found in the parasite, whereas DHFR is present in both human erythrocytes and *Plasmodium* cells.

Pyrimethamine is safe for human use, as it binds to parasite DHFR with a much higher affinity than to human DHFR. SP treatment is, however, especially vulnerable to resistance development. SP has been observed to have a short useful therapeutic life, meaning there is a high risk of drug resistance developing (Nzila *et al.*, 2000). One of the main reasons for this, is that the long elimination half-lives of the SP drugs can lead to long term exposure of the *Plasmodium* parasites to the drugs at sub-therapeutic doses. This increases selective pressures on the *Plasmodium* parasites, accelerating the development of drug resistance. Noncompliance and inadequate dosing are thought to contribute to this effect. Point mutations in the *dhfr* and *dhps* genes, which convey resistance, have appeared in *Plasmodium* strains in East Africa, South America, and South East Asia (Gatton *et al.*, 2004). While SP is still effective in many areas, the spread of resistance threatens to reduce the efficacy of this treatment.

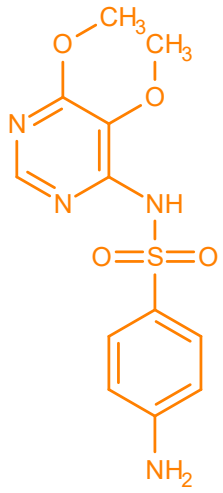

Figure 1.4: Molecular structure of sulfadoxine (Chemicalize)**.**

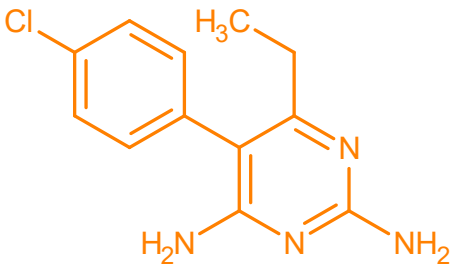

Figure 1.5: Molecular structure of pyrimethamine (Chemicalize).

1.2.5.3 Artemisinins

Artemisinin was isolated from ancient Chinese traditional medicines and first derived from the Chinese plant, *Artemisia annua*, in 1973 (Cragg and Newman, 2013; Haynes *et al.*, 2013). Since then, other compounds have been derived from artemisinin, including, dihydroartemisinin (DHA), artesunate, artemether, and arteether (Anthony *et al.*, 2012). The molecular structure of artesunate is displayed in Figure 1.6. These compounds are collectively referred to as the artemisinins or artemisinin derivatives. Artemisinins are structurally unique,

as they contain a peroxide bridge between two oxygen atoms linked in a 6 membered ring, referred to as a 1,2,4-trioxane (Haynes *et al.*, 2013). Despite the low bioavailability, low solubility, poor metabolic stability, and short half-lives that are characteristically displayed by the artemisinins, they are still considered the most effective antimalarial compounds available (Haynes *et al.*, 2006; World Health Organization, 2018). They demonstrate a high level of efficacy, target all the blood stages of the parasite's lifecycle, and are selectively taken up into parasitized erythrocytes, allowing them to reduce the parasitaemia in a patient to a greater extent than any other antimalarial drug.

The mode of action of the artemisinins is still under debate (Haynes *et al.*, 2013). What is agreed upon is that the peroxide bridge is the active pharmacophore and is essential for the artemisinins' mode of action. Compounds derived from artemisinins that lack the peroxide bridge are not cytotoxic towards *Plasmodium* parasites (Krishna *et al.*, 2004).

The artemisinins present low metabolic stability as they are rapidly metabolized by the liver cytochrome P450 enzyme CYP3A4 (Haynes *et al.*, 2006). This means monotherapies involving artemisinins promote the development of resistance in the *Plasmodium* parasite (Phan Trong Giao *et al.*, 2001). Any parasites that survive the short and potent artemisinin treatment may be able to replicate, which increases the likelihood of resistance-mediating genes becoming established within a population.

Recrudescence is another concern that arises when artemisinins are used in monotherapies (Chen *et al.*, 2014). Artemisinins have been shown to induce dormancy in ring-stage parasites, removing symptoms of the disease and making it appear that the patient has been cured. The short half-lives of these compounds can allow the dormant parasites to survive and become active again, leading to the re-appearance of symptoms. To evade recrudescence and resistance development, artemisinins are partnered with drugs that have a longer half-life in order to eliminate any parasites that survive exposure to the artemisinins. Artemisinin-based combination therapies (ACT) are the current first-line treatment in most malaria-endemic countries and are favoured over other antimalarial therapies, such as SP (Muller and Hyde, 2010; World Health Organization, 2018). There are many types of ACTs in development or use, but the major ones used are: artemether partnered with lumefantrine, artesunate partnered with amodiaquine, or DHA partnered with piperaquine (Anthony *et al.*, 2012). ACTs are effective, as they require short-term treatments of three days, which reduces the chance of patient noncompliance, inhibits gametocyte transmission, reduces the chance of resistance

development to the partner drug, and seem to be well tolerated by patients with few side effects (Xie *et al.*, 2009).

Despite the use of drug combinations, the ACTs are currently threatened by the development of drug resistance. *P. falciparum* resistance to artemisinins was first reported along the border separating Cambodia and Thailand in 2008 and has now spread to five countries in the Greater Mekong region (Noedl *et al.*, 2008; World Health Organization, 2018). Artemisinin resistance is clinically defined as reduced parasite clearance and is expressed as a prolonged parasite clearance half-life or detection of persistent parasites after three days of treatment with an ACT (Ariey *et al.*, 2013). Currently, the ACTs are still effective, however, as a consequence of delayed clearance, the dose of the artemisinins used in ACTs has been increased by at least twofold (Harmse *et al.*, 2015). The failure rate of ACTs has also increased in the areas with the highest burden of malaria. In Cambodia, failure rates have reached 90%, and in Vietnam, 30% (Roberts, 2017). It is important to note that, in the case of failures to standard ACT treatments, patients are dosed with tailored combinations of clinical antimalarials, which so far are capable of treating malaria infection. However, this practice is becoming increasingly frequent, which emphasizes the extent of drug resistance. There are many unknown factors, and much research is being done to assess the situation. The exact cause of artemisinin resistance is unknown, but it has been linked to mutations in the Kelch 13 (K13) propeller domain in *P. falciparum* (Ariey *et al.*, 2013). One hypothesis is that the resistant mutants are able to down-regulate their metabolism during the early stages of erythrocyte infection when the artemisinins are most effective (Mok *et al.*, 2011). They then upregulate their metabolic activity later in the blood stage when the artemisinins are less effective as a result of their chemical instability.

The rise of chloroquine resistance was a serious loss in the war against malaria and, if the resistance to the artemisinins is not contained, history could repeat itself. If ACT-resistant *Plasmodium* strains spread across the globe, the consequences would be devastating, and the success achieved in the past few decades could be reversed (Flannery *et al*., 2013).

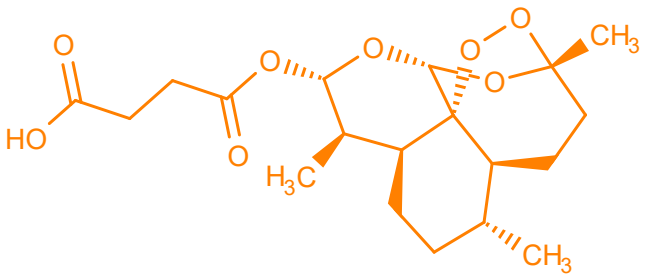

Figure 1.6: Molecular structures of artesunate (Chemicalize).

1.2.6 The Future

The fight against malaria has currently stalled. The WHO reported a decrease in the rate of reduction of malaria mortalities in the past few years (World Health Organization, 2018). For example, an increase in global mortalities was seen from 2015 to 2016 where the global incidences increased from 219 million to 231 million cases respectively and since then the number of incidences have plateaued (World Health Organization, 2019). The global incidence rate (number of cases per 1000 people) has overall decreased since the start of the decade when it was 71 per 1000 people and is currently at 57 per 1000 people. However, the bulk of this reduction occurred during the beginning of the decade when the incidence rate dropped from 60 per 100 people in 2013 to 57 per 1000 people in 2014 (World Health Organization, 2019). The incidence rate has unfortunately remained almost the same for the past 4 year. One of the reasons for this stalled progress is a decrease in funding, which hinders control and treatment programmes and reduces the availability of funds for new measures. The other major reasons are the rise in insecticide resistance and the decrease in efficacy of the ACTs. With insecticides being less effective, more pressure is placed on drug treatment schemes to combat malaria. However, with the growing threat and impact of ACT resistance, these treatment programs are

vulnerable and may be unable to sustain their success. To avoid this, and continue to combat malaria, new antimalarial drugs, with novel mechanisms of action, need to be developed.

There are several approaches that can be taken to develop new antimalarials. A short-term approach is altering the drug combinations used in the ACTs. Mefloquine, piperaquine, and lumefantrine are all currently used as partner drugs with the artemisinins (World Health Organization, 2018). There is controversy over the cause for ACT failure, as resistance to partner drugs has also been detected. Therefore, altering the drug combinations may reverse failing treatments and contain the resistant strains (Pink *et al.,* 2005; Roberts, 2017). However, this approach may only prolong the time it takes for artemisinin resistance to develop further and is unlikely to lead to the eradication of malaria.

Another short-term approach is testing known antimicrobial agents for antimalarial activity, reducing the time and cost required to develop new drugs (Pink *et al.,* 2005). An example is DB289, which was originally developed to treat *Pneumocystis* pneumonia caused by the fungus *Pneumocystis jirovecii,* and has proven to be an excellent antimalarial (Yeates, 2003). This approach is not always viable as most drugs are owned by pharmaceutical companies, that may not want their drugs being tested for non-commercial or alternative commercial purposes (Pink *et al.,* 2005).

A medium-term approach is to create analogues of current antimalarials. For example, a drug called ferroquine contains the chloroquine nucleus with a ferrocenic group attached (Biot *et al.,* 2011). Ferroquine is non-toxic and effective against chloroquine-resistant *Plasmodium* strains. This is a medium-term approach as it shortens the drug discovery leg of the drug pipeline, but not the development stage. A series of analogues needs to be synthesized and screened, which takes time. This approach is only successful if the drug presents a novel mechanism of action that provides efficacy against drug-resistant strains (Pink *et al.,* 2005). Short- and medium-term approaches may be effective but, to ensure malaria is halted and reversed, long term approaches where novel antimalarials are developed, are required.

Novel antimalarials need to abide by a strict set of criteria to be effective. These criteria are known as Single Exposure Radical Cure and Prophylaxis (SERCaP) treatment (Burrows *et al.,* 2013). Firstly, new drugs need to have a novel mechanism of action to avoid existing drug resistance and be more effective in combination with current drugs. New antimalarials need to possess novel mechanisms of action because all known drugs are unable to fulfil the SERCaP criteria (Flannery *et al*., 2013). Novel drugs also need to be active against multiple stages in

the parasite lifecycle, to prevent transmission and to clear infection. These drugs need to be cheap to manufacture, ideally at $0.15 per dose, as malaria is a disease of poverty (Burrows *et al.*, 2013).

New drugs also need to be stable at high temperatures, so that they do not require refrigeration. Refrigeration is not available in the poorest regions of the world. Drugs need to be able to be taken orally so that patients do not need to go to a clinic every day, a requirement which leads to noncompliance, which accelerates the development of drug resistance. Ideally, new drugs should be able to be administered as a single dose to reduce costs and the likelihood of noncompliance.

The use of novel antimalarials in combination with the current drugs or analogues of the current drugs may be enough to avoid drug resistance and eradicate the disease (Flannery *et al.*, 2013). Novel antimalarials can be synthesized with the use of combinatorial chemistry or isolated from natural products. Historically, the most effective antimalarials have been isolated from nature and, therefore, natural products are the ideal source to begin the search for novel antimalarial compounds.

1.3 Natural Products in Drug Discovery and Development

1.3.1 Introduction

Natural products can be defined as pharmacologically active chemical compounds isolated from living, biological systems (Mathur and Hoskins, 2017). Natural products have been a dominant source of antimicrobial agents in the past. The first example of natural products used as medicine is from 2600 BC in ancient Mesopotamia, where cypress, myrrh, and poppy were used to treat fevers and other maladies (Borchardt, 2002). Ancient Egyptian and Chinese traditional medicines provide a vast collection of treatments and remedies for a spectrum of diseases (Chan, 1994; Borchardt, 2002). Most traditional medicines were sourced from plants and developed by experimentation over hundreds of years (Kinghorn *et al.*, 2011; Dias *et al.*, 2012). Traditional medicines were also developed by observing which plants animals eat or avoid, a process known as zoopharmacognosy (Rodriguez and Wrangham, 1993).

There are many examples of clinically-used drugs developed from natural products from plants (Der Marderosian and Beutler, 2014). A well-known example is the analgesic and antipyretic drug, acetylsalicylic acid, also known as aspirin. Salicylic acid was originally isolated from the bark of the willow tree (*Salix alba*) and improved by derivatization into acetylsalicylic acid. Foxglove (*Digitalis purperea*) has been used in European medicine for centuries, but the active constituent, digitoxin, was only isolated in the 1700s (Der Marderosian and Beutler, 2014). Digitoxin is a cardiotonic glycoside used to treat cardiac conditions by enhancing cardiac conduction (Dias, Urban and Roessner, 2012).

Plants are not the only source of natural products, as microorganisms such as fungi and bacteria are well-known producers of bioactive compounds. Paclitaxel, sold under the brand name Taxol®, is a potent anticancer drug isolated from the bark of the Pacific yew tree (*Taxus brevifolia*). It is actually produced by an endophytic fungus, *Taxomyces andrenae*, located in the phloem of the Pacific yew (Rowinsky and Donehower, 1995).

The antibiotic, penicillin, is the most well-known example of a fungal natural product, isolated from *Penicillium notatum* in 1929 by Sir Alexander Fleming (Fleming, 1929; Abraham *et al*., 1941). Members of the bacterial phylum, *Actinobacteria*, are another famous source of natural products and produce a wide range of antibiotics that have been used in medicine. Streptomycin was isolated from *Streptomyces griseus* and was used to treat tuberculosis (*Mycobacterium tuberculosis*) and the black plague (*Yersinia pestis*) (Waksman *et al*., 1946). The discovery of penicillin in 1929 and, streptothricin, streptomycin and actinomycin in the 1940s, initiated the Golden Age of Antibiotics from the 1940s to the 1960s (Fleming, 1929; Waksman and Woodruff, 1942; Bérdy, 2005). During this time, hundreds of fungi and bacteria were screened for antibiotics (Davies, 2006). It is estimated that half the number of drugs currently known were isolated during this period. The term antibiotic was coined by Selman A. Waksman in 1942, who defined it as, "any microbial product that is antagonistic to the growth of another microorganism"(Waksman and Woodruff, 1942). The Golden Age of Antibiotics initiated many natural product drug discovery and development projects run by pharmaceutical companies, not just for antibacterial and antifungal antibiotics, but also other classes of drugs, such as anticancer and antiparasitic drugs (Dias *et al.,* 2012).

1.3.2 The Drug Discovery and Development Pipeline

The process by which new molecules are identified, tested, and improved to produce new drugs is known as the drug discovery and development pipeline. First, a new molecule is identified, then evaluated for efficacy and safety *in vitro*, before moving on to preclinical testing (Katzung *et al.*, 2012). In preclinical testing, the *in vivo* pharmacokinetics, efficacy and toxicity are evaluated in animal models. If the compound passes these tests, it is moved forward into clinical trials in humans where it is tested in three different phases before reaching the public market. A fourth and final phase of safety monitoring and data gathering occurs before the drug is officially declared safe (Figure 1.7) (Katzung *et al.*, 2012).

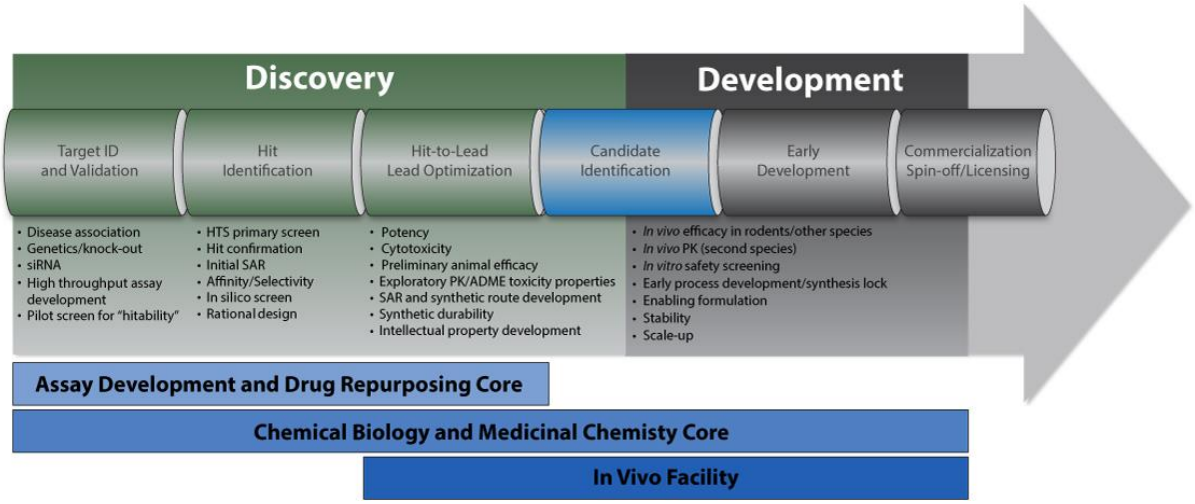

Figure 1.7: Summary of the drug discovery and development pipeline (Michigan State University)**.**

The drug discovery and development pipeline is an expensive and time-consuming procedure with a low success rate. Only approximately 1 out of every 5000 candidate molecules is developed into a commercial drug (Gibson, 2009). It is estimated that it costs $800 million–$1 billion and requires 10–15 years of dedicated study to develop a new drug for clinical use (Katzung *et al.*, 2012). Most drugs fail at some point during testing and either need to be derivatised into improved analogues or abandoned, and the process has to be restarted. Dedicated researchers across multiple disciplines using expensive instruments are required to develop a new drug. This is why the process is so expensive and time-consuming. However, the investment in time, effort and money is worth it, as the pharmaceutical market is worth

billions of dollars. For example, in 2001 the global profit from prescription pharmaceuticals was estimated to be $364 billion dollars (Katzung *et al.*, 2012).

This investigation will focus on the first part of the pipeline, drug discovery, where molecules are screened for activity against a specific disease or disorder (Hughes *et al.*, 2011). Drug screening involves a series of experiments that test a large number of samples in quantitative assays *in vitro* or sometimes *in vivo* (Katzung *et al.*, 2012). Drug screens produce a list of compounds that display reproducible and desired activity, known as hit candidates (Hughes *et al.*, 2011). The list of hit candidates is evaluated to identify the best or lead candidate to evaluate in preclinical tests. This involves *in vitro* testing against drug-resistant strains, cytotoxicity testing against host cell lines to determine selectivity, mechanism of action and ADME (absorption, distribution, metabolism and excretion) studies. ADME studies includes a range of assays which predict the pharmacokinetics and pharmacodynamics of hit candidates. Some examples of ADME assays include kinetic solubility, lipophilicity, metabolic stability, and plasma stability.

1.3.3 Advantages of Natural Products in Drug Discovery

The main sources of compounds for drug screens in drug discovery are synthesized molecules and natural products (Hughes *et al.*, 2011). Focusing on natural products for drug discovery and development has a number of advantages. Natural products exhibit extremely diverse chemical structures and represent a vast source of new chemical compounds (Clardy and Walsh, 2004). Diverse chemical structures lead to diverse biological functions, which is why these structures are sought after (Bérdy, 2005). For example, natural products have more stereogenic centres and chemical complexity than most synthetic molecules.

The chemical diversity exhibited by natural products is a function of their biosynthesis. Natural products are produced by secondary and, to a lesser extent, primary metabolism. Primary metabolism refers to the breakdown and biosynthesis of carbohydrates, lipids, proteins, and nucleic acids. Primary metabolism is generally very conserved, as it is required for growth and replication (Dewick, 2002).

Secondary metabolism is not required for growth and generates molecules that may be unique to specific groups or individual organisms (Bérdy, 2005). Secondary metabolites are produced

to allow an organism to adapt to its environment and can function as defence mechanisms, forms of communication, transporters and metabolic regulators (Demain and Fang, 2000). Secondary metabolites are biosynthesised from the intermediates produced by primary metabolism, such as amino acids and acetyl CoA. With just a few intermediates, a wide range of diverse molecules can be produced by using different tailoring enzymes or incomplete processing in some cases (Sarker *et al.*, 2006). For example, it has been theorized that amino acids are partially processed by the acetate and shikimate pathways to generate shunt, or intermediate metabolites, to create unique secondary metabolites (Clardy and Walsh, 2004; Sarker *et al.*, 2006).

Natural products often provide excellent efficacy and selectivity for drug targets (Cragg and Newman, 2013). This could be due to unique and diverse structures, which allow very specific binding and, thus, strong responses and reduced toxicity. Another hypothesis is that natural products are already biologically validated (Brohm *et al.*, 2002). Because the precursors of primary and secondary metabolites are limited and existed in primitive life forms, they have co-evolved over thousands of years to interact (Ginsburg and Deharo, 2011).

Natural products can also act as excellent scaffolds for further study and improvement. Many natural product drugs do not function as drugs in their original biological form and are instead derivatized to produce improved compounds. Examples include aspirin and the artemisinin derivatives used in the ACTs (Krishna *et al.*, 2004; Der Marderosian and Beutler, 2014). Since natural products have not evolved as drug compounds, they often need chemical modification to improve their efficacy or pharmacokinetic parameters (Ginsburg and Deharo, 2011).

The final advantage is the untapped potential of natural products. There are many natural sources that have never been screened for bioactive compounds. It is estimated that only 6% of terrestrial plant species have been screened pharmacologically (Farnsworth *et al.*, 1985; Basso *et al.*, 2005). The oceans cover most of the Earth's surface and contain the bulk of the planet's biodiversity, but improvements in technology have only recently allowed exploration of marine products (Faulkner, 2000). Despite, only recent exploration, drugs based on marine natural products have already been developed, emphasising their potential. One of the first marine-based natural products was a non-narcotic analgesic drug Ziconotide®, isolated from marine cone snails (*Conus* sp.) (Wallace, 2006).

However, while natural products have many advantages, there are also a number of disadvantages, which led to the end of the Golden Age of Antibiotics (Dias *et al*., 2012). Issues caused by rediscovery of known compounds, high cost of productions and the long duration of natural products screening led to pharmaceutical companies favouring semi-synthetic and synthetic methods instead.

1.3.4 Disadvantages of Natural Products in Drug Discovery

There are many reasons why natural products were abandoned as a source of drug-like compounds. Natural product research is a time-consuming process which increases the cost and labour required for screening and development projects (Wagenaar, 2008). While the complexity and diversity of natural products can create interesting molecules and effective drug compounds, these characteristics can make it more difficult to isolate and purify them (Li and Vederas, 2009). Thus, more resources and time are required to determine how to successfully isolate these molecules. Molecules may also be unstable, making it nearly impossible to isolate them. Once isolated, elucidating the structure of a complex molecule can be very difficult and require extremely sensitive instruments (Dias *et al*., 2012).

In some cases, the isolated natural product cannot be synthesized due to its unique structure (Clardy and Walsh, 2004; Basso *et al.*, 2005). Only an estimated 40% of microbial natural products can be synthesized (Bérdy, 2005). This can prevent large scale production and, therefore, sale as a therapeutic agent. Therefore, the labour and financial investment into these projects cannot always be justified.

Once isolated, scaled-up production of natural products may not be achievable (Dias *et al*., 2012). Many natural products are produced in very small quantities and sourcing the material can be difficult (Basso *et al.*, 2005; Guantai and Chibale, 2011). For example, it is difficult to cultivate the Pacific yew as a source of paclitaxel (Nikolic *et al.*, 2011). The Pacific yew grows slowly and is an endangered species making it an inefficient source for large scale production. Sources, such as sea sponges, may produce highly active compounds, but only occur in certain reef systems and may not be viable to farm (Faulkner, 2000).

Other sources, like plants or animals, may be endangered or protected by traditional laws. While an advantage of natural products is the untapped biodiversity they represent, there are

often reasons these sources have not been explored. For example, most bacteria are unculturable in a laboratory environment, depriving us of access to an enormous number of diverse molecules (Bérdy, 2005; Davies, 2006).

A major problem that affects all natural product screening programmes is dereplication. Dereplication is the process of rediscovering known compounds in different strains or species of organisms (Sarker *et al*., 2006). It was a major challenge faced during the Golden Age of Antibiotics, and, over time, fewer and fewer new natural products have been discovered. Between 1930 and 1962, 20 different classes of antibiotics were discovered (Coates *et al.*, 2011). Since then, only two new classes have been discovered. Between the 1970s and 1990s, the number of discovered natural products continued to increase, but most of them were analogues of known compounds (Bérdy, 2005). The cost of conducting this research had increased and, with the chances of discovering novel compounds diminishing, it was no longer viable for pharmaceutical companies to screen natural products.

Today, natural products represent a much smaller proportion of drugs. For example, between 1981 and 2002, only 5% of all drugs approved by the US Food and Drug Administration (FDA) were natural products and 23% were natural product derivatives (Newman *et al*., 2003). Synthetic methods, such as combinatorial chemistry, have replaced natural products in drug discovery. However, with the advent of new technology and techniques developed in many fields, such as chemistry, genomics, and metabolomics, it is possible to overcome these difficulties and increase the chances of finding natural products with novel structures.

1.3.5 The Present and Future

In the 1980s, many pharmaceutical companies shifted from natural product screening to synthetic approaches, such as semisynthesis and combinatorial chemistry, as a source of new drug compounds (Dias, *et al.*, 2012).

Semisynthesis is a type of synthesis that modifies known natural product structures to improve its efficacy and pharmacokinetics (Clardy and Walsh, 2004). While natural products can make excellent lead candidates in the drug discovery and development pipeline, they are rarely used in their original state (Guo, 2017). Modifications to the molecular structure of active candidates are often necessary to improve efficacy, reduce toxic side effects and improve its

pharmacokinetic profile such as by altering its lipophilicity or solubility. This can be achieved by removing redundant substructures that are not involved in the natural product's activity or by adding more functional groups that change the nature of the compound. One example of a successful semisynthetic natural product derivative is telavancin from vancomycin. Vancomycin is an antibiotic isolated from *Amycolatopsis orientalis* in the 1950s which is effective against Gram-positive bacteria such as the pathogen *Staphylococcus aureus* (Levine, 2006). Vancomycin is able to bind to the terminal D-alanyl-D-alanine moieties of the peptidoglycan bacterial cell wall which prevents its formation and results in cell death (Higgins *et al.*, 2005). Vancomycin resistant bacteria have a D-lactate instead of a D-alanine terminal moiety which inhibits vancomycin's action. In 2009, the semisynthetic lipoglycopeptide telavancin was approved by the FDA to combat vancomycin and combat drug resistant bacteria (Saravolatz *et al*., 2009). Telavancin acts by binding to growing D-alanyl-D-alanyl moieties of peptidoglycan chains and prevents transpeptidation which prevents cell wall formation and causes cell death (Higgins *et al.*, 2005; Saravolatz *et al*., 2009). This makes telavancin effective against vancomycin and other drug resistant pathogens. For example, telavancin was shown to be inhibit methicillin resistant *S. aureus* (Higgins *et al.*, 2005). Telavancin was synthesised by the addition of an aliphatic chain to vancomycin's amino sugar moiety (Saravolatz *et al*., 2009). Additionally, a polar amino-phosphonic acid group is linked to vancomycin's biphenyl moiety. These alterations allow telavancin to anchor into the lipophilic cell membrane which improves it stability at its target site and its affinity for peptidoglycan. Other examples of the use of semisynthesis to improve natural products include the artemisinin derivatives from artemisinin and aspirin from salicylic acid (Krishna *et al*., 2004; Der Marderosian and Beutler, 2014).

Combinatorial chemistry uses different techniques to generate a large and diverse array of chemical molecules, known as a chemical library, by repetitive covalent linkage of a set of building blocks or precursors (Liu *et al.*, 2017). Chemical libraries can produce millions of new compounds, and improvements in technology have facilitated the study of these massive libraries. The development of automated high throughput screening (HTS) of whole-cell and drug-target based assays allows these libraries to be screened in a matter of days (Dias *et al*., 2012). This model offered the potential to solve several challenges faced by natural product screening, as combinatorial chemistry was faster, sourcing compounds was no longer an issue, and all the structures were known. It was predicted that these libraries could produce highly active molecules (Liu *et al.*, 2017). Many drugs have been produced synthetically, such as Sorafenib, an anticancer drug that was approved by the FDA in 2005 (Kingston and Newman,

2005). However, over time it became clear that the chemical libraries produced could not match the chemical diversity of natural products and fewer drug candidates and leads have so far been developed by combinatorial chemistry than anticipated (Clardy and Walsh, 2004; Liu *et al.*, 2017; Harvey *et al*., 2015).

Nature has spent billions of years evolving and developing diverse secondary metabolites to act in a variety of biological systems, so it is not surprising that matching this diversity and functionality is difficult (Basso *et al.*, 2005; Cragg and Newman, 2013). What has been more effective is using natural products or their pharmacophores as the building blocks for chemical libraries (Brohm *et al.*, 2002; Cragg and Newman, 2013). This was demonstrated by Brohm *et al.* (2002), who created a series of biologically-diverse analogues of the dysidiolide phosphatase inhibitors using solid phase synthesis techniques (Brohm *et al.*, 2002). Natural products are already biologically validated, and their architecture could be a potent driving force in developing improved chemical libraries. Combinatorial chemistry could help modify natural products to improve their absorption, transport, and other *in vivo* parameters (Bérdy, 2005). This is similar to semisynthesis of natural products, but on a much larger scale. This would never be possible without the development of combinatorial chemistry and efforts need to be made to combine the two systems. However, to achieve this, new and improved natural product libraries need to be created, which first requires isolation of new natural products.

With the advent of modern technology, the past challenges of natural products can be overcome. Advanced chromatographic techniques developed to separate chemical libraries can be used to isolate natural products at an accelerated rate (Baker *et al.*, 2007). The inaccessible biodiversity of microorganisms can be investigated with the use of genomic techniques, such as genome mining, and improved culture methods, such as the use of Ichip chambers that isolate unculturable species (Nichols *et al.*, 2010; Liu *et al.*, 2013). Detection methods, such as high resolution mass spectrometry (HRMS) and nuclear magnetic resonance spectroscopy are more sensitive than before and can be linked to much larger chemical libraries to identify new molecules and avoid the isolation of known molecules (Baker *et al.*, 2007). Synthesis methodologies have also improved, making it possible to synthesise compounds previously out of reach (Bérdy, 2005). These techniques can be combined and even automated to streamline the drug discovery process (Dias *et al*., 2012). With the threat of drug resistance growing, not just in malaria, but in the majority of pathogens, new and improved methods and models need to be implemented (Bérdy, 2005). While there are still major challenges to be faced, the evidence suggests that natural products warrant renewed interest for drug discovery.

1.3.6 Natural Products in Malaria Drug Discovery

In the context of malaria, natural products have been very successful drugs in the past (Guantai and Chibale, 2011; Dias *et al.,* 2012). As discussed previously, quinine and artemisinin were both isolated from plants and developed into first-line treatments. There are other examples, such as the semisynthetic clindamycin and doxycycline, both of which are used as antibacterial antibiotics, but were also found to be effective antimalarials (Kremsner, 1990; Magill *et al.*, 2011). Currently, natural products are not being developed into antimalarials and there are currently no antimalarial compounds in clinical trials that have originated from natural products (Guantai and Chibale, 2011; Tse *et* al., 2019). With the availability of new methods and equipment, and the history of natural products in antimalarial drug discovery, natural products are a potential source of antimalarials.

Plants have been the predominant source of natural products in antimalarial drug discovery, predominantly due to their importance in traditional medicines (Bourdy *et al.*, 2008; Wells, 2011). However, screening of plants has produced little success in recent years. From 2005 to 2008, only 20 new highly active antimalarial compounds were isolated, and none were developed further (Bero *et al.*, 2009). While plants represent a viable source of natural products, screening new sources of natural products may yield better results (Bérdy, 2005; Guantai and Chibale, 2011; Wells, 2011). As discussed previously, members of the phylum *Actinobacteria* are a well-known source of antibiotics and were key contributors during the Golden Age of Antibiotics. Despite this impressive history, their antimalarial producing potential is not well studied.

1.4 Actinobacteria

1.4.1 Taxonomy and Physiology

The phylum, *Actinobacteria*, is composed of Gram-positive bacteria with a distinctive high guanine + cytosine DNA content (Barka *et al.*, 2016). The phylum *Actinobacteria* represents one of the largest lineages of the domain *Bacteria* and includes a diverse array of species

ranging from the human pathogen *Mycobacterium tuberculosis*, the causative agent of tuberculosis, to the soil-dwelling saprophytic *Streptomyces*, a genus of antibiotic producing microorganisms. The actinobacteria display a range of morphologies, such as rods, cocci, and filamentous forms (Barka *et al.*, 2016). The filamentous species are known as the actinomycetes and are the main source of bacterial bioactive compounds. For the purpose of this review, discussion and investigation, the focus will be on the filamentous actinobacteria. The actinomycetes are typically aerobic mesophiles, but there are exceptions (Lechevalier and Lechevalier, 1965). Actinomycetes are mostly free-living and can be found in both terrestrial and aquatic/marine environments. Some examples of actinomycete genera are *Streptomyces, Kitasatospora, Salinispora, Actinomadura, Streptosporangium, Micromonospora*, and *Kribbella* (Barka *et al.*, 2016).

Actinomycetes have a unique morphology, as they produce a mass of hyphae to form a mycelium and many reproduce by sporulation (Flärdh and Buttner, 2009; van Dissel *et al*., 2014). In the past, the actinomycetes were considered to be fungi or a transitional form between bacteria and fungi because of their filamentous morphology. Almost all actinomycetes form a substrate mycelium when grown on solid medium, with the only exception being members of the very rare genus *Sporichthya* (Flärdh and Buttner, 2009). Actinomycetes are also known to produce pigments with many different colours depending on growth medium and culture age (Lechevalier and Lechevalier, 1965).

Briefly, the actinomycete lifecycle (Figure 1.8) begins from a spore, which germinates and develops into branched multinucleoid vegetative hyphae, which form the substrate mycelium in the agar (Ohnishi *et al.*, 2008). The substrate mycelium grows by tip extension and branching (Barka *et al.*, 2016). When stressed, such as during nutrient starvation, actinomycetes produce aerial hyphae above the colony, which differentiate into spores for reproduction. The actinomycetes are sessile; therefore, in order to survive adverse conditions, they produce spores. Spores can be formed by subdivision of the aerial hyphae, fragmentation, swelling, or endogenous spore formation (Reponen *et al.*, 1998). The end result is chains of uninucleoid spores (Ohnishi *et al.*, 2008).

The spore morphology, chain length, and number of spores produced all differ greatly between actinomycete genera (Barka *et al.*, 2016). Spores are dispersed by air and water to places where they can germinate and grow when the conditions are favourable. Spores can remain dormant and viable for long time periods under a range of conditions (Reponen *et al.*, 1998). To develop

aerial hyphae during adverse conditions, the actinomycetes trigger a programmed cell-death mechanism (Wildermuth, 1970; Miguélez *et al*., 1999). This programmed cell death breaks down the vegetative hyphae and scavenges its components. These include amino acids, polysaccharides, nucleic acids, lipids, and other nutrients required for aerial hyphae production and sporulation. This collection of nutrients is often targeted by neighbouring, competing microorganisms; therefore, during this time antibiotics are produced as a defence mechanism (Bibb, 2005). Antibiotics can be produced during other stages of the lifecycle, but the majority are produced during times of stress (Martin and Demain, 1980).

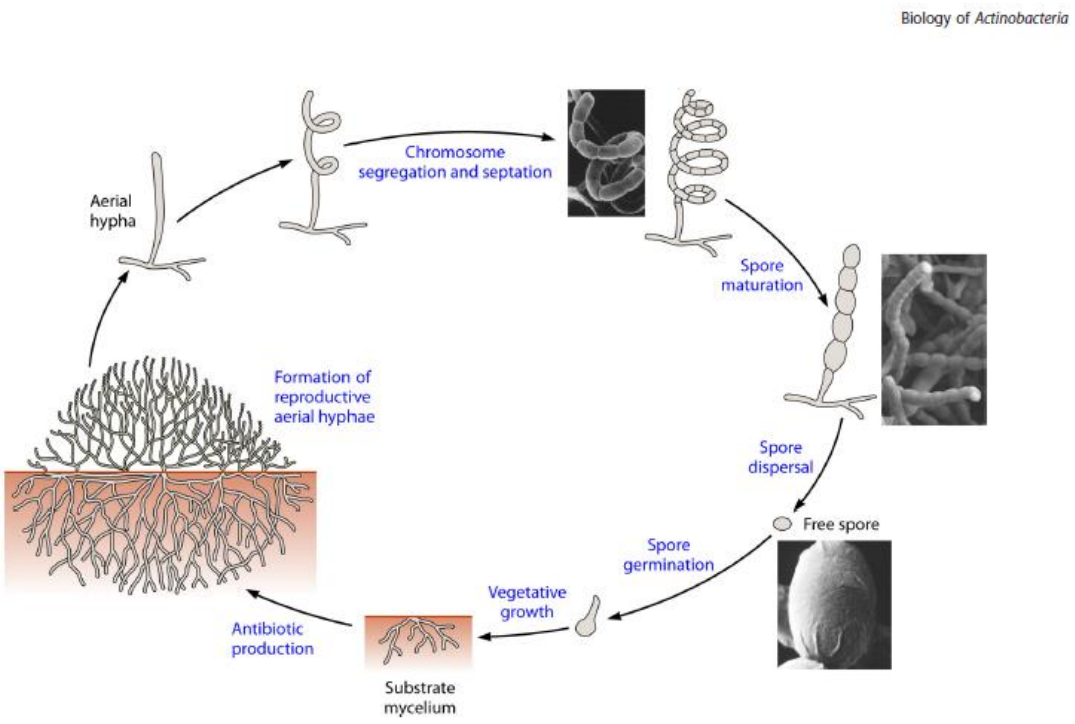

Figure 1.8: Lifecycle of the actinomycetes (Barka *et al.*, 2016). This image was used with permission under the American Society for Microbiology copyright license.

1.4.2 Secondary Metabolism of Filamentous Actinobacteria

1.4.2.1 Antibiotics

The actinomycetes are one of the best sources of natural products in the world. They were heavily exploited during the Golden Age of Antibiotics, initiated by the discovery of streptothricin, streptomycin, and actinomycin from *Streptomyces* strains in the 1940s (Waksman and Woodruff, 1942; Waksman, 1947). Of the approximately 10 000 antibiotics known, an estimated 50% originate from actinomycetes (Subramani and Aalbersberg, 2012). In addition to their ability to produce such an array of compounds, actinomycetes, and microorganisms in general, have another advantage over other natural product sources. Once isolated, microorganisms can generally be cultivated on a larger scale and with higher production rates than plants, animals, and marine organisms (Bérdy, 2005).

The bulk of the compounds produced by the actinomycetes, approximately 70%, originate from one genus, *Streptomyces* (Okami and Hotta, 1988; Bérdy, 2005). The genus *Streptomyces* consists of hundreds of species, and *Streptomyces* strains are the easiest actinomycetes to isolate and culture in a laboratory (Bérdy, 2005).

Streptomyces are thought to be able to produce such an array of diverse secondary metabolites due to their extremely large genomes (Goshi *et al.*, 2002). They contain hundreds of transcription factors, giving them fine control over their secondary metabolism. This allows *Streptomyces* to react and adapt to a range of environments. The list of antibiotics produced by the *Streptomyces* is too great for the scope of this review, but some examples include, aminoglycosides (e.g. streptomycin), macrolides (e.g. erythromycin), β lactams (e.g. the cephamycins), ansamycins (e.g. rifamycin) and tetracyclines (e.g. doxycycline) (Okami and Hotta, 1988; Liras, 1999; Gaynor and Mankin, 2003; Vakulenko and Mobashery, 2003; Kang *et al*., 2012). More examples are shown in Figure 1.9, which demonstrates the large number of antibiotics discovered in the 1960s and the subsequent decrease in the rate of discovery over time.

Other actinomycete genera, known as the rare actinomycetes, because they are more difficult to isolate, are also capable of producing unique natural products (Bérdy, 2005). These genera represent a massive source of untapped microbial biodiversity. They have a history of

producing unique, and sometimes very complicated compounds, which display excellent bioactivity and selectivity. Some examples include *Micromonospora purpurea*, which produces the aminoglycoside gentamicin and *Actinomadura verrucosospora* subspecies *neohibisca* strain E-40, which produces the pradimicins (Furumai *et al.*, 1993; Lazzarini *et al.*, 2000). There has been an increase in the study of the secondary metabolites of the rare actinomycetes over the past few years (Tiwari and Gupta, 2012). Genetically diverse actinomycetes have a greater potential to produce chemically diverse novel compounds. This makes developing new cultivation techniques and improving the understanding of the rare actinomycetes crucial when investigating potential antibiotics.

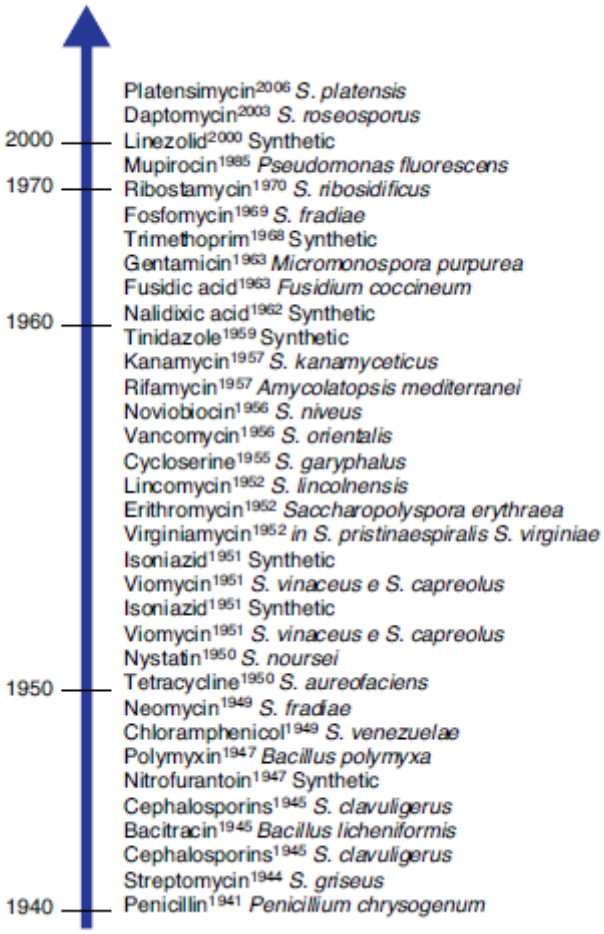

Figure 1.9: Timeline and list of antibiotics from the 1940s until the 2000s (de Lima Procópio *et al.*, 2012)**.** Note how the majority were isolated from *Streptomyces*. This image was used with permission under ScienceDirect's Creative Commons license.

While actinomycetes can produce many different antibacterial antibiotics through a variety of biosynthetic mechanisms, they can produce many different types of antimicrobial compounds. In a comprehensive biological and statistical review, Bérdy (2005) showed that the actinomycetes produce many compounds that are active against multiple pathogens, or exhibit multiple pharmacological effects. He estimated that of 10,100 bioactive secondary metabolites isolated from actinomycetes, 8,700 were antibacterial and 2,400 of these had other bioactivities (Bérdy, 2005). The remaining 1,400 were bioactive, but not antibacterial. According to Bérdy (2005), this was much greater than any other source of microbial secondary metabolites, such as fungi, but not as many as produced by plants.

The actinomycetes are able to produce a range of antibiotics, not only those with antibacterial qualities. For example, the antifungal agent, validamycin A, was isolated from *Streptomyces hygroscopicus* var. *limoneus* in 1968 (Barka *et al.*, 2016). Validamycin A was used to treat rice sheath blight disease (*Rhizoctonia solani*). Another antifungal agent is kasugamycin, which was isolated from *Streptomyces kasugaensis* and used to treat rice blast disease (*Pyricularia oryzae cavara*) (Umezawa *et al.*, 1965). Actinomycetes also produce natural products with anticancer properties. One example is salinosporamide A, produced by the marine actinomycete *Salinispora tropica* (Feling *et al.*, 2003). Salinosporamide A was found to be a proteasome inhibitor and submitted for Phase I clinical trials. Actinomycetes have also been shown to produce natural products with antiviral, herbicidal, and anti-inflammatory properties (Renner *et al.*, 1999; Sacramento *et al.*, 2004; Sousa *et al.*, 2008). More interestingly, Bérdy (2005) estimated that actinomycetes produced 5000–10,000 inactive secondary metabolites. These inactive molecules share many structurally similarities with known active compounds, and it is hypothesized that these molecules do, in fact, have some inherent bioactivity. However, they have just not been screened against the correct targets (Bérdy, 2005).

Expanding screening efforts may link unique structures and features with less well-studied disease pathways. This was seen in the past with hundreds of compounds originally classified as inactive molecules, but discovered to be active later when screened using different testing systems. Secondary metabolites are produced to adapt to an organism's environment and, therefore, have evolved to exert some function, the exact function just needs to be determined. While the antibacterial antibiotic potential of the actinomycetes drew them into the scientific spotlight, it is clear that that is just a small part of what they are capable of. Theoretically, the

diversity and versatility of actinomycete natural products is inexhaustible. Due to this they represent one of the best chances to combat the threats of drug resistance we face today.

1.4.3 Antimalarial Compounds from Filamentous Actinobacteria

Actinomycetes have been shown to produce potent antimalarial compounds. For example, the semisynthetic antibiotics doxycycline, clindamycin, and azithromycin have all been shown to be effective antimalarials (Kremsner, 1990; Magill *et al.*, 2011; van Eijk and Terlouw, 2011).

Azithromycin is a semisynthetic derivative of erythromycin and clindamycin is a semisynthetic derivative of lincomycin (Birkenmeyer and Kagan, 1970; Jelić and Antolović, 2016). Both of which are produced by actinomycetes. Doxycycline is still used as a prophylactic treatment, but it is not recommended for children as it can disrupt bone growth (Magill *et al.*, 2011). More recently, there has been an increase in the search for antimalarials produced by actinomycetes. For example, gancidin-W, a potent low-toxicity antimalarial, was isolated from the endophytic *Streptomyces* strain SUK-10 (Baba *et al.*, 2015). Salinosporamide A was shown to be a very effective antimalarial in *in vivo* studies, with activity matching that of chloroquine (Prudhomme *et al.*, 2008). While these examples indicate that actinomycetes can produce antimalarials, more research needs to be conducted. Most of the compounds mentioned were antibiotics repurposed as antimalarials, and little screening has been done solely on the antimalarial potential of the actinomycetes (Pérez-Moreno *et al.*, 2016). Therefore, further work is required to fully explore the antimalarial potential of the actinomycetes.

1.5 Conclusion

With the threat of drug resistance, the spread of insecticide resistance, and the lack of a vaccine, progress towards the eradication of malaria has stalled (Feachem *et al.*, 2019). New measures need to be implemented and developed to eradicate the disease. While it cannot be the only new measure, it is critical that novel drugs, with novel mechanisms of action, are developed. Historically, natural compounds have produced the best antimalarials. While interest has waned in natural products as drug sources, the advent of new technologies, methodologies, and

knowledge can allow us to overcome their past limitations. This makes natural products an ideal source for new antimalarial drugs.

The filamentous actinobacteria have a long history of producing bioactive compounds and have been shown to be capable of producing unique compounds with different bioactivity profiles. However, limited research has been conducted on the antimalarial potential of the filamentous actinobacteria. This warrants further research to determine whether the filamentous actinobacteria produce natural products capable of being developed into novel and effective antimalarials.

1.6 Scope of the Study

The aim of this investigation was to screen filamentous actinobacteria for antiplasmodial activity, determine if activity was due to novel antiplasmodial compounds and if these novel compounds could be developed into new antimalarial compounds. This was to be achieved by pursuing four objectives:

- The first objective was to screen filamentous actinobacterial strains for antiplasmodial activity against the drug-sensitive strain of *P. falciparum*, NF54. The activity of each strain was used to select the best candidate for further study.
- The second objective was to purify the active compounds from the selected filamentous actinobacteria by bioassay-guided fractionation. The intention was to develop a purification method with as few steps as possible.
- The third objective was to elucidate the structures of the active compounds and determine whether they are novel. This was achieved by using HRMS and NMR spectroscopy.
- The final objective was to evaluate the isolated compounds antiplasmodial efficacy and host selectivity to determine if they are suitable for further development. This objective was subdivided into the following categories:
    1. Activity against the drug-sensitive strain and multi-drug resistant strain of *P. falciparum*, NF54 and K1 respectively.
    2. Mammalian cytotoxicity against the Chinese Hamster Ovary and HepG2 cell lines.
    3. Haemotoxicity against human erythrocytes.

2 Screening of Filamentous Actinobacteria for Antiplasmodial Activity

Abstract

Uncharacterized environmental actinobacterial strains from the Meyers laboratory (University of Cape Town, South Africa) culture collection and the type strains of new actinobacterial species identified and characterized in the Meyers laboratory, were screened for antiplasmodial activity against *P. falciparum*, NF54. The cultivation conditions selected for antiplasmodial compound production were the same as those shown to result in antibacterial antibiotic production. Liquid cultures were extracted using the mid-polar solvent, ethyl acetate, with the aim of discovering drug-like molecules that can be administered orally. Thirty-one strains of actinobacteria belonging to eight genera (*Actinomadura*, *Amycolatopsis*, *Gordonia*, *Kribbella*, *Micromonospora*, *Nocardia*, *Nonomuraea*, and *Streptomyces*) were screened revealing fourteen candidates. By applying strict *in vitro* conditions required to qualify for further investigation, eight strains were found to be suitable for antiplasmodial purification and isolation studies. Of these eight candidates, *Streptomyces* strain PR3 was selected as it showed excellent antiplasmodial efficacy, no cytotoxicity against the Chinese Hamster Ovary or liver HepG2 cell lines, no haemotoxicity, and was easy to culture.

2.1 Introduction

The aim of the investigation was to screen filamentous actinobacteria metabolites for antiplasmodial activity. Actinobacterial strains were selected, cultivated in liquid medium, extracted, and tested for antiplasmodial activity. Crude extracts that showed promising activity were then evaluated further.

Actinobacterial strains were not isolated as part of this investigation. Instead, strains from Dr Paul Meyers' culture collection in the Department of Molecular and Cell Biology, University of Cape Town, were screened. These strains represent a unique biodiversity having never been screened for antiplasmodial activity. Only recently isolated, uncharacterized strains or novel strains isolated and characterized by Dr Meyers' laboratory were selected. The intention behind selecting biodiverse strains was to improve the probability of isolating unique chemical molecules as biological diversity underpins chemical diversity. Genetic diversity enables strains to produce chemically-diverse molecules, which may be new secondary metabolites with unique functions (Bérdy, 2005; Tiwari and Gupta, 2012). Actinobacterial strains shown to have antibacterial or antifungal antibiotic potential were prioritized in the hopes of isolating compounds with activity against a spectrum of pathogens. However, strains with no known antibiotic activity were also screened. Only pure cultures of the strains were used, and purity was checked before, during and after cultivation by Gram staining and streaking for single colonies (Bartholomew and Mittwer, 1952; Shirling and Gottlieb, 1966).

Due to the impressive record of *Streptomyces* strains as antibiotic producers, the bulk of the strains screened were novel isolates belonging to the *Streptomyces* genus (de Lima Procópio *et al.*, 2012). *Streptomyces* species were also readily available from the culture collection. The other strains tested belonged to rarer, non-*Streptomyces*, genera. As discussed in Chapter 1, the rare actinomycetes are capable of producing unique and potent antibiotic compounds and warrant screening (Tiwari and Gupta, 2012).

The simplest way to test the antiplasmodial activity of actinobacteria is to test the crude solvent extracts of each strain. To the author's knowledge, there is no bioautographic overlay technique or similar technique available to accelerate antiplasmodial testing.

To obtain crude extracts, strains were cultivated in liquid medium. The cultivation conditions required for antiplasmodial compounds were considered to be the same as the ones required

for antibacterial antibiotic production. This is an accepted assumption for all non-antibiotic secondary metabolites, such as pigments and plant growth factors (Martin and Demain, 1980). In nature, actinomycetes usually produce antibiotics under stress conditions, such as nutrient depletion. When grown in batch culture, actinomycetes grow exponentially during the exponential (log) phase, then enter the stationary phase as nutrients become limiting and growth slows down (Martin and Demain, 1980). In the stationary phase, primary metabolites produced during the log phase are used in the biosynthesis of antibiotics and other secondary metabolites. Therefore, culture incubation was set for a period shown to be suitable by the Meyers group to ensure sufficient time in the stationary phase (Meyers *et al.*, 2003; Wood *et al.*, 2007).

Most actinomycetes are aerobic and require oxygen to grow and produce antibiotics; therefore, all cultures were shaken (Iwai and Omura, 1982). This ensures homogenous, well-aerated liquid cultures.

Actinomycetes can be fastidious, and it is well known that they produce different secondary metabolites based on their growth and nutrient conditions (Martin and Demain, 1980). Therefore, it is possible that a selected strain can produce antiplasmodial compounds, but not in the medium or conditions it was exposed to. However, the chance of locating novel compounds is predicted to be higher when screening more strains simultaneously than fewer strains under different growth conditions (Tiwari and Gupta, 2012). Therefore, each strain was grown in the medium it was originally isolated in.

Before extraction, the broth and cell mass were separated. This simplified the extraction, and if one source (the cells or the spent culture broth) was inactive, it could be discarded in future extractions. It is also possible that different compounds are found in the cells and the culture broth. Extraction is based on the partitioning of compounds into solvents with similar physiochemical properties, such as polarity (Zhang *et al*., 2018). When selecting extraction solvents to use, it is important to understand what type of molecules you need to isolate. As discussed in Chapter 1, new antimalarials ideally need to be administered orally. The lipophilicity of a compound has been shown to be an important factor in determining its absorption and distribution. Hydrophilic compounds are typically unable to penetrate the lipophilic cell membrane of the gastrointestinal tract (GIT) without cell transporters (Lipinski, 2000). Conversely, lipophilic molecules can pass through the GIT cell membranes, but do not dissolve in water. Therefore, they may bind preferentially to proteins or food in the GIT or

remain in cells (Katzung *et al*., 2012). Mid-polar compounds have been shown to be better oral drugs as they dissolve better in water and pass through lipophilic membranes (Lipinski, 2004; Bhal, 2020). The partition coefficient (*P*) describes the likelihood of a neutral solute to dissolve in an immiscible biphasic system of fats (organic solvents, lipids) and water (Bhal, 2020). If a solute has a positive log*P* it is hydrophobic/lipophilic while if it has a negative log*P* it has a higher affinity for aqueous environments. Solutes with a log*P* of 0 are mid-polar as they partition equally between the organic and aqueous layers. Solvents tend to extract solutes with the same log*P* following the old rule "like dissolves in like" (Zhang *et al*., 2018). Therefore, the selected solvent should have a similar log*P* value. Ethyl acetate (EtAc) was selected as the main extraction solvent as it has a log*P* of 0.7 (National Center for Biotechnology Information, 2020). This does not mean that all compounds extracted by EtAc will make good oral drugs, but it does increase the likelihood of extracting compounds with the correct lipophilicity. Methanol (MeOH), a polar solvent, was used in the first cell mass solvent wash with EtAc to disrupt hydration layers. This was predicted to improve the extraction as it allowed the EtAc to mix more efficiently with the actinobacterial hyphae.

To test for antiplasmodial activity, a phenotypic assay against the asexual blood stage of *P. falciparum* was selected. This stage was used, because it is the easiest to culture *in vitro,* presents a number of druggable targets, and represents a large proportion of the parasite's lifecycle (Cowman *et al.,* 2016; Hovlid and Winzeler, 2016). Phenotypic or whole-cell assays are tests that expose the entire microorganism to drug candidates and changes in phenotype are monitored (Hovlid and Winzeler, 2016).

The alternative to phenotypic screening is target-based screening. Target-based screening involves exposing purified protein targets required for the pathogen's survival to drug candidates (Swinney, 2013). When screening natural products, phenotypic screens have several advantages over target-based screens (Hovlid and Winzeler, 2016). Firstly, compounds that are unable to penetrate cell membranes are eliminated. Secondly, molecules that act synergistically can be detected. Most importantly for natural-product screening, knowledge of the drug target is not required; therefore, the identity of the test molecule(s) is not necessary and unknown mechanisms of action can be discovered (Swinney, 2013; Katsuno *et al.,* 2015). While not preferred for hit selection, target-based screens are very useful in discovering the targets of drug candidates during later development (Katsuno *et al.*, 2015).

The parasite lactate dehydrogenase (pLDH) assay was used to measure antiplasmodial activity. The basis of this assay relies on the ability of the lactate dehydrogenase (LDH) enzyme of *P. falciparum* to use 3-acetyl pyridine (APAD) as a coenzyme to oxidize lactate to pyruvate (Makler *et al.*, 1993). APAD is reduced to APADH, which subsequently reduces nitro blue tetrazolium (NBT) to a formazan precipitate. Reduction of the tetrazolium produces a colour change from yellow to purple, which can be measured spectrophotometrically and correlated to parasite survival. The greater the colour change, the greater the parasite survival (Makler *et al.*, 1993).

Human erythrocytes also contain the LDH enzyme; however, it carries out the same reaction at a much slower rate in the presence of APAD. Therefore, erythrocytes produce very little background signal. The pLDH assay can detect the presence of *P. falciparum in vitro* at parasitaemia levels of 0.02% (Makler *et al.*, 1993). NB, when discussing efficacy results from *in vitro* assays, the activity is referred to as antiplasmodial activity (Fan *et al.*, 2018). Antimalarial activity refers to activity seen against the disease as a whole, such as in *in vivo* or clinical studies.

Each crude culture extract sample was tested for antiplasmodial activity against NF54, a fully drug-sensitive strain of *P. falciparum* (Dowler, 1995). A drug-sensitive strain was selected to establish baseline activity. Once purified, active compounds were tested against the multi-drug resistant strain, K1 (Thaithong *et* al., 1983).

The basis of antibiotic drug therapy is selective toxicity, where drugs must selectively inhibit the pathogenic target without harming the human host (Peternel *et al.*, 2009). Therefore, when screening natural products, it is important to discern between antiplasmodial activity and host cytotoxicity. Cytotoxicity refers to the effect of chemical compounds as evidenced by host cell death, cell growth inhibition, altered cell morphology or failure of cells to attach to surfaces (Slater, 2001).

Cytotoxicity can be measured using a number of different techniques, and there is no single generally accepted method (Peternel *et al.*, 2009). *In vitro* assays are commonly used to determine cytotoxicity and have a number of advantages over *in vivo* studies (Stone *et al.*, 2009). They are faster and thus more suitable for high-throughput screening, relatively easy to maintain and analyse, less expensive than *in vivo* models and more ethical than testing on animals. The obvious disadvantage of *in vitro* cytotoxicity, and indeed many *in vitro* screening techniques, is that they do not represent the complex set of interactions between multiple organs

and cell types that occur in living systems. Drug candidates can be cytotoxic against a range of cell types at the same concentration or display cell-type-specific toxicity (Peternel *et al.*, 2009). These toxic effects could be missed *in vitro,* and, ultimately, compounds of interest must be tested for *in vivo* toxicity in animal and human models to be declared safe.

An important issue with early *in vitro* cytotoxicity results is interpretation. Crude extracts are a mixture of chemicals and mixtures may not display the same properties as pure compounds (Altenburger *et al*., 2003). Other components in the crude extract may exert a synergistic or antagonistic effect, which could lead to an increase or decrease in an active compound's cytotoxicity, respectively. Concentrations are also affected in mixtures. For example, an antiplasmodial active compound may be cytotoxic, but could be diluted in a crude extract to the extent that cytotoxicity is not detected. Alternatively, the crude extract may contain compounds that are cytotoxic, but are not responsible for antiplasmodial activity of the mixture. For these reasons, in the past, cytotoxicity screening was left for when compounds were purified or close to pure (Peternel *et al.*, 2009). However, this led to late toxicology identification and increased drug attrition rates, which could have been avoided by earlier cytotoxicity screening (Kola and Landis, 2004). Therefore, in this study cytotoxicity screening was employed at every major purification step.

To better asses cytotoxicity, crude extracts, fractions, and pure compounds were tested against three different cell types. The first was the Chinese Hamster Ovary (CHO) cell line, an epithelial cell line derived from the ovary cells of Chinese hamsters (Lai *et al*., 2013). CHOs are widely used in cytotoxicity experiments during drug discovery and development projects. The second cell line tested was the HepG2 line, a human liver cancer cell line (Miret *et al*., 2006).

Cell viability was determined by the colorimetric 3-*(*4,5-dimethylthiazol-2-yl*)*-2,5-diphenyl tetrazolium bromide (MTT) assay (Mosmann, 1983). This assay measures mitochondrial enzyme activity, such as succinate dehydrogenase, as a measure of cell viability (Stone *et* al., 2009). In this assay, MTT is reduced to a purple formazan crystal by NADH in viable cells, and the colour change can be measured spectrophotometrically (Mosmann, 1983; Aslantürk, 2018). Higher levels of cell viability generate a greater absorbance measurement.

Lastly, cytotoxicity was also tested against human erythrocytes (O^+). Although uncommon, some compounds display toxicity specific to erythrocytes, an effect known as haemotoxicity (Ziegler *et al.*, 2002; Jilani *et al*., 2013). In these cases, the pLDH assay will a yield positive

results, but the mechanism of action of the tested compound is deprivation of the parasite of its host environment due to inhibition of the erythrocyte. This is a false-positive results and would lead to toxic host side effects if the tested compound was developed further. To measure haemotoxicity, an in-house assay was developed. This assay is relatively simple, in that it is a modified version of the pLDH assay. Uninfected blood was used instead of parasitized red blood cells. The experimental set-up was the same as the pLDH assay (i.e. complete medium was used to dilute drug samples and to make up haematocrit, the uninfected haematocrit was kept to 1% as per the pLDH assay etc). These conditions were maintained to obtain results that could be directly compared to antiplasmodial readings. Therefore, if similar results were obtained from both assays, antiplasmodial activity could be attributed to haemotoxicity, rather than selective action against the *P. falciparum* parasites.

The ultimate goal of natural-product screening programs is not to identify the perfect candidate, but rather generate a list of potential hit compounds that can be chemically modified and improved during later drug development (Bugelski *et al.*, 2000; Peternel *et al.*, 2009). By running cytotoxicity screening in parallel with antiplasmodial screening, one can identify very toxic compounds early on and identify compounds that may be less potent, but safer. These compounds could theoretically be dosed at a higher concentration to improve their selective effect.

The aim of this investigation was to:

- Grow selected actinobacterial strains in liquid media until sufficient cell mass was produced.
- Extract the broth and cell mass of each actinobacterial strain.
- Determine and evaluate the antiplasmodial efficacy of each crude extract against the drug-sensitive strain of *P. falciparum*, NF54.
- Determine and evaluate the *in vitro* cytotoxicity of selected candidates against the Chinese Hamster Ovary, HepG2 cell lines, and their haemotoxicity against human erythrocytes.

2.2 Methodology

2.2.1 Cultivation of Actinobacteria

Spore suspensions or 15% (*v/v*) glycerol stock solutions were used to inoculate 15 mL of liquid medium in a 250 mL Erlenmeyer flask, and incubated with shaking at 25 oscillations per minute at 30°C for 4–6 days. If sufficient growth had occurred during this time, the entire culture was used to inoculate 100 mL of the same liquid medium in a 1 L Erlenmeyer flask, which was incubated for 10–14 days at 30°C with shaking at 25 oscillations per minute.

Four different liquid media were used depending on the strain tested. These were yeast extract-malt extract medium (International *Streptomyces* Project medium 2; ISP-2) (Shirling and Gottlieb, 1966), DSMZ (German Culture Collection) medium #553 (German Culture Collection, 2007), Hacène's Medium (HM) (Hacène and Lefebvre, 1995) and Japan Collection of Microorganisms (JCM) medium #61 (Ara and Kudo, 2007). All media were autoclaved before use to ensure sterility. Before inoculation, upscaling, and extraction, the purity of the culture was determined by streaking for single colonies on agar plates and by Gram staining (Bartholomew and Mittwer, 1952; Shirling and Gottlieb, 1966).

2.2.2 Culture Extraction

Once sufficient cell mass was obtained, the secondary metabolites could be extracted from the actinobacterial cultures. After culture purity was checked, the filamentous cell mass was separated from the culture medium (broth) by filtration through two coffee filters (size 1 x 4, House of Coffees, South Africa). The broth fraction was extracted by liquid-liquid extraction, where the broth (approximately 100 mL) was mixed with 30 mL of EtAc (≥ 98%, Merck, Darmstadt, Germany) and left to stand in a separating funnel at room temperature for 60 minutes. The EtAc was removed and the broth was extracted with a second 30 mL of EtAc. The two EtAc layers obtained were pooled and allowed to stand in a separating funnel overnight. This separated any remaining water and emulsified layers from the EtAc layer. The EtAc layer was collected and allowed to dry in a glass beaker in a fumehood.

The cell mass was mixed with 5 mL of MeOH (>99%, Kimix Chemical and Lab Supplies, Cape Town, South Africa) and 50 mL of EtAc. The cell mass and solvents were mixed by gentle agitation in a Schott bottle on a Labnet™ Orbit 1000 multipurpose shaker at 120 rpm for 60 minutes. The solvent was separated from the cell mass by filtration through two coffee filters. Another 50 mL of EtAc was added to the extracted cell mass and the extraction process was repeated. The two cell mass EtAc extracts were pooled and allowed to dry in a glass beaker in a fumehood.

The broth and cell mass dried extracts were re-dissolved in 1 mL each of EtAc and transferred into a clean pre-weighed plastic benchtop tube (Inqaba Biotec, Pretoria, South Africa). One millilitre of MeOH was then added to each glass beaker to dissolve remaining compounds and transferred into a separate clean pre-weighed plastic benchtop tube. Based on the calculated mass of each crude extract, the concentration of each solution was adjusted to 2 mg/mL with the same solvent used to prepare the solution. This produced four crude extracts per strain: broth EtAc, cell mass EtAc, broth MeOH and cell mass MeOH.

2.2.3 *Plasmodium falciparum* Cultivation

The culture medium was made with 10.4 g/L RPMI 1640 (with glutamine and without $NaHC0_3$), 4 g/L glucose, 6 g/L Hepes buffer, 0.088 g/L hypoxanthine, 5 g/L albumax, and 102 ml/L (0.05 g/L) gentamicin (Sigma-Aldrich, South Africa). The medium was filtered twice, first with 0.45 µm filters followed by filtration with 0.22 µm filters. Complete medium (CM) was made by adding 8.4 ml of 5% bicarbonate per 200 ml culture medium.

The drug-sensitive strain of *P. falciparum*, NF54 was obtained from the Malaria Research and Reference Reagent Resource (MR4) depository (Dowler, 1995). *P. falciparum* was continuously cultured in human O^+ erythrocytes as described by Trager and Jensen (Trager and Jensen, 1976). Human blood, donated by anonymous donors, was obtained from the Western Cape Blood Service (Cape Town, South Africa). Cultures were centrifuged at 700 x *g* for 3 minutes, the resultant supernatant was aspirated, and a thin blood smear made.

Smears were fixed with MeOH, stained with 10% Giemsa stain and left to stand for 5 minutes. Parasitaemia was estimated and blood-stage determined via light microscopy. The parasitaemia was calculated as the ratio of parasitized erythrocytes to uninfected erythrocytes. The

parasitaemia of each culture was estimated by counting 500-700 cells at 1000 X magnification. If cells were predominantly in the mature trophozoite phase, cultures were diluted to approximately 5% parasitaemia using red blood cells and 40 mL of CM.

If the culture was predominantly in the immature trophozoite phase (ring phase), it was subjected to sorbitol lysis to lyse mature trophozoites present and synchronise the culture. Mature trophozoite and schizont cells are more sensitive to changes in osmotic pressure than immature trophozoites, and thus sorbitol lysis ensures that only immature trophozoites are present and viable. Sorbitol lysis was conducted by adding 15 mL of 5% sorbitol, warmed to 37ºC, to the culture and leaving it to stand for 10 minutes. Afterwards, the culture was centrifuged at 700 rcf for 3 minutes, the supernatant aspirated and 40 mL of CM was added.

Each culture was gassed with a mixture of 3% O_2, 4% CO_2 and 93% N_2 for 30–60 seconds in a sealed gassing chamber before incubation at 37°C.

2.2.4 Parasite Lactate Dehydrogenase Assay

The pLDH assay was performed according to a modified version of the method described by Makler *et al.* (1993). All crude extracts were weighed to 3 decimal places using an accurate mass balance and diluted to a stock concentration of 20 mg/mL. Crude extract and stock samples were diluted in CM, and the starting concentration was adjusted depending on the sample. However, during the initial screening of actinobacteria for antiplasmodial activity, crude culture extracts were tested at a starting concentration of 5 µg/mL. One hundred microlitres of CM was added to every row of a 96-well titration plate except row 3. Two hundred microliters of the test sample was added in quadruplicate to row 3. The sample was then serially diluted 2-fold from rows 3–12 to generate a concentration gradient.

Only cultures of mature trophozoites were used. Cultures were counted (section 2.2.3) and diluted to a 2% suspension using CM, uninfected red blood cells, and parasitized red blood cells. One hundred microlitres of a 2% haematocrit solution served as a blank and was added to row 1. One hundred microlitres of the 2% parasitaemia suspension was added to row 2 and served as a positive control for parasite growth. One hundred microlitres of 2% parasitaemia was then added to each well in rows 3–12. Ten millilitres of the 2% parasitaemia suspension was required per 96-well plate tested. The final volume of each well was 200 µL and the final

parasitaemia was 1%. Each plate was covered with a lid, labelled and placed in a gassing chamber.

The chamber was sealed and gassed for 2 minutes with a mixture of 3% O_2, 4% CO_2 and 93% N_2. The chamber was incubated at 37ºC for 48 hours, one full blood stage lifecycle. After incubation, the red blood cells in the plates were lysed by freezing at -80°C for 1 hour, followed by thawing at 37°C. Next, the contents of each well were thoroughly resuspended with an automatic pipette to ensure each sample was homogenous.

Malstat lysis buffer was prepared by adding 400 µL Triton*100, 4 g of L-lactate, 1.32 g tris(hydroxymethyl)aminomethane (Tris) buffer, 22 mg of APAD and the solution was adjusted to a pH of 9 in 200 mL Millipore water (Sigma-Aldrich, South Africa).

One hundred microlitres of Malstat lysis buffer was added to each well on a new plate, and 15 µL of each test sample was transferred to the corresponding well on the new plate. The new plates were left to stand for 30 minutes to ensure complete lysis of all the parasite cells in each well and thus an accurate reading. Bubbles were removed from the new plate by drying them with a hairdryer prior to reading. Bubbles interfere with absorbance readings and must be removed. Afterwards, 25 µL of NBT was added to each well.

NBT was made by adding 160 mg NBT and 8 mg phenazine ethosulphate to 100 mL H_2O. The plates were kept in a cupboard until they had fully developed, as NBT is light sensitive. Once developed, the absorbance was measured at 620 nm using a Turner BioSystems, Inc. Modulus™ II Microplate Reader. Nonlinear regression analysis of the data on the GraphPad PRISM version 4.00 program was used to determine the concentration of compound required to inhibit the absorbance signal by 50% (Maron *et al.*, 2016). This value is known as the half maximal inhibitory concentration (IC_{50}) and represents the concentration of the tested compound required to inhibit the growth of half of the population of the tested cell type.

Chloroquine and artesunate were used as positive controls in each pLDH assay, as they are well described antimalarial compounds. The acceptable ranges of chloroquine's and artesunate's IC_{50}s were considered to be 2–10 ng/mL and 0.5–8 ng/mL, respectively. If either of the controls displayed activity not within the selected ranges, the results were discarded, and the experiment repeated. Factors such as incorrect parasitaemia calculation, culture contamination or gas chamber leaks could cause these assay failures.

2.2.5 Cultivation of Cell Lines

Both cell lines (CHO and HepG2) were continuously cultured by Mrs Sumaya Salie and Mr Virgil Verhoog at the Division of Clinical Pharmacology, Department of Medicine at the University of Cape Town.

CHO cells were cultured continuously in cell-culture medium consisting of 10% foetal calf serum (FCS, Celtic Molecular Diagnostics, Mowbray, South Africa) 45% Dulbecos Modified Eagles Medium (DMEM, Highveld Biologicals, Lyndhurst, South Africa) and 45% HAMS-F12 medium ((1:1), Sigma, St Louis, MO, USA). HepG2 cells were cultured in 90% DMEM and 10% foetal calf serum. Both cell lines were kept in gas flow incubators at 37ºC, 5% CO_2. Cells were subcultured in preparation for cytotoxicity assays, with only confluent cultures selected. Confluency of cells was checked periodically via microscopy, and if cultures were not confluent the medium was changed.

If the cells were confluent, the medium present was poured off, and flasks were rinsed twice with 10 mL of sterile phosphate buffered saline (PBS). A 0.25% trypsin solution was warmed to 37ºC and added to the washed flasks. Trypsin is a protease that degrades the anchoring proteins causing cells to lift from the flask's surface. The flasks were incubated with trypsin for 2 minutes and agitated slightly to lift cells. Care must be taken, as the cells must not be incubated with the trypsin for too long, to avoid extensive degradation. Once it was determined that all cells had lifted (via light microscopy), 5 mL of cell medium was added to inhibit the trypsin. The flasks contents were then transferred into a 50 mL centrifuge tube and centrifuged for 3 minutes at 700 rpm. The supernatant was poured off, and the resultant pellet was resuspended in 5 mL cell medium.

2.2.6 MTT Assay

Cytotoxicity assays were conducted by Mrs Sumaya Salie and Mr Virgil Verhoog at the Division of Clinical Pharmacology, Department of Medicine at the University of Cape Town.

Twenty microlitres of the selected confluent cell culture was transferred into a benchtop centrifuge tube and mixed with 20 µL of 1% crystal violet dye for cell counting. All of the

mixture was placed in a counting chamber, and the number of cells was counted via light microscopy. From the count, the cell concentration was determined, and a dilution was made to obtain a standard cell concentration of 10^5 cells/mL. Fifteen millilitres of the diluted cell suspension was used per plate. One hundred microlitres of cell suspension was added to each well in rows A–G of a 96 well plate. One hundred microlitres of cell medium was then added to the same wells in rows A–G. Two hundred microlitres of cell medium was added to each well in row H, which served as a blank. The plates were incubated at 37ºC for 24 hours.

Cells were checked by microscope to ensure that they had attached to the bottom of each well. Each test sample and control was diluted to generate 6 concentrations of 200, 20, 2, 0.2, 0.02, and 0.002 µg/mL. The medium was carefully aspirated from each well so that only a thin layer was left covering the cells. Two hundred microlitres of cell medium was added to each well in rows G and H. Row G served as the positive control for MTT reduction and therefore cell growth. One hundred microlitres of each drug dilution was added in triplicate to separate rows, starting with row E. One hundred microlitres of cell medium was added to each well in rows A–E. This generated a total volume of 200 µL in each well with a compound concentration range of 100–0.001 µg/mL. Plates were covered and incubated in gas flow incubators at 37ºC, 5% CO_2 for 48 hours.

After incubation, plates were developed by adding 25 µL of sterile MTT to each well and further incubated for 4 hours at 37ºC. Plates were centrifuged at 200 rpm for 10 minutes, and the medium was aspirated off. One hundred microlitres of dimethyl sulfoxide (DMSO) was added to dissolve the MTT formazan derivative, and the plates were softly agitated for 2 minutes to ensure a homogenous mixture. The plates were then read at 540 nm using a Turner BioSystems, Inc. Modulus™ II Microplate Reader. The data were analysed by nonlinear regression analysis using the GraphPad PRISM version 4.00 program to determine the IC_{50} of each compound. Once the IC_{50} has been calculated the selectivity index (SI), can be determined. The SI is the ratio of a compound's cytotoxicity vs its antiplasmodial efficacy and is calculated using the equation below:

$$\text{Selectivity Index (SI)} = \text{Cytotoxicity } (IC_{50}) / \text{ Antiplasmodial Efficacy } (IC_{50})$$

Emetine was used as a cytotoxicity control, and the acceptable IC_{50} range was set as less than 30 ng/mL against both the CHO and HepG2 cell lines. If emetine did not display acceptable

cytotoxicity, the results were discarded, and the assay repeated. Incorrect cell counting or contamination could cause these results.

2.2.7 Haemotoxicity Assay

An in-house assay was developed to determine haemotoxicity by measuring the absorbance of haemoglobin present after 1% haematocrit was exposed to test samples for 48 hours. Haemotoxic compounds can cause apoptosis or disrupt the membrane of erythrocytes, which increases the amount of haemoglobin released into the environment (Hayter *et al.*, 2014). Haemoglobin has a unique absorbance profile and absorbs light at 540 nm and 575 nm. This allows the amount of haemoglobin to be measured spectrophotometrically. Triton X-100 was used as a positive control for erythrocyte lysis. Triton X-100 is a non-ionic surfactant used to lyse cells for protein extraction or to permeabilize cell membranes (Borner *et al.*, 1994).

Human blood (O^+) donated by anonymous donors, was obtained from the Western Cape Blood Service (Cape Town, South Africa). Ten millilitres of 2% haematocrit solution was made up per plate tested. Complete medium (CM) (section 2.2.3) was used to dilute all samples and test solutions. One hundred microlitres of CM was added to each well except row F. Drugs were diluted to 200 µg/mL in CM. Two hundred microlitres of each sample was added to row F in triplicate. The samples were then serially diluted two-fold to produce a concentration gradient of 100–0.001 µg/mL from row A–F. A 2% solution of Triton 100 was made up in CM, and 100 µL was added to each well in row G. One hundred microlitres of the 2% haematocrit was added to each well to generate a final haematocrit of 1%, the same concentration tested in the pLDH assay (section 2.2.4). Row H consisted of only erythrocytes in CM to act as a blank and negative control for erythrocyte lysis. After incubation for 48 hours at 37°C, the plates were centrifuged at 200 rpm for 10 minutes. One hundred microlitres of the supernatant was transferred from each well to the corresponding wells in a clean 96 well plate. Care was taken not to disturb the pellet when transferring the supernatant. The absorbance was measured at 540 nm and 575 nm using a BMG Labtech® FLUOstar Omega multi-mode microplate reader. The data were analysed using nonlinear regression analysis in the GraphPad PRISM version 4.00 program to determine the IC_{50} of each compound.

2.3 Results and Discussion

Each crude culture extract sample was tested at a starting concentration of 5 µg/mL. If inhibition greater than 50% was seen in all test rows, further studies, at lower starting concentrations, were conducted in certain cases, depending on the amount of extract available. Thirty-one actinobacterial strains were tested for antiplasmodial activity against the drug-sensitive *P. falciparum*, NF54 during this investigation (Table 2.1). Fourteen strains showed antiplasmodial activity against NF54 (Table 2.2).

Table 2.1: Antiplasmodial activity of actinobacterial strains against *P. falciparum*, NF54, N=1 biological repeat with 4 technical repeats.

Strain Name	Growth Medium	Antiplasmodial activity against *P. falciparum*, NF54
Actinomadura napierensis strain B60^T	ISP-2	+
Actinomadura rudentiformis strain HMC1^T	ISP-2	-
Amycolatopsis roodepoortensis strain M29^T	ISP-2	-
Amycolatopsis speibonae strain JS72^T	ISP-2	-
Gordonia lacunae strain BS2^T	ISP-2	-
Kribbella karoonensis strain Q41^T	ISP-2	-
Kribbella swartbergensis strain HMC25^T	ISP-2	-
Kribbella strain SK5	ISP-2	-
Micromonospora strain RS10	DSMZ #553	-

+ antiplasmodial activity with IC_{50} < 5 µg/mL was observed ,

- antiplasmodial activity with IC_{50} > 5 µg/mL was not observed.

Table 2.1 (continued): Antiplasmodial activity of actinobacterial strains against *P. falciparum*, NF54, N=1 biological repeat with 4 technical repeats.

Strain Name	Growth Medium	Antiplasmodial activity against *P. falciparum*, NF54
Nocardia gamkensis strain CZH20^T	ISP-2	-
Nonomuraea candida strain HMC10^T	JCM #61	+
Streptomyces strain CS1	JCM #61	-
Streptomyces strain CS12	JCM #61	-
Streptomyces strain CS18	JCM #61	-
Streptomyces strain CS3	DSMZ #553	-
Streptomyces strain CW2	DSMZ #553	+
Streptomyces strain CW5	JCM #61	+
Streptomyces strain L2	ISP-2	+
Streptomyces speibonae strain PK-Blue^T	HM	+
Streptomyces strain PR3	ISP-2	+
Streptomyces strain PR10	ISP-2	+
Streptomyces strain RS3	DSMZ #553	+
Streptomyces strain RS6	DSMZ #553	-
Streptomyces strain RS7	DSMZ #553	+
Streptomyces strain RS9	DSMZ #553	-
Streptomyces strain RS13	DSMZ #553	+
Streptomyces strain RS15	DSMZ #553	+
Streptomyces strain RS18	DSMZ #553	-
Streptomyces strain RS19	JCM #61	+
Streptomyces strain UK1	HM	+
Streptomyces strain UK2	ISP-2	-

+ antiplasmodial activity with IC_{50} < 5 µg/mL was observed ,

- antiplasmodial activity with IC_{50} > 5 µg/mL was not observed.

Table 2.2: Antiplasmodial activity of each active actinobacterial strain, N=1 biological repeat with 4 technical repeats.

Strain Name	Antiplasmodial activity against *P. falciparum*, NF54 IC_{50} (ng/mL)			
	Broth (EtAc)	Broth (MeOH)	Cell Mass (EtAc)	Cell Mass (MeOH)
Actinomadura napierensis strain B60^T	< 312	> 5000	> 5000	> 5000
Nonomuraea candida HMC10^T	2296	>5000	>5000	3269
Streptomyces strain CW2	40	< 125	311	> 5000
Streptomyces strain CW5	128	< 312	> 5000	> 5000
Streptomyces strain L2	>5000	> 5000	2648	> 5000
Streptomyces speibonae strain PK-Blue^T	1333	> 5000	196	> 5000
Streptomyces strain PR3	110	147	80	2370
Streptomyces strain PR10	< 125	< 125	< 125	< 125
Streptomyces strain RS3	> 5000	3270	> 5000	> 5000
Streptomyces strain RS7	70	< 312	21	< 312
Streptomyces strain RS13	4493	> 5000	> 5000	> 5000
Streptomyces strain RS15	2293	> 5000	1631	2000
Streptomyces strain RS19	1933	2722	> 5000	> 5000
Streptomyces strain UK1	> 5000	> 5000	174	> 5000

* Strains that showed antiplasmodial activity suitable for further study are marked in red.

To simplify data presentation, the mean values of the positive controls (chloroquine and artesunate), from each pLDH assay done when screening the filamentous actinobacteria, are displayed separately (Table 2.3). The raw data for each experiment is displayed in a supplementary chapter (Table 8.1, Appendix). The controls were within the acceptable ranges for all screening experiments.

Table 2.3: Mean antiplasmodial activity of the positive controls, chloroquine and artesunate, obtained from the filamentous actinobacteria screening experiments, N=18 biological repeats with 4 technical repeats.

Control	Antiplasmodial activity against *P. falciparum*, NF54 IC_{50} (ng/mL)
Chloroquine	5.4 ± 1.4
Artesunate	4.1 ± 1.3

To ensure solvent toxicity was not responsible for the antiplasmodial activity measured, 100% solutions of EtAc and MeOH were diluted in CM in the same manner as the crude extracts, i.e. from 2 mg/mL stock concentration to 5 µg/mL test concentration. This correlates to a final concentration of 0.25% (*v/v*) and each diluted sample was tested for antiplasmodial activity (section 2.2.4). No antiplasmodial activity at 0.25% (*v/v*) or less, was seen in the solvent blanks (Table 8.2, Appendix). Therefore, the activity observed is solely due to compounds present in the crude extracts. The controls were within the acceptable ranges.

Initial screens revealed a relatively high number of hits, 14 of the 31 actinobacterial strains screened showed antiplasmodial activity with IC_{50}s less than 5 µg/ml. Twelve of the 14 active strains belong to the genus *Streptomyces.* Despite the focus on their antibacterial and antifungal capabilities, there are many examples of antimalarials from *Streptomyces*. The anticancer trioxacarcin series, isolated from *Streptomyces ochraceus* and *Streptomyces bottropensis*, were shown to be potent antiplasmodial compounds (Maskey *et al.*, 2004). Triacsin C and D, two acetyl-CoA synthetase inhibitors isolated from *Streptomyces aureofaciens*, were shown to be potent antiplasmodial agents (Yoshida *et al.*, 1982; Ahmad *et al.*, 2017). One of the most recent antimalarials described from *Streptomyces* was gancidin W, isolated from *Streptomyces* strain SUK10 (Zin *et al.*, 2017). The bafilomycins, munumbicins and coronamycins also represent antimalarials isolated from *Streptomyces* species (Jensen *et al.*, 2002; Ezra *et al.*, 2004; Castillo

et al., 2006; Ahmad *et al.*, 2017). These compounds have unique structures with different mechanisms of action.

There were few hits from the rarer actinomycetes, with only *A. napierensis* B60^T and *N. candida* HMC10^T displaying antiplasmodial activity. This is not the first time antiplasmodial activity has been seen in *Actinomadura* and *Nonomuraea* species. For example, kijanimicin was isolated from *Actinomadura kijaniata* strain SCC 1256 and displays potent antimalarial activity against *Plasmodium berghei in vivo* (Waitz *et al.*, 1981). The antibiotic simaomicin A, produced by *Actinomadura madurae* subsp. *simaoensis*, was also shown to possess antimalarial activity (Carter *et al.*, 1989; Ui *et al.*, 2007). Maduramicin, isolated from *Actinomadura rubra* strain ATCC 27031^T, was shown to be a potent antiplasmodial agent, which acts on an ion transport mechanism in *P. falciparum* gametocytes (Fleck *et al.*, 1978; Maron *et al.*, 2016). Antibiotics affecting ion transport represent a new mechanism of action for antimalarials (Maron *et al.*, 2016). *Nonomuraea rhodomycinica* NR4-ASC07^T was shown to produce two compounds with weak activity against *P. falciparum in vitro* (Supong *et al.*, 2018).

As a relatively small number of strains were screened, it is difficult to assess the antiplasmodial potential of the filamentous actinobacteria overall. The relatively high hit rate observed in this work does, however, suggest that they are a good source of antiplasmodial compounds and further screening is warranted. This is supported by the literature on actinobacterial antimalarial compounds.

The second aim of the investigation was to isolate the active compounds and identify them to determine if they are novel antiplasmodial compounds. This is a step towards revealing if the actinobacteria produce antiplasmodial agents that can be developed into effective, novel antimalarials drugs. It was not within the scope of this investigation to isolate each active compound from all the active extracts. Therefore, the best candidate was selected for further investigation based on its antiplasmodial efficacy.

While the crude actinobacterial broth extracts were screened at 5 µg/mL, only extracts that displayed IC_{50}s of 1 µg/mL or less were considered for further study. This is, according to many authorities on antimalarial drug development, such as Medicines for Malaria Venture (MMV), Drugs for Neglected Disease initiative (DNDi), and the Bill and Melinda Gates Foundation a good target value for initial antiplasmodial activity screening (Pink *et al.*, 2005; Wells, 2011; Katsuno *et al.*, 2015). The same authorities state that pure compounds need to be active against both drug-sensitive and resistant strains of *P. falciparum* at a concentration of

100 ng/mL or less. These efficacy targets need to be strict for a few reasons. Firstly, few compounds are present in patients at concentrations near 1 µg/mL for a significant amount of time (Wells, 2011). Therefore, to be clinically relevant, compounds must be effective at lower concentrations. Secondly, as the efficacy cut off value is lowered, there are fewer chances of random, non-specific interactions within or between cells which reduces the chance of toxic off-target effects (Hann *et al*., 2001). Generally there are a high number of *in vitro* hits reported against *P. falciparum*, but very few molecules can be developed further (Katsuno *et al.*, 2015). Thirdly, as the drug discovery and development pipeline is an expensive and timely process, by setting stringent *in vitro* requirements more time and resources can be assigned to hit candidates that have a better chance of being developed further.

Considering these guidelines, the strains that displayed sufficient antiplasmodial activity to be considered for further investigation were; *Actinomadura napierensis* strain B60^{T}, *Streptomyces* strain CW2, *Streptomyces* strain CW5, *Streptomyces* strain RS7, *Streptomyces speibonae* strain PK-Blue^{T}, *Streptomyces* strain PR3, *Streptomyces* strain PR10, and *Streptomyces* strain UK1 (highlighted in Table 2.2).

Under the criteria set by MMV, DNDi, and the Bill and Melinda Gates Foundation, the minimum selectivity index (SI) of a compound should be 10 minimum (Pink *et al.*, 2005).

Before selection for further study, the most active crude extract of strain PR3 (cell mass EtAc fraction) was tested for cytotoxicity and haemotoxicity (sections 2.2.6 and 2.2.7 respectively) (Table 2.5). The crude extracts of strain PR3 displayed no cytotoxicity up to 100 µg/mL against the CHO or HepG2 cell line nor any haemotoxicity against human erythrocytes. The cytotoxicity displayed by the control (emetine) was within the acceptable range.

2.4 Conclusion

Due to its potent antiplasmodial activity, lack of cytotoxicity and lack of haemotoxicity, and ease of cultivation, strain PR3 became the focus of this study. It should be noted that strain PR3 was selected as the lead strain very early on in the investigation. Further screening of new strains for antiplasmodial activity continued in parallel to the purification of strain PR3's active compounds, to better evaluate the antiplasmodial potential of the actinobacteria. Additionally, strains that showed the required antiplasmodial efficacy for further study were kept in reserve

in case any problems were encountered with strain PR3 (e.g. the strain stopped producing its active compounds) and for future studies.

Table 2.4: Mean antiplasmodial activity, cytotoxicity, and haemotoxicity of strain PR3's cell mass EtAc fraction, N=2 biological repeats with 4 technical repeats

Sample	Antiplasmodial activity against *P. falciparum* NF54 IC_{50} (ng/mL)	Cytotoxicity against Chinese Hamster Ovary IC_{50} (µg/mL)	Cytotoxicity against HepG2 IC_{50} (µg/mL)	Haemotoxicity Human Erythrocyte IC_{50} (µg/mL)	Selectivity Index (Cell IC_{50}/ NF54 IC_{50})
Strain PR3 Cell Mass EtAc Fraction	90.0 ± 13	> 100	> 100	> 100	> 1250
Emetine	-	0.0012 ± 0.0002	0.002 ± 0.00011	-	-

3 Bioassay-Guided Fractionation of the Crude Culture Extracts of *Streptomyces* strain PR3

Abstract

Bioassay-guided fractionation principles were followed to purify and isolate the antiplasmodial compounds produced by *Streptomyces* strain PR3. The cultivation and extraction processes were improved to increase the yields obtained from strain PR3. A variety of techniques, such as solid phase extraction and high performance liquid chromatography, were employed to purify and isolate the active antiplasmodial compounds. High resolution mass spectrometry and nuclear magnetic resonance spectrometry were used to estimate the purity of the isolated compounds. During bioassay-guided fractionation, two contaminants, compounds 540 and 870, were mistakenly identified as the highly active compound produced by *Streptomyces* strain PR3. During method development compound 540 disappeared for unknown reasons, however compound 870 presented unique proton nuclear magnetic resonance and mass spectra and a two-step, reproducible SPE method was developed to purify it.

3.1 Introduction

After selecting *Streptomyces* strain PR3 as a candidate producer of antiplasmodial compounds, the next goal was the isolation and purification of its antiplasmodial compounds by bioassay-guided fractionation. Bioassay-guided fractionation is a general concept, also known as activity guided/directed fractionation or bioactivity screening (Weller, 2012). It involves the separation of the molecules in a complex mixture and the association of a fraction or compound, with biological activity at each step of the purification process. Multiple separation steps are often required to achieve purification of the biologically active compound. Once purified, the compound of interest is identified and characterised. Bioassay-guided fractionation can be used in many different fields, including environmental analysis, toxicology, and natural products screening.

The goal of the separation steps is to avoid the simultaneous presence of multiple different compounds in the biologically-active fraction (Weller, 2012). Chromatographic techniques are the standard methods when it comes to separating complex mixtures. In chromatography, molecules are separated by their affinity between two layers, a stationary phase and a mobile phase (Coskun, 2016). The two phases have contrasting physiochemical properties, such as polarity or charge. The different affinity of each compound, in the mixture, for these phases leads to their separation. Two different types of chromatographic techniques are used: normal phase, where the stationary phase is polar and the mobile phase is non-polar, and reverse phase, where the stationary phase is non-polar, and the mobile phase is polar.

The most widely used method of separation is liquid chromatography (LC), where a liquid sample is injected into liquid mobile phases, then passed through a solid stationary phase column (Coskun, 2016). Examples of LC are counter current chromatography (CCC), solid phase extraction (SPE) and high performance liquid chromatography (HPLC). In CCC, a liquid phase is held in place by centrifugal force in the column and interacts with the injected sample and other liquid phase (Berthod *et al.*, 2009). In SPE, samples in solution are added to a solid stationary phase cartridge, and the mobile phase is passed through the cartridge at set volumes and concentrations in individual wash steps. Comparatively, in HPLC, pumps continuously wash mobile phase through the stationary phase column. An HPLC method can make use of a gradient, where the concentration of the components of the mobile phase changes over time, or isocratic, where the conditions are maintained throughout the method. LC conveys several advantages over other techniques. First, it can be automated and run repeatedly for long periods of time (Weller, 2012). Second, it can be coupled to fraction collectors, autosamplers, and detectors. This allows real-time tracking and identification of compounds of interest. However, LC also presents a number of challenges. Synergistic compounds can be missed due to intensive separation, volatile or labile samples may be lost, and the cost of equipment and solvents can be substantial.

The principle method of detection at each separation step is biological activity. However, biological activity does not provide structural data and often cannot be used in real time. For example, the pLDH assay, used to determine antiplasmodial activity, requires a minimum of three days to produce a result and uses a moderate amount of material. A better method of detection is correlating a physiochemical signal to the active fraction. This signal could be a mass to charge ratios (*m/z*), ultraviolet-visible light (UV-Vis) or infrared (IR) absorbance. This signal can be used to track the putative active compound(s) while enough material is collected

for further separation or elucidation. Care must be taken as the signal may not be from the active compound, but an impurity. To avoid collecting the incorrect sample, biological activity must be confirmed intermittently during collection and reproducibly measured at the beginning of each new separation step.

When it comes to analysing small molecules in complex systems, the best analytical instrument available is a mass spectrometer (Cooke, 2003). Mass spectrometers detect ions based on their mass to charge ratios and broadly consist of three components. The first is the ioniser where the sample is vaporised and ionised, the second is the mass analyser which separates the ions based on their *m/z*, and the final component is the detector which measures the intensity of each ion. There are many different types of mass spectrometers that can analyse different samples. The most common types are triple quadrupoles, quadrupole ion traps, and time of flight (TOF) instruments. Quadrupoles are mass analysers consisting of two pairs of electricity-conducting rods that stabilise ions with selected *m/z*'s, when specific radio frequencies and direct currents are applied. Triple quadrupoles are made up of three sets of quadrupoles which allows them to perform full ion scans, single ion monitoring (SIM), neutral loss, precursor, and tandem scans (Cooke, 2003). In tandem mass spectrometry (MS/MS), a fragmentation chamber and second mass analyser are utilised. Compounds are separated by their *m/z* in the first mass analyser, then fragmented by bombardment by inert gases, such as N_2, in the fragmentation chamber. These molecular fragments can then be analysed in the second mass analyser, providing more in-depth structural information about the sample and be used to separate molecules with the same parent *m/z*. An ion trap is a series of electrodes that concentrates ions of selected *m/z*'s (Cooke, 2003). Selected ions are then released to the detector by applying specific voltages to destabilise their orbits. This increases the sensitivity of the instrument as ions present in small amounts can be accumulated. TOFs involve accelerating a set of ions through a mass analyser at the same energy. The time taken for each ion to reach the detector is measured and can be used to calculate an *m/z*. For example, heavier ions take longer to reach the detector. TOF instruments are more selective than other systems, which allow them to identify the exact mass of an ion and its fragments to four or more decimal points. This allows ions to be distinguished from other molecules with very similar masses. This is known as high resolution mass spectrometry (HRMS). A quadrupole can be coupled to TOF systems to fragment ions and increase selectivity even further. Mass spectrometers offer advantages over other detection methods in terms of improved selectivity and sensitivity and can be coupled to LC systems

with ease (Wolfender, 2009). However, these methods are destructive, and the equipment is very expensive.

A common detector option that is non-destructive and suitable for unknown samples is ultraviolet-visible (UV-Vis) light detectors (Wolfender, 2009). UV-Vis detectors measure the absorbance of UV-Vis light (10–700 nm) by chromophore structures in a sample. Different chromophores absorb different wavelengths, which can be used to determine the identity of the sample. For example, the flavonoids absorb light at 350 nm (Hasler *et al* ., 1992). However, this technique relies on the presence of chromophores in a sample and suffers from lower sensitivity and selectivity compared to that of mass spectrometry.

There are many other detector options, such as fluorescence and IR absorbance. Due to the structural diversity of natural products, there is no standard detection method for all molecules, and a range of detectors needs to be used (Adnani, *et al* ., 2012). Once purified, the structure of the active compound needs to be elucidated so that it can be determined whether it is a known or novel molecule. This is achieved using HRMS and nuclear magnetic resonance (NMR) analysis. These techniques are discussed in more detail in Chapter 4.

The aims of this investigation were to:

1. Improve the cultivation conditions and extraction protocol of *Streptomyces* strain PR3, to increase the amount of active material produced.
2. Develop a purification method for isolating the active antiplasmodial compound(s) produced by *Streptomyces* strain PR3. This method had to be reproducible and involve as few steps as possible.

A wide array of methods were used during this stage of the investigation. An overview of the method development process is displayed in Figure 3.1.

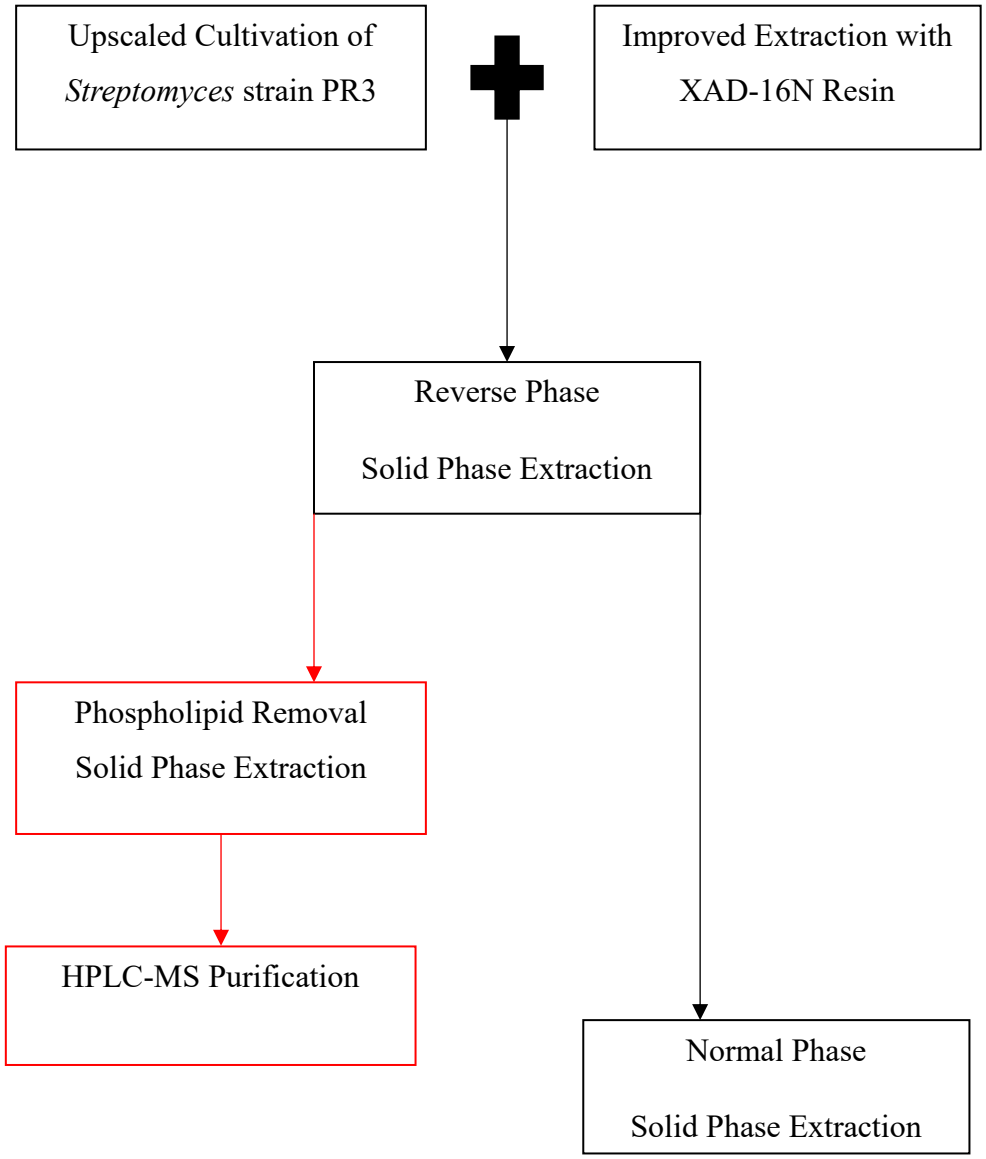

Figure 3.1: Overview of the purification method development. Red lines and arrows represent unsuccessful purification techniques. Black lines and arrows represent successful purification methods.

3.2 Methodology

3.2.1 Scaled Up Bacterial Cultivation

Streptomyces strain PR3 glycerol stocks (15%, *v/v*) were used to inoculate 15 mL of ISP-2 liquid medium in a 250 mL Erlenmeyer flask. The culture was incubated at 30°C with shaking at 25 oscillations per minute for 3–4 days. The entire culture was then used to inoculate 100 mL liquid ISP-2 medium in a 1L Erlenmeyer flask. This culture was incubated at 30°C with shaking at 25 oscillations per minute for 3–4 days. After this time, the entire culture was used to inoculate 1 L of ISP-2 liquid medium in a 5 L Erlenmeyer flask. This third culture was incubated at 30°C for 10 days with shaking at 25 oscillations per minute. The purity of each culture was assured, at each upscaling and inoculation step, by Gram staining and streaking for single colonies on agar plates (Bartholomew and Mittwer, 1952; Shirling and Gottlieb, 1966).

3.2.2 Modified Extractions

3.2.2.1 Extraction of Upscaled Culture

The bacterial cell mass was separated from the broth (culture medium) by filtration through two coffee filters. Fifty millilitres of methanol (MeOH) and 200 mL of ethyl acetate (EtAc) were added to the filtered cell mass, and the mixture was agitated on a Labnet™ Orbit 1000 multipurpose shaker at 120 rpm for 90 minutes at room temperature. The bacterial cell mass was separated from the solvent using two coffee filters, and the solvent was collected in a glass beaker. A second volume of 200 mL EtAc was added to the already-extracted cell mass and agitated on a Labnet™ Orbit 1000 multipurpose shaker at 120 rpm for a further 90 minutes at room temperature. The EtAc was separated from the cell mass by filtering through two coffee filters, the solvent was pooled with the first solvent wash (MeOH and EtAc) in the glass beaker, and the combined extracts were left to dry in a fume hood at room temperature.

The broth (spent culture medium), approximately 1 L, was shaken vigorously with 250 mL of EtAc in a 2 L separating funnel and left for 90 minutes at room temperature to allow the phases to separate. The EtAc and aqueous culture broth layers were collected in separate glass beakers.

The culture broth was extracted with a second 250 mL volume of EtAc, placed in the 2 L separating funnel, shaken vigorously and the phases were allowed to separate for 90 minutes at room temperature. The EtAc layer and broth layers were collected in separate glass beakers. The two EtAc fractions (culture broth extracts) were combined and placed in a clean 2 L separating funnel and left overnight at room temperature to allow separation of the EtAc from the residual aqueous component. The final EtAc fraction was collected in a glass beaker and allowed to dry in a fume hood at room temperature. The broth crude extract was redissolved in 5 mL of EtAc and transferred into clean pre-weighed plastic benchtop tubes.

3.2.2.2 XAD-16N Resin Extraction

Fourteen to sixteen hours before extraction of the strain PR3 culture, 50 g of XAD-16N was added to each 1 L culture, under nonsterile conditions. The XAD-16N resin consists of a styrene-divinylbenzene matrix with a mean pore size of 200 Å (Sigma, 1998). XAD-16N resin is non-polar and adsorbs organic materials from aqueous or polar systems. XAD-16N binds to molecules with small to medium molecular weights. These properties make it ideal for compound extraction from liquid bacterial cultures. After 14-16 hours, the culture and resin were filtered through coffee filters and the culture broth was discarded. Two hundred millilitres of MeOH was added to the filtered cell mass plus resin and agitated on a Labnet™ Orbit 1000 shaker at 140 rpm for 60 minutes at room temperature. The MeOH was then recovered by filtering through two coffee filters, and the MeOH was discarded.

Two hundred millilitres of EtAc was added to the cell mass plus resin and agitated on a Labnet™ Orbit 1000 shaker at 140 rpm for 90 minutes at room temperature. The EtAc was filtered from the cell mass and resin with two coffee filters and collected in a glass beaker. Another 200 mL of EtAc was added to the filtered cell mass plus resin and agitated on a Labnet™ Orbit 1000 shaker at 140 rpm for 90 minutes at room temperature. The EtAc was recovered (as before) and combined with the first EtAc wash in a glass beaker. The pooled EtAc fractions were left in a fume hood overnight to dry at room temperature. Each crude extract was redissolved in 20 mL of EtAc and transferred into a clean pre-weighed plastic benchtop tube.

3.2.2.3 Blank Extraction

The ISP-2 and JCM #61 blank samples were created by incubating 1 L of uninoculated ISP-2 or JCM #61 media in a 5 L Erlenmeyer flask for 10 days at 30°C with shaking at 25 oscillations per minute. These conditions mimic the conditions under which strain PR3 was cultured and extracted. Next, the medium was extracted as if it were a broth (section 3.2.1). Fifty millilitres of MeOH was added to mimic the cell mass extraction conditions.

3.2.3 Solid Phase Extraction (SPE)

3.2.3.1 SPE Method #1: Reverse Phase

The SPE cartridges used were Phenomenex® Strata™ X-33 µm Reverse Phase C18 SPE cartridges (Separations, Johannesburg, South Africa) with a sorbent mass of 200 mg and a total volume of 3 mL. A SPEEDISK® 48 manifold was used to wash solvents and dissolved crude extract samples through the C18 cartridge under pressure. The C18 cartridges were equilibrated before use by washing 2 mL MeOH (99.9%, Honeywell, Johannesburg, South Africa) through each cartridge followed by 2 mL water under pressure. The crude extracts were dissolved in 2 mL of water and passed through the equilibrated C18 cartridge under pressure. Thirty to fifty milligrams of crude extract sample was used per cartridge. After the sample had been washed onto the column, 2 mL of solvents, of decreasing polarity, were added one after another. The solvents, in order of use, were water, water/MeOH (1:1), MeOH, Acetonitrile (ACN, 99.9%, Honeywell, South Africa) dichloromethane (DCM, 99.9%, Honeywell, Johannesburg, South Africa), hexane (≥ 97%, Sigma-Aldrich, Johannesburg, South Africa) and acetone (99.8%, Honeywell, Johannesburg, South Africa). Acetone was used last, despite not being the most non-polar solvent, as it cleans the cartridge, which allows for repeated uses. Each fraction was collected and dried under N_2 in a clean pre-weighed plastic benchtop tube.

3.2.3.2 SPE Method #2: Reverse Phase

The cartridges and equipment used are the same as described in section 3.2.3.1. Thirty to fifty milligrams of crude extract sample were used per cartridge. The crude extract sample was dissolved in 2 mL water/MeOH (1:1) then passed through the C18 cartridge under pressure. Solvents of decreasing polarity were used. The solvents used, in order, were water/MeOH (1:1), water/MeOH (2:3), water/MeOH (3:7), water/MeOH (1:4), water/MeOH (1: 9), MeOH and acetone. Acetone served to clean the cartridges for repeated use of the cartridges. Each C18 cartridge was used three times before being discarded.

3.2.3.3 SPE Method #3: Reverse Phase

The cartridges and equipment used were the same as described in section 3.2.3.1. Thirty to fifty milligrams of crude extract sample were used per cartridge. The crude extract sample was dissolved in 2 mL water/MeOH (1:1) then passed through the C18 cartridge under pressure. Two millilitres water/MeOH (1:1) was passed through the cartridge and the fraction discarded. Next, 2 mL water/MeOH (1:4) was passed through the cartridge and the fraction discarded. The active compound was eluted with 2 mL MeOH, and the fraction was collected. Finally, the cartridge was washed with 2 mL acetone to ensure as much inactive material was removed so that the cartridge can be used again. Cartridges were used three times before being discarded.

3.2.3.4 SPE Method #4: PHREE

To remove lipids, Phenomenex® phospholipid removal (PHREE) cartridges (Separations, Johannesburg, South Africa) were used. A SPEEDISK® 48 manifold was used to pass solvents and dissolved samples, through the C18 cartridge under pressure. The MeOH fraction produced by SPE Method #3 (section 3.2.3.3) was dried under N_2 at 37°C and redissolved in 200 µL of MeOH. This was added to a PHREE cartridge along with 800 µL of MeOH/1% formic acid. The samples were passed through the PHREE cartridges under pressure, dried under N_2 at 37°C and weighed in centrifuge tubes.

3.2.3.5 SPE Method #5: Normal Phase

The SPE cartridges used were ISOLUTE® silica SPE cartridges (Shimadzu, Roodepoort, South Africa) with a sorbent mass of 200 mg and a total volume of 3 mL. SPE cartridges were equilibrated by passing 2 mL of MeOH followed by 2 mL of hexane. Samples were dissolved in 2 mL hexane/EtAc (9:1) and washed through the silica cartridges by gravity. After adding the sample, solvents of increasing polarity were passed through the silica cartridges. The list of solvents in order of use was: hexane, hexane/EtAc (2:1), hexane/EtAc (1:1), EtAc, EtAc/MeOH (4:1), EtAc/MeOH (2:1) and MeOH. When using silica cartridges, the sorbent was not allowed to dry as this alters the retention of compounds in the subsequent wash steps. Therefore, 2.5 mL of solvent was added in each step, and approximately 0.5 mL of each solvent was left behind (i.e. only 2 mL of each fraction was collected).

3.2.4 Nuclear Magnetic Resonance Spectrometry

Samples were submitted to two different institutes for ^{1}H and ^{13}C NMR analysis depending on availability.

The institutes, analysts and methods were:

Mr Kojo Acquah (Ph.D. student) with assistance from Dr Godwin Dziworn, from the Department of Chemistry at the University of Cape Town. Samples were dissolved in deuterated MeOH. A BRUKER Ascend 600 NMR spectrometer was used with a Prodigy cryoprobe at to obtain NMR spectra.

Dr Jaco Brandt from the Central Analytical Facility, University of Stellenbosch, South Africa. The samples were dried and dissolved in deuterated acetone and transferred into a new NMR tube. An Agilent^{Unity}*Inova* 600 NMR spectrometer with a 5 mm dual-channel IDpfg probe was used obtain NMR spectra.

3.2.5 High Performance Liquid Chromatography - Mass Spectrometry

3.2.5.1 HPLC-MS Method #1

An AB Sciex® X500R QTOF coupled to an AB Sciex® Exion LC system was used for high resolution analysis. The Exion LC system consisted of a column oven, autosampler, solvent valve, degasser, controller, and two pumps. Spectral data was obtained using information dependent acquisition (IDA). Samples were scanned from 50–1200 Da. All methods, batches, and data were processed using OS Sciex® v1.2. The declustering potential was 80 V, the curtain gas (N_2) was at 25 pounds per square inch (psi), the ion spray voltage was 5500 V, and the source temperature was 450°C. Ion source gas 1 and 2 were at 45 and 55 psi, respectively. The collision energy was 10 eV for the MS scans and 20-50 eV for MS/MS scans. The IDA intensity threshold was 50 cycles per second. An in-house HPLC method, developed in the Division of Clinical Pharmacology, University of Cape Town, by Ms Alicia Evans, was used for HPLC-QTOF analysis. This method is a routine drug screening HPLC method; used to separate a wide range of molecules with different polarities. The aqueous mobile phase used was 1 mM ammonium formate in water, and the organic mobile phase was MeOH/0.5% formic acid. The method was a gradient method starting at 2% organic and ending at 98% organic phase, with a flow rate of 600 µL/min and a run time of 18 minutes. A Kinetex® Evo C18 LC column (5 µm, 100 Å, 50 mm x 2.1 mm), with a column protector was used. All solvents were sonicated for 10 minutes before use to remove bubbles. Nontarget regression analysis was used to analyse the MS, and MS/MS spectra obtained.

3.2.5.2 HPLC-MS Method #2

A SCIEX® API 2000 mass spectrometer coupled to an Agilent™ 1260 Infinity binary pump system and an Agilent™ 1100 autosampler was used for Q1 mass analysis. The declustering and entrance potential were set to 50 V and 10 V, respectively. The curtain gas (N_2) was set at 20 psi, the ion spray voltage was 5500 V, and the source temperature was 300°C. Ion source gas 1 and 2 were set to 60 and 40 psi, respectively. All methods, batches, and data were processed using Analyst® v1.6.2. A semi-preparative Luna® C18 column (5 µm, 100 Å, 250mm x 4.6 mm) with a column protector was used. Water was the aqueous mobile phase and MeOH

was the organic phase. A gradient at flow-rate of 1 mL/min was used (Table 3.1). All solvents were sonicated for 10 minutes before use to remove bubbles.

Table 3.1: Gradient method used for HPLC-MS Method #2.

Time (minutes)	Aqueous (%)	Organic (%)
0	90	10
7	10	90
45	10	90
45.1	90	10
50	90	10

3.2.5.3 HPLC-MS Method #3

A modified version of HPLC Method #2 (section 3.2.5.2) was used with a change in gradient method. The maximum organic concentration was increased to 95% (Table 3.2).

Table 3.2: Gradient method used for HPLC-MS Method #3.

Time (minutes)	Aqueous (%)	Organic (%)
0	95	5
7	5	95
45	5	95
45.1	95	5
50	95	5

3.2.5.4 HPLC-MS Method #4

A modified version of HPLC Method #2 (section 3.2.5-.2) was used. Changes were made to the gradient method and mobile phase composition. Water was used as the aqueous phase and the organic phase was 95% MeOH, and 5% water. The organic phase concentration was increased from 95% to 100% (Table 3.3).

Table 3.3: Gradient method used for HPLC Method #4.

Time (minutes)	Aqueous (%)	Organic (%)
0	90	10
7	0	100
45	0	100
45.1	90	10
50	90	10

3.2.6 MZMine2 Data Processing

Raw HRMS data produced by HPLC-MS Method #1 was converted to mzXML format by ProteoWizard tool MSconvert (version 3.0.10051, Vanderbilt University, United States) (Chambers *et al.*, 2012). The converted data was then analysed using the processing software MZMine2 (Pluskal *et al.*, 2010). The parameters set were based on the recommendations of MZMine2. After the raw data was imported the peaks were detected using the Mass Detection feature. For MS 1 detection, centroid data was selected, and the noise level cut-off was set to 500. For MS2 peak detection, centroid data was also selected, and the noise level cut-off was set to 5. Next a chromatogram was created using the ADAP Chromatogram Builder feature (Myers *et al.*, 2017). To generate chromatograms the detected mass features were selected and the minimum group size in number of scans was set to 5, the group intensity threshold was set to 250, the minimum highest intensity was set to 500 and the *m/z* tolerance was set to 0.1. At this point the *m/z* signals had been detected for MS1 and MS2, and a chromatogram had been created using these signals. Next, isobars (atoms of different chemical elements with the same number of nuclei) need to be removed by deconvoluting the chromatograms. This was achieved by using the Chromatogram Deconvolution feature. The baseline cut-off algorithm was selected, and the minimum peak height was set to 1000, peak duration was set to 0.1-3.0 min and baseline level was 500. For the remaining settings, the *m/z* center calculation was set to median, *m/z* range for MS2 scan pairing was set to 0.02 and the retention time range for MS2 scan pairing was set to 0.1 min. Lastly, isotopic peaks were grouped to remove redundancies, using the Isotope Peak Grouper function. The *m/z* tolerance was set to 0.1, the retention tolerance was set to 0.1 min and the maximum charge was set to 3.

3.3 Results and Discussion

3.3.1 Upscaled Actinobacterial Cultivation and Modified Extraction

In many natural product screening projects, the amount of active material is a major limiting factor (Basso *et al.*, 2005). To manage this challenge, the cultivation conditions and extraction methodologies for *Streptomyces* strain PR3 were investigated. A new cultivation method was used to grow two 1 L cultures of strain PR3 (section 3.2.1). Volumes of ISP-2 larger than 1 L could not be used as larger Erlenmeyer flasks were not available and the shaker in the 30°C incubator lacked the space for larger flasks. Both cultures were extracted separately using a modified extraction method (section 3.2.2.1) and the broth and cell mass crude extracts produced were tested for antiplasmodial activity against *P. falciparum*, NF54 (section 2.2.4). The results revealed that larger crude extract masses were obtained, and the antiplasmodial activity of the crude extracts was maintained (Table 3.4). The assay controls, chloroquine and artesunate, displayed activity within the acceptable ranges.

Both culture broth and cell mass crude extracts redissolved in MeOH were less active than the EtAc samples (Table 2.2). Due to this, they were discarded and instead, multiple EtAc washes were performed.

Despite upscaling to a larger culture volume, the amount of material remained a limiting factor. As it was not possible to upscale to larger volumes, the extraction protocol was further developed. To improve yields, an extraction resin was added to the cultures prior to extraction. The resin selected was Amberlite® XAD-16N 20-60 mesh (Sigma, 1998).

To determine if the XAD-16N resin improved extraction yields and maintained antiplasmodial activity, two 1 L cultures of strain PR3 were grown (section 3.2.1) and extracted with a modified extraction method which included XAD-16N resin (section 3.2.2.2). The crude extracts were tested for antiplasmodial activity against *P. falciparum*, NF54 (section 2.2.4). The antiplasmodial activity results showed that the MeOH cell mass extract was inactive, the EtAc cell mass extract was moderately active, and the EtAc broth extract was inactive (Table 3.5). Both controls were within the acceptable ranges.

Table 3.4: Mean antiplasmodial activity against *P. falciparum*, NF54 of strain PR3 crudes from different media volumes, N=2 biological repeats with 4 technical repeats.

Culture Volume (mL)	100		1000	
Crude Extracts	Antiplasmodial activity against *P. falciparum*, NF54 IC_{50} (ng/mL)	Mass of crude extract (mg)	Antiplasmodial activity against *P. falciparum*, NF54 IC_{50} (ng/mL)	Mass of crude extract (mg)
Broth (EtAc)	177 ± 23	3.7 ± 1.2	200 ± 36	12.8 ± 1.4
Cell Mass (EtAc)	90 ± 13	2.5 ± 0.9	110 ± 14	8.3 ± 1.7
Chloroquine	5.2 ± 2.4			
Artesunate	4.3 ± 1.6			

Table 3.5: Mean antiplasmodial activity of XAD-16N crude extracts against *P. falciparum*, NF54, N=2 biological repeats with 4 technical repeats.

Crude Extract	Antiplasmodial activity against *P. falciparum*, NF54 IC_{50} (ng/mL)
Cell Mass MeOH	> 2000
Cell Mass EtAc	361.0 ± 52.0
Broth EtAc	> 2000
Chloroquine	4.8 ± 1.9
Artesunate	4.1 ± 0.5

The adsorption of the active antiplasmodial compound(s) to the XAD-16N resin was interesting and suggested that it is mid to non-polar. The active compound(s) had greater affinity for the non-polar resin than the polar culture broth and could not be washed off the resin with polar MeOH. This is shown by the lack of activity displayed by the MeOH cell mass and EtAc broth extracts (Table 3.5).

Using the XAD-16N resin improved the amount of sample extracted and streamlined the extraction method. Yields were erratic as the amount of cell mass varied from culture to culture, but overall yields were greater than those seen without the resin and ranged from 70–90 mg (compare with Table 3.4). Weaker activity was seen in the crude extracts, however, this was likely due to the increased amount of material extracted, not a change in the biosynthesis of the compound(s) by strain PR3 (compare with Table 3.4). The broth EtAc extract was believed to be inactive due to the active antiplasmodial compound(s) adsorbing to the resin. Due to this the broth extract could be discarded which decreased the number of steps involved in the extraction process, which allowed more cultures to be extracted simultaneously. Four 1 L cultures of strain PR3 could be extracted at the same time, allowing the accumulation of even more crude extract than was previously feasible. When following the previous method without resin, both the broth and cell mass extracts required extracting. Therefore only two 1 L cultures could be effectively extracted at once, and less material was obtained per 1 L culture.

3.3.2 Reverse Phase Solid Phase Extraction

Initial fractionation of strain PR3's crude extracts was achieved using reverse phase (RP) SPE. The goal was to develop a purification method where the active compound is retained on the SPE cartridge, allowing inactive polar material to be washed off using polar solvents. The active compound could then be eluted with mid-polar solvents leaving more non-polar constituents on the cartridge, allowing significant purification. Crude extract samples were fractionated using SPE Method #1 (section 3.2.3.1) and each sample was tested for antiplasmodial activity against NF54 (section 2.2.4). From the results, it is clear that the active compound eluted exclusively in the MeOH wash step (Table 3.6). Both controls were within the acceptable ranges. Further study investigated if the active compound could be eluted with different combinations of MeOH and water, to improve selectivity of the SPE method.

Table 3.6: Antiplasmodial activity against *P. falciparum*, NF54 of RP SPE fractions obtained by SPE Method #1, N=1 biological repeat and 4 technical repeats.

SPE Wash Step	Antiplasmodial activity against *P. falciparum*, NF54 IC_{50} (ng/mL)
Water (#1)	> 5000
Water/MeOH (1:1) (#2)	> 5000
MeOH (#3)	< 125
ACN (#4)	> 5000
DCM (#5)	> 5000
Hexane (#6)	> 5000
Acetone (#7)	1414
Chloroquine	5
Artesunate	5

A modified SPE protocol, SPE Method #2 (section 3.2.3.2) was developed and each fraction was tested for antiplasmodial activity against NF54 (section 2.2.4). Improved dissolution of all crude extract samples was seen when the starting solvent combination was water/MeOH (1:1). This is advantageous, as solid material can block the SPE cartridge and hinder separations. As the ACN, DCM, and hexane wash steps produced inactive fractions, they were omitted from SPE Method #2. The results found that that the active compound still eluted in the MeOH fraction as it was the most active fraction with a mean IC_{50} of 40.0 ± 1.5 ng/mL (Table 3.7). However, the MeOH fraction was not the only active fraction as the water/MeOH (1:9) step displayed moderate activity with a mean IC_{50} 878 ± 123 ng/mL. This activity suggested that the active compound was partially eluting in the water/MeOH (1:9) wash step. The controls in these assays were within the acceptable ranges.

Taking this into account, a final RP SPE method was generated, referred to as SPE Method #3 (section 3.2.3.3). Two washes of water/MeOH (1:1) were used to remove polar compounds. The water/MeOH (1:4) step was added to further remove inactive material, without the risk of eluting the active compound. Followed by the final elution of the active compound in MeOH.

Table 3.7: Mean antiplasmodial activity against *P. falciparum*, NF54 of SPE Method #2 fractions, N=2 biological repeats with 4 technical repeats.

SPE Wash Step	Antiplasmodial activity against *P. falciparum*, NF54 IC_{50} (ng/mL)
Water/MeOH (1:1) (#1)	> 2000
Water/MeOH (2:3) (#2)	> 2000
Water/MeOH (3:7) (#3)	> 2000
Water/MeOH (1:4) (#4)	> 2000
Water/MeOH (1:9) (#5)	878 ± 123
MeOH (#6)	40.0 ± 1.5
Acetone (#7)	1532 ± 130
Chloroquine	6.2 ± 1.3
Artesunate	3.7 ± 0.8

One milligram of the RP SPE MeOH fraction obtained from SPE Method #3 (section 3.2.3.3) was submitted for ^{1}H NMR analysis at the University of Cape Town (section 3.2.4). The annotated ^{1}H NMR spectrum of the RP SPE MeOH fraction is shown in Figure 3.2. Briefly, NMR spectrometry involves disturbing the precession of isotopic nuclei such as ^{1}H in a constant magnetic field using radio waves of differing frequencies (Silverstein *et al*., 2005). This alters the spin state of the nuclei which generates a signal that can be detected by an NMR spectrometer. The circulation of electrons around these nuclei alters their chemical environment, therefore different chemical groups generate different signals. Therefore, the NMR spectrum of a sample can provide information on the chemical groups present and their location in the molecule (Dayrit and Dios, 2017). In Figure 3.2, strong signals were observed in the δ_H 3.3-3.7 range and δ_H 0.9-1.4 range. The signals from δ_H 3.3-3.7 are represent protons that are deshielded suggesting they are attached to or located close to heteroatoms such as oxygen or nitrogen (Silverstein *et al*., 2005). Therefore, these signals could be from protons attached to ether groups or be protons with neighbouring amine or hydroxyl groups. The signals from δ_H 0.9-1.4 represent shielded proton signals suggesting they are from methyl or methylene groups situated in a hydrocarbon chain or a 5-6 membered ring. Alternatively, they could be protons attached to a free amine group without any neighbouring functional groups (Silverstein *et al*., 2005). A signal at δ_H 4.8 was also detected, and is believed to be from water not removed from the sample. Unfortunately, many peaks of different intensities were detected in these

ranges on the spectrum making further analysis difficult. Once an ^{1}H NMR spectrum has been obtained the next step would have been to integrate each peak to determine the number of protons present in each signal. However, due to the overlapping bases and varying signals in the ^{1}H NMR spectrum, it was not possible to accurately integrate each peak or identify which peaks are related to the active compound(s) and which ones are not. This suggested that the sample contained impurities not linked to the active compound and further purification steps were required.

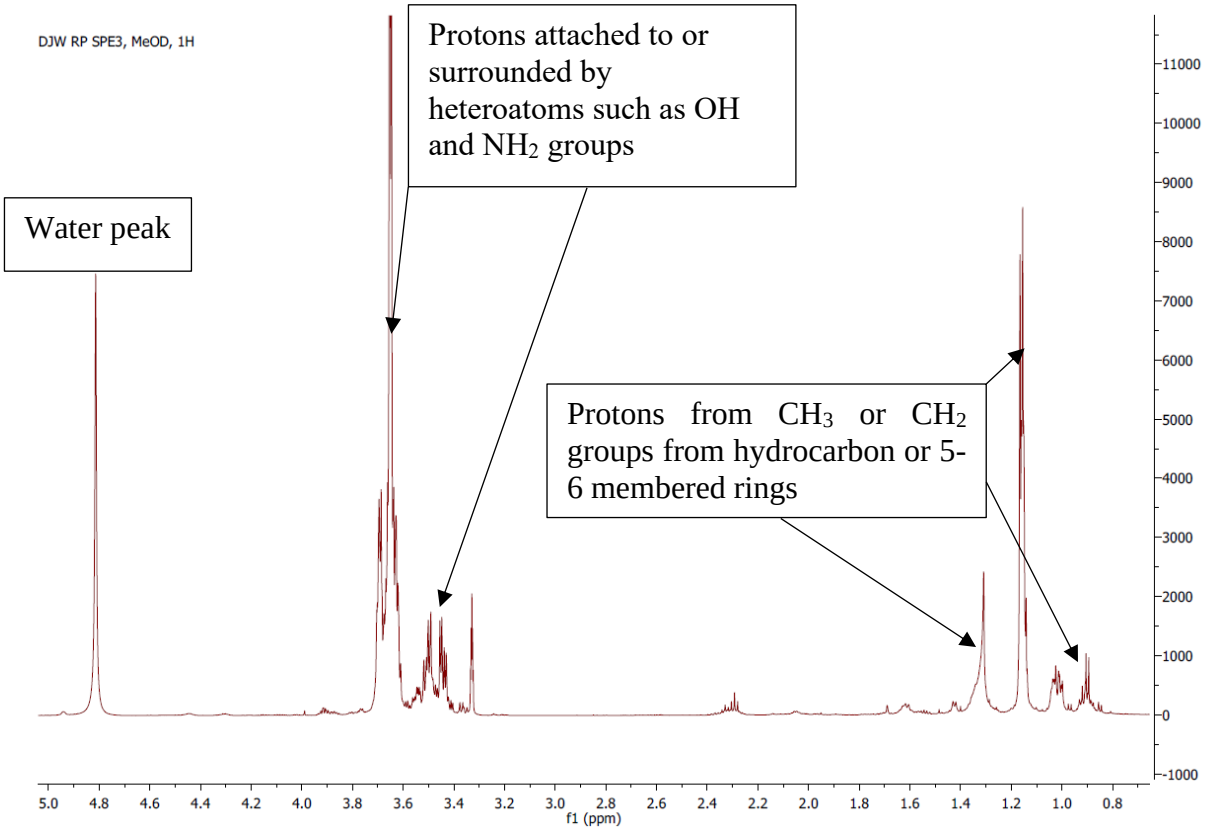

Figure 3.2: ^{1}H NMR spectrum of RP SPE MeOH sample (SPE Method #3).

It was hypothesised that lipids were present in the sample due to the strong signal seen in the aliphatic regions of the ^{1}H NMR spectra of the RP SPE MeOH sample (Dayrit and Dios, 2017). Phospholipids form the bulk of the bacterial cell membrane and were likely extracted from the cell mass (Sohlenkamp and Geiger, 2016). It was predicted that phospholipids could have eluted in the RP SPE MeOH wash and contaminated the sample. To remove these lipids, a Phenomenex® phospholipid removal (PHREE) cartridge was used according to SPE Method #4 (section 3.2.3.4) (Phenomenex, 2013).

Before further NMR analysis, samples were taken before and after being passed through the PHREE cartridge and tested for antiplasmodial activity against NF54 (section 2.2.4). The results show that the active compound did not retain to the PHREE SPE cartridge as antiplasmodial activity was unchanged (Table 3.8). The RP+PHREE SPE fraction was tested for *in vitro* cytotoxicity (section 2.2.6) and haemotoxicity (section 2.2.7). The RP SPE MeOH fraction displayed no cytotoxicity up to 100 µg/mL and had calculated selectivity indices (SI) greater than 100 (Table 3.9). This suggested the active compound(s) present are selectively targeting the *Plasmodium* parasites and further study was warranted.

Table 3.8: Mean antiplasmodial activity against *P. falciparum*, NF54 of RP SPE MeOH (SPE Method #3) sample before and after PHREE separation (SPE Method #4), N=2 biological repeats with 4 technical reports.

Sample	Antiplasmodial activity against *P. falciparum*, NF54 IC_{50} (ng/mL)
Before PHREE	40.0 ± 5.0
After PHREE	39.7 ± 4.0
Chloroquine	5.1 ± 2.0
Artesunate	4.7 ± 1.0

To determine if contaminants and background material had been removed, and if more structural data could be obtained ^{1}H NMR spectrometry was undertaken. One and half milligrams of the RP+PHREE SPE MeOH sample was submitted for ^{1}H NMR analysis at the University of Cape Town (section 3.2.4). The ^{1}H NMR spectrum of the RP+PHREE SPE MeOH fraction is shown in Figures 3.3. The signals observed in the PHREE ^{1}H NMR spectrum are very similar to the signals from the RP SPE MeOH fraction (compare Figure 3.2). Strong signals were observed in the δ_H 3.3-3.7 range and δ_H 0.9-1.4 range which was the same as the signals observed in the SPE MeOH fraction (compare Figure 3.2). The ^{1}H NMR of the MeOH sample was repeated under the same conditions used to analyse the PHREE sample to allow an accurate comparison (section 3.2.4). The two spectra were overlaid and compared (Figure 3.4). Weaker signals in the ^{1}H NMR spectrum of the PHREE sample were seen at δ_H 1.15, 1.3 and 3.65. It is likely that these signals are linked to phospholipids or aliphatic compounds as that is what the PHREE SPE cartridges target (Phenomenex, 2013). The decrease in aliphatic signals

and unchanged antiplasmodial activity suggested that the PHREE SPE was able to remove impurities without affecting the active compound(s). However, the ^{1}H NMR spectrum of the active PHREE SPE sample still contained too many overlapping and varied peaks to accurately integrate the signals and further purification was required to elucidate the structure of the active compound.

Table 3.9: Mean antiplasmodial and cytotoxicity data of RP+PHREE SPE MeOH fraction against NF54, CHO, HepG2, and human erythrocytes, N=2 biological repeats and 4 technical reports.

Sample	Antiplasmodial activity against *P. falciparum*, NF54 IC_{50} (ng/mL)	Cytotoxicity against Chinese Hamster Ovary IC_{50} (µg/mL)	Cytotoxicity against HepG2 IC_{50} (µg/mL)	Haemotoxicity against Human Erythrocyte IC_{50} (µg/mL)	Selectivity Index (SI) (Cell IC_{50}/ NF54 IC_{50})
RP+PHREE SPE MeOH	39.7 ± 4	> 100	> 100	> 100	> 2564
Emetine	-	0.0024 ± 0.001	0.015 ± 0.002	-	-

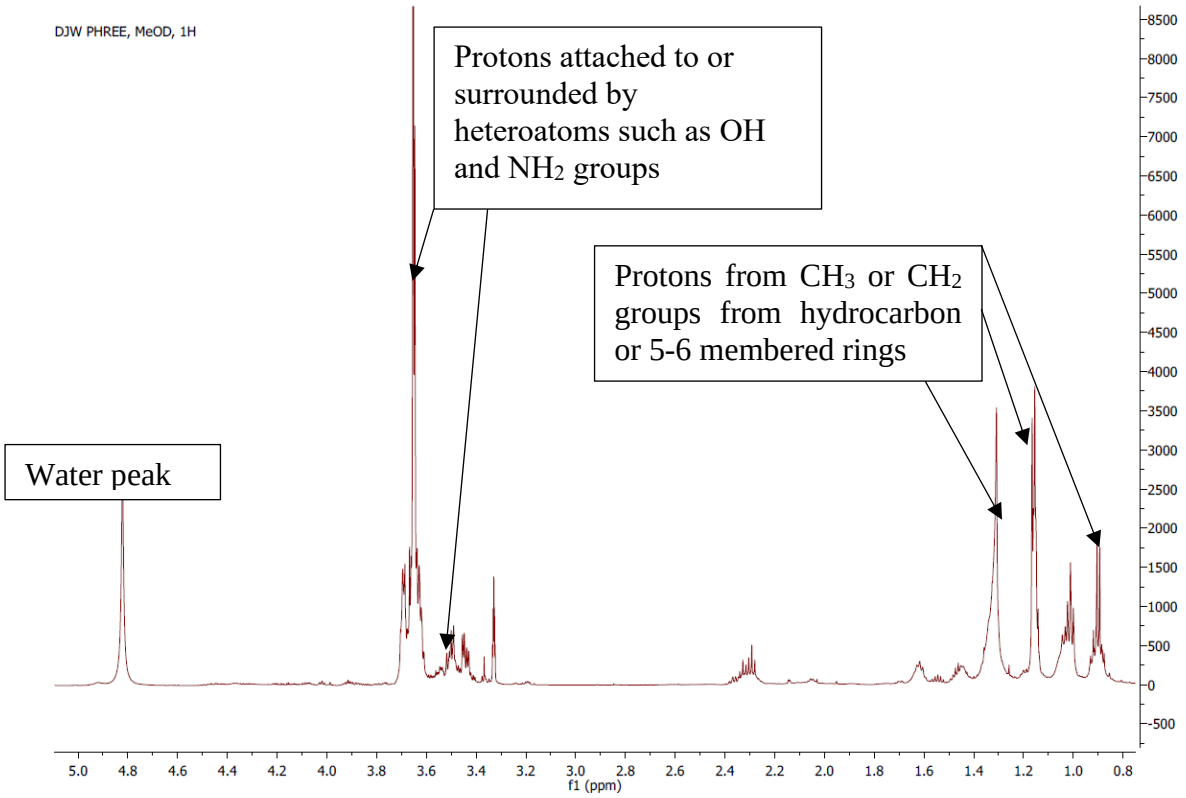

Figure 3.3: ^{1}H NMR spectrum of RP+PHREE SPE MeOH sample.

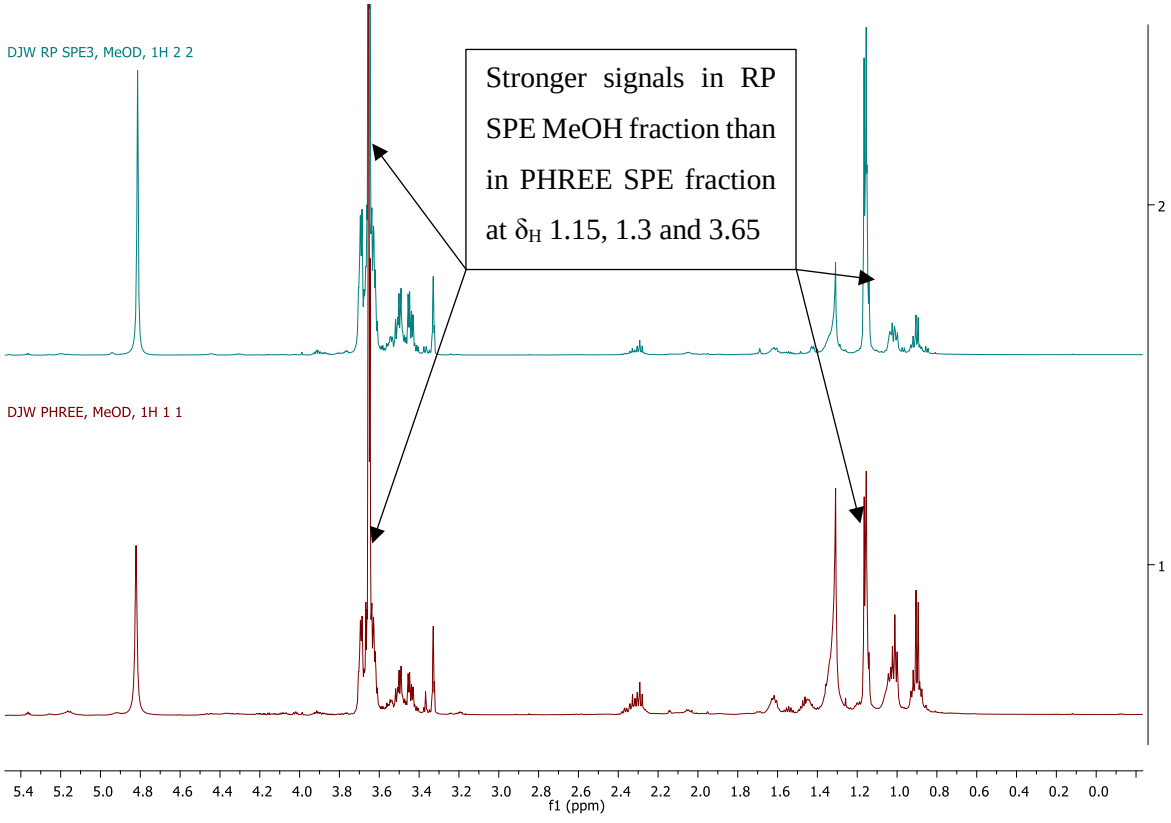

Figure 3.4: Comparative overlay of RP SPE MeOH and RP PHREE SPE active samples.

3.3.3 HPLC-MS Guided Purification

At this stage of the investigation, the active compound(s) was still impure and, more importantly, very little structural information was known. To identify the mass of the active compound and gain structural data, HRMS analysis, with a quadrupole time of flight (QTOF) instrument, was conducted using HPLC-MS Method #1 (section 3.2.5.1).

Samples were processed by independent data acquisition (IDA) scanning. The first step in an IDA method is a survey scan where all ions are passed through the first mass analyser, in radio frequency (RF) only mode (Sciex, 2017). In RF only mode, only ions with a *m/z* greater than a set limit will pass through the mass analyser. In the case of this investigation, the set limit was a *m/z* greater than 50 Da. The ions are scanned and pass through the collision cell, with very low collision energy, so no fragmentation occurs. Next, the ions pass through the TOF mass analyser, onto the detector and each ion is assigned an accurate *m/z*. QTOFs generally display a mass error less than 10 ppm (Kind and Fiehn, 2007). Next, precursor ions are selected from the survey scan based on intensity and exclusion parameters and transmitted through the first mass analyser again. These are scanned, then fragmented in the collision cell and analysed in the TOF chamber before reaching the detector. This results in high-resolution MS and MS/MS data on ions and their fragments in complex mixtures. It also separates signals from different molecular ions with the same *m/z*. The MS, MS/MS and retention times can then be used to identify or aid elucidation of the compound. IDA produces very accurate MS data on almost all ions present; however, because such a large quantity of data is obtained, it can be difficult to analyse unknown compounds. To solve this issue, non-target screening analysis can be conducted. In this analysis, an active sample and an inactive blank sample are processed in the same manner by HPLC-QTOF IDA, and the MS, MS/MS data and retention times are overlaid. Ions seen in the active sample, but not in the blank, are potentially responsible for antiplasmodial activity. If the active sample is pure, then the blank can simply be the solvents used to dilute the active sample. In the case of this investigation, NMR had shown that the active RP+PHREE SPE MeOH sample still contained impurities with the active compound(s), so a more sophisticated blank was required.

An ISP-2 blank was created as discussed in section 3.2.2.3. Next, the extracted blank was fractionated by RP+PHREE, using SPE Methods #3 and #4 (sections 3.2.3.3 and 3.2.3.4 respectively). A sample of the blank liquid medium was streaked on an ISP-2 agar plate before

extraction, and no growth was observed, indicating no microbial presence in the blank. Theoretically, this extracted sample contains almost all the molecules from the growth medium and solvents used to prepare the active sample, without any bacterial cell components or metabolites.

Ten microlitres of a 10 µg/mL sample of the RP+PHREE SPE MeOH active and blank sample were analysed using HPLC-MS Method #1 (section 3.2.5.1). Molecular ions that appeared at moderate to high intensities in the active sample and were not present in the blank sample were selected as candidate ions that could be the active compound. Candidate ions were selected in this fashion because the RP+PHREE SPE sample displayed potent antiplasmodial activity (see Table 3.9) and therefore *m/z* signals linked to the active compound should be present at relatively high concentrations. This was supported by the improvement in antiplasmodial efficacy of the fractionated active sample compared to the original activity of the crude extract (compare Table 3.5 and Table 3.9). It was possible that selected candidate compound ions were not responsible for antiplasmodial activity. To overcome this, after selection all candidate ions were separated by HPLC and tested for antiplasmodial activity.

Three candidate ions were selected for further purification: *m/z* 285.0758, *m/z* 301.0711 and *m/z* 540.3823 (Figures 3.5, 3.6, and 3.7, respectively). Once selected, candidate ions had to be isolated and tested to determine which were responsible for antiplasmodial activity.

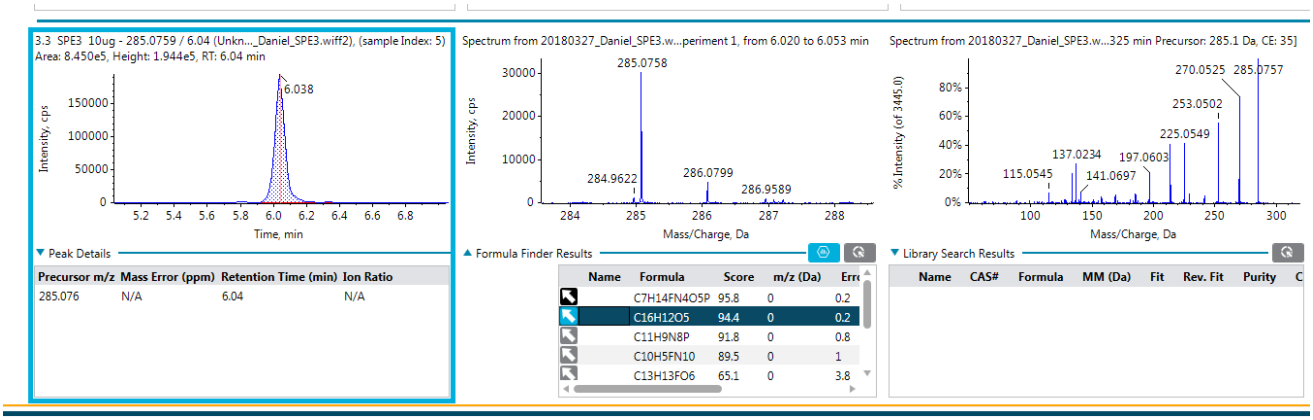

Figure 3.5: The high-resolution mass spectrum, predicted formulae and MS/MS spectrum of candidate compound with *m/z* 285.

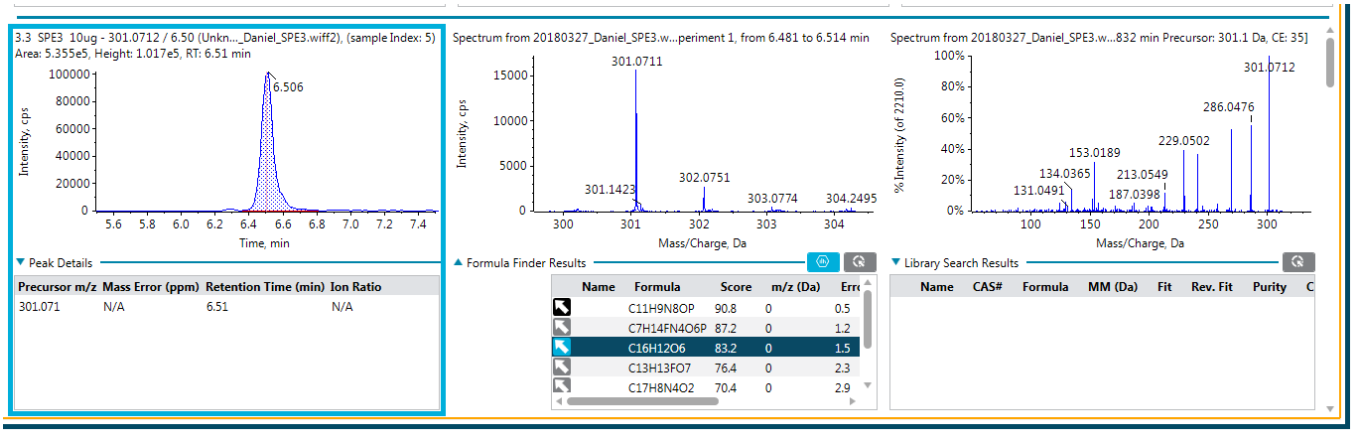

Figure 3.6: The high-resolution mass spectrum, predicted formulae and MS/MS spectrum of candidate compound with *m/z* 301.

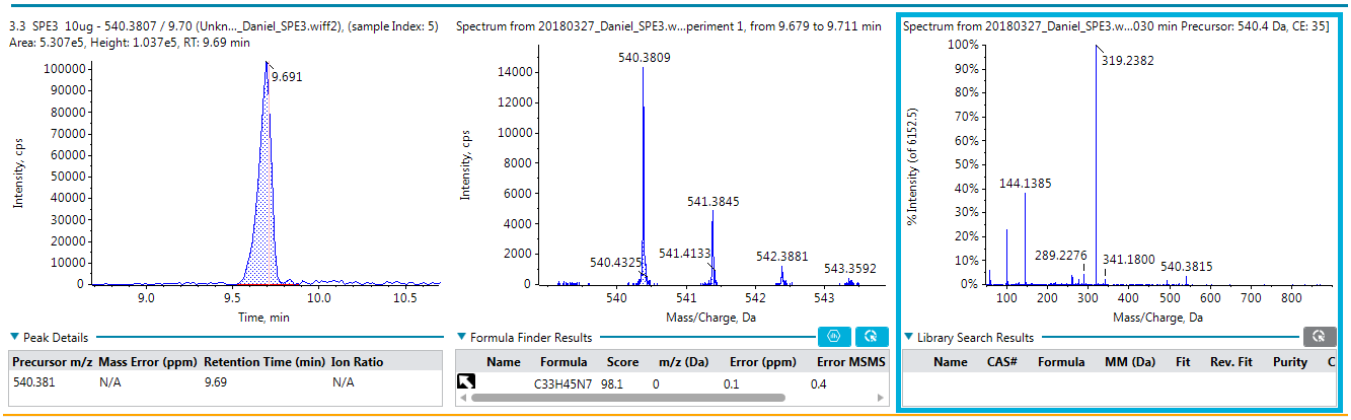

Figure 3.7: The high-resolution mass spectrum, predicted formula and MS/MS spectrum of candidate compound with *m/z* 540.

A HPLC-MS method was developed to separate the three candidate ions. The method used was HPLC-MS Method #2 (section 3.2.5.2). From the SPE experiments, it was known that the active compound(s) adsorbed strongly to a C18 column and only eluted at close to 100% MeOH. Therefore, the final organic concentration reached was set to 90% MeOH which, from the SPE experiments, was shown to elute the active compound (see Table 3.7). The gradient was held at 90% MeOH for the bulk of the HPLC run to ensure the candidate ions eluted. One hundred microlitres of 20 mg/mL RP+PHREE SPE MeOH fractionated sample was injected. HPLC-MS Method #2 was unable to elute *m/z* 540 with *m/z* 285 and 301 (Figure 3.8 and 3.9). A MeOH blank was injected onto the column directly after the RP+PHREE SPE sample to determine if *m/z* 540 could be washed off. If it could then the HPLC method needed to be

altered. One hundred microlitres of MeOH was injected and processed using HPLC-MS Method #2 (section 3.2.5.2) as a blank run. This blank MeOH injection was able to elute *m/z* 540 (Figure 3.10). This suggested that *m/z* 540 required a higher MeOH concentration to elute in the same method as *m/z* 285 and 301, and the method was altered to HPLC-MS Method #3 (section 3.2.5.3). In this method, the maximum MeOH concentration was increased to 95%. With the new method, *m/z* 540 eluted with the other candidate ions, *m/z* 285 and 301 (Figure 3.10).

One hundred microlitres of 20 mg/mL RP+PHREE SPE MeOH fractions was injected, and each candidate ion was collected. When one of the candidate ion peaks was detected, the waste line was run into a glass collection tube, and the sample was dried under N_2 gas at 37°C. Approximately 95% of the sample was diverted to waste, which allowed larger sample injection volumes without risking contaminating the source of the mass spectrometer. Candidate ions *m/z* 285 and 301 eluted close together with no baseline separation, so were collected together (Figure 3.9).

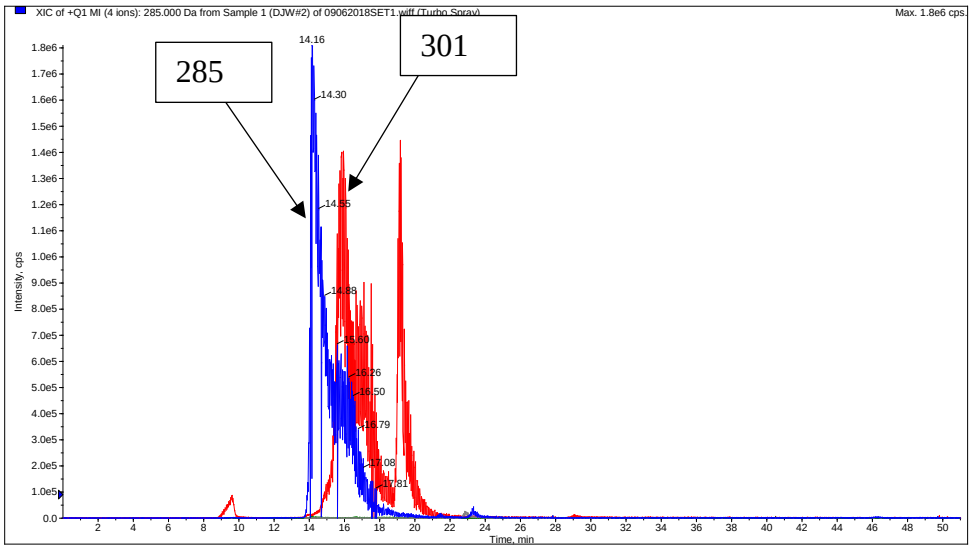

Figure 3.8: HPLC Method #2 showing only *m/z* 285 (blue) and *m/z* 301 (red) eluting.

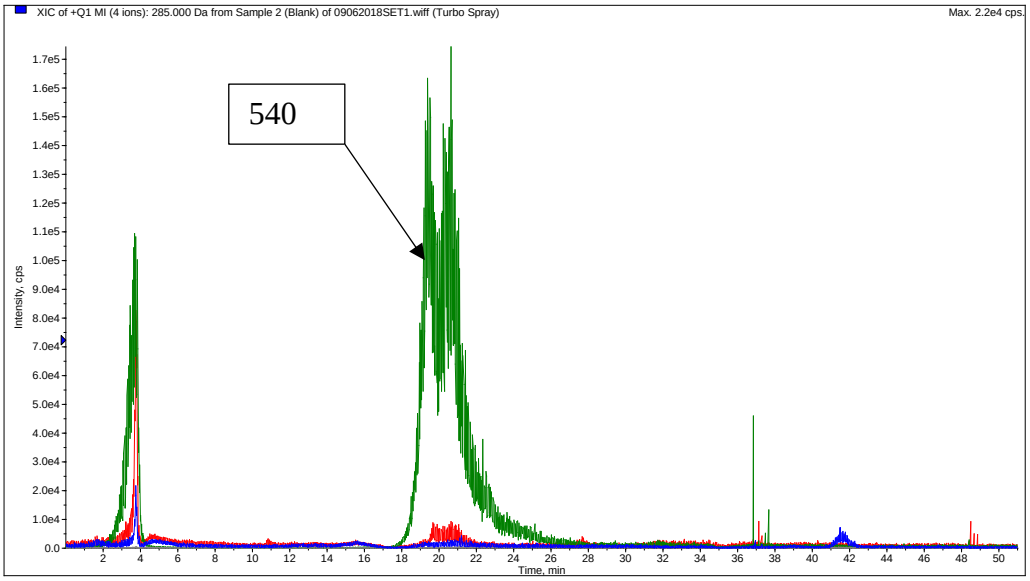

Figure 3.9: Blank injection after active sample showing *m/z* 540 (green) eluting due to incorrect chromatography conditions.

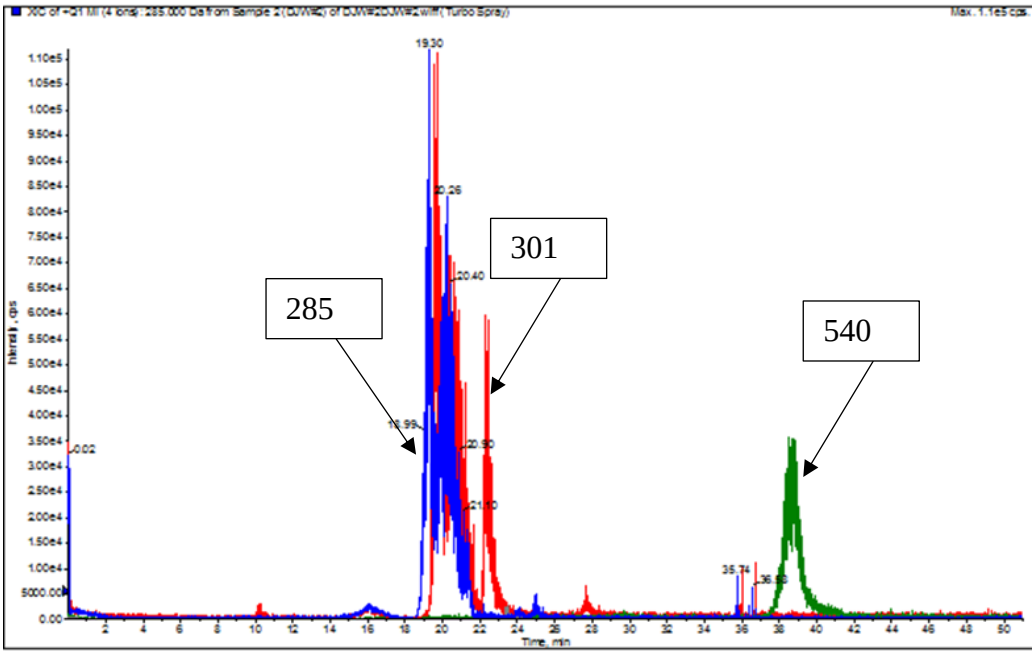

Figure 3.10: Chromatogram of candidate ions (HPLC-MS Method #3). The blue peak represents *m/z* 285, the red represents *m/z* 301, and the green peak represents *m/z* 540.

The two samples (fractions 285+301 and 540) were tested for antiplasmodial activity against NF54 (section 2.2.4). Not only was the fraction containing *m/z* 540 the only sample to display antiplasmodial activity, but it displayed potent activity with a mean IC_{50} of 27 ± 7 ng/mL (Table 3.10). The ISP-2 blank displayed no antiplasmodial activity proving that the compounds responsible for the inhibition of the *Plasmodium* parasites was being produced by strain PR3. The controls were within the acceptable ranges.

Table 3.10: Mean antiplasmodial activity of HPLC-MS purified fractions, N =2 biological repeats with 4 technical repeats.

Fractions	Mean antiplasmodial activity against *P. falciparum* NF54 IC_{50} (ng/mL)
285+301	> 2000
540	27.0 ± 7.0
ISP-2 Blank	> 5000
Chloroquine	6.7 ± 2.0
Artesunate	4.2 ± 0.5

This HPLC-MS purification method (section 3.2.5.3) allowed a mass ion to be associated with antiplasmodial activity, which greatly improved the purification process. Once antiplasmodial activity had been correlated to a *m/z* signal, it was possible to track the active compound during future separations without needing to carry out antiplasmodial testing each time a new culture was grown and fractionated.

Fraction 540 was tested for cytotoxicity (section 2.2.6) and haemotoxicity (sections 2.2.7) and displayed SIs greater than 100, which suggests its activity is parasite selective (Table 3.11). The control emetine displayed cytotoxicity within the acceptable range. Once fraction 540 was shown to be active against *P. falciparum* and non-toxic against the CHO, HepG2 and erythrocytes up to 100 µg/mL, further purification was undertaken to collect more material for further study. A modified HPLC method, HPLC-MS Method #4 (section 3.2.5.4) was implemented for the purification of fraction 540. The organic phase was changed to 95% MeOH + 5% water, and the maximum organic concentration was set to 100%. The mixing of the mobile phases, water and MeOH leads to an exothermic reaction, which generates bubbles that can affect both chromatography and equipment over long repeated runs. As little active sample was recovered from each HPLC-MS run (approximately 2%), many injections and long

run times were required. To reduce this effect, water and MeOH were mixed as the organic phase and degassed by sonication before use.

Table 3.11: Mean antiplasmodial and cytotoxicity data of fraction 540 against CHO, HepG2 and human erythrocytes, N=2 biological repeats with 4 technical repeats.

Sample	Antiplasmodial activity against *P. falciparum* NF54 IC_{50} (ng/mL)	Cytotoxicity against Chinese Hamster Ovary IC_{50} (µg/mL)	Cytotoxicity against HepG2 IC_{50} (µg/mL)	Haemotoxicity against Human Erythrocyte IC_{50} (µg/mL)	Selectivity Index (SI) (Cell IC_{50}/ NF54 IC_{50})
Fraction 540	27.0 ± 7.0	> 100	> 100	> 100	> 3703
Emetine	-	0.013 ± 0.009	0.021 ± 0.003	-	-

The purified fraction 540 was analysed by HRMS by injecting 10 µL of 10 mg/mL sample using HPLC Method #1 (section 3.2.5.1). The X500R's OS Sciex software features were unable to provide a molecular formula or any other information about the *m/z* 540 signal. Further study was conducted by processing the raw data using MZMine2 (section 3.2.6) and screening the *m/z* 540 in the Massbank, Pubchem and Kyoto Encyclopedia of Genes and Genomes (KEGG) databases (Pluskal *et al.*, 2010). Both KEGG and Massbank matched exclusively to the aminoglycoside apramycin (Figure 3.11). Apramycin has a mass of 539.2802 Da and a chemical formula of $C_{21}H_{41}N_5O_{11}$ (MassBank, 2016). This represents a close match to fraction 540's observed mass of 539.3809 Da with a small mass error of 0.0907. The aminoglycosides are a well-known group of antibiotics produced by the filamentous actinobacteria and include streptomycin, gentamicin and neomycin (Kotra *et al*., 2000). The aminoglycosides act by inhibiting protein synthesis through binding to the 16S rRNA subunit and causing conformation changes. This leads to codon misreading which results in the production of faulty protein products and ultimately kills the cell. The aminoglycosides exert

an antibacterial effect on a wide range of Gram positive and negative bacterial pathogens (Krause *et al.*, 2016). For example, the first isolated aminoglycoside was streptomycin, which is still used to treat *M. tuberculosis* (Waksman *et al*., 1946). The use of the aminoglycosides has been limited in humans due to potent ototoxicity and nephrotoxicity as well as drug resistance in parts of the world (Krause *et al.*, 2016). The aminoglycosides are structurally characterized by a group of amino sugars bound by glycosidic linkages to one or more dibasic aminocyclitols (Mingeot-Leclercq *et al*., 1999). Apramycin is a broad spectrum antibiotic used to treat a veterinary infections in livestock and was originally isolated from *Streptomyces tenebrarius* in the 1977 (Ryden and Moore, 1977). Apramycin contains a unique central deoxygenated bicyclic octose moiety flanked by a 5-amino pyranose sugar and a monosubstituted 2-deoxystreptamine (Figure 3.11) (Walton, 1978). This is not seen in most aminoglycoside antibiotics and allows apramycin to retain activity against aminoglycoside resistant bacteria and to display reduced ototoxicity in animal studies (Matt *et al.*, 2012; Hao *et al.*, 2020). Apramycin has no recorded antimalarial activity according to the current literature. This may be solely to a lack of study on the antiplasmodial activity of apramycin as other aminoglycosides have been shown to have antiplasmodial properties. Gentamicin and amikacin were both shown to repress the growth of the blood stage of *P. falciparum in vitro* (Krugliak *et al*., 1987). Their predicted mechanism of action is the inhibition of the parasite's phospholipase which has been linked to the feeding mechanism of *P. falciparum*. It is possible that apramycin exerts a similar effect to gentamicin and amikacin and is the active compound produced by strain PR3.

While the precursor mass of compound 540 and apramycin are a close match with a low mass error, the consensus MS/MS spectrum from Massbank of apramycin (Figure 3.12) does not match *m/z* 540's MS/MS spectrum (Figure 3.14). Figure 3.13 shows the MS/MS spectrum of apramycin from Massbank when analysed with a collision energy of 30 eV, which is similar to the collision energy used in HPLC Method #1 (MassBank, 2016). There are a number of peaks missing from compound 540's MS/MS spectrum which could identify it as apramycin, such as the typical *m/z* 217 and 378 peak which represents the loss of one half of the central octose moiety and the 5-amino pyranose ring respectively (Kaufmann and Maden, 2005; MassBank, 2016). The mass shifts in the major peaks of apramycin's and 540's MS/MS spectra are also different. For example the double 175 Da mass shift (see Figure 3.14) seen in 540's spectrum is not seen in apramycin's. Overall, this suggests that apramycin is not compound 540, despite the precursor ion match to the KEGG and Massbank databases. Analysis of compound 540's

MS/MS spectrum shows a mass shift of 46 Da, 44 Da and two shifts of 175 Da. It is possible that the mass shift of 46 Da corresponds to a CH_2O_2 group which could signify the presence of carboxylic acids (Ma *et al.*, 2014). Another possibility is that the 46 Da mass shift corresponds to a NO_2 unit which could suggest that 540 contains a nitroamine. The mass shift of 44 Da is commonly seen as the loss of a CO_2 group which could signify the presence of carboxylic acids or aldehydes (Ma *et al.*, 2014). The double mass shift of 175 Da does not match any commonly lost structures nor do the mass fragments *m/z* 319.2 and 144.1. However, the repeated mass shift suggests that compound 540 could be a dimer or have a cyclic structure (Jia *et al.*, 2006).

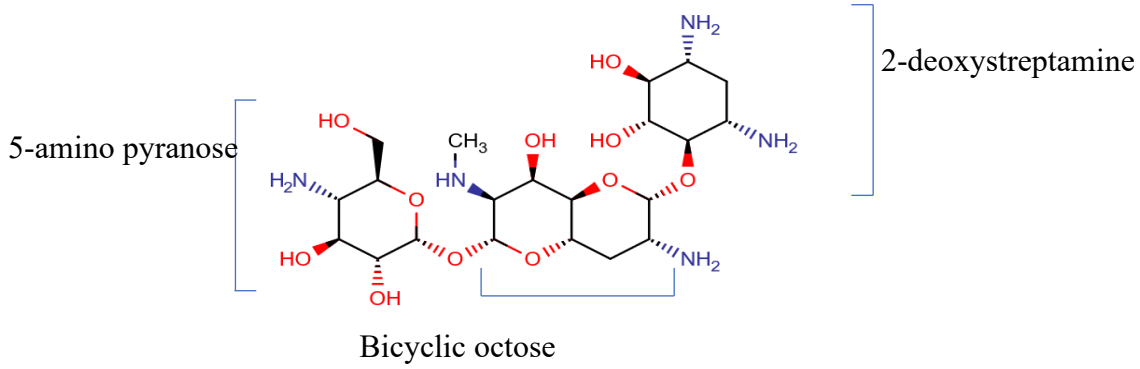

Figure 3.11: Annotated molecular structure of apramycin (Chemicalize, 2019)**.**

ID	Common Name	Formula	Mass difference
KO008806	Apramycin; LC-ESI-IT; MS2; m/z: 540; [M+H]+	C21H41N5O11	0.0907
KO002247	Apramycin; LC-ESI-QQ; MS2; CE:50 V; [M+2H]++	C21H41N5O11	0.0907
KO002246	Apramycin; LC-ESI-QQ; MS2; CE:40 V; [M+2H]++	C21H41N5O11	0.0907
KO002245	Apramycin; LC-ESI-QQ; MS2; CE:30 V; [M+2H]++	C21H41N5O11	0.0907
KO002244	Apramycin; LC-ESI-QQ; MS2; CE:20 V; [M+2H]++	C21H41N5O11	0.0907
KO002243	Apramycin; LC-ESI-QQ; MS2; CE:10 V; [M+2H]++	C21H41N5O11	0.0907
KO002242	Apramycin; LC-ESI-QQ; MS2; CE:50 V; [M+H]+	C21H41N5O11	0.0907
KO002241	Apramycin; LC-ESI-QQ; MS2; CE:40 V; [M+H]+	C21H41N5O11	0.0907
KO002240	Apramycin; LC-ESI-QQ; MS2; CE:30 V; [M+H]+	C21H41N5O11	0.0907
KO002239	Apramycin; LC-ESI-QQ; MS2; CE:20 V; [M+H]+	C21H41N5O11	0.0907
KO002238	Apramycin; LC-ESI-QQ; MS2; CE:10 V; [M+H]+	C21H41N5O11	0.0907
CO000075	Apramycin; LC-ESI-QTOF; MS2; CE:50 eV; [M+H]+	C21H41N5O11	0.0907
CO000074	Apramycin; LC-ESI-QTOF; MS2; CE:40 eV; [M+H]+	C21H41N5O11	0.0907
CO000073	Apramycin; LC-ESI-QTOF; MS2; CE:30 eV; [M+H]+	C21H41N5O11	0.0907
CO000072	Apramycin; LC-ESI-QTOF; MS2; CE:20 eV; [M+H]+	C21H41N5O11	0.0907
CO000071	Apramycin; LC-ESI-QTOF; MS2; CE:10 eV; [M+H]+	C21H41N5O11	0.0907

Figure 3.12: : Library match results showing that *m/z* 540 matched to apramycin repeatedly under different conditions in the Massbank database.

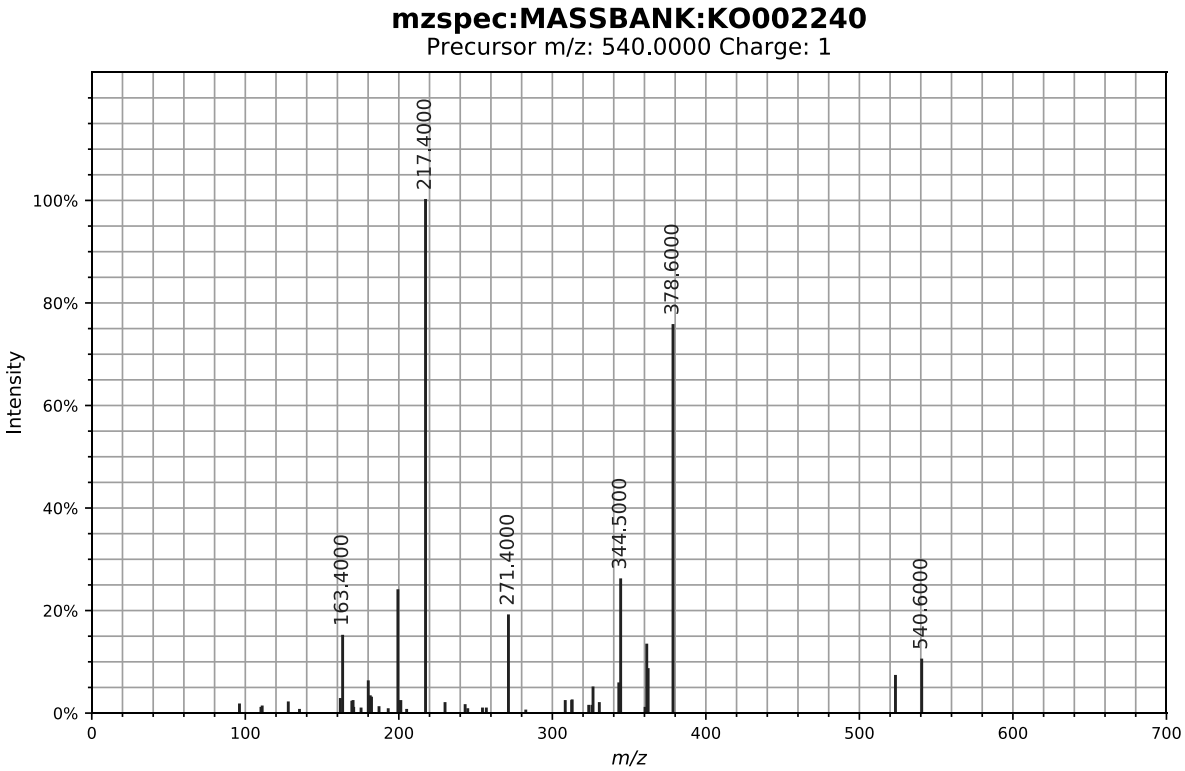

Figure 3.13: The consensus mass spectrum of apramycin from Massbank (MassBank, 2016)**.**

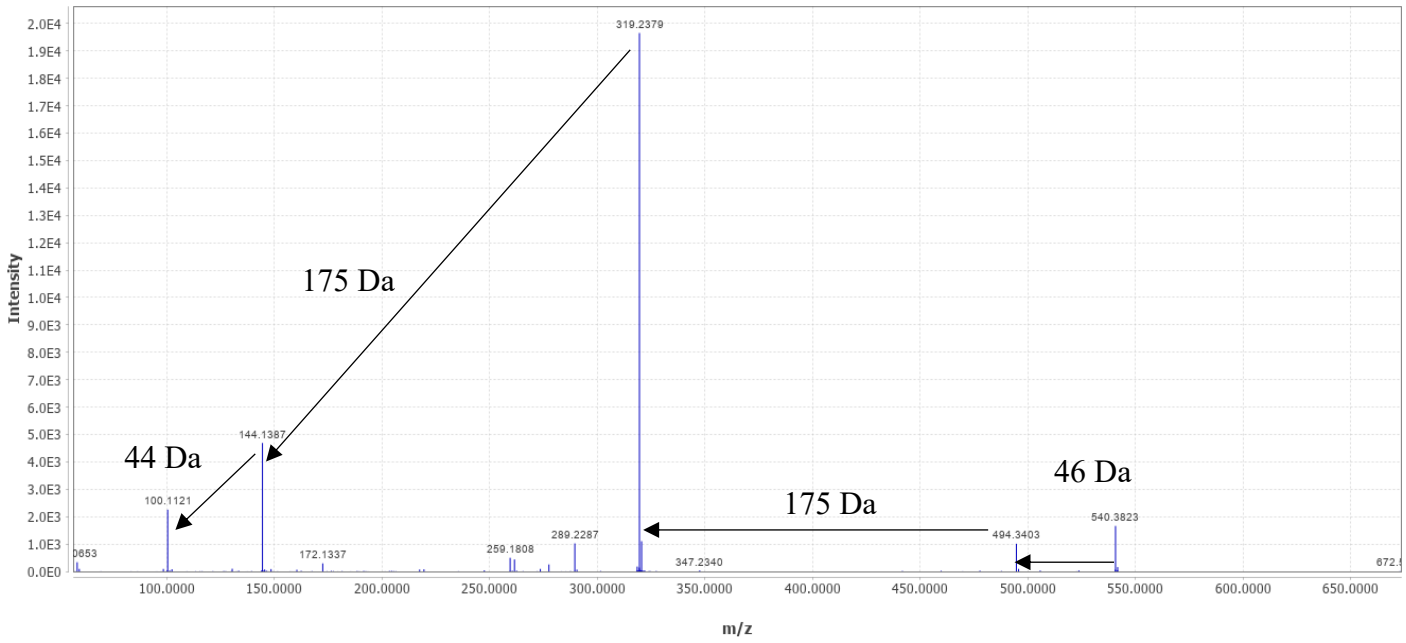

Figure 3.14: Annotated MS/MS spectrum of *m/z* 540. Arrows indicate a mass shift between major peaks and are annotated with the size of the mass shift.

Despite the close analysis of compound 540's MS/MS spectrum, very little structural information could be obtained. To obtain more structural data, large volumes of strain PR3 were cultured (section 3.2.1), extracted (section 3.2.3) and fractionated by RP+PHREE SPE (sections 3.2.3.3 and 3.2.3.4 respectively) to obtain enough material for ^{1}H NMR analysis. One hundred microlitres of 20 mg/mL RP+PHREE SPE MeOH fractions were repeatedly injected and separated until 1.1 mg of fraction 540 had been collected for ^{1}H NMR analysis at the University of Cape Town (section 3.2.4). The annotated ^{1}H NMR spectrum of fraction 540 is displayed in Figure 3.15. Signals from δ_H 0.75-1.5 represent shielded protons and were predicted to be from protons from methyl or methylene groups from hydrocarbon chains or 5-6 membered rings, or from protons bound to free amine groups (Silverstein *et* al., 2005). Signals from δ_H 3.25-3.75 represented deshielded signals due to protons bound to or neighbouring heteroatoms such as oxygen or nitrogen. The signal at δ_H 4.75 represents water not removed from the sample. These signals are very similar to the previous ^{1}H NMR spectra obtained from RP SPE and PHREE SPE (see Figures 3.2 and 3.3). While the ^{1}H NMR provided some structural data, a precise integration of the peaks was not possible as there were too many signals in the spectrum. Despite predicting some structural features from both the HRMS and NMR analysis of fraction 540, not enough data was available to accurately elucidate that active compound's structure. Therefore, further modifications and additions to the purification method were required.

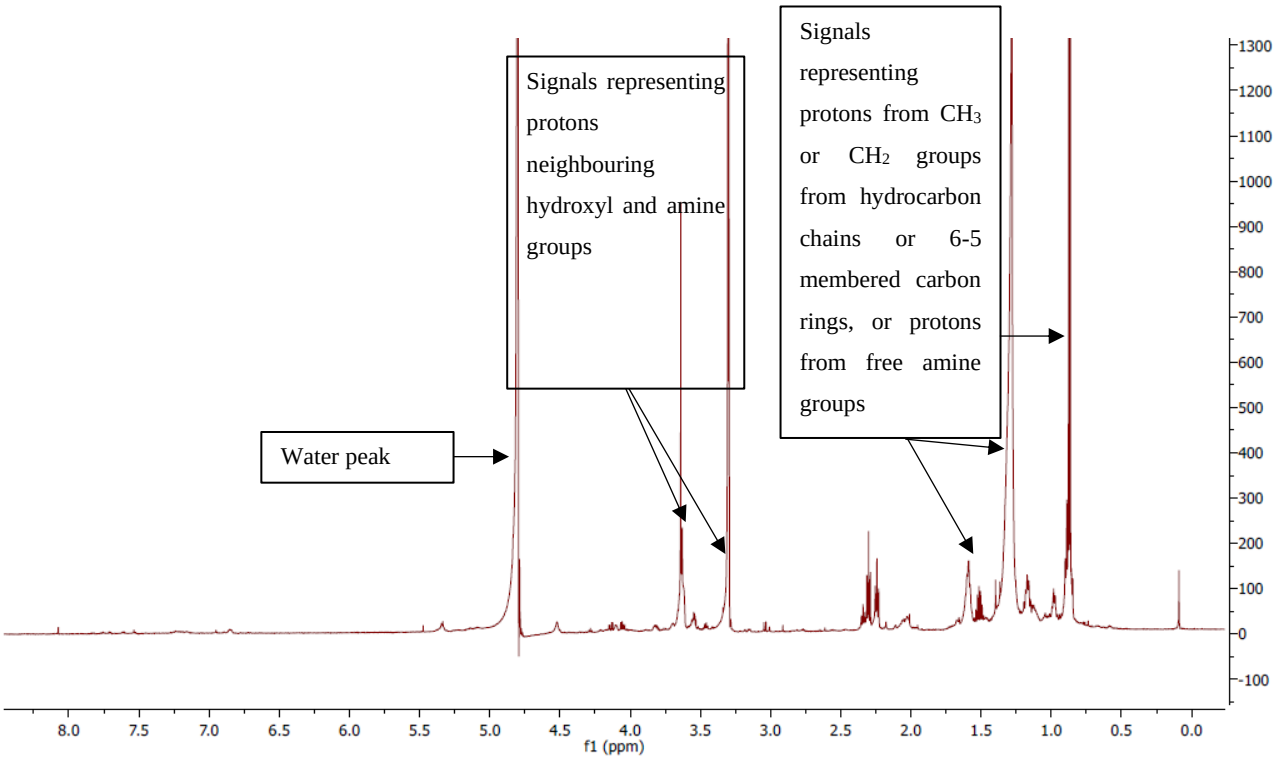

Figure 3.15: ^{1}H NMR spectrum of fraction 540

3.3.4 Culture Medium Alteration

It was hypothesised that, by altering the growth medium of strain PR3, the purity of fraction 540 could be improved by reducing the number of molecules co-extracted with the antiplasmodial molecules from the culture medium. *Streptomyces* strain PR3 was cultured and extracted (sections 2.2.1 and 2.2.2 respectively) in 100 mL of four media, DSMZ #553 (German Culture Collection, 2007), Czapek solution agar (CZ) (Atlas, 2010), JCM #61 (Ara and Kudo, 2007) and HM (Hacène and Lefebvre, 1995). The crude extracts were then tested for antiplasmodial activity against NF54 (section 2.2.4). The results showed that strain PR3 produced antiplasmodial active crude extracts when cultured in DSMZ #553, JCM #61 and HM with activity against *P. falciparum*, NF54 similar to that of ISP-2 extracts (Table 3.12). The controls were within the acceptable ranges. HM was not selected as it contains the same components as ISP-2, in addition to NaCl, so its use would not reduce the number of unwanted molecules extracted. When grown in DSMZ #553, strain PR3 grew slowly, and very little cell mass was produced, making it a poor choice, despite the antiplasmodial activity displayed. Therefore, JCM #61 was selected for further study as it has fewer complex nutrient components than ISP-2 and led to the production of crude extracts with matching antiplasmodial efficacy against *P. falciparum* strain NF54. ISP-2 medium is composed of yeast extract, malt extract, and glucose (Shirling and Gottlieb, 1966). JCM #61 is composed of starch, yeast extract, $MgSO_4$, and K_2HPO_4 (Ara and Kudo, 2007).

To determine if strain PR3 produced its antiplasmodial active compounds in larger JCM #61 volumes, two cultures of strain PR3 were cultured in 1 L volumes of JCM #61 (section 3.2.1), extracted with XAD-16N resin (section 3.2.3) and tested for antiplasmodial activity (section 2.2.4). The results showed that when strain PR3 was grown in JCM #61 it produced active extracts (Table 3.13). When the JCM #61 crude extracts were separated using RP+PHREE SPE (sections 3.2.3.3 and 3.2.3.4 respectively), good activity was seen, but it was weaker than the activity displayed by previous ISP-2 RP+PHREE SPE MeOH fractions. This was an unexpected and undesirable result, as it suggested that the JCM #61 samples were less pure than when ISP-2 was used as the growth medium. However, the difference was not significant enough to discard the JCM#61 samples and further purification was carried out in the hope that HPLC-MS purification would isolate the compound responsible for antiplasmodial activity.

Table 3.12: Antiplasmodial activity of crude extracts from strain PR3 grown in different growth media, N=1 biological repeat with 4 technical repeats.

Sample	Antiplasmodial activity against *P. falciparum* NF54 IC_{50} (ng/mL)
ISP -2 Broth Extract	150
ISP-2 Cell Mass Extract	< 125
JCM #61 Broth Extract	< 125
JCM #61 Cell Mass Extract	< 125
CZ Broth Extract	> 2000
CZ Cell Mass Extract	> 2000
HM Broth Extract	< 125
HM Cell Mass Extract	134
DSMZ # 553 Cell Mass Extract	< 125
Chloroquine	3
Artesunate	4

Table 3.13: Mean antiplasmodial activity against *P. falciparum*, NF54 of ISP-2 and JCM #61 crude extracts and SPE+PHREE MeOH fractions, N=2 biological repeats with 4 technical repeats.

Sample	Antiplasmodial activity against *P. falciparum*, NF54 IC_{50} (ng/mL)
ISP-2 Cell Mass XAD16-N Extraction	361 ± 50
ISP-2 RP+PHREE SPE MeOH	40 ± 1.5
JCM #61 Cell Mass XAD16-N Extraction	497 ± 14
JCM #61 RP+PHREE SPE MeOH	129 ± 23
Chloroquine	7.3 ± 1.8
Artesunate	4.1 ± 0.6

Another possibility for the change in activity was a change in antibiotic synthesis. When the JCM #61 RP+ PHREE SPE fractions were purified using HPLC-MS Method #4, the *m/z* 540 signal was not detected. This was corroborated by HRMS analysis of the JCM #61 grown RP+PHREE SPE MeOH fraction.

The change in antiplasmodial activity and disappearance of *m/z* 540 suggested that, under the new cultivation conditions, strain PR3 was producing a new antiplasmodial compound. This would explain why antiplasmodial activity was weaker in JCM #61 fractions compared to ISP-2 fractions and why *m/z* 540 disappeared.

As discussed in Chapter 1, antibiotic synthesis usually occurs as nutrients are depleted, and cells enter the stationary phase. During the log phase, utilization of simple nutrient sources are favoured to promote cell growth (Rafieenia, 2013). To ensure that the nutrients are not diverted from being used for cell growth, simple and rapidly metabolised carbon, nitrogen, and phosphate sources can inhibit antibiotic biosynthesis. Inhibition can occur by many different pathways, such as transcriptional inhibition or inhibition of enzymes required for biosynthesis (Sánchez *et al.*, 2010). As these rapidly-utilized nutrients are depleted, cell growth slows, this inhibitory effect weakens, and secondary metabolism is activated. This explains why antibiotic production is often associated with slow growth rates (Sánchez *et al.*, 2010).

Along with the amount and nature of carbon, nitrogen, and phosphate sources present, aeration, pH, ion concentration, cultivation time, light, and temperature are also major factors that can influence secondary metabolism (Sánchez *et al.*, 2010). When changing the growth medium of strain PR3, the same cultivation times, temperature, shaking speed, and light exposure were used (cultures were incubated in the dark). The pH of the culture medium was maintained as well, as the pH of ISP-2 and JCM #61 are very similar, 7.3 and 7.2, respectively (Atlas, 2010; Shirling and Gottlieb, 1966).

The main change in strain PR3's biosynthesis was possibly caused by the change in carbon source from glucose in ISP-2 to starch in JCM #61. Glucose is a well-known inhibitor of antibiotic biosynthesis and inhibits a variety of transcriptional and metabolic pathways. For example, glucose inhibits actinorhodin produced by *Streptomyces lividans*, by inhibiting mRNA synthesis required for its biosynthesis *(Kim et al.,* 2001). When the carbon source for *S. lividans* was changed to glycerol, this effect was not observed. Using polysaccharides, such as starch, is more suitable for antibiotic production as it is utilized at a slower rate (Rafieenia, 2013). While starch is hydrolysed to glucose, the free glucose concentration is much lower,

therefore, it applies a weaker inhibitory effect. High phosphate concentrations promote growth, as phosphate is an essential component in RNA, DNA, and protein biosynthesis. Many antibiotics are only synthesised when phosphate becomes a limiting factor (Rafieenia, 2013). It is difficult to predict the effect of the change in phosphate sources between the two media as the concentration of phosphate in ISP-2 is unknown. The yeast extract concentration was identical in the two media; therefore it would not have influenced antibiotic production. Yeast extract acts as an excellent nitrogen source for antibiotic production, as due to its complex nature, it is utilized at a slow rate (Rafieenia, 2013).

It is impossible to accurately state how the changes in the cultivation medium altered the antiplasmodial biosynthesis by strain PR3 with the data at hand. To begin to understand this change, the focus of the investigation shifted, with the aim to isolate the active compound in fraction 540 and the JCM #61 RP+PHREE SPE MeOH samples. Once their structures had been elucidated, they could be compared to determine if they were related or not. To achieve this, strain PR3 was cultivated in both ISP-2 and JCM #61 liquid media.

When strain PR3 was cultured and extracted in ISP-2 (sections 3.2.1 and 3.2.3 respectively), the RP+PHREE SPE MeOH samples showed antiplasmodial activity comparable activity to extracts with *m/z* 540 (data not shown), but the *m/z* 540 itself was not be detected. This occurred despite culturing strain PR3 cultures under the same conditions with 15% (*v/v*) glycerol frozen stocks of cultures which had produced active extracts that contained the *m/z* 540 signal in the past. During cultivation, conditions that produced active crude extracts were strictly adhered to, as the fastidious nature of the actinomycetes is well-known. This suggested that *m/z* 540 was never produced by strain PR3 or that strain PR3 had lost the ability to produce it. It was theorized that *m/z* 540 was a contaminant however comparison to other common MS contaminants such as plasticizers and media revealed no matches (Fisher Chemicals, 2020). Overall, the loss of the *m/z* 540 signal remains unexplained, fortunately activity was not lost in any fractions from ISP-2 or JCM #61 cultures of strain PR3 and therefore the loss of *m/z* 540 did not impede the investigation. Additionally, the study of *m/z* 540 led to the development of a purification workflow that could be applied to future work.

3.3.5 High-Resolution Mass Spectrometry Analysis of JCM #61 Samples

With the loss of the primary candidate, more in-depth mass spectrometry analysis was required to identify the correct active compound. JCM #61 samples were selected for analysis instead of ISP-2 grown samples, because of the reduced background.

A JCM #61 blank was generated (section 3.2.2.3) and fractionated by RP+PHREE SPE (sections 3.2.3.3 and 3.2.3.4 respectively). Ten microlitres of a 10 µg/mL sample of the RP+PHREE SPE MeOH active and blank sample were analysed using HPLC-MS Method #1 (section 3.2.5.1). The best candidate ion that was present at a high intensity in the active sample (and absent from the blank) was an ion with *m/z* of 888.6620. This was shown to be an ammonium adduct ($M+NH_4^+$) with an observed mass of 870.6271 Da. The source of the ammonium ions is believed to the aqueous phase, ammonium formate in water. Note, that the HPLC-MS purified sample will be referred to as fraction 870 and the *m/z* signal used to monitor fraction 870 was *m/z* 888. The MS and MS/MS data of *m/z* 888 did not match any known compounds after processing by MZMine 2 and screening in the KEGG, Massbank and Pubchem databases (Pluskal *et al.*, 2010). Another reason for selecting fraction 870 as the new lead candidate was that *m/z* 888 was found in the HPLC-MS purified 540 fraction, but had been overlooked because it appeared at a lower intensity than *m/z* 540. This correlated antiplasmodial activity with the presence of *m/z* in multiple active samples from different sources. Analysis of the MS/MS spectrum of *m/z* 888 (Figure 3.16) revealed a repeating mass shift of 58 units. *m/z* 888's true mass is 870.6274 Da, which is wholly divisible by 58 to give 15. This suggests that *m/z* 888 is a polymer with 15 subunits, however the structure of the monomer was unknown. To obtain more structural information about the monomer fraction 870 had to be purified and analysed by NMR spectrometry.

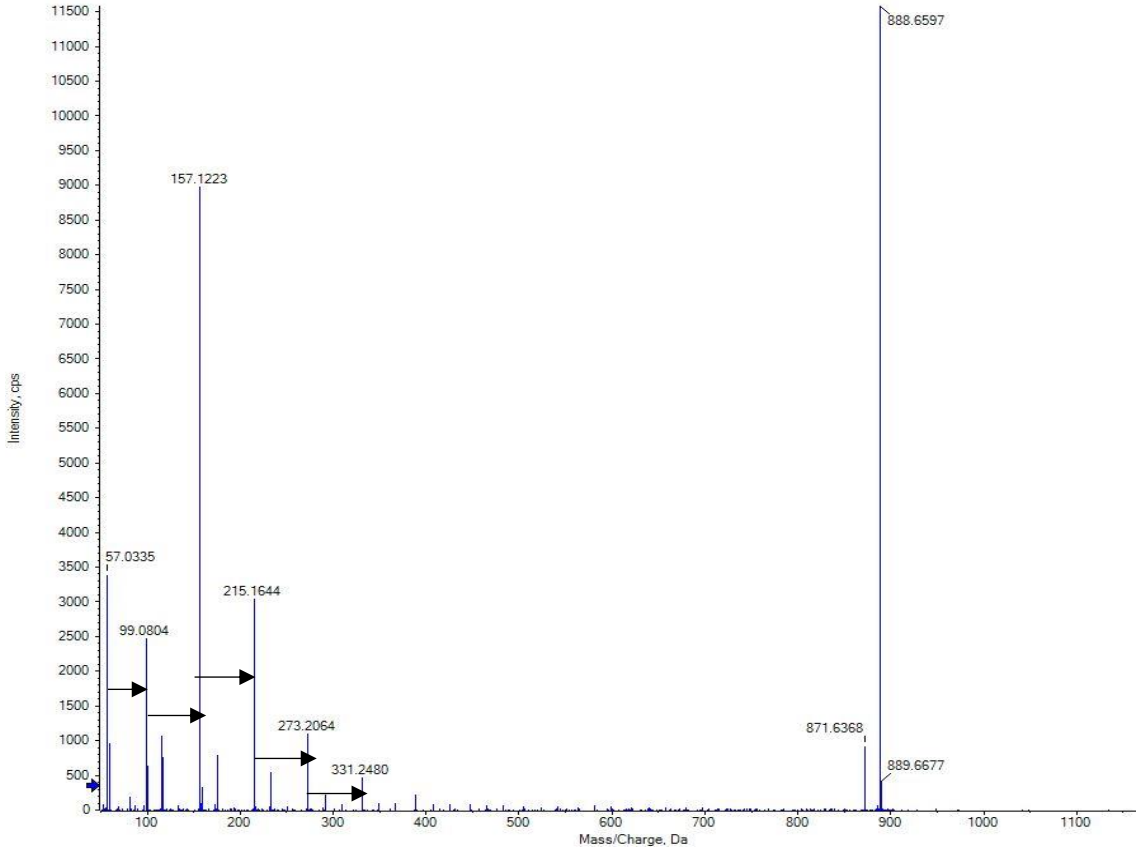

Figure 3.16: MS/MS spectrum of fraction 870. Black arrows represent repeated mass shifts of 58 Da.

JCM #61 crude extracts were separated by RP+PHREE SPE (sections 3.2.3.3 and 3.2.3.4), 100 µL of 20 mg/mL was injected and analysed using HPLC-Method #4 (section 3.2.5.4). Fraction 870 was collected and tested for antiplasmodial activity (section 2.2.4). Fraction 870 displayed good antiplasmodial activity with a mean IC_{50} 128 ± 12 ng/mL (Table 3.14). The JCM #61 blank was also tested and displayed no antiplasmodial activity confirming that the active compound in the extracts are natural products produced by strain PR3. Fraction 870 was tested for cytotoxicity and haemotoxicity (sections 2.2.6 and 2.2.7 respectively) and displayed no toxicity up to 100 µg/mL, which strongly suggested it was selectively targeting the *P. falciparum* parasites (Table 3.15). The antiplasmodial and cytotoxicity controls were within the acceptable ranges.

Table 3.14: Mean antiplasmodial data of fraction 870 and JCM #61 blank, N=2 biological repeats with 4 technical repeats.

Sample	Antiplasmodial activity *P. falciparum*, NF54 IC_{50} (ng/mL)
Fraction 870	128.0 ± 12
JCM #61 Blank	> 5000
Chloroquine	10.1 ± 2.0
Artesunate	4.2 ± 0.3

Dozens of 1 L cultures of strain PR3 were cultured in JCM #61 and extracted (sections 3.2.1 and 3.2.3). The crude extracts were separated by RP+PHREE SPE (sections 3.2.3.3 and 3.2.3.4 respectively) and the MeOH fraction was separated by HPLC-MS Method #4 (section 3.2.5.4). This was done continuously until 1.8 mg of fraction 870 had been collected for NMR analysis. Fraction 870 was submitted for ^{1}H NMR analysis at University of Stellenbosch (section 3.2.4). The annotated ^{1}H NMR spectrum of fraction 870 is displayed in Figure 3.17. Much like the ^{1}H NMR spectra of the previous active fractions (see Figures 3.2, 3.3 and 3.15) strong signals were detected from δ_H 0.75-1.5 and δ_H 3.25-3.75. These could represent protons from methyl or methylene groups from hydrocarbon chains or 5-6 membered rings and protons attached to or surrounded by heteroatoms such as OH and NH_2 groups respectively (Silverstein *et al*., 2005). However, additional signals were detected in this NMR analysis not seen in the previous spectra. Signals from δ_H 1.8-2.3 were detected at a greater intensity in fraction 870 than in previous samples and could be protons from methyl or methylene groups bound to alkenes or aldehydes. Signals were detected at δ_H 4.0-4.15 and could be from protons attached to methine or methylene groups conjugated or in close proximity to other functional groups (Silverstein *et al*., 2005). The signals at δ_H 6.89, 7.15 and 7.45 could be from protons attached to nitrogens in amide bonds. This suggests that a peptide could be present in the sample. However, the signals are extremely weak and may be from an impurity. Despite this improvement in the ^{1}H NMR spectrum of the active sample, the spectrum peaks could still not be integrated or correlated accurately. Therefore, no structural information could be garnered to aid the identification of the 58 Da monomer hypothesised to constitute *m/z* 888 and additional fractionation steps were required.

Table 3.15: Mean antiplasmodial and cytotoxicity data of fraction 870 against *P. falciparum* NF54, CHO, HepG2, and human erythrocytes, N=2 biological repeats with 4 technical repeats.

Sample	Antiplasmodial activity against *P. falciparum* NF54 IC_{50} (ng/mL)	Cytotoxicity against Chinese Hamster Ovary IC_{50} (µg/mL)	Cytotoxicity against HepG2 IC_{50} (µg/mL)	Haemotoxicity against Human Erythrocyte IC_{50} (µg/mL)	Selectivity Index (SI) (Cell IC_{50}/ NF54 IC_{50})
Fraction 870	128 ± 12	> 100	> 100	> 100	> 781
Emetine	-	0.024 ± 0.001	0.016 ± 0.002	-	-

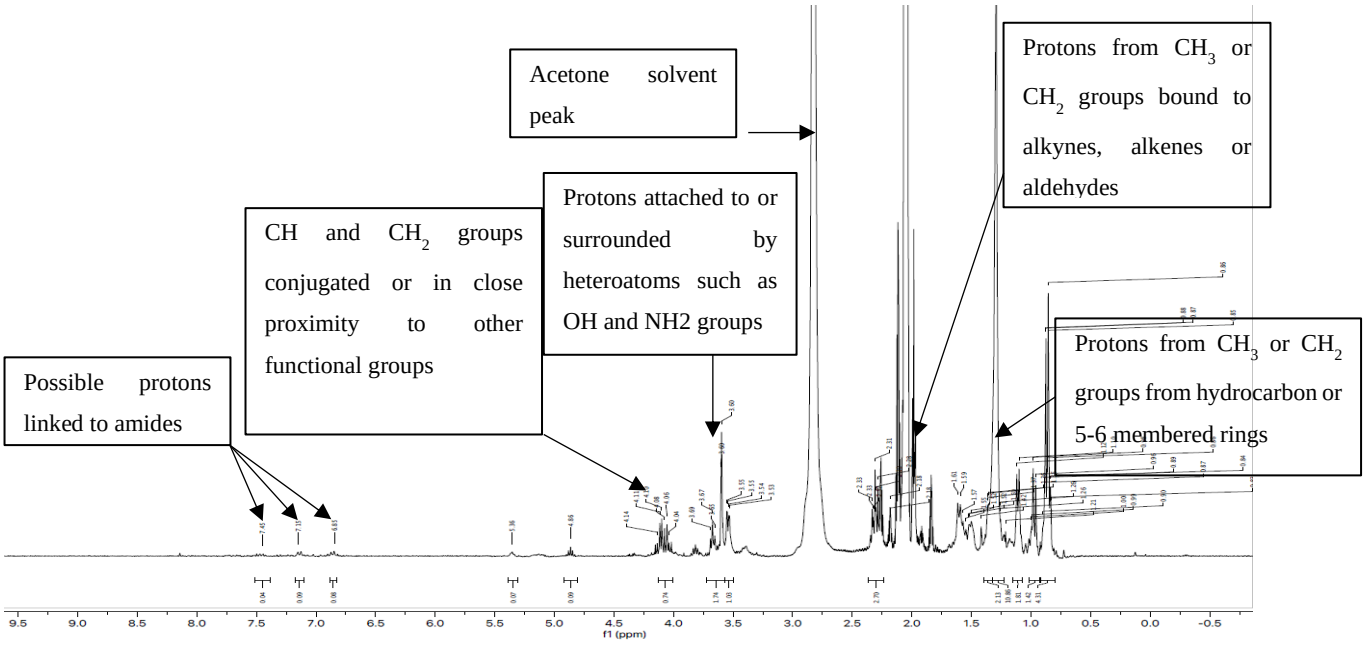

Figure 3.17: ^{1}H NMR spectrum of compound 870 partially purified by HPLC-MS.

3.3.6 Normal Phase Solid Phase Extraction

After the use of several reverse phase SPE and HPLC methods, normal phase SPE was utilized to fractionate the active samples. While the HPLC-MS technique was very useful at assigning a *m/z* to the antiplasmodial compound, the yield of material was very low. For both fraction 540 and 870, dozens of HPLC injections of 20 mg/mL RP SPE MeOH samples were required to obtain just over a milligram of active sample. To reduce the time required to purify fraction 870, normal phase (NP) SPE was used after RP SPE. PHREE separation was not used as NP was predicted to be capable of separating lipids and non-polar molecules from fraction 870. The active MeOH fraction generated by SPE Method #3 (section 3.2.3.3) was separated by NP SPE using SPE Method #5 (section 3.2.3.5).

Each fraction was collected, dried under $N_{2,}$ and made to 10 µg/mL in MeOH and 10 µL of each NP SPE was injected and scanned by IDA using HPLC-MS Method #1 (section 3.2.5.1). The results were analysed by nontarget regression analysis with the JCM #61 blank. The only fraction that contained *m/z* 888 was NP SPE EtAc fraction (#4).

Each NP SPE fraction was tested for antiplasmodial activity against *P. falciparum*, NF54 (section 2.2.4) to confirm that the activity of the pure compound 870 sample matched the HPLC-MS acquired fraction 870. A small sample of the RP SPE MeOH fraction was not purified and kept for antiplasmodial testing, to verify that the previous fractions were active. The activity of compound 870, found in the EtAc fraction (#4) and highlighted in red, did not match the activity of the HPLC-MS fraction 870 sample (Table 3.16). Fraction 870 displayed good antiplasmodial activity with a mean IC_{50} 128 ± 12 ng/mL, while the pure compound 870 displayed much weaker activity with a mean IC_{50} of 1873 ± 308 ng/mL. The controls were within the acceptable ranges. This suggested that compound 870 was not the main active antiplasmodial compound produced by strain PR3.

However, as compound 870 displayed novel MS and MS/MS spectra further study was undertaken. Ten 1 L cultures of strain PR3 were grown in JCM #61 and extracted (sections 3.2.1 and 3.2.3 respectively). These crude extracts were then separated by RP+NP SPE (sections 3.2.3.3 and 3.2.3.5 respectively). A total of 1.6 mg of fraction 870 was obtained and submitted for ^{1}H NMR analysis at the University of Cape Town (section 3.2.4). The ^{1}H NMR spectrum of fraction 870 (Figure 3.18) revealed that the sample was pure enough to attempt

structural elucidation. This can be seen by the low number of overlapping base signals and similar signal intensities (Silverstein *et* al., 2005).

As this is now a relatively pure sample it will henceforth be referred to as compound 870. Compound 870 was then submitted for more advanced 2D NMR spectrometry and the structural elucidation of compound 870 is discussed in detail in Chapter 4.

Table 3.16: Mean antiplasmodial activity of the crude MeOH RP fraction, NP SPE fractions and compound 870, N=2 biological repeats with 4 technical repeats. Fraction containing compound 870 is highlighted in red.

NP SPE Fraction	Antiplasmodial activity against *P. falciparum* NF54 IC_{50} (ng/mL)
Fraction 870	128 ± 12
RP SPE MeOH	152 ± 13
Hexane (#1)	> 5000
Hexane/EtAc (2:1) (#2)	117 ± 7.0
Hexane/EtAc (1:1) (#3)	686 ± 61
Compound 870/EtAc (#4)	1873 ± 308
EtAc/MeOH (4:1) (#5)	> 5000
EtAc/MeOH (2:1) (#6)	> 5000
MeOH (#7)	> 5000
Chloroquine	6 ± 2.1
Artesunate	2 ± 1.5

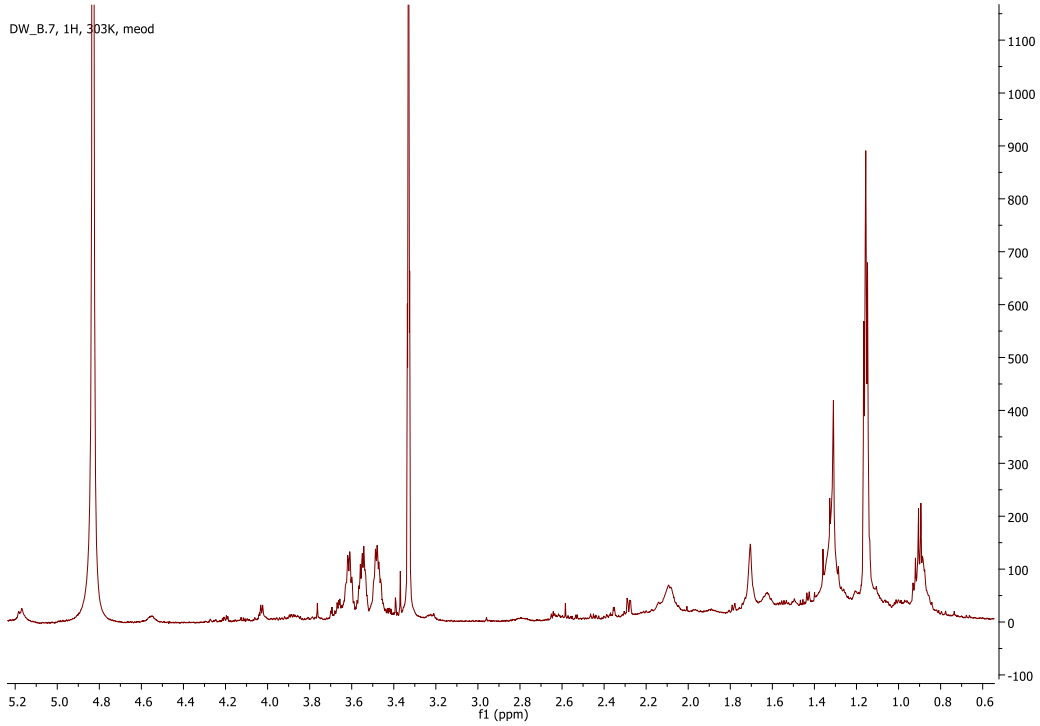

Figure 3.18: ^{1}H NMR spectrum of fraction 870 purified by RP+NP SPE.

3.4 Conclusion

In summary, many methods were developed in an attempt to purify the antiplasmodial compounds produced by *Streptomyces* strain PR3. The final purification method for compound 870 met the requirements set at the beginning of this chapter in that it uses two different SPE methods, which are quick, reproducible and can produce a pure sample. However, antiplasmodial tests revealed that compound 870 is not the major antiplasmodial compound produced by strain PR3.

The next objectives of the investigation were the structural elucidation of compound 870 and the identification of the main active compounds produced by strain PR3. Because the ^{1}H NMR and high-resolution mass spectra of compound 870 did not match that of any known compounds, it was studied further. Once the compound responsible for antiplasmodial activity in the JCM #61 fractions had been identified, the ISP-2 fractions could be analysed to determine if the same antiplasmodial compound(s) was present. The elucidation and identification of compound 870 is discussed in detail in Chapter 4. The identification of the main antiplasmodial active compound(s) produced by strain PR3 is discussed in Chapter 5.

4 Structural Elucidation of the Methylated Crown Ethers

Abstract

During bioassay-guided fractionation studies, compound 870 was associated with antiplasmodial activity and subsequently purified. Upon purification, it was discovered that compound 870 displayed weak antiplasmodial activity and was not responsible for the potent antiplasmodial activity exhibited by *Streptomyces* strain PR3. However, compound 870 displayed unique HRMS and ^{1}H NMR spectra, which did not match any known compounds. Due to this, it was studied further and discovered to be a new class of crown ether derivatives, here named methylated crown ethers (MCE). These MCEs were found to be derivatives of polypropylene glycol (PPG) found in the XAD-16N extraction resin and not natural products. The MCEs were shown to form by the cyclization of PPG oligomers, possibly by nucleophilic substitution in the presence of proton donators. The MCEs displayed weak antiplasmodial activity and exhibited no cytotoxicity against the Chinese Hamster Ovary, HepG2 cell lines or human erythrocytes, unlike crown ethers and PPG. This is the first time these structures have been reported and associated with selective inhibition of *P. falciparum* parasites.

4.1 Introduction

After the isolation of compound 870, the next step was its structural identification and elucidation. Structural identification is the process where the spectra of a compound under investigation are compared to that of known compounds (Elyashberg, 2015). If these spectra do not match any known compounds, then the compound is considered novel, and the next step is structural elucidation. The term structural elucidation refers to a full *de novo* characterization of the structure resulting in a complete molecular connection table with correct stereochemical assignments (Kind and Fiehn, 2010).

The optimum approach to structural identification and elucidation is through the use of a set of independent techniques to obtain stereochemical information. The two best techniques in this regard are NMR and HRMS.

Many atomic nuclei rotate about their own axis in a process known as spin (Dayrit and Dios, 2017). The spin of charged nuclei generates a magnetic field and creates their own magnetic moment. At a molecular scale, each atom spins in a random direction, and their magnetic fields generally cancel each other out (Bruker, 2019). However, the magnetic moments of these nuclei allow them to be aligned when exposed to a strong magnetic field. In NMR spectroscopy, a sample is exposed to a strong magnetic field forcing the nuclear magnetic moments to align parallel to this field. These nuclear magnetic moments are extremely weak and therefore do not interfere with the orientation and movement of atoms in a molecule; thus, NMR spectroscopy does not alter the molecule's structure. This is one of the benefits of using NMR in structural elucidation. While exposed to this magnetic field, the sample is irradiated with a short burst of radio waves containing well-defined resonance frequencies, a process known as Fourier transform. Specific resonance frequencies deflect different nuclear magnetic moments, which starts a rotational movement known as precession. These frequencies can be detected by an NMR spectrometer and are known as the chemical shift. The local circulation of electrons around a nucleus can shield it from the external magnetic field which alters the precession frequency of nuclei depending on the electrons around them (Silverstein *et al*., 2005). Therefore, nuclei in different chemical groups or with different neighbouring atoms will have different electron circulation and will generate unique, characteristic chemical shifts. This allows functional groups to be detected and correlated to elucidate structures (Silverstein *et al*., 2005). Shielded nuclei signals will be observed at lower precession frequencies (to the right of the NMR spectrum) and deshielded are observed at a higher precession frequency (to the left of the NMR spectrum) (Wehrli and Wirthlin, 1976).

There are different types of NMR analyses that can be conducted, each providing different kinds of information. The standard NMR approaches are ^{1}H and ^{13}C NMR spectroscopy, also known as one dimensional NMR (1D-NMR). Hydrogen is present in almost all organic molecules in its major isotopic form (^{1}H) (Dayrit and Dios, 2017). ^{1}H has an abundance of 98.9 % and displays a unique resonance frequency depending on its location in the molecule and couplings to other atoms in the same molecule. The term couplings refers to the interaction between magnetic nuclei. The chemical shifts generated by these unique ^{1}H atoms can be used to provide an immense amount of structural data. ^{12}C lacks nuclear spin and cannot be measured

by NMR spectroscopy, therefore, the ^{13}C isotope is analysed. ^{13}C is only present in an abundance of 1.1% and thus generates weaker signals than ^{1}H. This means greater amounts of sample and longer processing times are required for ^{13}C NMR than ^{1}H NMR spectroscopy. However, as ^{13}C atoms can be surrounded by more than one pair of electrons, they generate a wider range of unique chemical shifts. Therefore, ^{13}C NMR spectroscopy provides more accurate structural data than ^{1}H NMR. 1D-NMR provides very useful data about molecular structures, which makes it a very effective tool in the study of natural products. In Chapter 3, ^{1}H NMR spectroscopy was used to estimate the purity of purified fractions. However, even when the sample is pure 1D-NMR can still produce spectra with overlapping signals. To elucidate structures, 2D-NMR techniques are required.

2D-NMR spectroscopy provides information plotted on two frequency axes instead of one (Elyashberg, 2015). This allows overlapping signals to be separated. There are many forms of 2D-NMR spectroscopies, but the ones used in this investigation were heteronuclear single quantum coherence (HSQC), correlation spectroscopy (COSY) and heteronuclear multiple-bond coherence (HMBC) (Berger and Braun, 2004). HSQC displays direct heteronuclear correlations between ^{13}C and protons (Berger and Braun, 2004). COSY analysis provides information about homonuclear correlations between vicinal hydrogens separated by three bonds. This allows the identification of neighbouring carbon atoms separated by a chemical bond. HMBC analysis reveals heteronuclear correlations between ^{1}H and ^{13}C separated by two or three chemical bonds. These techniques allow each signal from ^{1}H and ^{13}C NMR to be correlated to one another and allows the determination of the two dimensional structure of the molecule.

NMR has a number of advantages over other techniques, such as its non-destructive nature, simpler sample preparation requirements, and ability to analyse any sample as long as it contains hydrogen and carbon atoms (Dayrit and Dios, 2017). However, the equipment required is expensive, the analysis is complicated, milligrams of material are required, processing times can be lengthy, and it can suffer from limited sensitivity. Due to these limitations, HRMS needs to be used in combination with NMR to accurately elucidate molecular structures. As discussed in Chapter 3, HRMS is extremely sensitive, can analyse samples at intensities in parts per million, provides data about parent and fragment ions, and predicts molecular formulae.

In this chapter, the structural elucidation of compound 870 is discussed. The aims of the chapter were to:

1. Elucidate the structure of compound 870 by NMR and HRMS analysis.
2. Determine if compound 870 is a known or novel compound.
3. Evaluate the antiplasmodial efficacy, cytotoxicity and haemotoxicity of compound 870.

4.2 Methodology

4.2.1 High Performance Liquid Chromatography-Mass Spectrometry

4.2.1.1 Method #5

A modified version of HPLC-MS Method #1 (section 3.2.5.1) was used to obtain accurate MS/MS data. The only variation in the method was the increase in collision energy (CE) to 55-85 eV.

4.3 Results and Discussion

4.3.1 Structural Elucidation of [150]crown-15

By the end of the investigations described in Chapter 3, a set of methods had been developed, which allowed purification of compound 870. Analysis of the purified sample by ^{1}H NMR spectroscopy (section 3.2.4) confirmed that the sample was pure enough to elucidate the structure of compound 870. At this stage, the ^{1}H NMR and MS and MS/MS spectra of compound 870 did not match those of any known compound in the ChemSpider, Mass Bank, or SciFinder databases. The final structure was elucidated by 1D and 2D NMR (section 3.2.4) and HRMS. HRMS analysis was conducted using HPLC-MS Method #1 and HPLC-MS Method #5 (sections 3.2.5.1 and 4.2.1 respectively). HPLC-MS Method #5 used a higher collision energy to obtain more structural data.

Compound 870 was isolated as a brown amorphous solid with an observed mass of 870.6271 Da based on HRMS analysis. As discussed previously, analysis of compound 870's MS/MS spectrum (Figures 3.16 and 4.1) revealed a repeating pattern of 58 Da which suggested it was a polymer. Analysis of the MS/MS spectrum of compound 870 at a higher collision energy (section 4.2.1) revealed repeating mass shift of 58 Da adding further evidence that compound 870 was a polymer (Figure 4.2).

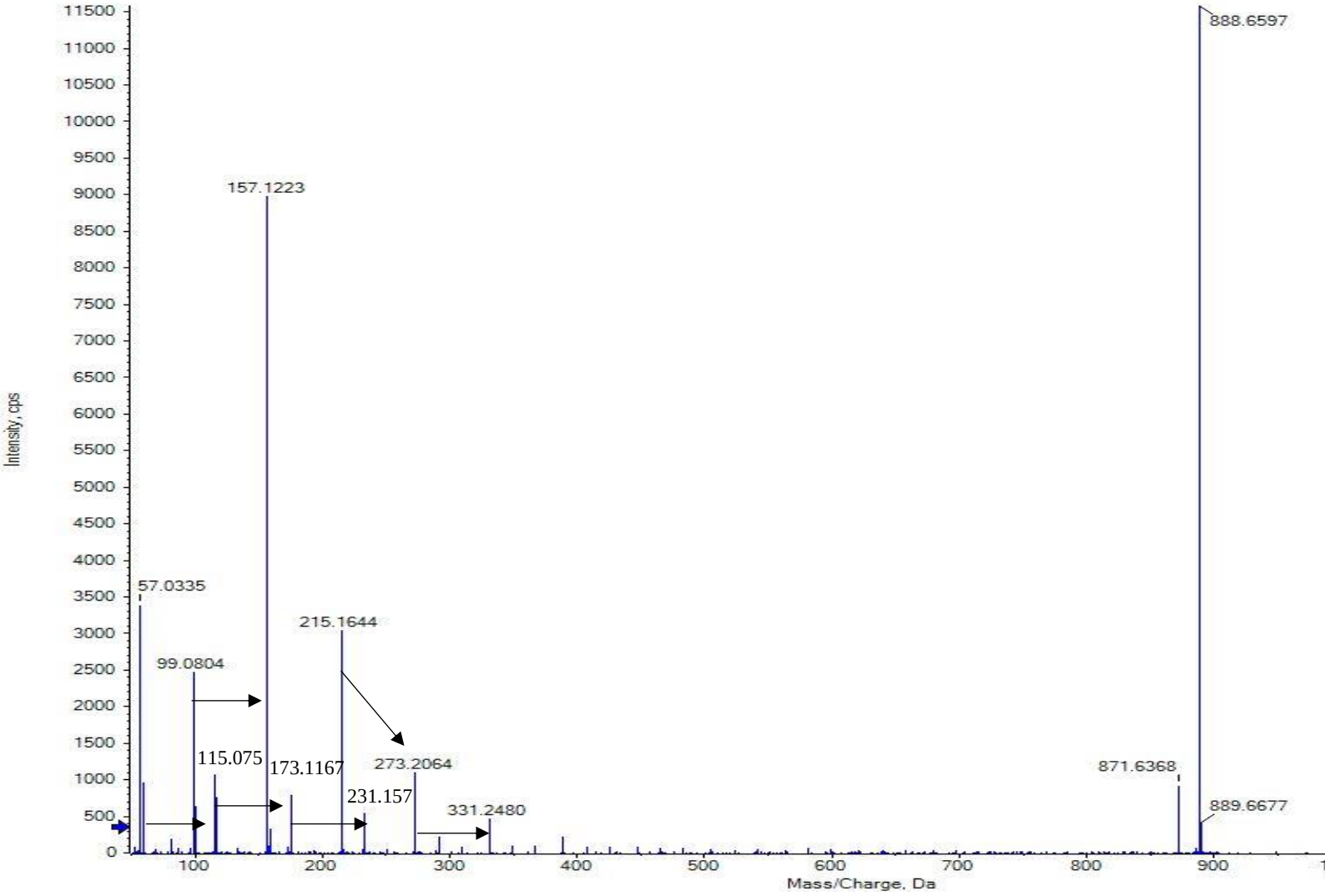

Figure 4.1: MS/MS spectrum of [150]crown-15 obtained by HPLC-MS Method #1 (lower collision energy). Black arrows represent neutral loss pattern of 58 Da.

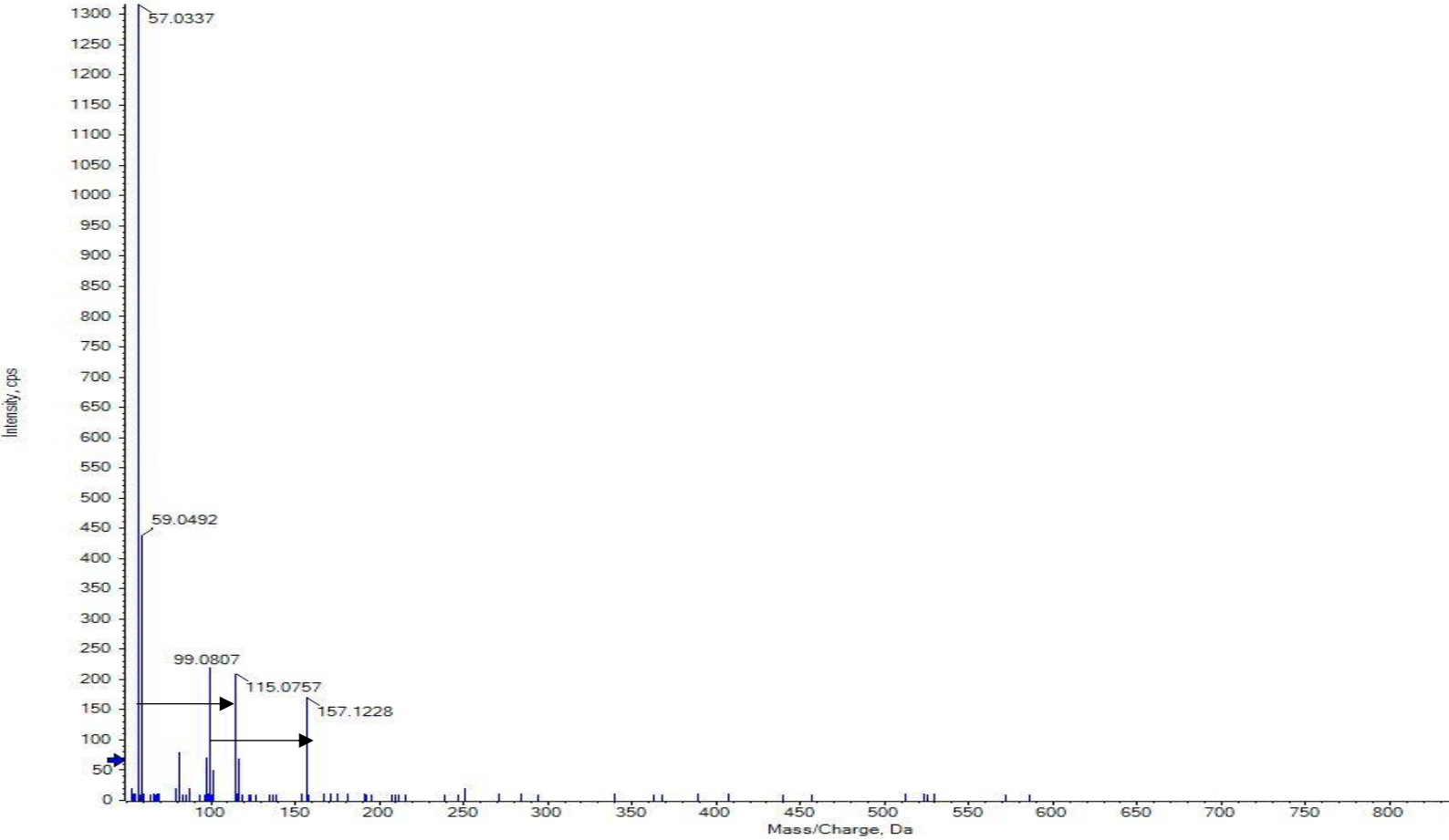

Figure 4.2: MS/MS spectrum of [150]crown-15 obtained by HPLC-MS Method #5 (higher collision energy). Black arrows represent neutral loss pattern of 58 Da.

However, no other information about the monomer could be obtained from the mass spectra. To identify the monomer and other possible groups that constitute compound 870, ^{1}H, ^{13}C, HSQC, COSY and HMBC NMR analysis were undertaken at the University of Cape Town (section 3.2.4). The major signals detected from the ^{1}H NMR spectrum of compound 870 (Figures 3.16 and 4.3) were δ_H 0.70, 1.16 and 1.30, 3.48, 3.55 and 3.63. The signals at δ_H 0.70 and 1.16 represent shielded signals as they are lower on the NMR spectrum and were predicted to be from protons in free methyl groups (Silverstein *et al*., 2005). The signal at δ_H 1.30 was predicted to correspond to a methylene group (Silverstein *et al*., 2005). The signals at δ_H 3.48, 3.55 and 3.63 were predicted to be signals corresponding to methylene and methine groups attached to either of the heteroatoms, oxygen or nitrogen. The ^{13}C NMR spectrum (Figure 4.4) revealed three main signals, one at δ_C 16.22 which represents a shielded carbon signal and corresponds to a carbon in a methyl group (Silverstein *et al*., 2005). Another signal was present at δ_C 29.00 which was predicted to correspond to the carbon in a free methylene group (Wehrli and Wirthlin, 1976). Two signals were detected at δ_C 72.87 and 75.3 which were believed to

correspond to the carbons in a methylene and methine group respectively. These chemical shifts represent deshielded signals and suggest that the methylene and methine groups are attached to a heteroatom, in this case the specific chemical shifts suggest an oxygen group (Silverstein *et al*., 2005, Wehrli and Wirthlin, 1976). The HSQC spectrum correlated the three signals at δ_C 16.22, 72.87 and 75.3 from the ^{13}C NMR spectrum to the signals at δ_H 3.48, 3.55, 3.63 and 1.16 from the ^{1}H NMR spectrum (Figure 4.5). The HSQC spectrum also correlated both methylene signals at δ_H 3.48 and 3.55 to one carbon which suggested that they are two diastereotopic protons attached to a chiral carbon. The HSQC revealed that the signal at δ_C 29.00 is an impurity as it was not linked to any other signals. The ^{1}H-COSY spectrum shows that the methine group is linked to the methylene and methyl group and that the two methylene signals at δ_H 3.48 and 3.55 are linked together (Figure 4.6). This corroborates the results obtained from the HSQC spectrum. The HMBC provides further support for these correlations and links the methyl group to the methine and the methylene signals to the methine group (Figure 4.7). The other signals detected in the ^{1}H and ^{13}C NMR spectra are therefore impurities as they did not correlate to any other signals in the ^{1}H-COSY, HSQC or HMBC. From the NMR spectra it was deduced that a methyl, a methylene and a methine group were present and linked together. From the ^{13}C NMR spectrum (Figure 4.4) it was hypothesised that the methylene and methine were attached to an oxygen group. This generates a molecular formula of C_3H_6O which has a theoretical mass of 58.041 Da. This matched perfectly to the predicted monomer seen in HRMS. The signals from the ^{1}H and ^{13}C NMR spectra (Figure 4.3 and 4.4) were not properly resolved which suggested that the signals were generated by the same groups in different parts of the molecule. This suggests that these groups are repeated many times in the compound 870 which supported the hypothesis that compound 870 is a polymer. Analysis of the groups suggested that the monomer that constitutes compound 870 is an ether as the methylene and methine groups are bound to an oxygen, but no other groups were detected. The proposed ether monomer's structure is displayed in Figure 4.8 with corresponding ^{1}H-COSY and HMBC signals and has been annotated onto the ^{1}H, ^{13}C, ^{1}H-COSY, HSQC and HMBC NMR spectra (Figures 4.3-4.7). The NMR results for the ether monomer are summarized in Table 4.1. It was previously predicted that compound 870 was comprised of 15 58 Da subunits as its mass is equal to 15 multiplied by 58. This implies that compound 870 is cyclic, only comprised of repeating subunits as no capping or tail end groups were detected by HRMS and NMR. Therefore, the final proposed structure of compound 870 is a cyclic polyether comprised of 15, 58 Da ether monomers (Figure 4.9).

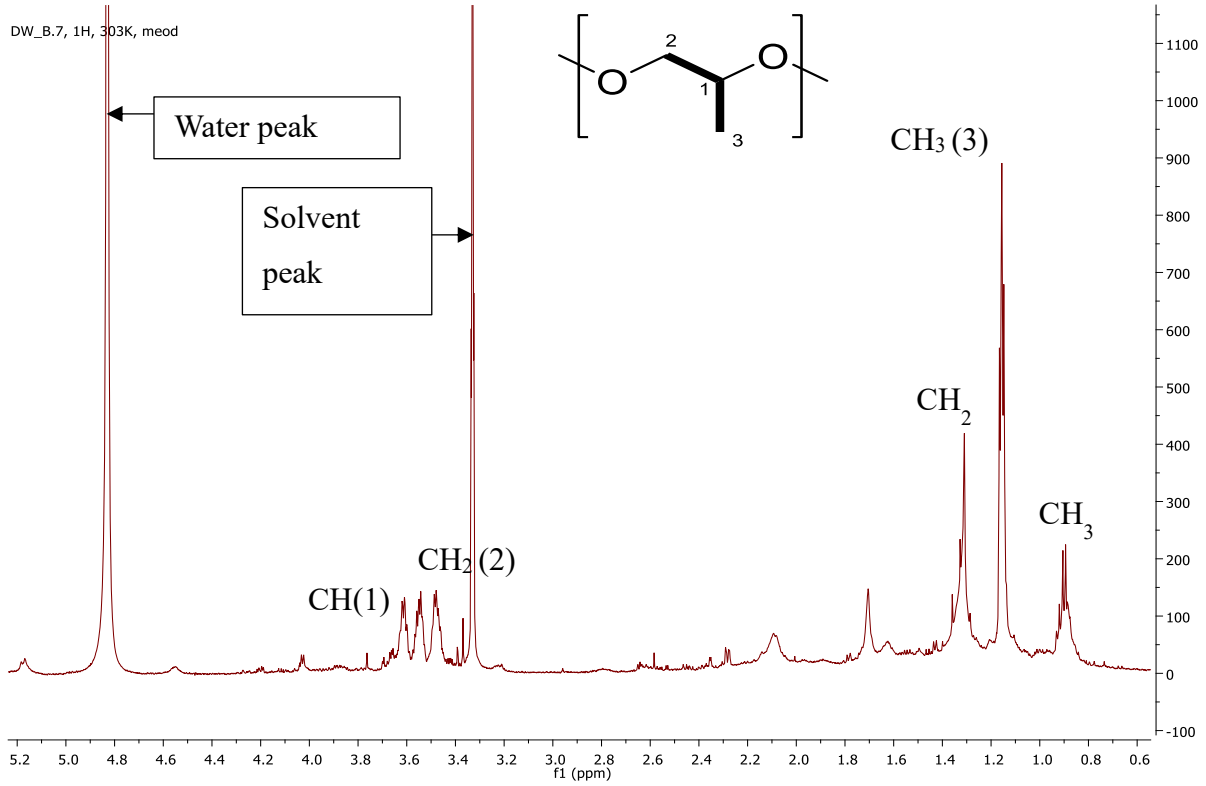

Figure 4.3: ^{1}H NMR spectrum of compound 870 annotated with protons linked to ether monomer and impurities. The structure of the ether monomer is presented with each group numbered.

The proposed structure of compound 870 is displayed in Figure 4.8 Compound 870 resembles a crown ether and, therefore, was named following crown ether convention. Crown ethers are named as [m]crown-n, where m represents the total number of atoms and n represents the number of oxygens present in the macrocycle (Liu *et al.*, 2017). Henceforth, compound 870 will be referred to as [150]crown-15. [150]crown-15 has a chemical formula of $C_{45}H_{90}O_{15}$ with a theoretical mass of 870.6274 Da with an observed mass of 870.6271 Da, mass error -0.3 ppm.

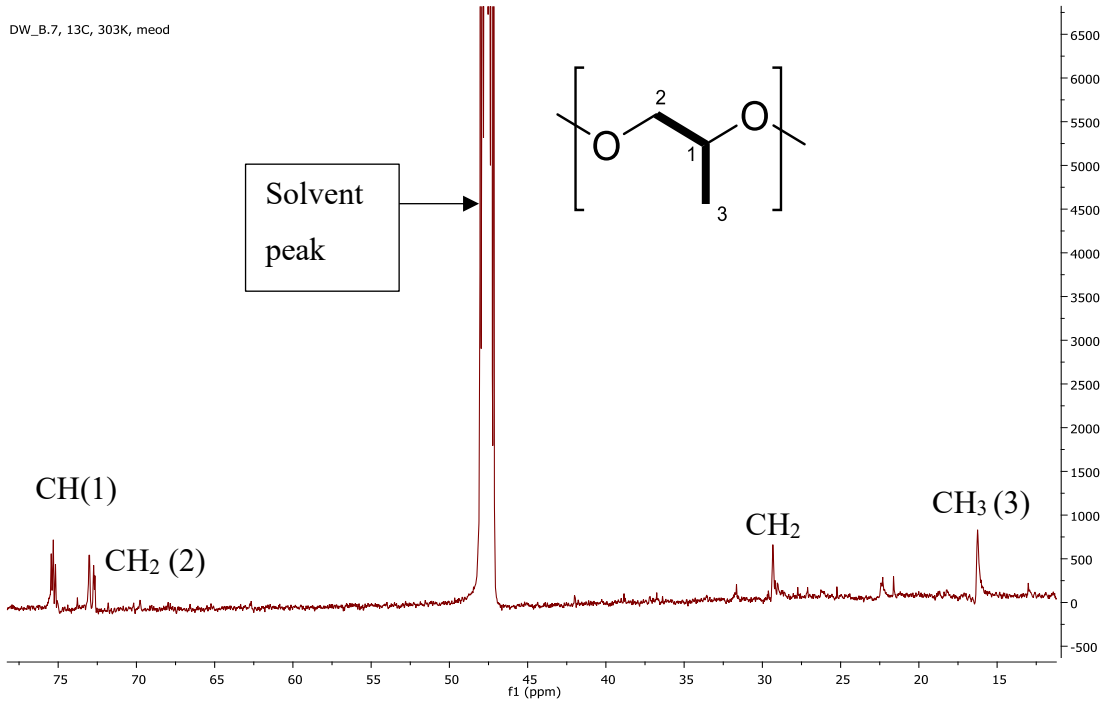

Figure 4.5: ^{13}C NMR spectrum of compound 870 annotated with carbon signals from ether monomer. The structure of the ether monomer is presented with each group numbered.

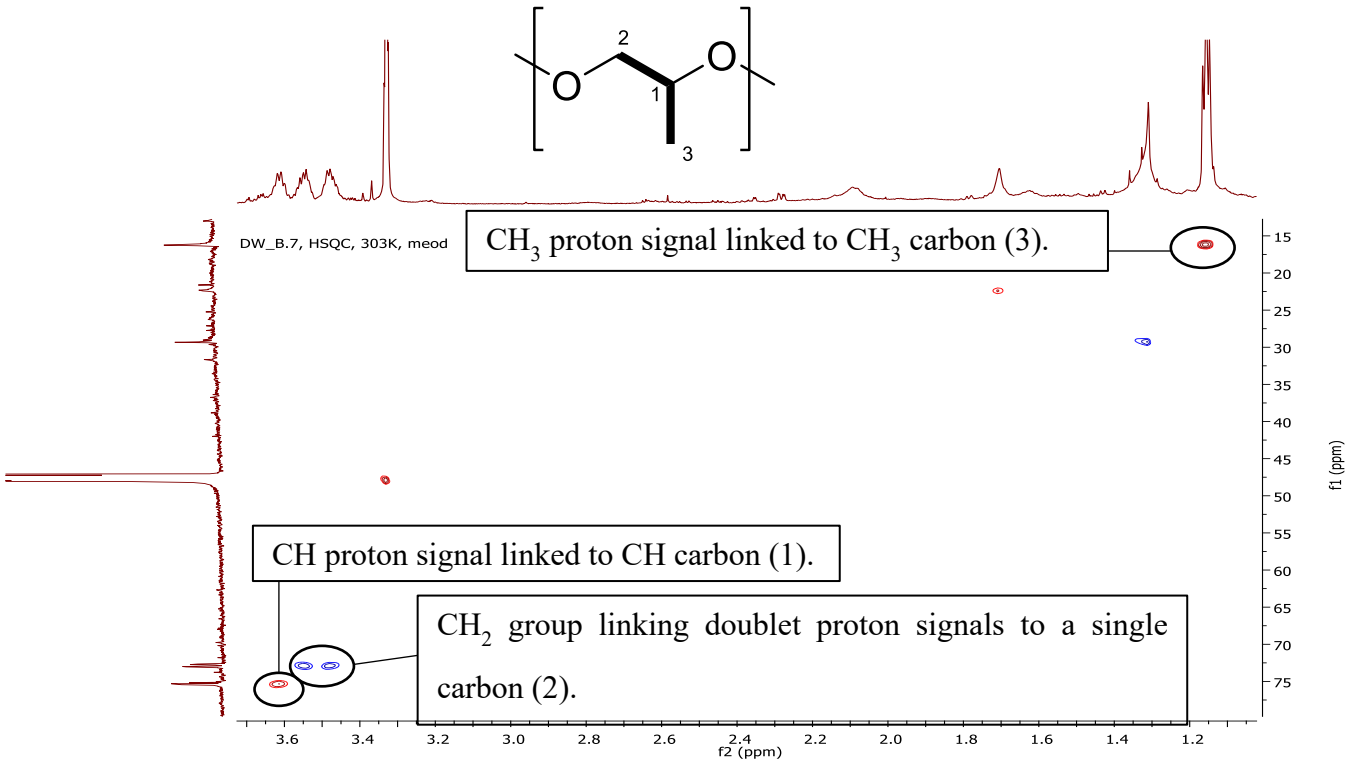

Figure 4.4: HSQC NMR spectrum of compound 870 annotated with proton carbon signal correlations. The red signals represent CH or CH_3 groups and the blue signals represent CH_2 groups.

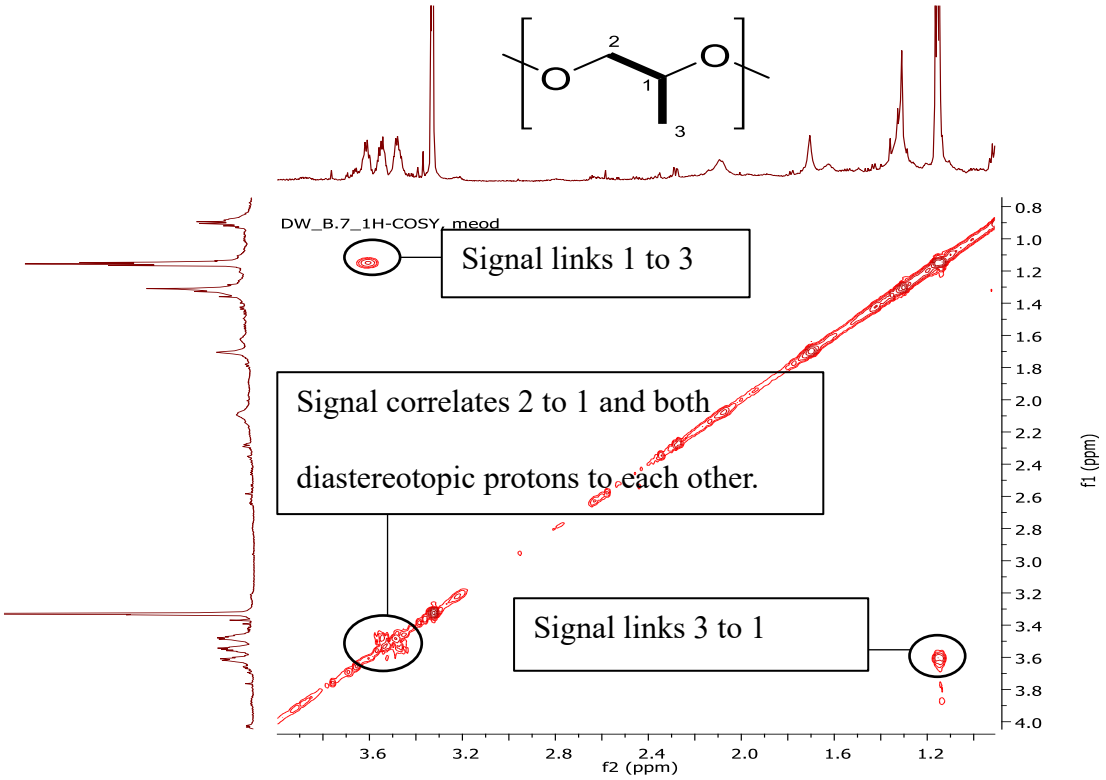

Figure 4.6: ^{1}H COSY spectrum of compound 870 annotated with each correlation. The structure of the ether monomer is presented with each group numbered.

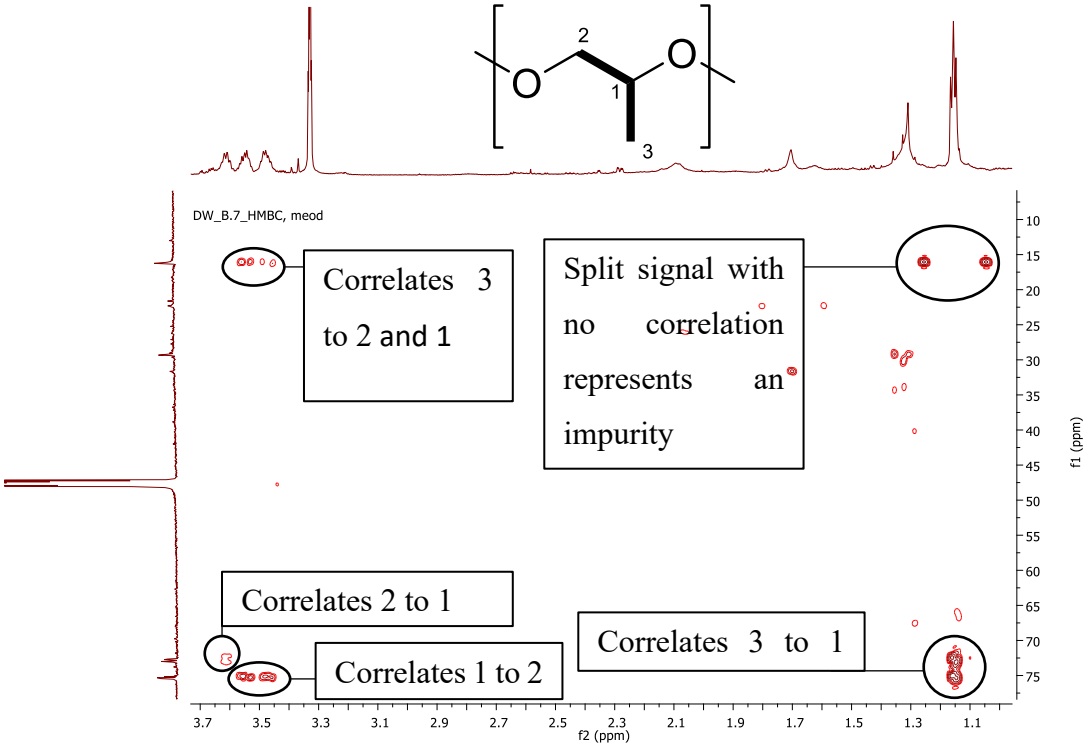

Figure 4.7: HMBC spectrum of compound 870 annotated with signal correlations.

Table 4.1: Selected ^{13}C, ^{1}H, COSY and HMBC data for [150]crown-15.

Position	^{13}C	^{1}H mult	^{13}C-^{1}H COSY	^{13}C-^{1}H HMBC
1	75.3, CH	3.63 m	2,3	2,3
2	72.87,CH_2	3.55 3.48 m	1	1,3
3	16.22, CH_3	1.16 m	2	1,2

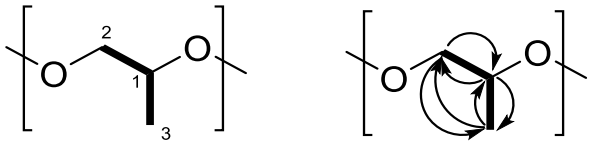

Figure 4.8: Structure and COSY (—) and HMBC (→) correlations for C_3H_6O monomer. This image was provided by K. Acquah.

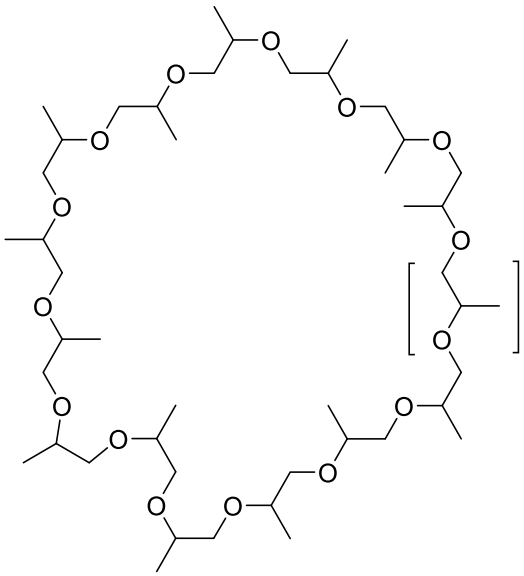

Figure 4.9: Predicted structure of [150]crown-15. The ether monomer is highlighted by the square brackets. This image was provided by G. Dziworn.

4.3.2 Characterization of the Methylated Crown Ethers

Crown ethers are synthetic macrocyclic oligomers of ethylene oxide with the formula $(-CH_2CH_2O-)_n$ where n is 4 or greater (Liu *et al.*, 2017). They are named crown ethers, as they look like a crown on the head of a monarch. Crown ethers can bind alkaline earth and transition metal cations, such as Na^+ and K^+ (Pedersen, 1967). Stable complexes are formed with the cation in the centre of the ether ring by ion-dipole interactions between the ion and oxygen atoms (Hayvali *et al.*, 2014) (Figure 4.10).

Changes in the ring size and adding functional groups to the core crown ether motif change the cation affinity (Gokel *et al*., 2004). For example, [18]crown-6 has a high affinity for K^+ ions, while [15]crown-5 has a higher affinity for Na^+ ions. Crown ethers are neutral ionophores, which means they lack their own ionisable groups, but can bind cations and transport them through hydrophobic environments such as lipid membranes. This has led to many applications in chemistry, as the discovery of crown ethers triggered massive development in the synthesis and development of macrocycles. This development led to an improved understanding of molecular recognition, binding, and mechanics. Crown ethers also have a biological effect and display a range of antibiotic properties, such as antibacterial, antifungal, antiviral, and anticancer activity (Ziedan *et al.*, 2010; Flipo *et al.*, 2011; Hayvali *et al.*, 2014).

Transport of molecules and ions across cell membranes is an important function of cellular physiology (Campbell *et al.*, 2008). It is essential in maintaining homeostasis by bringing in nutrients, transporting wastes, and maintaining electrochemical gradients. In a cell, a delicate balance of ions on each side of the lipid membrane produces a voltage across the membrane known as the membrane potential. The membrane potential drives the transport of ions in and out of the cell. The voltage of the membrane potential ranges from -50 to -200 mV, therefore the cytosol of a cell is negatively charged compared to the exterior of the cell. This membrane potential favours the transport of cations into the cell and anions out of the cell.

Ions also move down a chemical concentration gradient typically from the exterior to the interior of the cell. These two forces create an electrochemical gradient, which is essential for cell survival. If there is a pH difference between the interior and exterior of the cell, it produces another driving force across the cell membrane known as the proton motive force (Fong, 2016).

Crown ethers and other neutral ionophores bind cations and facilitate their passive diffusion down the electrochemical gradient. The increased transport of cations into the cell decreases the membrane potential across the cell membrane. This collapses the electrochemical gradient, which alters ion transport and has downstream cytotoxic consequences. This is why the crown ethers display activity against such a wide range of microorganisms and cells.

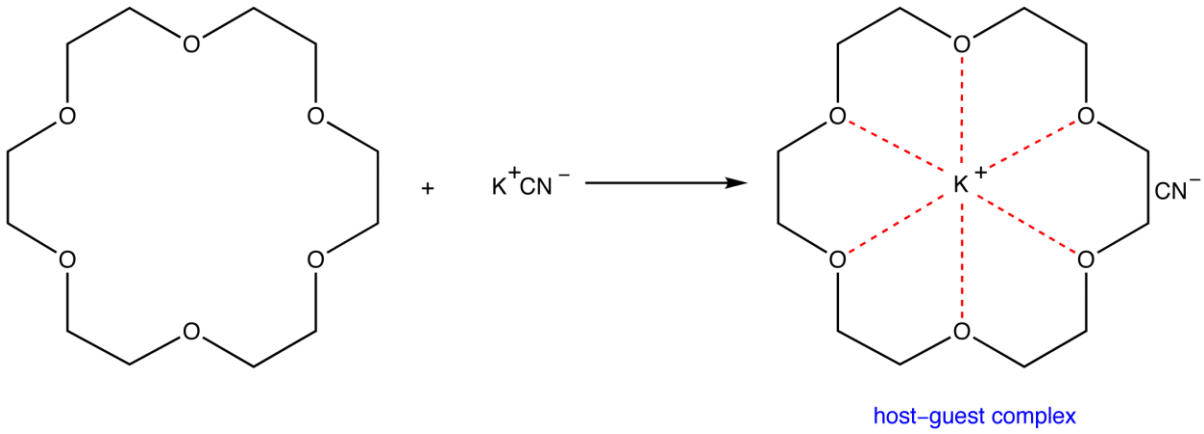

Figure 4.10: [18]Crown-6 ether forming a stable complex with a K^+ ion in the centre of the ring (OChemPal).

After searching literature and multiple databases (SciFinder, Pubchem, Chemspider, KEGG and Massbank), one match was found reporting the same formula and mass spectra as those of [150]crown-15 (Rindelaub *et al.* 2019).

In an investigation of the extractable profiles of 3D printed medical implants, plastic oligomers were isolated that had the same formula and mass spectra as [150]crown-15 (Rindelaub *et al.*, 2019). In this investigation, medical implants were exposed to three different solvents: water, isopropyl alcohol, or hexane, while shaking at 50°C for 72 hours. The extracts were then analysed by LC-HRMS and GC-MS. The MS and MS/MS results of the isopropyl alcohol samples matched those of [150]crown-15. This sample was reported to contain polypropylene glycol (PPG) oligomers, which leached out of the implants. PPG is comprised of the same 58 Da subunit as [150]crown-15, with a hydroxyl group at each end of the chain. PPG has a variety of applications in many fields. It is used as a plasticizer, lubricant, and intermediate in the synthesis of polyurethane (Oudhoff *et al.*, 2003). PPG is copolymerized with polyethylene glycol (PEG) to create a stronger composite plastic used to manufacture many plastic products. In addition, PPG has uses outside the manufacturing of plastics. For example, PPG-PEG has been used as a vessel in drug delivery and been shown to improve drug solubility *in vivo* (Yapar and Ýnal, 2013).

To confirm if [150]crown-15 was an oligomer of PPG, the next step was to determine if *Streptomyces* strain PR3 was producing [150]crown-15 or if it was being isolated from background components. To achieve this, a new blank of JCM #61 medium was created. The previous JCM #61 blank (section 3.3.5) did not contain [150]crown-15 and was not active against *P. falciparum*, NF54 (Table 3.14). However, the previous JCM #61 blank sample had not been processed with the XAD 16-N resin or separated by NP SPE. Therefore, the new JCM #61 blank was generated with XAD 16-N resin and fractionated liquid medium was incubated for 10 days at 30°C, while shaking, extracted with XAD-16N resin (section 3.2.2.2 and 3.2.2.3), fractionated by RP+NP SPE (sections 3.2.3.3 and 3.2.3.5). Each fraction was collected, dried down, re-dissolved, and 100 µL of 10 µg/mL was injected and processed by HPLC-MS Method #1 (section 3.2.5.1). A sample was taken from the JCM #61 blank, Gram stained and streaked for single colonies. No microbial growth or presence was detected verifying that only the media components were present. The HRMS results revealed that [150]crown-15 was present in the crude blank, RP SPE MeOH fraction and the NP SPE EtAc (#4) blank. This proved that [150]crown-15 was not a natural product produced by strain PR3, but was likely a PPG oligomer.

PPGs are routinely used to calibrate mass spectrometers, as they display characteristic MS and MS/MS signals, such as a neutral loss pattern of 58 Da and a peak of *m/z* 175 Da (Matsuo *et al.*, 1979; Rindelaub *et al.*, 2019). A calibration sample of PPGs (Sciex®, Johannesburg, South Africa) at a concentration of $1*10^{-5}$ M, was tested using HPLC-MS Method #1 (section 3.2.5.1). [150]crown-15 was found to be present in this PPG calibration sample. The more typical, linear form of PPG were also detected. MS/MS spectra characteristic of linear PPGs, with 175 Da peaks and neutral losses of 58 Da, were detected in the PPG calibration sample (Figure 4.11) (Rindelaub *et al.*, 2019). These linear chains were not found in the JCM #61 blank or strain PR3 extracted active samples.

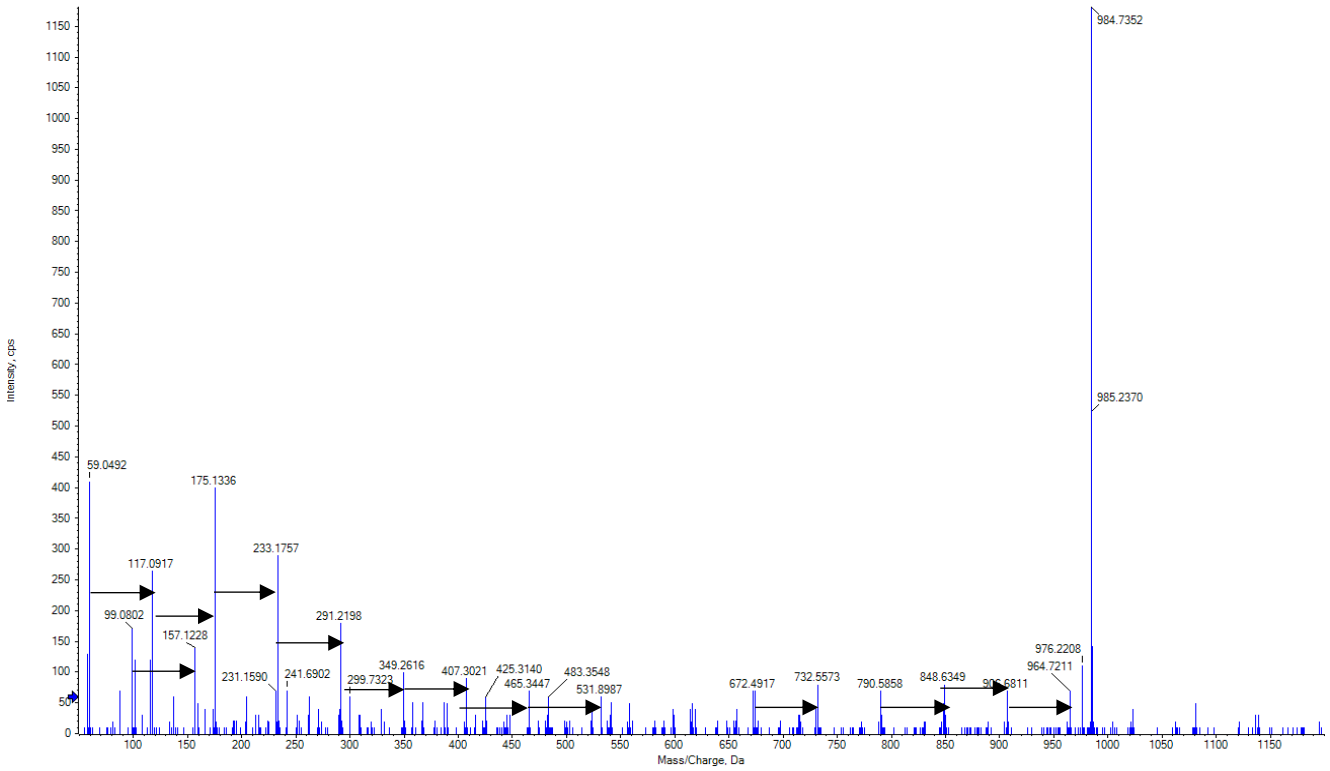

Figure 4.11: Linear PPG MS/MS with characteristic *m/z* peak of 175 Da and neutral loss pattern of 58 Da. Black arrows represent mass shifts of 58 Da.

At this point in the investigation, it had been confirmed that [150]crown-15 was not a natural product, but likely an oligomer of PPG. However, there were two major questions that needed to be answered.

Firstly, what was the source of [150]crown-15? [150]crown-15 was found in the crude blank sample extracted from JCM #61 medium. This showed that it was coming from a component used in the extraction process and not leaching out of plastic products, such as pipette tips and benchtop centrifuge tubes, during fractionation.

Each component used in the crude extraction was examined by HRMS to identify the source of [150]crown-15. Ten microlitres of each of the solvents used in the extraction process (MeOH and EtAc) were injected directly, without dilution, and analysed using HPLC-MS Method #1 (section 3.2.5.1). The coffee filters and XAD-16N resin used in the extraction methods were washed repeatedly with the same extraction solvents separately and tested in the same manner. None of these samples contained [150]crown-15.

The ingredients used to make the growth media for strain PR3 were also examined. [150]crown-15 was found in both ISP-2 and JCM #61 media, and the only ingredient common to both media was the yeast extract. Therefore, 5 g of dry yeast extract was washed with 50 mL of EtAc for 30 minutes. The solvent was filtered through coffee filters into a glass beaker, then reconstituted in a glass vial, and 10 µL of a 100 µg/mL sample was tested using HPLC-MS Method #1 (section 3.2.5.1). This sample also lacked [150]crown-15.

The second question was, if [150]crown-15 is a PPG oligomer, how is it cyclizing? PPG is a linear chain made up of propylene oxide monomers capped by a hydroxyl group at each end (Rindelaub *et al.*, 2019). As discussed earlier, the HRMS and NMR strongly suggested that [150]crown-15 is cyclic. This meant that either the data was incorrect and the molecules were linear, or [150]crown-15 is formed by the cyclization of PPG oligomers during the extraction process.

Both questions were answered in collaboration with Dr Joel Rindelaub from the Department of Chemistry at the University of Auckland, New Zealand. He hypothesised that the PPG oligomers could indeed cyclize by nucleophilic substitution and this would likely occur in the presence of proton donators, such as under aqueous or acidic conditions. Dr Rindelaub proposed a mechanism of cyclization (Figure 4.12). To determine if this mechanism was correct, 100 µL volume of water was added to the EtAc and MeOH-washed samples (filters, resin and yeast extract). Ten microlitres of each mixed sample was resubmitted for HRMS analysis by HPLC-MS Method #1 (section 3.2.5.1). [150]crown-15 was found in the MeOH and EtAc XAD-16N resin samples after water was added.

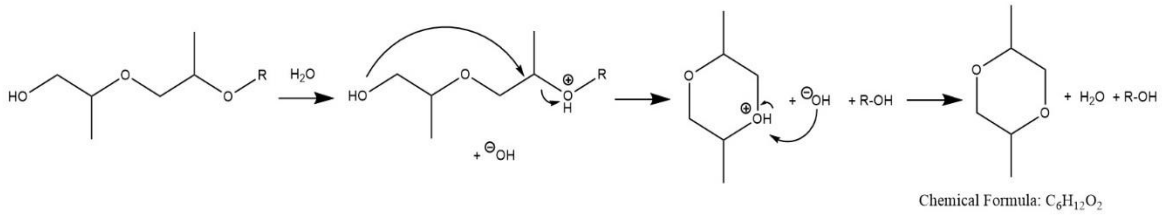

Figure 4.12: Possible mechanism of cyclization of PPG chains into methylated crown ethers. This diagram was provided by J. Rindelaub.

Thus, the mystery of the origin of [150]crown-15 was solved. It was now known that the XAD-16N resin was the source of [150]crown-15, which explains why it was not in the original JCM

#61 blank. XAD-16N resin was not used in the preparation of that blank sample. The PPGs could not have come from the resin itself, as the resin has a styrene-dibenzyl structure and shares no structural similarity with PPG oligomers (Sigma, 1998). Proton donators such as water, are required for the nucleophilic substitution reaction, which is why [150]crown-15 was only seen in the EtAc and MeOH washed resin when water was added. It also could explain how [150]crown-15 forms in terms of the extraction process followed. When extracting the culture broth of strain PR3, the XAD-16N resin is added to the liquid culture prior to solvent extraction, then the PPGs introduced with the resin are exposed to the required aqueous environment and cyclize. The resulting MCEs are then extracted into the organic solvent and purified during the SPE purification steps.

Rindelaub *et al.* (2019) reported multiple oligomers with a mass difference of 58 Da between them. Using the IDA explorer tool on OS Sciex, the HRMS sample containing [150]crown-15 was analysed for other compounds with similar fragmentation patterns. The search parameters were set to find compounds that contained the major fragments of [150]crown-150: *m/z* 57, 157, 215 and 331, as well as fragments with a neutral loss of 58 Da.

A range of compounds with matching MS/MS patterns were seen (Figure 4.13). Each compound had a mass difference of 58 Da from the next and a unique retention time, which implies that they are distinct and separate molecules and not fragments of a larger compound. The series of compounds related to [150]crown-15 is annotated in the blue ellipse in Figure 4.13. Each of these is an ammonium adduct and contains the same MS/MS fragmentation pattern as [150]crown-15. This suggests that there are multiple MCEs present. This correlates with the unresolved peaks signals seen in the NMR data. The NMR signals from the ether

subunit were not only generated multiple times from within one structure, but from many structures.

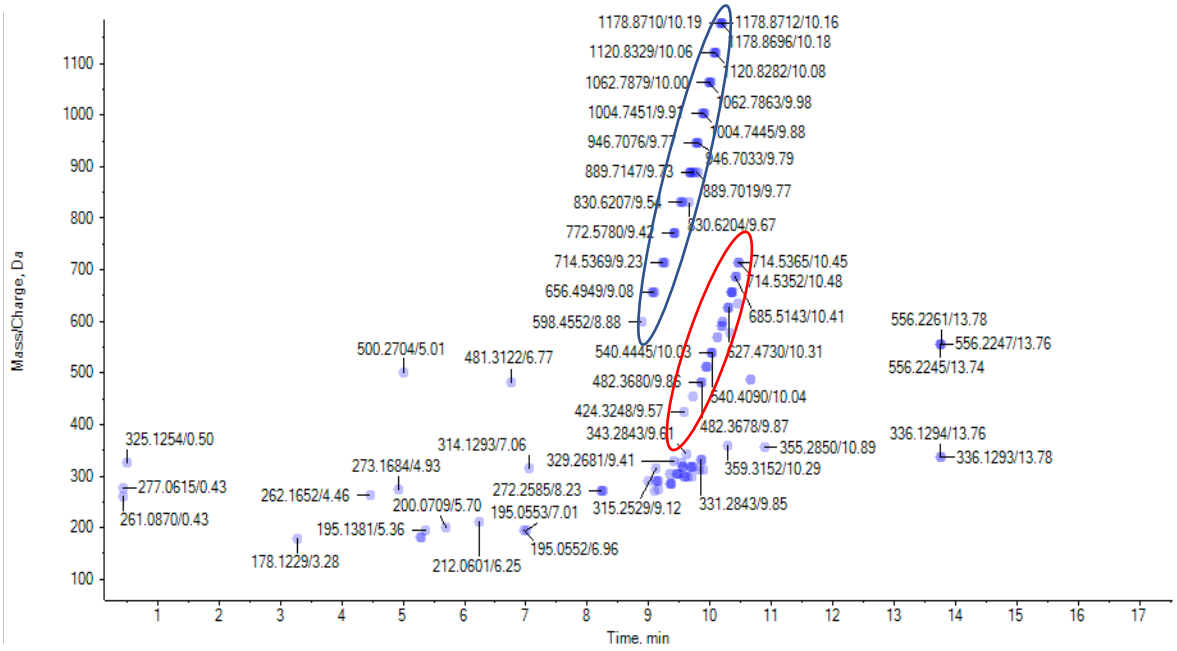

Figure 4.13: The series of methylated crown ethers is presented. The blue ellipse shows the series of singly charged methylated crown ethers. The red ellipse highlights the series of multiply charged methylated crown ethers. The numbers next to each data point are the accurate mass and retention time.

A smaller series of MCEs was seen running parallel to the main series at a later retention time. This parallel series is shown in the red ellipse and was reported to have a lower *m/z* than the larger series shown in blue. This is contradictory to our understanding of these compounds, because larger MCEs would be more non-polar and therefore should have a later retention time when separated by reverse phase chromatography. Further analysis showed that the compounds in the parallel series, shown in the red ellipse, were carrying multiple charges. Therefore, they had a larger true mass than the ones indicated by the blue ellipse, but displayed a lower *m/z*. Ten microlitres of a 100 µg/mL solution of the purified sample containing [150]crown-15 and the related compounds were analysed by HPLC-MS Method #1 (section 3.2.5.1). The method was modified by changing the mass range from 50–1200 Da to 1000–2000 Da. The same fragmentation search parameters were applied as before, and more related MCEs were detected (Figure 4.14). The number of different related compounds produced is erratic, however, there were at least 16 different MCEs with the same structural motif as [150]crown-15 detected (Figures 4.13 and 4.14). All the m/z's represent ammonium adducts and, thus, their true mass

is their ionised mass – 18.0347 Da divided by 58. The smallest MCE observed had a *m/z* 366.2865, composed of 6 subunits. The largest MCE observed had a *m/z* of 1566 Da, which is composed of 27 subunits. The empirical formula of these compounds is C3nH6nOn, where n is the number of 58 Da monomers.

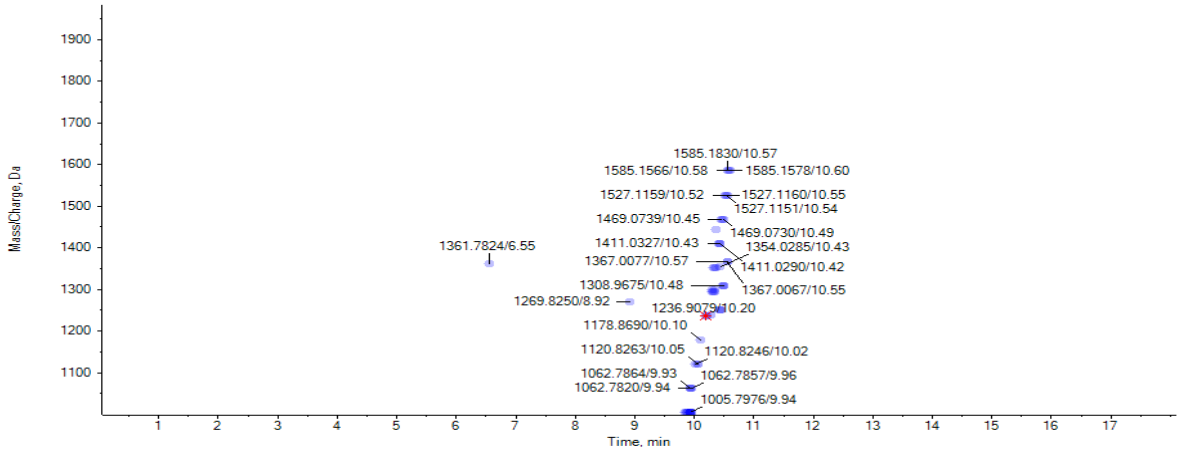

Figure 4.14: Series of larger (*m/z* >1000) methylated crown ethers. The numbers next to each data point are the accurate mass and retention time.

The MS PPG calibration sample was also examined for multiple MCEs. The PPG calibration sample contained the same MCE series as seen in the isolated fraction (Compare Figure 4.15 to Figures 4.13 and 4.14). This provides further evidence that the MCEs originate from PPG.

In summary, the data presented strongly suggests that the compounds isolated in Chapter 3 are a series of MCEs formed by the cyclization of PPG oligomers in the presence of proton donators. It must be noted that the presented mechanism is only a proposed mechanism of cyclization and, while it seems proton donators such as water, are required for cyclization; the exact mechanism could be different and needs to be studied further.

While the NMR and HRMS spectra suggest that the structure of [150]crown-15 is accurate, the exact three-dimensional structure is unknown. Molecular models have predicted that PPG oligomers can form a doughnut shape, which correlates to the crown ether structures, or a disc-coil shape (Sandell, 1970). These models were determined mathematically, and no NMR data was generated on these oligomers in solution, so a direct comparison with the isolated MCEs is impossible. Other than those predictions, to the author's knowledge, MCEs and the cyclization of PPG oligomers into MCEs have not been reported. PPG is an extremely common and well-known molecule; therefore it is odd that this phenomenon has not been described. It

is possible that these MCEs have been found by other researchers, but were not separated from linear PPG chains or did not display any interesting characteristics, so were not studied further.

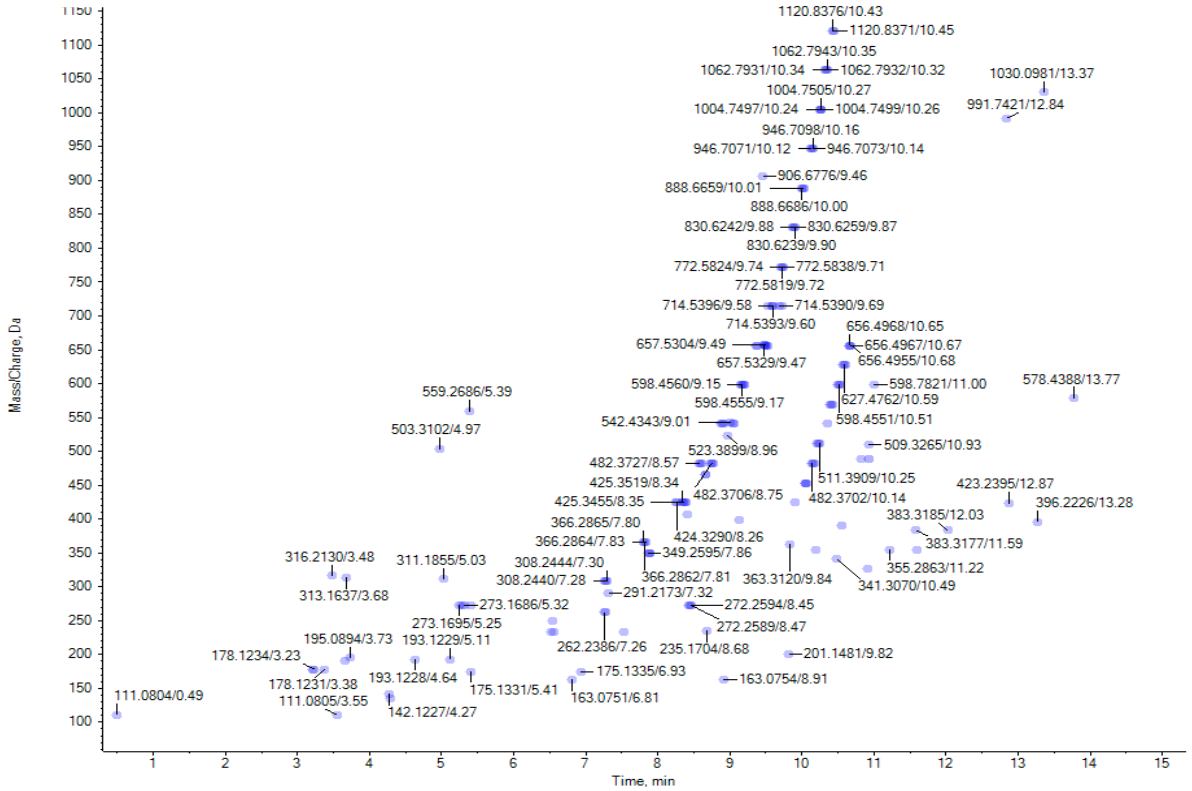

Figure 4.15: Series of methylated crown ethers displayed in PPG calibration sample. The numbers next to each data point are the accurate mass and retention time.

4.3.3 Antiplasmodial Efficacy and Selectivity of the Methylated Crown Ethers

The discovery of the MCEs has potential significance in the field of chemistry. More work needs to be done to understand if these structures have other applications. While the cyclization of the PPGs into the MCEs is an interesting phenomenon, it is not the main focus of this investigation and to determine if the MCEs could be lead drug candidates, they were tested for antiplasmodial activity against NF54 (section 2.2.4).

The PPG MS calibration sample was used as a comparison in these studies as it contained both the linear PPGs and MCEs according to HRMS analysis (Figures 4.13, 4.14, and 4.15). If no difference in activity between the two samples was detected, this would suggest that the MCEs

are solely responsible. Alternatively, a difference in antiplasmodial activity would suggest that the linear PPGs are active against *P. falciparum*. RP+NP SPE Fraction #4 produced by SPE Method #5 (section 3.2.3.5), shown to contain the pure MCEs was used for antiplasmodial activity determination (section 2.2.4). The MCEs displayed weak antiplasmodial activity with a mean IC_{50} of 1873 ± 308 ng/mL (Table 4.2). PPG displayed good antiplasmodial activity with an IC_{50} of 190 ± 20 nM. The controls were within the acceptable ranges.

Table 4.2: Mean antiplasmodial activity of the methylated crown ethers against *P. falciparum* NF54, N=2 biological repeats with 4 technical repeats.

Sample	Antiplasmodial activity against *P. falciparum*, NF54 IC_{50} (ng/mL)
Methylated Crown Ethers	1873 ± 308
Polypropylene Glycol	190 ± 20
Chloroquine	5 ± 1.1
Artesunate	2 ± 0.5

The MCEs are predicted to act as neutral ionophores due to their proposed ring structure which is the active pharmacophore in other crown ether species (Gokel *et* al., 2004). The MCEs lack ionisable groups but, were able to form adducts. For example, [150]crown-15 formed multiple adducts detected by MS, the *m/z* 888.6659 Da ($M+NH_4^+$) was the dominant ion, likely due to the high concentration of ammonium formate in the mobile phase. The other adducts seen were proton, *m/z* 871.6368 Da ($M+H^+$), sodium, *m/z* 893.6148 Da ($M+Na^+$) and potassium, *m/z* 909.5994 Da ($M+K^+$). This is supported by Rindelaub *et al*. (2019) who reported that the leached PPGs oligomers formed NH_4^+, Na^+, K^+ and H^+ adducts. These adducts are likely forming by stable dipole interactions between the cation and oxygen groups in the centre of the crown ether ring, as discussed earlier. Their ring structure and adduct formation strongly indicates that the MCEs are also ionophores.

Ionophores are known to possess antimalarial activity and a series of ionophores, including gramicidin D, nigericin, lonomycin, and monensin, were found to display potent antimalarial activity *in vitro* and *in vivo* (Gumila *et al.*, 1997). The *Plasmodium* parasites rely on a suite of ion gradients in the human erythrocyte. As discussed in Chapter 1, the *Plasmodium* parasites remodel the human erythrocyte. Part of this remodelling is a large-scale increase in cation transport capacity. Some examples of the change in cation transport systems are increases in

K^+, Na^+, and Cl^- transport systems and the inhibition of erythrocyte ATPase membrane pumps (Ginsburg, 1994). This creates a list of targets that could be used to selectively inhibit *P. falciparum* infected erythrocytes. For example, the breakdown of globin into its peptide constituents produces ammonium wastes, which has been shown to be lethal to the parasites if not removed (Zeuthen *et al.*, 2006). Binding to NH_4^+ ions and transporting them back into the parasite or preventing their removal could be an effective mechanism of action for an antiplasmodial drug. Changes in intracellular Na^+ concentrations have been shown to impact the development of *P. falciparum* and disrupt lifecycle stage transitions (Vaidya *et al.*, 2014). The list of possible ionophore targets in *P. falciparum* is very long, and further investigation is required to determine the exact mechanism of action of these MCEs.

The PPG calibration sample was only available as a mixture of PPG chains with an unknown percentage of each oligomer. The concentration provided by the distributor stated that the mixture had a concentration of 10 µM. Therefore it was assumed that the sample stock concentration was 10 µM. The PPG MS calibration sample displayed surprisingly good antiplasmodial activity with an IC_{50} of 190 ± 20 nM against NF54. As this is a mixture of compounds this antiplasmodial activity cannot be assumed to be accurate. To determine exact IC_{50}'s each PPG chain would have to be purified and retested. This was not within the scope of this investigation and the antiplasmodial result obtained was used as an estimate for activity. The exact molecular mass of the MCEs and PPG samples is unknown, so the IC_{50}s cannot be converted into the same units. Using the results obtained it was estimated that the PPG calibration sample was more active than the MCEs. This suggested that the linear forms of PPG are contributing to this increased activity, as they are not present in the MCE sample. This could be due to a cytotoxic effect induced by the PPGs rather than selective inhibition of the *P. falciparum* parasite. However, these can only be used to estimate activity and further study on each pure individual PPG chain and cyclic oligomer would have to be done to allow a direct comparison.

To determine if the MCEs and the PPGs were selectively targeting the *P. falciparum* parasite, cytotoxicity and haemotoxicity studies (sections 2.2.6 and 2.2.7 respectively). The MCEs exhibited no signs of cytotoxicity or haemotoxicity *in vitro* up to 100 µg/mL (Tables 4.3 and 4.4). The PPGs showed no cytotoxicity at 5 µM, but did display moderate haemotoxicity with an IC_{50} of 4.22 ± 0.4 µM (Tables 4.3 and 4.4). The PPGs could not be tested at a higher concentration as they were only available at a maximum concentration of 10 µM, which was

diluted by a minimum of 2 fold during the MTT assay (section 2.2.6). The control emetine displayed toxicity within the acceptable ranges in all experiments.

Studies have shown that short- to moderate-sized PPG molecules (200–1200 Da) have acute oral toxicity (Bingham and Cohrssen, 2012). The much longer chains (MW >2000) are much less cytotoxic. PPG has also been shown to cause haemolysis of human erythrocytes (Reed and Yalkowsky, 1985). This supports the data reported here (Table 4.4). The haemotoxicity reported here suggests that the linear PPGs are interfering with the human erythrocyte. This may be why the PPG MS calibration sample was estimated to have a greater antiplasmodial effect than the MCEs.

Table 4.3: Mean antiplasmodial activity against *P. falciparum* NF54 and mean cytotoxicity against CHO and HepG2 of the methylated crown ethers and polypropylene glycol, N=2 biological repeats with 4 technical repeats.

Sample	Antiplasmodial activity against *P. falciparum,* NF54 IC_{50}	Cytotoxicity against Chinese Hamster Ovary IC_{50}	Cytotoxicity against HepG2 IC_{50}	Selectivity Index (SI) (Cell IC_{50}/ NF54 IC_{50})
Methylated Crown Ethers	1873 ± 308 ng/mL	> 100 µg/mL	> 100 µg/mL	> 54
Polypropylene glycol	190 ± 20 nM	> 10 µM	> 10 µM	> 52
Emetine	-	0.009 ± 0.002 ng/mL	0.013 ± 0.002 ng/mL	-

Table 4.4: : Mean antiplasmodial activity against *P. falciparum,* NF54 and mean haemotoxicity against human erythrocytes of the methylated crown ethers and polypropylene glycol, N=2 biological repeats with 4 technical repeats.

Sample	Antiplasmodial activity against *P. falciparum* NF54 IC_{50}	Haemotoxicity Human Erythrocytes IC_{50}	Selectivity Index (SI)(Erythrocyte IC_{50}/ NF54 IC_{50})
Methylated Crown Ethers	1873 ± 308 ng/mL	> 100 µg/mL	> 54
Polypropylene glycol	190 ± 20 nM	4.22 ± 0.4 µM	22.2

An interesting quality of the MCEs compared to other crown ethers is their lack of toxicity *in vitro*. Crown ethers are known to be cytotoxic to mammalian cells and cause acute central nervous system failure in mice (Hendrixson *et al.*, 1978; Arenaz *et al.*, 1992). The MCEs presented SIs greater than 100 with no signs of cytotoxicity or haemotoxicity up to 100 µg/mL, indicating that the MCEs are selectively targeting the *P. falciparum* parasites in the erythrocyte. This implies that the MCEs could have biomedical applications by modifying ion gradients or ionophores safely in living systems. However, these tests are simple *in vitro* assays, and more study needs to be done to verify that the MCEs are, in fact, non-toxic.

Despite their selectivity, the discovery of compounds with such weak antiplasmodial activity would usually have eliminated them from further investigation. However, further study suggested that the addition of MCEs to the most active NP SPE fraction of strain PR3 led to a synergistic improvement in antiplasmodial activity. This is of great interest, and the identification of the active component in this NP SPE fraction and the relationship between it and the MCEs was investigated further. This is reported and discussed in Chapter 5.

5 Identification of Cyclodepsipeptides and their Relationship with the Methylated Crown Ethers

Abstract

After isolating and purifying the methylated crown ethers, the compounds responsible for the high antiplasmodial activity remained unknown. Through molecular networking, genome mining, and nuclear magnetic resonance analysis, a group of cyclodepsipeptides was successfully identified as the active compounds. These included the well-known valinomycin, montanastatin and other analogues recently identified in literature. Study of their tandem mass spectrum (MS/MS) spectra, comparison to literature and knowledge of their biosynthesis allowed the elucidation of the structures of two new cyclodepsipeptides. Unfortunately, it was found that the cyclodepsipeptides could not be purified further with the chromatographic method developed. The most active solid phase extraction fraction containing the cyclodepsipeptides was tested for antiplasmodial activity against drug-sensitive and resistant strains of *P. falciparum*, cytotoxicity against the HepG2 and Chinese Hamster Ovary cell lines, and haemotoxicity against human erythrocytes. While the results were promising, they showed similarity to pure valinomycin, which presents host toxicity, and, without further purification, it is unknown if the cyclodepsipeptide analogues could be lead candidates for further development. However, the tested cyclodepsipeptide fraction displayed suitable antiplasmodial activity with mean IC_{50}s of 25 ± 3.5 ng/mL and 101 ± 1.0 ng/mL against the drug-sensitive, NF54 and multidrug-resistant, K1 strains of *P. falciparum* respectively. The cyclodepsipeptide fraction also displayed favourable host selectivity with no cytotoxicity against the CHO cell line nor human erythrocytes and moderate toxicity against the HepG2 cell line. Overall, these results suggest that further study and purification of the cyclodepsipeptides is warranted. Lastly, antiplasmodial activity of past impure samples from earlier in the investigation was found to be comparable to the purest active cyclodepsipeptide fraction. High-resolution mass spectrometry analysis revealed the presence of the cyclodepsipeptides and MCEs in the active impure samples. This association led to the hypothesis that the methylated crown ethers and cyclodepsipeptides interacted in a synergistic manner. Combination studies using two models suggested that combining the methylated crown ethers with the cyclodepsipeptides elicits a synergistic response against *P. falciparum*, NF54.

5.1 Introduction

At this stage of the investigation, the compound(s) responsible for the potent antiplasmodial activity displayed by *Streptomyces* strain PR3's crude extracts and partially-purified fractions, was still unknown. Bioassay-guided fractionation supported by nontargeted high resolution mass spectrometry (HRMS), had led to the discovery of the novel methylated crown ethers (MCE). However, it was later shown that the MCEs were not entirely responsible for activity, but were thought to be co-eluting with the unknown active compound(s). The nontargeted HRMS approach that was adopted in Chapter 3 was deemed too crude, and a more direct mass spectrometry approach supported by additional methods of detection was needed to correctly identify the active compound(s). To this end, a set of systems biology approaches were implemented.

Systems biology is the integrated study of the molecular components within a biological system, at different scales (organism, organ, tissues, cells), and their connection to physiological functions and phenotypes through quantitative reasoning, computational models, and high throughput experimental technologies (Tavassoly *et al.*, 2018). Systems biology approaches involve several fields such as genomics, proteomics, and metabolomics. The two approaches that suited this investigation were metabolomics and genomics.

Metabolomics is a relatively new field in systems biology and refers to the study of all the metabolites produced by an organism at a specific time and under specific conditions (Tawfike *et al.*, 2013). In metabolomics, metabolites are analysed by spectroscopic methods such as HRMS, nuclear magnetic resonance (NMR), ultraviolet-visible light (UV-Vis), or infrared (IR), and the results are processed by computational tools and statistical models. This allows metabolites to be identified by the use of spectral libraries, the relationship between metabolites to be studied, and even the discovery of new molecules by comparison to known compounds. Metabolomics is used in a variety of fields such as toxicology, physiology, and of course, natural products chemistry.

A recently created metabolomic platform is the Global Natural Products Social molecular networking (GNPS) (https://gnps.ucsd.edu/) . GNPS is an online open-access knowledge base for the sharing of raw, processed and identified mass spectrometry (MS) and tandem mass

spectrometry (MS/MS) data from thousands of researchers around the globe (Wang *et al.*, 2016). GNPS links to other well-known MS libraries and repositories such as MassBank, and mzCloud. After validation, researchers can upload their own findings to GNPS, which creates a living database that is continuously growing and learning. This allows improved library searches to identify unknown compounds and therefore easy dereplication. One of the most useful tools provided by GNPS is molecular networking (Wang *et al.*, 2016). Molecular networking is a spectral correlation and visualization approach that matches MS/MS spectra to known spectra. A molecular network is visualized in the form of nodes clustered and linked to one another. Each node represents a mass spectrum and each link or edge represents a spectrum to spectrum alignment. By comparing fragmentation patterns of compounds, novel analogues with different parent masses and additional groups can still be matched, allowing the discovering of new compounds without the need to purify them (Allard *et al.*, 2016). It can also aid dereplication by easily and accurately identifying known compounds, which saves time and resources during fractionation studies. Alternatively, it could highlight a new molecule of interest and direct fractionation studies (Allard *et al.*, 2016; Wang *et al.*, 2016).

Another system biology approach seeing increased application in natural products screening is genomics. Genomics is the study of the function, mapping, and evolution of an organism's genome (Trivella and de Felicio, 2018). All natural products are produced by metabolic processes, which are governed by an organism's genetics. In the filamentous actinobacteria, these biosynthetic genes are organised into clusters known as biosynthetic gene clusters (BGC). BGCs are the core organisation of the biosynthetic pathways at a genomic level in bacteria and encode proteins, such as multidomain enzymes and binding factors, which are required to create and tailor metabolites (Tietz and Mitchell, 2016; Trivella and de Felicio, 2018). Analysing a genome sequence to identify known BGC sequences is known as genome mining and can be used to predict or identify structures present in a crude extract or fraction. Natural products are broadly made in a two-step process where a core backbone or scaffold is made and then tailored. Therefore, analogues can be predicted or identified if known genes are located in new BGCs. Conversely, chemical knowledge of a molecule can be used to analyse the biosynthetic genes of an organism.

In the past, whole genome sequencing (WGS) was incredibly expensive and difficult, but advances in understanding and technology have made WGS relatively inexpensive and faster (Tietz and Mitchell, 2016). Today, thousands of genomes have been sequenced and are available online for comparison through platforms, such as the National Center for

Biotechnology Information's (NCBI) GenBank (Benson *et al.*, 2012). Genome sequences can then be analysed by programs such as antiSMASH, which searches for natural product biosynthesis signatures (Medema *et al.*, 2011). antiSMASH provides sequence information on a wide range of different natural product classes, such as similarity to known BGCs and closely-related genes, making it a very robust and useful tool. Overall, genome mining can be used in conjunction with biological, physiochemical, and spectrometric techniques to accelerate or improve natural product screening (Tietz and Mitchell, 2016).

Resources such as GNPS and antiSMASH are the reason natural products are again a viable source of novel compounds in drug discovery. The challenges of the past, such as dereplication, time consuming and laborious fractionation and misidentification of active compounds can now be avoided or reduced (Tawfike *et al*., 2013; Allard *et al.*, 2016).

Aims of this investigation:

1. Prove that the main antiplasmodial active compound(s) in the active fractions are produced by *Streptomyces* strain PR3 and are not background impurities.
2. Modify the normal phase solid phase extraction methodology to improve the purity of the antiplasmodial active compound(s) produced by *Streptomyces* strain PR3.
3. Identify the active antiplasmodial compound(s) produced by *Streptomyces* strain PR3 by molecular networking and genome mining.
4. Determine whether there is a synergistic relationship between the methylated crown ethers and the active antiplasmodial compound(s) produced by *Streptomyces* strain PR3.

5.2 Methodology

5.2.1 SPE Method #6: Normal Phase

The SPE cartridges used were ISOLUTE® silica SPE cartridges with a sorbent mass of 200 mg and a total volume of 3 mL. SPE cartridges were equilibrated by passing 2 mL of MeOH followed by 2 mL of hexane through each cartridge. Samples were dissolved in 2 mL hexane/ethyl acetate (EtAc) (9:1) and passed through the silica cartridges by gravity. After adding the sample, solvents of increasing polarity were passed through the silica cartridges. The list of solvents in order of use was: hexane, hexane/EtAc (8:1), hexane/EtAc (7:1), hexane/EtAc (6:1), hexane/EtAc (5:1), hexane/EtAc (4:1), hexane/EtAc (3:1), hexane/EtAc (2:1), hexane/EtAc (1:1), EtAc, EtAc/methanol (MeOH) (4:1), EtAc/MeOH (2:1) and MeOH. When using silica cartridges, the sorbent was not allowed to dry, as this alters the retention of compounds in the subsequent wash steps. Therefore, 2.5 mL of solvent was added in each step, and approximately 0.5 mL of each solvent was left behind (i.e. only 2 mL of each fraction was collected).

5.2.2 Global Natural Products Social Molecular Networking

Raw HRMS data produced by HPLC-MS Method #1 was converted to mzXML format by ProteoWizard tool MSconvert (version 3.0.10051, Vanderbilt University, United States) (Chambers *et al.*, 2012). The converted files were uploaded to the GNPS molecular networking server and analysed by the molecular networking workflow published by Wang *et al*., 2016. A molecular network was created using the online workflow (https://ccms-ucsd.github.io/GNPSDocumentation/) on the GNPS website (http://gnps.ucsd.edu). The data were filtered by removing all MS/MS fragment ions within +/- 17 Da of the precursor m/z. MS/MS spectra were window filtered by choosing only the top 6 fragment ions in the +/- 50 Da window throughout the spectrum. The precursor ion mass tolerance was set to 2.0 Da with a MS/MS fragment ion tolerance of 0.5 Da. A network was then created where edges were filtered to have a cosine score above 0.7 and more than 6 matched peaks. Further, edges between two nodes were kept in the network if, and only if, each of the nodes appeared in each other's respective top 10 most similar nodes. Finally, the maximum size of a molecular family

was set to 100, and the lowest scoring edges were removed from molecular families until the molecular family size was below this threshold. The spectra in the network were then searched against GNPS' spectral libraries. The library spectra were filtered in the same manner as the input data. All matches kept between network spectra and library spectra were required to have a score above 0.7 and at least 6 matched peaks. The results were visualized using Cytoscape v3.7.2 (Shannon *et al.*, 2003).

5.2.3 Whole Genome Sequencing

Streptomyces strain PR3 was submitted to the Belgian Co-Ordinated Collection of Microorganisms/Laboratorium voor Microbiologie (BCCM/LMG; Ghent, Belgium) for WGS and analysis. Strain PR3 was recovered on ISP-2 and checked for growth and purity after 1 day of incubation at 28°C under aerobic conditions. Genomic DNA was isolated using a Maxwell® 16 Tissue DNA Purification Kit (cat.# AS1030) and a Maxwell® 16 Instrument (cat.# AS2000) after a prior enzymatic lysis step. The integrity and purity of the DNA were evaluated on a 1.0% (w/v) agarose gel and by spectrophotometric measurements at 234, 260, and 280 nm. A Quantus™ fluorimeter and a QuantiFluor™ ONE dsDNA System (Promega Corporation, Madison, WI, USA) were used to estimate the DNA concentration. WGS analysis was performed by the Oxford Genomics Centre (University of Oxford, United Kingdom). Library preparation was performed using an adapted protocol of the NEB prep kit. Paired-end sequence reads (PE150) were generated using the NovaSeq 6000 platform (Illumina Inc., San Diego, CA, USA). Quality checking trimming of the raw sequence reads and genome assembly (*de novo*) were performed using the Shovill pipeline (https://github.com/tseemann/shovill), aiming at an average genome coverage of 100x. Contigs shorter than 500 base pairs (bp) were excluded from the final assembly. Quality checking of the assemblies was performed using QUAST (Gurevich *et al.*, 2013).

5.2.4 antiSMASH and BLASTP Analysis

Putative biosynthetic gene clusters in the sequenced genome were identified using antiSMASH 5.0 (Blin *et al.*, 2019). The corresponding amino acid sequence of genes of interest were then analysed by BLASTP v2.10.0+ (Altschul *et al*., 1997) against the NCBI database (https://www.ncbi.nlm.nih.gov/). This allowed the identification of protein products encoded by the identified gene clusters.

5.2.5 Cultivation and Antiplasmodial Efficacy Against the Multidrug-Resistant Strain of *P. falciparum*, K1

The *P. falciparum* K1 strain, which is resistant to chloroquine, cycloguanil, sulfadoxine and pyrimethamine, was obtained from the Malaria Research and Reference Reagent Resource (MR4) depository. The K1 strain was originally isolated from a patient in Thailand in 1982 (Thaithong *et al*., 1983). The cultivation of, and antiplasmodial efficacy testing against, the K1 strain of *P. falciparum* was conducted by Mrs Sumaya Salie and Mr Virgil Verhoog at the Division of Clinical Pharmacology, University of Cape Town (sections 2.2.3 and 2.2.4).

The acceptable range of artesunate remained the same as the one selected for *P. falciparum*, NF54 activity determination (0.5–8 ng/mL), as it is not affected by any of the resistance mechanisms of K1. The K1 strain of *P. falciparum* is chloroquine resistant, therefore the efficacy of the chloroquine control was an indicator of resistance. The acceptable efficacy range of the chloroquine control was 150–250 ng/mL. If the efficacy of the chloroquine control fell below the acceptable range, it would indicate that the strain tested was not suitable for resistance tests.

5.2.6 Fixed-Ratio Isobologram Method

Combination studies were conducted using a modified version of the method described by Fivelman *et al.,* 2004. Briefly, drug stock solutions were made up such that their approximate IC_{50}s are obtained after 3–5 two-fold dilutions. The drug stocks were then mixed to make six different volumetric ratios. The ratios and concentrations of each sample are displayed in Table 5.1. The antiplasmodial activity against *P. falciparum*, NF54 of each compound, in each mixture, was determined using the pLDH methodology (section 2.2.4).

Table 5.1: Fixed fraction ratios and concentrations of the methylated crown ethers and cyclodepsipeptide fractions, used in the modified fixed-ratio isobologram method from (Fivelman *et al.,* 2004**).**

Ratio Number	Fixed Ratio	Cyclodepsipeptides Concentration (µg/mL)	Methylated Crown Ethers Concentration (µg/mL)
1	5:0	1.6	0
2	4:1	1.28	8
3	3:2	0.96	16
4	2:3	0.60	24
5	1:4	0.32	32
6	0:5	0	40

5.2.7 Determination of Synergy by CompuSyn

Raw data obtained from the fraction combination studies (section 5.2.6) were inputted into CompuSyn version 1.00 (Chou and Martin, 2005). Combination index (CI) values were generated for each fixed drug ratio (Table 5.1).

5.3 Results and Discussion

5.3.1 Cultivation, Extraction and Fractionation in Glass

At this stage in the investigation, the identity of the main antiplasmodial active compound was still unknown. The detection of the MCEs suggested that plastics and other impurities were contributing to the antiplasmodial inhibition displayed by extracts and fractions of strain PR3. To prove that strain PR3 was producing an antiplasmodial active compound and background impurities were not responsible for the potent antiplasmodial activity observed, two 1 L cultures of strain PR3 were grown in JCM #61 (section 3.2.1), extracted without XAD-16N resin (section 3.2.2.1) and fractionated by RP+NP SPE (sections 3.2.3.3 and 3.2.3.5 respectively). Great care was taken to avoid sample exposure to plastics. Only glass containers such as beakers and HPLC vials, and no plastic containers, such as benchtop centrifuge tubes, were used. The only possible source of plastic contamination was predicted to be from automatic pipette tips and SPE cartridges. The RP+NP SPE fractions were tested for antiplasmodial activity against the drug-sensitive strain of *P. falciparum*, NF54 (section 2.2.4). Comparing the antiplasmodial results of the NP SPE fractions from the standard methodology (with XAD-16N resin and no avoidance of plastics) to the fractions from the glass methodology (no XAD-16N resin and minimal use of plastics) revealed only one major difference (Table 5.2). The EtAc fraction of the standard methodology displayed weak antiplasmodial activity which as discussed previously is proposed to be due to the MCEs. The EtAc fraction in the glass methodology was inactive, suggesting that the MCEs are not present. HRMS analysis of the glass methodology EtAc fraction confirmed the absence of the MCEs. This supports the results discussed in Chapter 4. The most active fractions from each methodology were from the Hexane/EtAc (2:1) wash step with mean IC_{50}s of 117 ± 7 ng/mL and 110 ± 5.0 ng/mL from the standard methodology and glass methodology fractions respectively. All controls were within the acceptable ranges. These results strongly suggest that strain PR3 is producing an active antiplasmodial compound and the potent activity is not derived from background contaminants.

Table 5.2: Mean antiplasmodial activity of NP SPE fractions (Method #5) obtained by extraction and fraction using the standard developed methodology and a glass methodology which limited exposure to plastics, N=2 biological repeats with 4 technical repeats.

NP SPE Fraction	Antiplasmodial activity against *P. falciparum* NF54 IC_{50} (ng/mL)	
	Standard Methodology	Glass Methodology
Hexane (#1)	> 5000	> 5000
Hexane/EtAc (2:1) (#2)	117 ± 7.0	110 ± 5.0
Hexane/EtAc (1:1) (#3)	686 ± 61	575 ± 78
EtAc (#4)	1873 ± 308	> 5000
EtAc/MeOH (4:1) (#5)	> 5000	> 5000
EtAc/MeOH (2:1) (#6)	> 5000	> 5000
MeOH (#7)	> 5000	> 5000
Chloroquine	6.1 ± 2.1	7.3 ± 0.9
Artesunate	2.4 ± 1.5	5.2 ± 2.0

5.3.2 Improved Normal Phase Solid Phase Extraction Purification

To purify the antiplasmodial active compound produced by strain PR3 the NP SPE methodology was improved. Previous experiments had shown that the hexane/EtAc (2:1) wash step of SPE Method #5 (section 3.2.3.5) contained the active antiplasmodial compound (Table 5.2). Due to the active compound eluting in this fraction, additional washes of hexane and EtAc, with a higher percentage of hexane, were used (section 5.2.1). It was hypothesized that this would remove inactive material and selectively elute the active compound(s).

Four litres of strain PR3 culture were grown (section 3.2.1), and extracted (section 3.2.3), then fractionated by RP SPE Method #3 (section 3.2.3.3). As the results had shown that background molecules were not responsible for antiplasmodial activity (section 5.3.1, Table 5.2), the standard extraction methodology, with the XAD-16N extraction resin, was used to obtain more material. Finally, SPE Method #6 (section 5.2.1) was used and each fraction was evaporated under N_2 at 37°C, weighed, and tested for antiplasmodial activity against NF54 (section 2.2.4). By increasing the concentration of hexane in the initial hexane/EtAc washes, the new SPE method was able to separate the active component to a greater extent than before. Four highly

active fractions were identified with the most active fractions being the hexane/EtAc (7:1) (#3) and hexane/EtAc (6:1) (#4) fractions (Table 5.3). These fractions displayed mean IC_{50}s of 31.3 ± 4.0 and 63.5 ± 17 ng/mL, respectively, values which are significantly lower than the previous NP SPE active fraction obtained by SPE Method #5 (section 3.2.3.5), which displayed an IC_{50} of 117 ± 7.0 ng/mL (Table 5.2). This suggested that the fraction's purity had increased. The controls were within the acceptable ranges for these pLDH assays. Note that the EtAc fraction (#10) displayed weak antiplasmodial activity with an IC_{50} of 2105 ± 146 ng/mL. The MCEs were detected in this fraction by HRMS and were believed to be the source of this activity.

The detection of strong antiplasmodial activity in four consecutive fractions suggested that multiple compounds were present. It was possible that these compounds were analogues of one another with the same pharmacophore. Due to this, they were eluting from the silica cartridge under similar conditions. It was also possible that one compound was eluted in the different wash steps and the SPE methodology was not selective enough to purify the active compound.

Table 5.3: Mean antiplasmodial activity of NP SPE Method #6 fractions against *P. falciparum*, NF54, N=2 biological repeats with 4 technical repeats.

Sample	Antiplasmodial activity against *P. falciparum*, NF54 IC_{50} (ng/mL)
Hexane (#1)	> 5000
Hexane/EtAc (8:1) (#2)	150 ± 53
Hexane/EtAc (7:1) (#3)	31.3 ± 4.2
Hexane/EtAc (6:1) (#4)	63.5 ± 17
Hexane/EtAc (5:1) (#5)	287 ± 14
Hexane/EtAc (4:1) (#6)	>5000
Hexane/EtAc (3:1) (#7)	>5000
Hexane/EtAc (2:1) (#8)	>5000
Hexane/EtAc (1:1) (#9)	>5000
EtAc (#10)	2105 ± 146
EtAc/MeOH (4:1) (#11)	>5000
EtAc/MeOH (2:1) (#12)	>5000
MeOH (#13)	>5000
Chloroquine	7.1 ± 2.1
Artemisinin	3.3 ± 1.3

To determine if the structure of the active compound could be identified or elucidated, more material was obtained by culturing three 1 L cultures of strain PR3 in JCM #61 (section 3.2.1) followed by extraction (section 3.2.2.1) and fractionation by RP+NP SPE Methods #3 and #6 (sections 3.2.3.3 and 5.2.1 respectively). The most active fractions, hexane/EtAc (7:1) (#3) and hexane/EtAc (6:1) (#4) from each culture were pooled and submitted for ^{1}H NMR analysis at the University of Cape Town (section 3.2.4). The ^{1}H NMR spectra of the two active fractions are displayed in Figures 5.1 and 5.2, respectively. Comparison of the ^{1}H NMR spectra revealed them to be nearly identical, which strongly suggested that the same molecules were present in both fractions. Both spectra had signals at δ_H 0.9 and 1.0 which were predicted to correspond to methyl groups either attached to a 5-6 carbon ring or hydrocarbon chain (Silverstein *et al*., 2005). Signals at δ_H 1.3, 1.4 and 2.3 were present in both spectra and believed to be from protons in methylene groups (Silverstein *et al*., 2005). Signals at δ_H 4.3, 4.4, 4.6 and 5.3 were also seen in both spectra and are proposed to be from methine groups attached to heteroatoms (Silverstein *et al*., 2005). Both ^{1}H NMR spectra were overlaid (Figure 5.3) to allow comparison and it was found that the spectra are extremely similar suggesting they contain the same compound(s). The similar antiplasmodial activity (Table 5.3) supports this observation. However, the ^{1}H NMR spectra also suggested that multiple analogues were present, as the base peaks of the most intense signals displayed overlapping signals and were not clearly resolved. To obtain more information, molecular networking was undertaken.

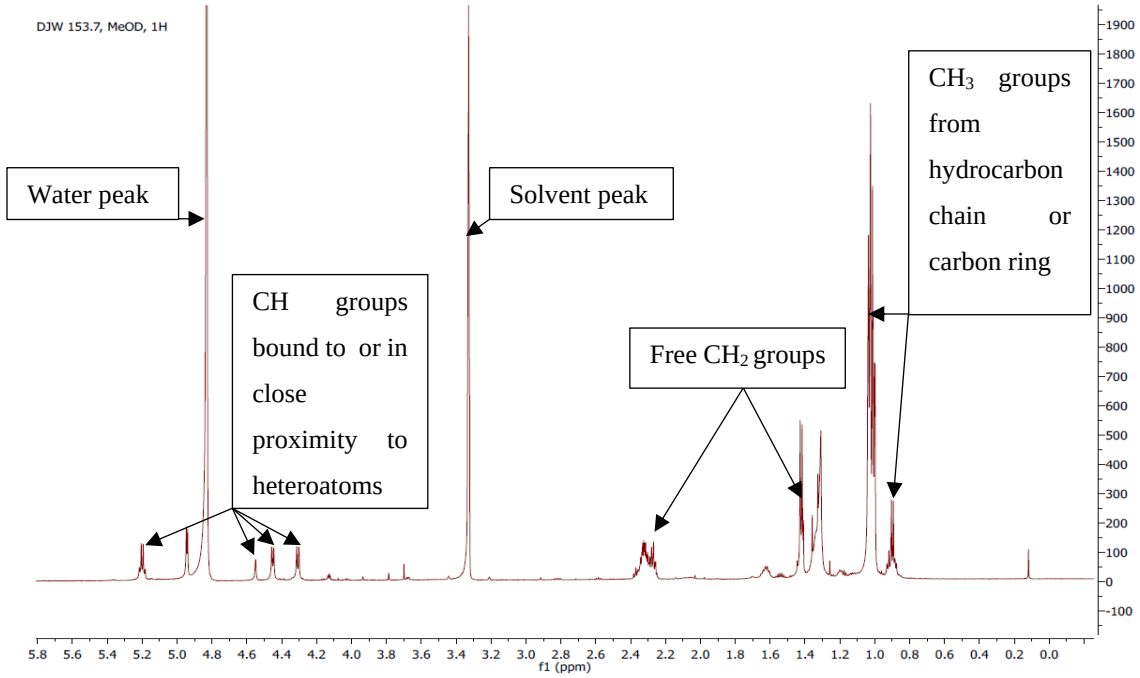

Figure 5.1: ^{1}H NMR spectrum of combined fraction #3 (hexane/EtAc 7:1) produced by SPE Method #6.

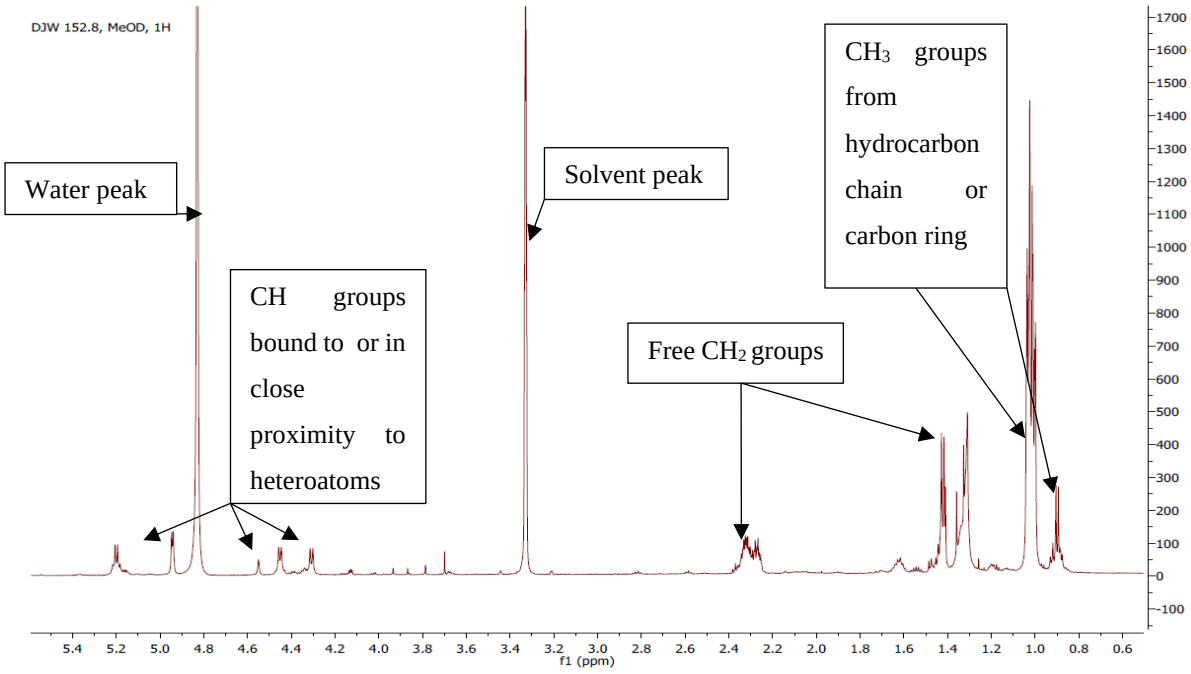

Figure 5.2: ^{1}H NMR spectrum of combined fraction #4 (hexane/EtAc 6:1) produced by SPE Method #6.

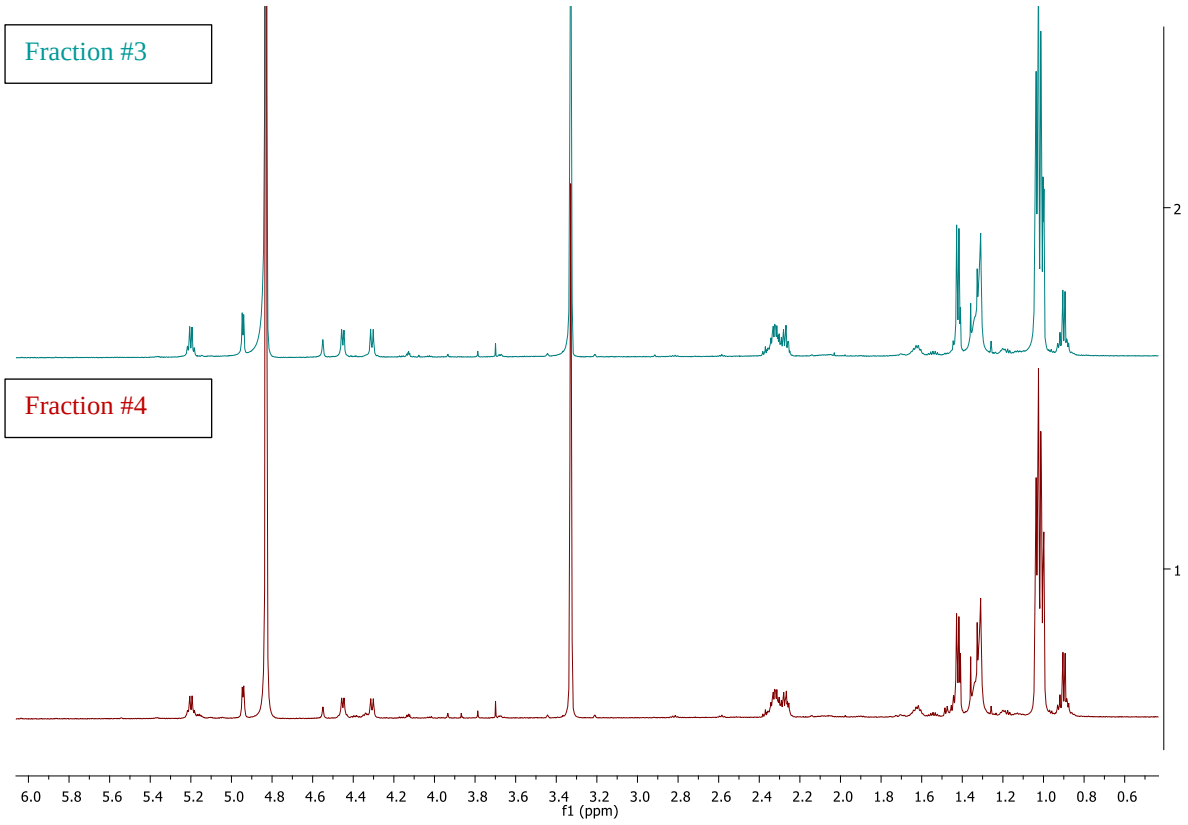

Figure 5.3: Overlaid 1H NMR spectra of fraction #3 (green) and fraction #4 (red) from NP SPE.

5.3.3 Identification of Cyclodepsipeptides by Molecular Networking, ^{1}H NMR and Genome Mining

The two most active fractions produced by SPE Method #6 (section 5.2.1), fractions #3 and #4, were diluted to 10 µg/mL in MeOH and 10 µL of each were injected and analysed by HPLC-MS Method #1 (section 3.2.5.1) to obtain HRMS data. Molecular network analysis was conducted on NP SPE Method #6 fractions #3 and #4 using the GNPS workflow (sections 5.2.1 and 5.2.2 respectively). A molecular network is visualized in the form of nodes clustered and linked to one another. Each node represents a mass spectrum and each link or edge between nodes represents a spectrum to spectrum alignment (Wang *et al.*, 2016). Therefore, spectra with similar fragmentation patterns will be linked together. The length of the edge is not representative of the similarity of the spectra. As discussed in the methodology (section 5.2.2) the molecular networking analysis parameters are set so that only closely matching spectra are

aligned. The only compounds of interest detected in both molecular networks were a series of cyclodepsipeptides. The cyclodepsipeptide molecular network cluster found in fraction #3 is shown in Figure 5.4. The full molecular network with all clusters, nodes and edges is displayed in Figure 8.1 in the Appendix. There were nine nodes detected by molecular networking, two corresponded to valinomycin, and two to montanastatin, both of which are known cyclodepsipeptides (Pettit *et al.*, 1999). Valinomycin was detected at *m/z* 1111.6409 ($M+H^+$) and 1128.6616 ($M+NH_4^+$). Montanastatin was detected at *m/z* 741.4288 ($M+H^+$) and 758.4552 ($M+NH_4^+$). Six nodes were clustered with valinomycin and montanastatin, indicating they have very similar fragmentation patterns and that they are cyclodepsipeptide analogues. All analogues were detected as ammonium adducts, and their observed *m/z*, corresponding masses and retention times are displayed in Table 5.4. As seen with previous adducts it is believed that the ammonium adducts are formed from the ammonium formate in the aqueous phase. With the exception of montanastatin there is a mass difference of 14 Da between each cyclodepsipeptide which could correspond to a methylene group (Ma *et al.*, 2014). The retention time increases as the size of the cyclodepsipeptide increases which suggests that the larger peptides are more non-polar as they retain to the C18 HPLC column slightly longer. This supports the addition of the aliphatic methylene groups to each peptide. These analogues did not match any compounds in the GNPS library (Wang *et al.*, 2016). The protonated forms of each cyclodepsipeptide can be observed in each of their MS/MS spectra which are displayed in the Appendix Figures 8.4-8.8.

The cyclodepsipeptide cluster from fraction #4's molecular network (Figure 5.5) and was found to be very similar to fraction #3's network (Figure 5.4), which corroborates the ^{1}H NMR results (Figures 5.1 and 5.2.) The only differences between the two molecular networks were the presence of an analogue with *m/z* of 1072.6 Da in fraction #3, not seen in fraction #4 and the presence of an analogue with *m/z* of 1156.6 Da in fraction #4, not seen in fraction #3. Overlaying the experimental MS/MS spectra of fraction #3 with the GNPS library MS/MS spectra of valinomycin and montanastatin revealed they were extremely similar, confirming their identities (Figures 5.6 and 5.7). The same overlays were conducted with the MS/MS spectra of valinomycin and montanastatin in fraction #4, and the results were the same as the overlays of fraction #3 (Figure 8.2 and 8.3).

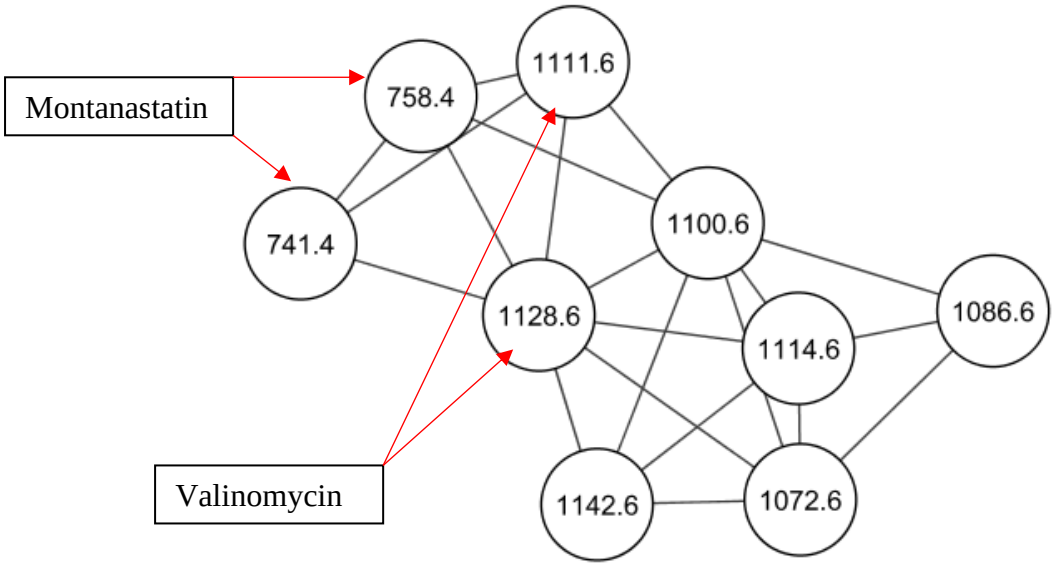

Figure 5.4: Molecular network of RP+NP SPE fractions #3, generated by SPE Methods #3 and #6. The nodes for valinomycin and montanastatin are highlighted by red arrows.

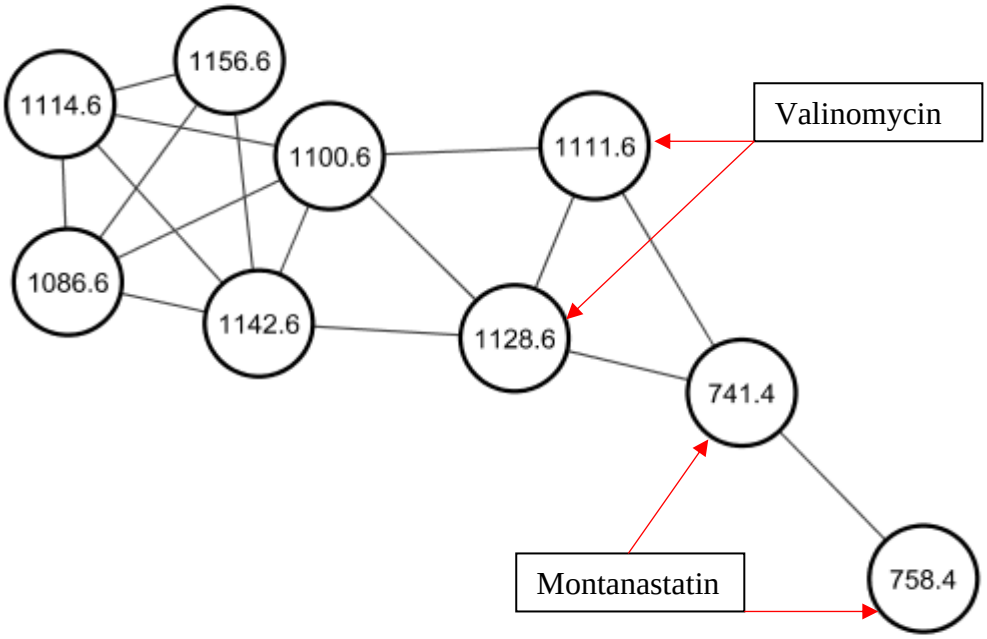

Figure 5.5: Molecular network of fraction #4 produced by RP + NP SPE Methods #3 and #6. The nodes for valinomycin and montanastatin are highlighted by red arrows.

Table 5.4: Detected ammonium adducts and experimental masses of cyclodepsipeptide analogues detected by HRMS.

Experimental Mass (Da)	*m/z* ($M+NH_4^+$)	Retention Time (minutes)
740.4218 (Montanastatin)	758.4552	10.21
1054.5671	1072.5997	10.27
1068.5820	1086.6151	10.33
1082.5984	1100.6308	10.46
1096.6130	1114.6461	10.56
1110.6339 (Valinomycin)	1128.6616	10.72
1124.6454	1142.6778	10.82
1138.6759	1156.6997	10.95

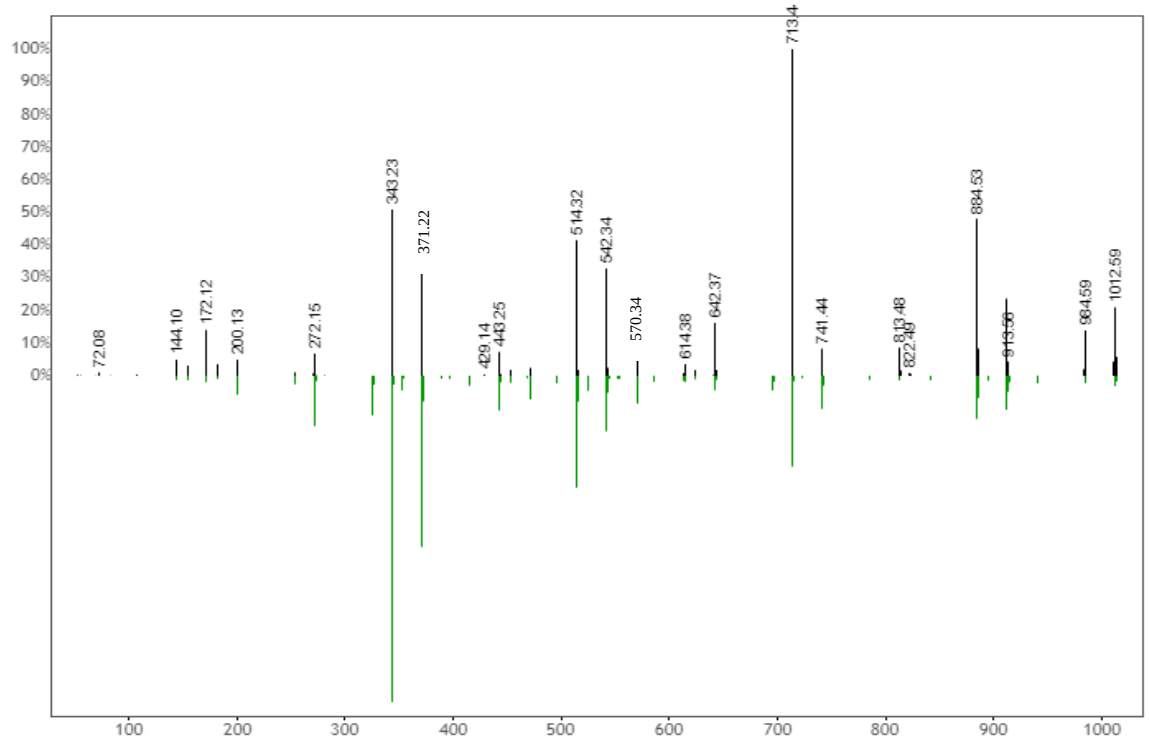

Figure 5.6: Valinomycin MS/MS spectral overlay of experimental spectrum (green) vs GNPS library spectrum (black).

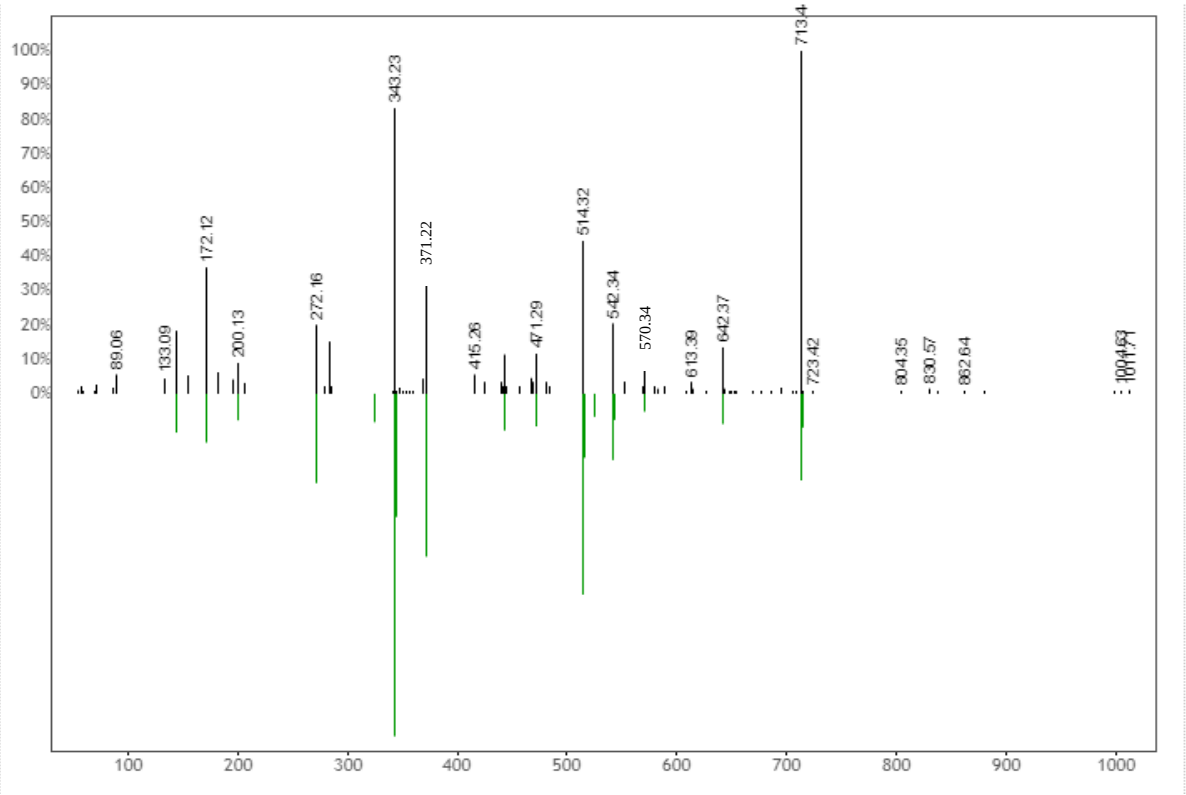

Figure 5.7: Montanastatin MS/MS spectral overlay of experimental spectrum (green) vs GNPS library spectrum (black).

Valinomycin is a cyclic depsipeptide consisting of the amino and hydroxy acids; L-Valine (Val) –D-α-hydroxyisovaleric acid (Hiv) –D-Val–L-Lactic acid (Lac) (L-Val–D-Hiv–D-Val–L-Lac–) repeated 3 times to produce a cyclic dodecamer (Ovchinnikov, 1979). The structure of valinomycin is displayed in Figure 5.8. Depsipeptides are peptides with one or more amino acids substituted for hydroxy acids and containing ester and peptide linkages (Kitagaki *et al.*, 2015). Valinomycin is commonly produced by many *Streptomyces* species and is a very well-studied antibiotic (Matter *et al.*, 2009). Valinomycin exhibits potent antibacterial, antiretroviral, antifungal, and anticancer activity (Ovchinnikov, 1979; Pettit *et al.*, 1999; Wu *et al.*, 2004; Ryoo *et al.*, 2006; Park *et al.*, 2008). More importantly, valinomycin has been shown to possess potent antiplasmodial activity, with an IC_{50} of 5.3 ng/mL against a drug-sensitive strain of *P. falciparum* (Gumila *et al.*, 1996). Valinomycin is a neutral ionophore, much like the crown ethers discussed in Chapter 4, with a lipophilic backbone and a central cavity where it can coordinate cations by ion-dipole interactions between its carboxylic oxygen atoms (Fong, 2016). Valinomycin binds and facilitates passive diffusion of cations through cell membranes and disrupts essential electrochemical gradients in cells, which is why it exhibits such a broad range of antibiotic activities. Valinomycin is highly selective for potassium ions (K^+), but can interact with several different cations with weaker selectivity. For example,

valinomycin is 10^3–10^4 times more stable when complexed with K^+ compared to Na^+ (Ovchinnikov, 1979).

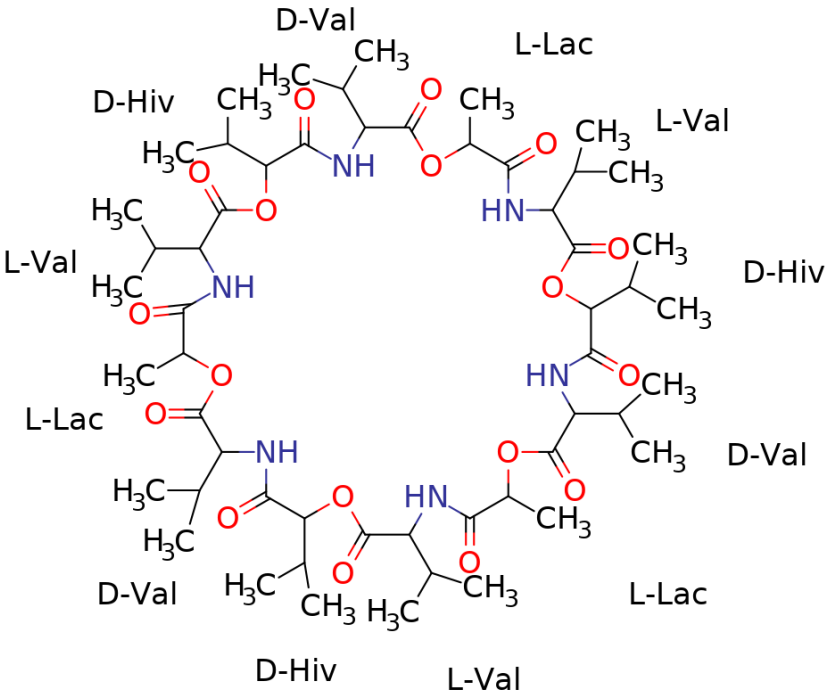

Figure 5.8: Molecular structure of valinomycin with each amino and hydroxy acid labelled (Chemicalize).

Montanastatin is a cyclodepsipeptide, which consists of the same sequence of amino and hydroxy acids as valinomycin (L-Val–D-Hiv–D-Val–L-Lac–), repeated twice instead of three times to form a cyclic octamer (Pettit *et al.*, 1999). The structure of montanastatin is displayed in Figure 5.9. Montanastatin was isolated from *Streptomyces anulatus* and exhibits moderate antibacterial and anticancer activity *in vitro* (Pettit *et al.*, 1999). Interestingly, in the same investigation valinomycin was shown to be substantially more active against the tested bacterial and cancer cell lines than montanastatin, despite their similar chemical compositions (Pettit *et al.*, 1999). This is thought to be due to montanastatin's smaller ring size, which is likely affecting ion selectivity and binding. Changes in ring size affects ion selectivity and thus possibly efficacy, which is also seen with the crown ethers (Pettit *et al.*, 1999; Gokel *et al.*, 2004). The exact mechanism of action of montanastatin has not been elucidated, but it is reasonable to believe it acts by electrochemical gradient disruption, much like valinomycin and other neutral ionophores. Other cyclodepsipeptides have been found to possess antiplasmodial activity. For example Paecilodepsipeptide A from the pathogenic fungus *Paecilomyces cinnamomeus* BCC 9616 exhibited weak antiplasmodial activity against the multi-drug resistant strain of *P. falciparum* K1 with an IC_{50} of 4.9 μM (Isaka *et al.*, 2007). Another example

is Chaiyaphumine-A, isolated from *Xenorhabdus* SP. PB614, which shows good antiplasmodial activity against *P. falciparum* (strain unknown) with an IC_{50} of 0.61 µM (Grundmann *et al.*, 2014).

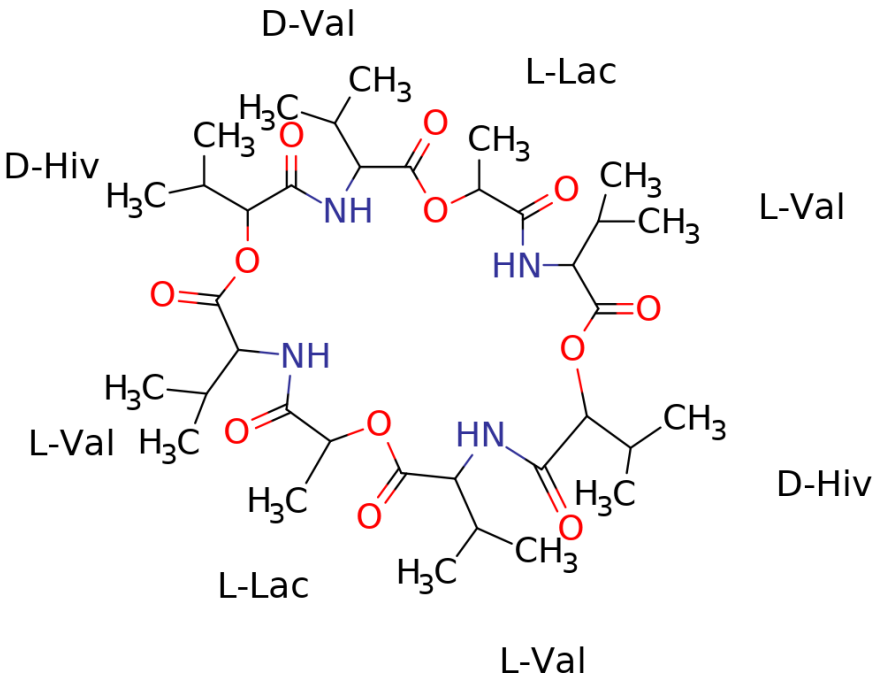

Figure 5.9: Molecular structure of montanastatin with each amino and hydroxy acid labelled (Chemicalize)**.**

While the GNPS molecular networking feature and library search are powerful tools it does not contain all known natural products and several other methods were employed to support the presence of the cyclodepsipeptides in fractions #3 and #4 and link their presence to antiplasmodial activity. Comparison of the ^{1}H NMR spectra of montanastatin and valinomycin published by Pettit *et al.* (1999), to the ^{1}H NMR spectra of NP SPE fractions #3 and #4 revealed matching signals (Figures 5.1, 5.2 and 5.3). Signals at δ_H 0.95, 0.96, 0.98 and 0.99 were observed and are theorized to represent methyl groups in Hiv and D-Val and L-Val respectively. Signals at δ_H 1.43 were proposed to represent methyl groups from L-Lac. Signals at δ_H 2.23 and 2.25 represent methine groups in branched chain in D-Val and L-Val, and Hiv respectively. Pettit *et al.* (1999) also reported signals at δ_H 4.25, 4.30, 5.00 and 5.05 which were assigned to methine groups attached to the peptide bond that form the backbone of valinomycin. Not all signals with these same chemical shifts were not observed in fraction #3 and #4's ^{1}H NMR spectra however similar signals at δ_H 4.3, 4.4, 4.6 and 5.3 were seen and

believed to correlate to methine protons attached to heteroatoms (Silverstein *et* al., 2005). The major matching signals missing in fraction #3 and #4's ^{1}H NMR spectra that are present in valinomycin's were at δ_H 6.96 and 6.94 which correspond to protons attached to nitrogens involved in amide bonds (Silverstein *et* al., 2005). Figure 5.10 is fraction #3's ^{1}H NMR spectrum and is annotated with the matching signals reported by Pettit *et al.* (1999). These results add further evidence to suggest that the cyclodepsipeptides are present. However, as the samples were not completely pure and only ^{1}H NMR analysis was done, it cannot be confirmed that these signals are from montanastatin and valinomycin.

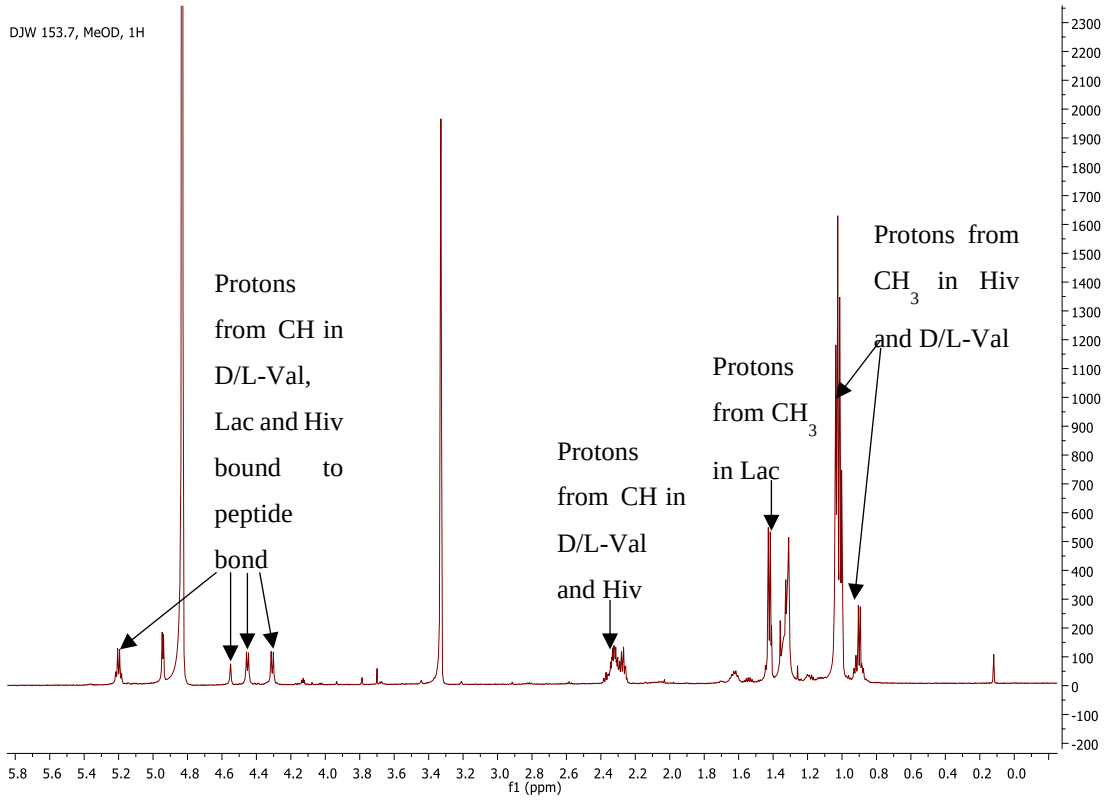

Figure 5.10: ^{1}H NMR spectrum of fraction #3 produced through SPE Methods #4 and #6 annotated with the matching signals from valinomycin (Pettit *et al.*, 1999)**.**

The HRMS data of all past active fractions produced from previous extractions and different purification methods were screened for the presence of cyclodepsipeptides. The *m/z* signals presented by the molecular networking results were used (Table 5.4). Valinomycin, montanastatin, and the cyclodepsipeptide analogues were detected in all of the past active fractions and in none of the inactive blank samples, suggesting that they are linked to the antiplasmodial activity displayed by strain PR3. The LC-MS data of each cyclodepsipeptide including observed *m/z*, retention time, peak height and peak intensity, in each active fraction is displayed in Figures 8.9 -8.15. Each cyclodepsipeptide was identified in each past active

fraction and were not found in any inactive fractions. The only missing peptide is *m/z* 1156.6997 from fraction #5, which displayed weak antiplasmodial activity (Table 5.3). It's not possible to determine if this lower activity is linked to the absence of *m/z* 1156.6997 with the data available. In Chapter 3, it was hypothesised that, when grown in ISP-2 or JCM #61, strain, PR3 produced different antiplasmodial compounds. This was found to be incorrect as analysis of crude extracts and fractions from cultures grown in both media, ISP-2 and JCM #61, contained the cyclodepsipeptides. The amount of each cyclodepsipeptide present could be altered by the different growth conditions, which could explain the differences in activity of the fractions generated from cultures grown in the two media.

Further evidence of the presence of the cyclodepsipeptides was achieved by sequencing the genome of strain PR3 followed by antiSMASH analysis (sections 5.2.3 and 5.2.4, respectively). antiSMASH analysis revealed that strain PR3 contained the BGC required to synthesise valinomycin (Figure 5.11).

Valinomycin and montanastatin are synthesised by non-ribosomal peptide synthetases (NRPS). Briefly, NRPSs consist of enzymatic domains each of which is responsible for a different action, such as activation, covalent binding, or modification of a substrate molecule, and finally condensation of the domain's product to that of the neighbouring domain in the enzyme (Mootz *et* al., 2002). Domains are organised into modules and each module is responsible for the binding of a single substrate. Amino acids and other substrates are covalently bound as thioesters to the enzyme attached 4′-phosphopantetheine (Ppant) prosthetic group. Following modifications, these bound substrates are then linked to the downstream domain's product by condensation. Possible modifications that can occur to each peptide include cyclization (to form a macrocycle), dehydration, methylation, acylation, and glycosylation. The NRPS product grows by step-wise chain extension from the N terminus to C terminus direction. The final product is cleaved from the last Ppant group and released. The type of NRPS described here is known as linear. Two other types exist, iterative and nonlinear. Iterative NRPSs use their modules or domains more than once to produce a single product. In nonlinear NRPSs, the domain order within a module can be different from the conserved order seen in the other two systems. This allows unique modifications, such as internal cyclization. NRPSs are able to incorporate unique amino acids and α-hydroxy carboxylic acids, as seen in valinomycin biosynthesis (Cheng, 2006). NRPS products can be linear, cyclic or branched cyclic, such as the macrocyclic lactones (Mootz *et al*., 2002).

Valinomycin biosynthesis is performed by an NRPS consisting of two core enzymatic units, VLM1 and VLM2, each of which is composed of two modules (Cheng, 2006; Paulo *et al.*, 2019). In valinomycin biosynthesis, D-α-hydroxyisovaleric acid (D-Hiv) is the starting component followed by the epimerization of L-valine (L-Val) to D-Val and its incorporation. Next L-lactic acid (Lac) is incorporated and finally L-Val is bound to form a tetradepsipeptide chain (Paulo *et al.*, 2019). Valinomycin biosynthesis is an example of iterative NRPS synthesis, as the process is repeated twice more by the same modules, to produce a linear twelve membered depsipeptide chain (Mootz *et al.*, 2002). This is cyclized by the VLM2 thioesterase, to produce the final cyclic dodecadepsipeptide (Paulo *et al.*, 2019). Montanastatin biosynthesis was recently shown to follow the same process with two iterations instead of three.

After the detection of the valinomycin BGC by antiSMASH analysis, BLASTP analysis was conducted on the genome sequence of strain PR3 (section 5.2.4) (Table 5.5). The BLASTP results revealed that strain PR3 contained genes which encode amino acid sequences with extremely high similarity to the consensus sequences of VLM1 and VLM2, originally sequenced from *Streptomyces tsusimaensis* strain ATCC 15141, in the NCBI database (Cheng, 2006). The genes that encode the VLM1 and VLM2 enzymes are referred to as *vlm1* and *vlm2*. The detection of the valinomycin BGC and amino acid sequence similarity to VLM1 and VLM2 proves that strain PR3 has the biosynthetic potential to produce valinomycin and montanastatin.

The antiSMASH results revealed that strain PR3 contained several additional genes flanking the core *vlm1* and *vlm2* gene sequences (Figure 5.11). The association of these genes with *vlm1* and *vlm2* suggests they may play a role in cyclodepsipeptide biosynthesis. If these additional genes code for enzymes with the ability to tailor the core valinomycin molecule, it could explain the presence of the cyclodepsipeptide analogues detected by molecular networking.

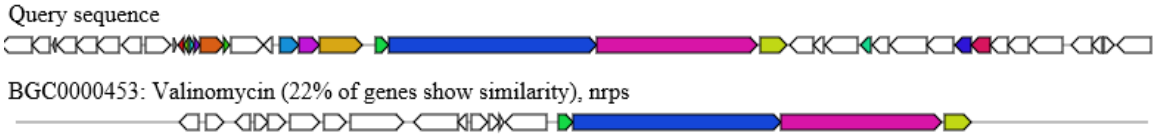

Figure 5.11: Biosynthetic gene cluster of strain PR3 (top) compared to the valinomycin biosynthetic gene cluster of *S. tsusimaensis* ATCC 15141 (bottom; accession number DQ174261) (Blin *et al.*, 2019)**.** The core module sequences, *vlm1* and *vlm2*, are shown in blue and pink, respectively.

Table 5.5: BLASTP results of the VLM-like proteins of strain PR3 (Benson *et al.*, 2012)**.**

Closest match	Max Score	Total Score	Query Cover (%)	Percent Identity (%)	Sequence accession number
VLM1 (*S. tsusimaensis* ATCC 15141*)*	6803	6803	100	99.47	ABA59547.1
VLM2 (*S. tsusimaensis* ATCC 15141*)*	5276	5276	100	100.00	ABA59548.1

In summary, molecular networking analysis of the active NP SPE fractions #3 and #4 of strain PR3 revealed the presence of the cyclodepsipeptides, valinomycin, montanastatin and related analogues. ^{1}H NMR analysis of the NP SPE active fractions and comparison to published spectra for valinomycin and montanastatin supported the proposal that cyclodepsipeptides were present. The detection of multiple cyclodepsipeptides with similar sequences and amino acids could explain the overlapping base signals seen in the ^{1}H NMR spectra (Figures 5.1 and 5.2). Finally, genome mining and BLASTP analysis revealed the presence of the biosynthetic genes required for valinomycin biosynthesis in strain PR3's genome. The core genes *vlm1* and *vlm2* were flanked by additional genes not seen in the consensus BGC of *S. tsusimaensis* ATCC 15141. These additional genes were suspected to be linked to the presence of the cyclodepsipeptide analogues detected by molecular networking. Overall, this provides strong evidence that the cyclodepsipeptides are present in strain PR3's fractions. Valinomycin is a known antibiotic and possesses potent antiplasmodial activity against *P. falciparum* (Gumila *et al.*, 1996). This activity is similar to the activity displayed by strain PR3's most active fractions. Analysis of the HRMS data of past active fractions showed that these cyclodepsipeptides were consistently present in the active fractions and extracts throughout the entire investigation and were not present in the blank or inactive samples (See Appendix, Figures 8.9-8.15. Confirmation of the presence of the cyclodepsipeptides by multiple methods, association with past active fractions, and review of the literature strongly suggests that the

cyclodepsipeptides are responsible for the antiplasmodial activity displayed by *Streptomyces* strain PR3.

5.3.4 Elucidation of Novel Cyclodepsipeptides

While the GNPS library search failed to identify the cyclodepsipeptide analogues, structures have been proposed in the literature. In a similar fashion to this investigation, Paulo *et al.* (2019) identified valinomycin, montanastatin, and five additional cyclodepsipeptides present in the EtAc extract of *Streptomyces* strain CBMAI 2042 using molecular networking and genome mining (Paulo *et al.*, 2019). They detected additional genes flanking the *vlm1* and *vlm2* core sequences and hypothesized that these could be responsible for the production of additional cyclodepsipeptides. This was also observed with strain PR3's valinomycin BGC and supports the theory that the additional genes detected by antiSMASH are responsible for the production of the cyclodepsipeptide analogues (Figure 5.11).

By studying the MS/MS spectra of the novel cyclodepsipeptides and the biosynthesis of valinomycin, Paulo *et al.* (2019) proposed structures for the detected cyclodepsipeptide analogues. Analysis of the MS/MS spectrum of a cyclic peptide can be used to elucidate its structure, as mass fragments represent alternating units that comprise the peptide backbone (Jia *et al.*, 2006). Knowledge of the biosynthesis of the compound of interest allows an understanding of the components available to produce analogues, simplifying the identification of these mass fragments (Paulo *et al.*, 2019). Any difference in a cyclodepsipeptide's MS/MS spectrum represents a deviation from the core structure of valinomycin and a change in the biosynthesis of the novel cyclodepsipeptide. Paulo *et al.* (2019) proposed that these cyclodepsipeptide analogues may be synthesised by a combination of two different mechanisms, the incorporation of Lac instead of Hiv and the incorporation of leucine or isoleucine (Leu/Ile) instead of Val (Challis *et al.*, 2000; Paulo *et al.*, 2019). Substitution of Leu/Ile for Val has been seen in other biosynthetic pathways with adenylation domains that bind Val, such as in lichenysin biosynthesis (Galli *et al.*, 1994). The cyclodepsipeptides elucidated by Paulo *et al.* (2019) are presented below (Tables 5.6 and 5.7).

Table 5.6: The predicted structures of the cyclodepsipeptide analogues identified by Paulo *et al.* (2019) and found in the molecular network of NP SPE fractions #3, and #4 of *Streptomyces* strain PR3.

m/z (Da) ($M+NH_4^+$)	Proposed structures
1100.6308	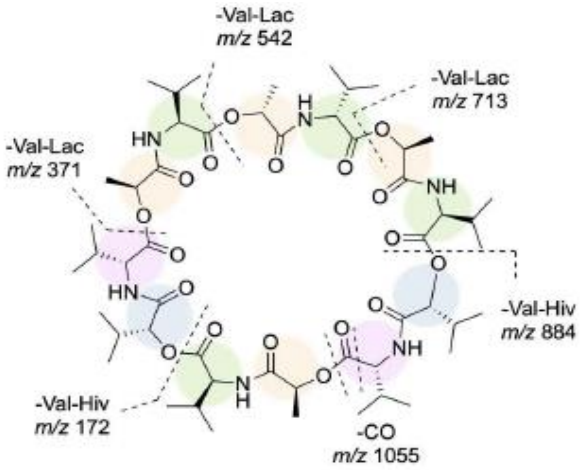
1114.6461	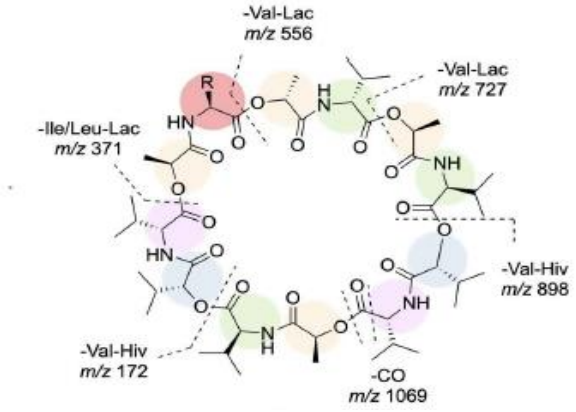

Each image displayed here was obtained and edited with permission from Bruno Sacchetto Paulo, author of Paulo et al., (2019). Each colour represents an amino or hydroxy acid to highlight the differences in biosynthesis. D-Hiv (blue), D-Val (pink), L-Lac (yellow), L-Val (green) and Leu/Ile (red) (Paulo *et al.*, 2019).

Table 5.7: The predicted structures of the cyclodepsipeptide analogues identified by Paulo *et al.* (2019) and found in the molecular network of NP SPE fractions #3 and #4 of *Streptomyces* strain PR3..

m/z (Da) ($M+NH_4^+$)	Proposed structures
1142.6778	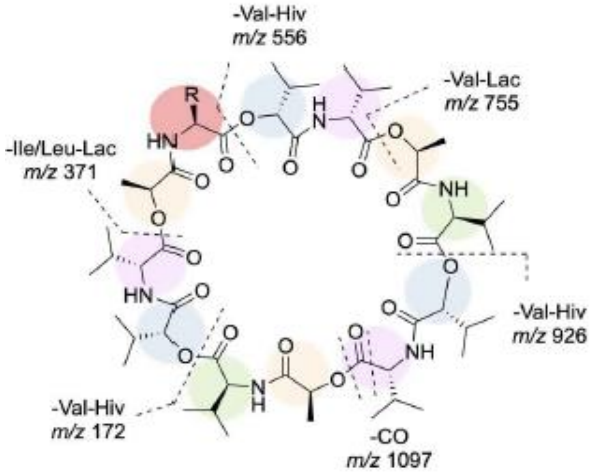
1156.6997	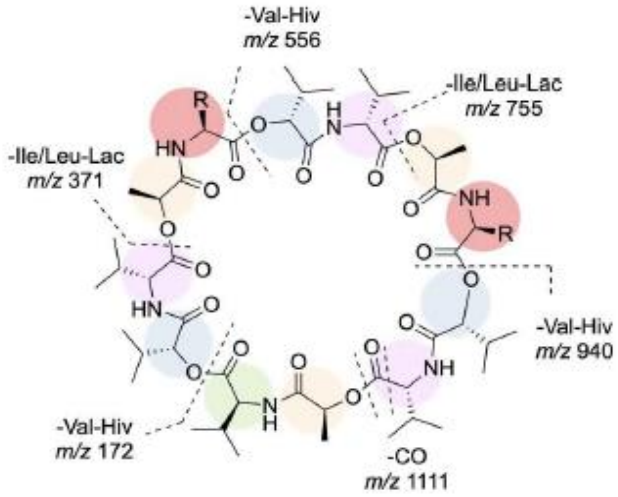

Each image displayed here was obtained and edited with permission from Bruno Sacchetto Paulo, author of Paulo et al., (2019). Each colour represents an amino or hydroxy acid to highlight the differences in biosynthesis. D-Hiv (blue), D-Val (pink), L-Lac (yellow), L-Val (green) and Leucine// Isoleucine (red) (Paulo *et al.*, 2019).

Two nodes, corresponding to compounds with *m/z* 1072.5697 and *m/z* 1086.6110 that were detected in the molecular network of fractions #3 of *Streptomyces* strain PR3 were not

elucidated by Paulo *et al.* (2019). These nodes were linked to the ammonium adducts of these compounds and their theoretical masses were calculated as 1054.5671 Da and 1068.5820 Da, respectively (Table 5.4). These will be referred to as compounds 1054 and 1068, respectively. Using the workflow and analysis done by Paulo *et al.* (2019) as a guide, the structures of compounds 1054 and 1068 were elucidated.

The molecular network matched compound 1054 and 1068 to valinomycin which suggests they have similar structures, therefore valinomycin's MS/MS was used as a starting point. Valinomycin's MS/MS spectrum displays a number of unique mass fragments that were used to compare and understand the structural differences between it and the cyclodepsipeptide analogues. When peptides fragment they produce fragments with either N-terminal charged ions (a,b) or fragments with C-terminal charged ions (yz) (Liu *et al.*, 2009). Cyclic peptides do not typically produce C-terminal charged fragments therefore only a and b fragments are detected. Fragments known as b ions are the amino acid residues + (H^+), b^o are b ions which have lost a H_2O group (-18.01056 Da) and a ions are b ions which have lost the C terminus CO group (-27.9950 Da) (Liu *et al.*, 2009). In the MS/MS spectra of valinomycin, compound 1054 and 1068 (Figures 5.12, 5.13, 5.15) there are a conserved set of mass fragments and mass shifts. These are the mass fragment of *m/z* 144.1012, 172.0959, 244.167, 343.2197 and 371.2158. The masses of the three core components of valinomycin, D/L Val, D-Hiv and L-Lac are 99.0684 Da, 100.0524 Da and 72.0211 Da respectively. The signals from *m/z* 144.1012 and 172.0959 represent the a and b type fragment ions of the Lac-Val dimer respectively. The mass shift of Da from *m/z* 144.1012 to 244.167 represents the addition of a Hiv group making *m/z* 244.167 a a fragment of the Lac-Val-Hiv trimer. The final shift of Da from *m/z* 244.167 to 343.2197 represent the addition of another Val. This makes *m/z* 343.2197 and 371.2158 the a and b ions of the Lac-Val-Hiv-Val tetramer. These peaks represent one pass of valinomycin synthesis. In valinomycin's MS/MS spectrum these masss shift patterns repeat twice more to produce the docdecadepsipeptide. For example the mass fragment *m/z* 713.4820 is the b fragment of two sets of Lac-Val-Hiv-Val fragments and represents two passes of valinomycin synthesis.The presence of these peaks in the MS/MS spectra of 1054 and 1068 reveals that these compounds contain at least one Lac-Val-Hiv-Val tetramer as valinomycin does. However, the MS/MS spectra of 1054 and 1068 vary from this point.

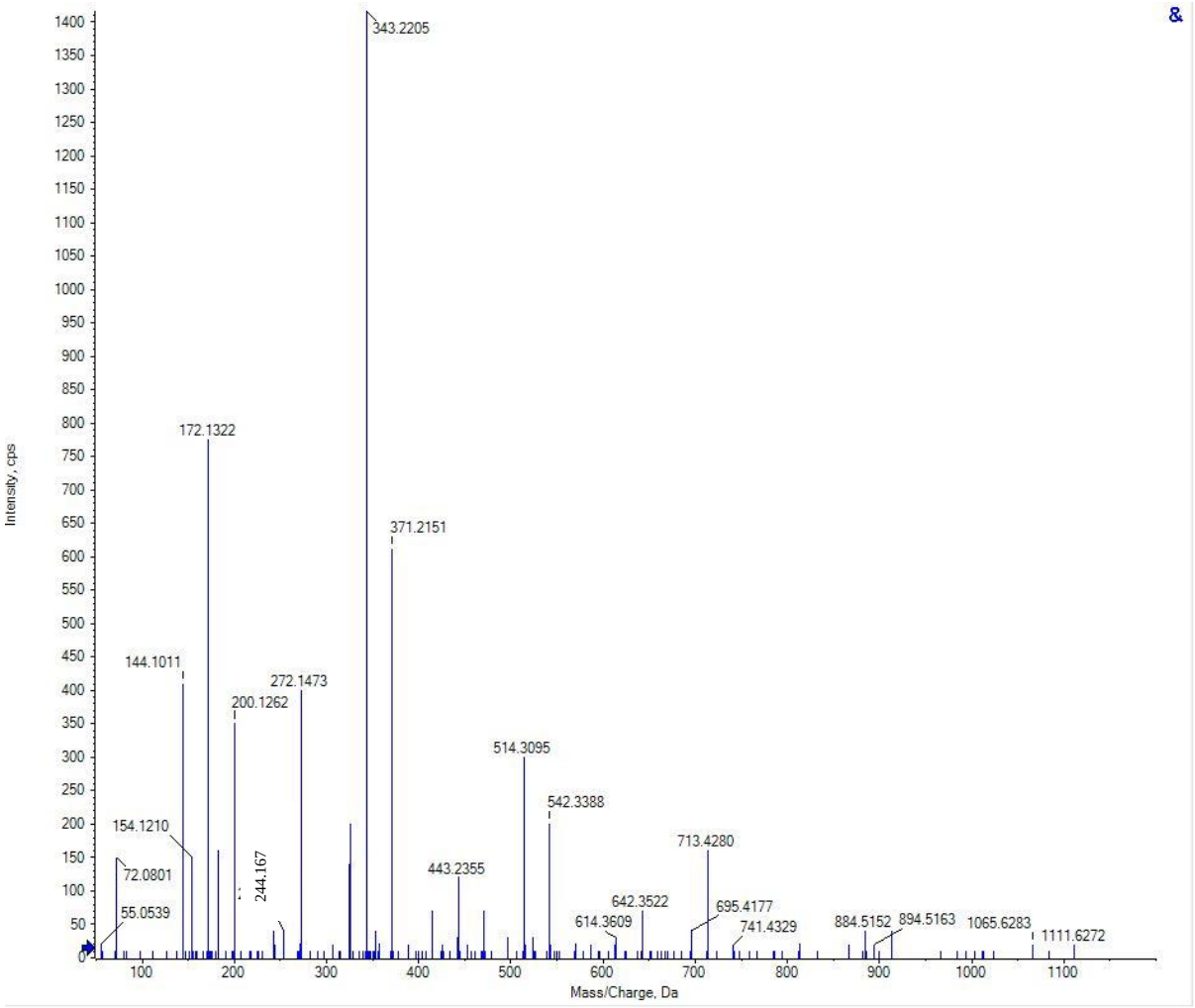

Figure 5.12: Valinomycin's MS/MS spectrum.

Compound 1054's MS/MS spectrum reveals that many more lactic acid groups are present in its structure compared to valinomycin's. A mass shift of 171.0895 Da from *m/z* 144.1012 to 315.1897 represents the addition of a Lac-Val group to form a Lac-Val-Lac-Val tetramer. This mass shift of 171.08 Da is repeated twice more to form a type fragments with *m/z* 486.2771 and 657.3654, these represent 3 and 4 sets of Val-Lac dimers respectively. The mass shifts from *m/z* 657.3654 to 757.4181 then to *m/z* 856.4829 and finally to *m/z* 1027.5727 represent the addition of a Hiv, Val and Lac-Val dimer respectively. These fragments represent one pass of valinomycin biosynthesis and support the previous hypothesis that there is one conserved pass of valinomycin biosynthesis involved in synthesising compound 1054. The fragment *m/z* 1027.5727 is a a type fragment and the addition of 27.995 (+CO) brings the final mass to *m/z* 1055.541, the protonated form of compound 1054. This suggests that compound 1054 contained 4 sets of Lac-Val dimers and one Val-Hiv-Lac-Val tetramer. This suggests that two Hiv units were replaced by two Lac units which has been seen in other related

cyclodepsipeptides as discussed previously (Paulo *et al.*, 2019). This correlates to the mass difference of 56.0668 Da between compound 1054 and valinomycin. The complete structural elucidation of compound 1054 is tabulated and displayed in Table 5.8 with each fragment, its observed and theoretical m/z, mass error and intensity. It must be noted that a few mass fragments display a high mass error which puts their accuracy into question. However, the proposed structure is consistent with all mass fragments and patterns which suggests it is accurate. The proposed structure of compound 1054 is displayed in Figure 5.13.The MS/MS spectrum of compound 1054, annotated with some of the major mass shifts and neutral losses is displayed in Figure 5.14. Compound 1054 has a predicted formula of $C_{50}H_{82}N_6O_{18}$ with a theoretical mass of 1054.5685 Da and a calculated mass of 1054.5671 with a low mass error of -1.3 ppm. A compound with the same mass and formula was located on the PubChem database (National Center for Biotechnology Information, 2019). However, the structure was defined as a cyclic peptide comprised of repeating valine-alanine units. The source was not given and no other reports of this structure were found, so further comparison was not possible. Searching other sources, such as the KEGG and MassBank databases yielded no matches.

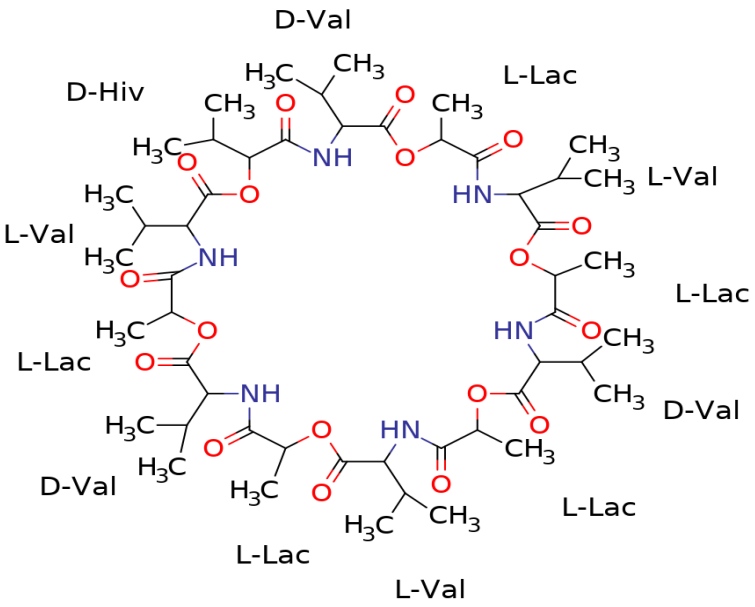

Figure 5.13: Proposed molecular structure of compound 1054 with each amino and hydroxy acid labelled (Chemicalize)**.**

Table 5.8: Identity of the mass fragments in compound 1054's MS/MS spectrum with observed and theoretical *m/z*'s, mass error and fragment ion type.

Name	Observed mass	Theoretical Mass	Mass error (ppm)	Fragment Type
Lac	72.0806	72.0211	825.7438	b
Lac-Val	144.1012	144.1023	-7.93186	a
Lac-Val	172.0959	172.0973	-8.38479	b
Val-Lac-Hiv	244.1167	244.1548	-155.942	a
2(Lac-Val)	315.1897	315.1919	-6.93546	a
Lac-Val-Hiv-Val	343.2197	343.2232	-10.1625	a
Lac-Val-Hiv-Val	371.2158	371.2182	-6.43287	b
Val-Lac-Hiv-Val-Lac	415.2043	415.2443	-96.3698	a
3(Lac-Val)	486.2771	486.2814	-8.90225	a
Val-Lac-Hiv-Val-Lac-Val	514.3079	514.3127	-9.39312	a
Lac-Val-Hiv-Val-Lac-Val	542.3024	542.3077	-9.83021	b
3(Lac-Val)-Lac	558.2994	558.3026	-5.65643	a
Lac-Val-Hiv-Val-Lac-Val-Lac	614.3225	614.3289	-10.3528	b
4(Lac-Val)	657.3654	657.3710	-8.47619	a
4(Lac-Val)	685.395	685.3660	42.35401	b
4(Lac-Val)-Hiv	757.4181	757.4234	-7.00137	a
4(Lac-Val)-Hiv-Lac	828.4538	828.4605	-8.1054	a
4(Lac-Val)-Hiv-Lac	856.4829	856.4555	31.97481	b
4(Lac-Val)-Hiv-Lac-Val-Lac	1027.572	1027.5451	26.21977	a
4(Lac-Val)-Hiv-Lac-Val-Lac	1055.541	1055.5401	0.702958	b
4(Lac-Val)-Hiv-Lac-Val-Lac	1072.57	1072.5666	2.86192	b ($+NH4^{+}$)

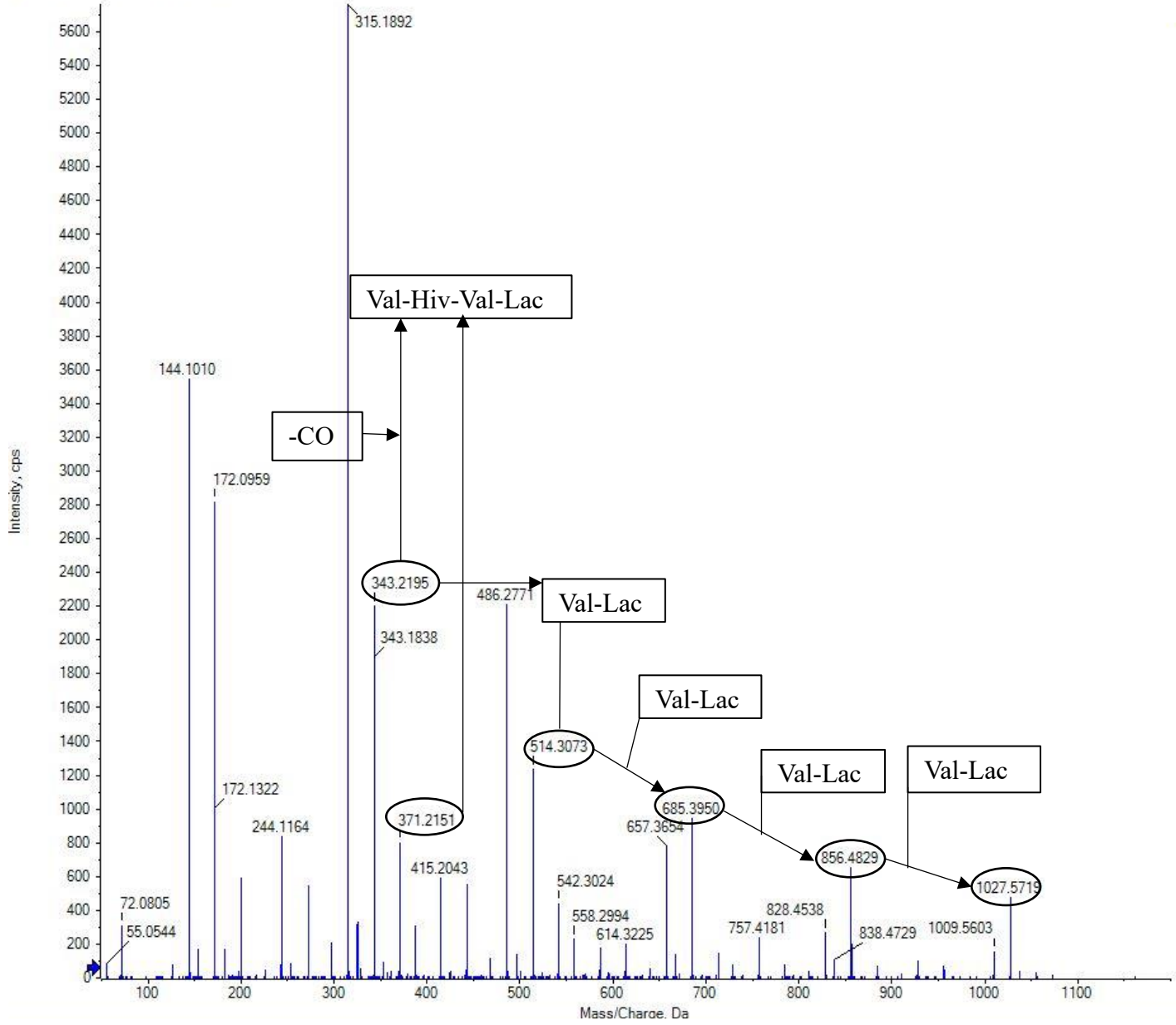

Figure 5.14: MS/MS spectrum of compound 1054 annotated with mass fragments and corresponding components.

The same workflow applied to compound 1054's MS/MS spectrum was used to elucidate compound 1068's structure. Starting from the matching peaks in valinomycin's MS/MS spectrum aided the elucidation. The mass shift of 171.9849 Da from *m/z* 343.2197 to 415.2046 adds a Val-Lac dimer to the Val-Hiv-Lac-Val tetramer. The next mass shift of 113.0838 Da

from *m/z* 415.2046 to 528.2884 suggests that a Leu/Ile groups is added. Paulo. *et al* (2019)'s proposes that Val groups can be substituted for a Leu/Ile and reported it in several cyclodepsipeptides (Paulo *et al.*, 2019). The mass shift of 171.08 Da from *m/z* 528.2884 to 699.4119 then to *m/z* 870.4919 and final to *m/z* 1041.5887 suggests the addition of Lac-Val dimers. These mass shifts are supported by additional shifts seen in 1068's spectrum. The 171.0885 Da mass shift from *m/z* 144.1012 to 315.1897 represents the addition of a Lac-Val dimer to form a a type Lac-Val-Lac-Val tetramer. Another 177.0879 Da mass shift is observed from *m/z* 315.1897 to 486.2776 which represents a a type 3 (Lac-Val) hexamer. These same mass shifts are seen in 1054's MS/MS spectrum (Figure) and suggests that the same 2 Lac substitutions for Hiv are seen in 1054 are also present in 1068's structure. The addition of a CO group seen by the mass shift of 27.995 Da from the a type fragment *m/z* 1041.5887 forms the b type *m/z* 1069.585 and completes the final proposed structure. In summary it is proposed that compound 1068 differs from valinomycin's structure by 2 Lac substitutions for 2 Hiv groups and 1 Ile/Leu substitution for 1 Val group. This correlates with the 42.0519 Da mass difference between valinomycin and compound 1068's masses. The complete strucutrual elucidation of compound 1068 is tabulated and displayed in Table 5.9 with each fragment, its observed and theoretical *m/z*, mass error and intensity. Again, it must be noted that a few mass fragments displayed a high mass error which puts their accuracy into question. However, the proposed structure is consistent with all mass fragments and patterns which suggests it is accurate. The proposed structure of compound 1068 is displayed in Figure 5.15. The MS/MS spectrum of compound 1068, annotated with some of the major mass shifts and neutral losses is displayed in Figure 5.16. Compound 1068 has a chemical formula of $C_{51}H_{84}N_6O_{18}$ with a theoretical mass of 1068.5842 Da and an experimental mass of 1068.5820 Da, with a low mass error of -2.0 ppm. No compounds with matching structures or chemical formulae were found in the GNPS library, PubChem, Massbank and KEGG. Therefore, both compounds 1054 and 1068 appear to be novel cyclodepsipeptides.

Table 5.9: Identity of the mass fragments in compound 1068's MS/MS spectrum with observed and theoretical m/z's, mass error and fragment ion type.

Fragment Name	Observed *m/z*	Theoretical *m/z*	Mass error (ppm)	Ion type
Lac-Val	144.1012	144.1023	-7.93186	a
Lac-Val	172.0959	172.0973	-8.38479	b
Val-Lac-Hiv	244.1167	244.1548	-155.942	a
2(Lac-Val)	315.1897	315.1919	-6.93546	a
Lac-Val-Hiv-Val	343.2197	343.2232	-10.1625	a
Lac-Val-Hiv-Val	371.2158	371.2182	-6.43287	b
Val-Lac-Hiv-Val-Lac	415.2046	415.2443	-95.6473	a
3(Lac-Val)	486.2776	486.2814	-7.87404	a
Val-Lac-Hiv-Val-Lac-Leu/Ile	528.2884	528.3284	-75.6745	a
Val-Lac-Hiv-Val-Lac-Leu/Ile	556.318	556.3234	-9.67243	b
Val-Lac-Hiv-Val-Lac-Leu/Ile-Lac-Val	699.4119	699.4179	-8.61288	a
Val-Lac-Hiv-Val-Lac-Leu/Ile-Lac-Val-Lac	771.4315	771.4391	-9.79079	a
Val-Lac-Hiv-Val-Lac-Leu/Ile-Lac-Val-Lac-Val	852.4919	852.4731	22.05982	b^o
Val-Lac-Hiv-Val-Lac-Leu/Ile-Lac-Val-Lac-Val	870.4919	870.5075	-17.8827	a
Val-Lac-Hiv-Val-Lac-Leu/Ile-Lac-Val-Lac-Val-Lac	942.5219	942.5286	-7.10429	a
Val-Lac-Hiv-Val-Lac-Leu/Ile-Lac-Val-Lac-Val-Lac-Val	1023.576	1023.5626	12.7617	b^o
Val-Lac-Hiv-Val-Lac-Leu/Ile-Lac-Val-Lac-Val-Lac-Val-Lac	1041.589	1041.5731	14.94125	a
Val-Lac-Hiv-Val-Lac-Leu/Ile-Lac-Val-Lac-Val-Lac-Val-Lac	1051.563	1051.5576	5.289677	b^o
Val-Lac-Hiv-Val-Lac-Leu/Ile-Lac-Val-Lac-Val-Lac-Val-Lac	1069.585	1069.5681	15.29814	b
Val-Lac-Hiv-Val-Lac-Leu/Ile-Lac-Val-Lac-Val-Lac-Val-Lac	1086.611072	1086.5947	15.05842045	b ($+NH4^+$)

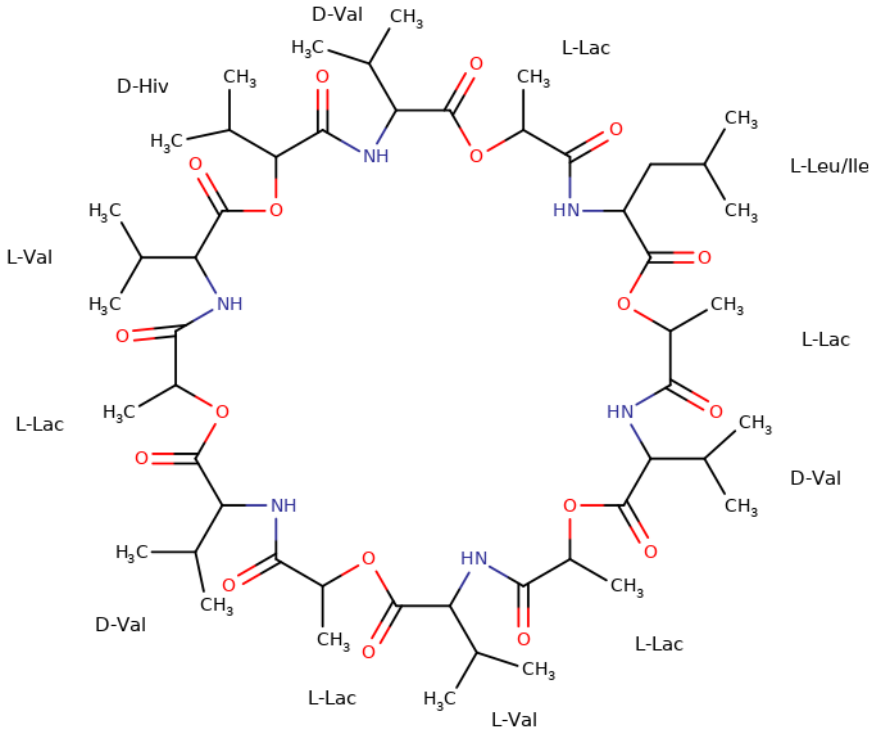

Figure 5.15: Proposed molecular structure of compound 1068 with each amino or hydroxy acid labelled. The structure was drawn using Chemicalize (Chemicalize).

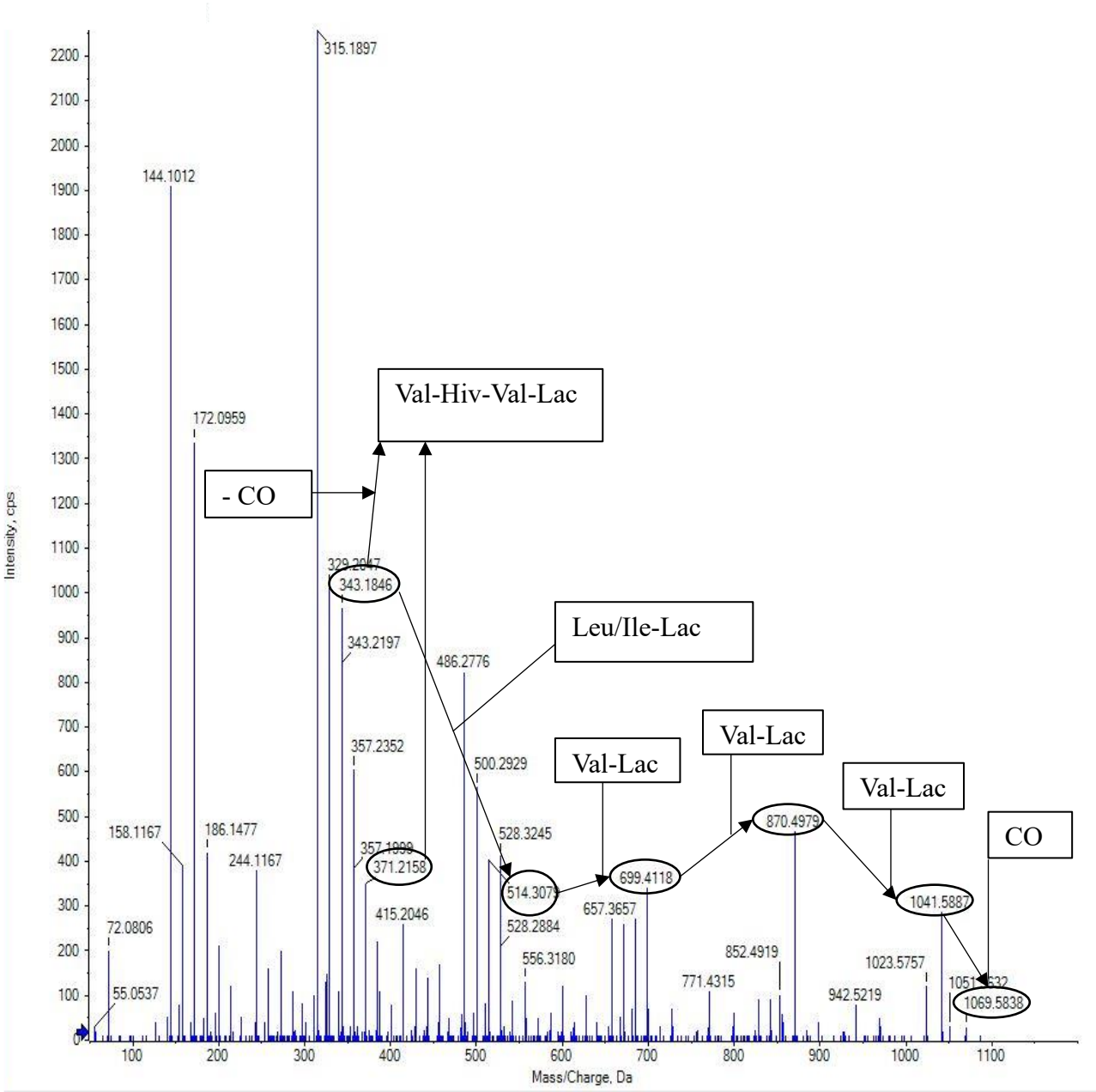

Figure 5.16: MS/MS spectrum of compound 1054 annotated with mass fragments and corresponding components.

The Metabolomics Standards Initiative (MSI) characterises the level of confidence that can be attached to a proposed structure based on the data used to elucidate it (Blaženović *et al.*, 2018). In the MSI ranking, level 0 refers to pure isolated compounds with fully elucidated stereochemistry and 3D structures. Level 1 refers to compounds with full 2D structural elucidation by techniques such as HRMS and 2D NMR. The methylated crown ethers discussed in Chapter 4 therefore have a level 1 confidence level. The cyclodepsipeptides 1054 and 1068

were elucidated based on biosynthetic logic and MS/MS spectrum analysis with comparison to literature and library searches. This attaches a level 2 confidence level to these structures, as they were determined by at least two orthogonal pieces of information including evidence that excludes all other candidates. To fully characterise the cyclodepsipeptide analogues proposed in this investigation and by Paulo *et al.* (2019), they either need to be purified and characterised or synthesised and characterised.

To purify each cyclodepsipeptide, more advanced chromatographic techniques would be required. After RP+NP SPE, active fractions could be separated by HPLC or Ultra Performance Liquid Chromatography (UPLC). UPLC is a chromatographic system that provides improved separation, with much shorter run times (Craige Trenerry and Rochfort, 2010). This is achieved by a combination of 1.7 µm reverse phase packing material and a system that can operate at 6000–15000 pressure per square inch (psi). Typically, HPLC systems use 3-5 µm packing material and operate at 2000–4000 psi. Reducing the particle size of the packing material of the solid phase and increasing the flow rate increases separation efficiency. This leads to greater resolution and sensitivity. Extensive HPLC separation steps have been shown to be able to separate montanastatin from valinomycin (Pettit *et al.*, 1999; Singh *et al.*, 2019). In both investigations, the recovery of montanastatin was poor and, to overcome this, the *Streptomyces* strains were grown in bioreactors to obtain large amounts of crude material. Theoretically, the same processes should be able to purify the cyclodepsipeptide analogues from the crude extracts of strain PR3. Singh *et al.* (2019) investigated the cultivation conditions and discovered that *Streptomyces lavendulae* strain ACR DA1 produced large quantities of cyclodepsipeptides at low temperatures (Singh *et al.*, 2019). While it is unknown if strain PR3 would respond in the same manner, more in-depth study of strain PR3's secondary metabolism under different cultivation conditions could improve cyclodepsipeptide production. Once purified, the cyclodepsipeptide structures could be fully elucidated by HRMS and 2D NMR and compared to the predicted structures. Alternatively, the predicted structures of the cyclodepsipeptide analogues could be synthesised for further study. A modified version of the method used to synthesise montanastatin may be suitable for the other analogues (Doi and Asano, 2002). The synthesis of the cyclodepsipeptides and the development of purification methods after culture optimisation and bioreactor cultivation of strain PR3 were beyond the scope of this investigation. To investigate if the cyclodepsipeptides could be developed further, fraction #3 (SPE Method #6) was selected for antiplasmodial efficacy and host selectivity evaluation.

Fraction #3 was selected as it was the most active fraction and was deemed to be moderately pure, as ^{1}H NMR analysis suggested it contained the cyclodepsipeptides and minor impurities.

5.3.5 Antiplasmodial Efficacy and Host Selectivity of the Cyclodepsipeptides

To better evaluate the antiplasmodial efficacy and host selectivity of the cyclodepsipeptide fraction, valinomycin (≥ 98% purity, Merck®, Germany) was subjected to the same series of tests to allow a comparison of the data. Fraction #3 and valinomycin were tested for antiplasmodial activity against the drug-sensitive strain of *P. falciparum*, NF54 (section 2.2.4). Antiplasmodial efficacy was also determined against the multidrug resistant strain of *P. falciparum*, K1 (section 5.2.5).

Fraction #3 displayed excellent antiplasmodial activity against NF54, with a mean IC_{50} of 25 ± 3.5 ng/mL (Table 5.10). Valinomycin displayed very potent activity against NF54, with a mean IC_{50} of 1.4 ± 0.4 ng/mL, which matched the efficacy displayed by the positive controls used (Table 5.10). This activity is comparable to the published antiplasmodial data for valinomycin (Gumila *et al.*, 1996). Fraction #3 exhibited good activity against the multidrug-resistant K1 strain, with a mean IC_{50} of 101 ± 1 ng/mL. This is within the acceptable range for *in vitro* activity of a candidate compound against resistant strains, discussed in Chapter 2 (Pink *et al.*, 2005). Valinomycin continued to display extremely potent activity and exhibited an IC_{50} of 8.4 ± 0.3 ng/mL against the K1 strain. The controls were within the acceptable ranges.

The resistance index (RI) is used to compare the antiplasmodial activity of a compound against drug-sensitive and resistant strains to estimate if its action is impacted by resistance. The RI is the ratio of the drug-resistant IC_{50} versus the drug-sensitive IC_{50} (K1 IC_{50}/NF54 IC_{50}). The RIs are compared to the positive controls that are affected by resistance, in this case, chloroquine. The RI of chloroquine was 32, while fraction #3, valinomycin and the second control, artesunate, had RIs of 4, 6 and 2, respectively (Table 5.10). The low RIs and IC_{50}s displayed, suggest that valinomycin and fraction #3 are not affected by the *Plasmodium* resistance mechanisms that reduce the effectiveness of chloroquine, cycloguanil, sulfadoxine and pyrimethamine.

Table 5.10: Mean antiplasmodial activity of fraction #3 (SPE Method #6) and valinomycin against *P. falciparum* strain NF54 (drug-sensitive) and strain K1 (multidrug-resistant), N=2 biological repeats with 4 technical repeats.

Sample	Antiplasmodial activity against *P. falciparum* NF54 IC_{50} (ng/mL)	Antiplasmodial activity against *P. falciparum* K1 IC_{50} (ng/mL)	Resistance Index (RI) (K1 IC_{50}/NF54 IC_{50})
Fraction #3	25 ± 3.5	101 ± 1.0	4
Valinomycin	1.4 ± 0.4	8.4 ± 0.3	6
Chloroquine	6.4 ± 0.5	205 ± 19.0	32
Artesunate	1.8 ± 0.1	4.0 ± 1.0	2

While valinomycin is an effective antibiotic, it displays very poor host selectivity and is barred from clinical use (Wu *et al.*, 2004; Paananen *et al.*, 2005). To determine if the isolated cyclodepsipeptide fraction displayed similar toxicity, both fraction #3 and valinomycin were tested for cytotoxicity and haemotoxicity (sections 2.2.6 and 2.2.7, respectively). Valinomycin displayed no haemotoxicity, but did display cytotoxicity against the CHO and HepG2 cell lines, with mean IC_{50}s of 12.4 ± 1.1 and 1.8 ± 0.8 µg/mL respectively (Tables 5.11 and 5.12). While data could not be found for the same cell lines, these results are comparable to studies of valinomycin in similar mammalian cell lines (Bugelski *et al.*, 2000). For example, valinomycin was shown to have an IC_{50} of 9.57 ng/mL against the Vero cell line (Wu *et al.*, 2004). Fraction #3 showed no cytotoxicity up to 100 µg/mL against the CHO cell line nor any haemotoxicity against human erythrocytes (Tables 5.11 and 5.12). However, it did show moderate cytotoxicity against the HepG2 cell line, with a mean IC_{50} of 10.3 ± 2.2 µg/mL. Despite this,

fraction #3 exhibited a SI above 100 against all the tested cell lines, which suggests it is selectively targeting *P. falciparum*.

Table 5.11: Mean antiplasmodial activity against *P.* falciparum, NF54 and mean cytotoxicity against the Chinese Hamster Ovary and HepG2 cell lines of fraction #3 (SPE Method #6) and valinomycin, N=2 biological repeats with 4 technical repeats.

Sample	Antiplasmodial activity against *P. falciparum* NF54 IC_{50} (ng/mL)	Cytotoxicity against Chinese Hamster Ovary IC_{50} (µg/mL)	Cytotoxicity against HepG2 IC_{50} (µg/mL)	Selectivity Index (SI) (CHO IC_{50})/ (*P. falciparum* NF54 IC_{50})	Selectivity Index (SI) (HepG2 IC_{50})/ (*P. falciparum* NF54 IC_{50})
Cyclodepsipeptides (Fractions #3)	25.0 ± 3.5	> 100	10.3 ± 2.2	> 4000	412
Valinomycin	1.41 ± 0.4	12.4 ± 1.1	1.8 ± 0.8	8794	1276
Emetine	-	0.01 ± 0.001	0.011 ± 0.004	-	-

Table 5.12: Haemotoxicity of fraction #3 (SPE Method #6) and valinomycin, N=2 biological repeats with 4 technical repeats.

Sample	Antiplasmodial activity against *P. falciparum* NF54 IC_{50} (ng/mL)	Haemotoxicity against Human Erythrocytes IC_{50} (µg/mL)	Selectivity Index (SI) (Erythrocytes IC_{50}/ NF54 IC_{50})
Fraction #3	25.0 ± 3.5	> 100	> 4000
Valinomycin	1.4 ± 0.4	> 100	> 71428

The discovery of these new cyclodepsipeptides could have an important impact in antimalarial drug development. Neutral ionophores are receiving increased interest as novel antimalarials. Ionophores have been found to present potent antiplasmodial efficacy and a recent study found that the neutral ionophore, maduramicin, was able to inhibit *Plasmodium* gametocytes (Gumila *et al.*, 1996; Sun *et al.*, 2015; Maron *et al.*, 2016). The inhibition of the development of the gametocyte stage prevents the transmission of the malaria parasite. This is one of the Single Exposure Radical Cure and Prophylaxis (SERCaP) parameters desired in future antimalarials (Burrows *et al.*, 2013). The study also found that *P. falciparum* infected erythrocytes are more sensitive to the actions of these neutral ionophores than uninfected erythrocytes (Maron *et al.*, 2016). The results obtained in this investigation support this observation. As discussed previously, the *Plasmodium* parasites remodel the erythrocyte upon infection and are heavily reliant on ion transport making them vulnerable to ionophore activity. These published studies and the results obtained in this investigation show the potential of neutral ionophores as novel antimalarials. Therefore, further study needs to focus on purifying the cyclodepsipeptides from *Streptomyces* strain PR3 and evaluating their antiplasmodial efficacy and host selectivity.

It must be noted that it is possible that valinomycin is the only antiplasmodial cyclodepsipeptide present and the efficacy and toxicity values determined for fraction #3 are from valinomycin being diluted by the other components in the mixture. This cannot be determined at this stage of the investigation, but the structural similarity predicted for the cyclodepsipeptide analogues suggests they could have a similar mechanism of action to valinomycin, which may equate to similar efficacy. The changes in structure could, however, lead to alterations in ion selectivity and binding, which could affect efficacy and selectivity. This is documented in the efficacy of MCEs (this study) compared to other crown ethers (Gokel *et al*., 2004). This is also observed with the cyclodepsipeptides. For example, while it displayed weaker antibacterial and anticancer activity, montanastatin was found to display better host selectivity than valinomycin (Pettit *et al.*, 1999). The cyclodepsipeptide analogues could be as toxic as valinomycin or less efficacious, but it is also possible that one or more of the analogues displays matching efficacy and improved selectivity. Not only is it possible that one or more display suitable parameters for clinical development, but they could also be used as scaffolds to synthesise improved derivatives. In summary, the efficacy and selectivity results for the fraction #3 cyclodepsipeptides, while inconclusive are still promising and the individual cyclodepsipeptides need to be purified before sound conclusions can be drawn.

5.3.6 Relationship Between Cyclodepsipeptides and Methylated Crown Ethers

During bioassay guided fractionation an interesting relationship between the cyclodepsipeptides and the MCEs was suspected. During the investigation, potent antiplasmodial activity was detected from an impure sample. This active sample was studied in Chapter 3 and referred to as fraction 540, as the *m/z* 540 was tracked and collected by HPLC-MS. Fraction 540 was found to have antiplasmodial efficacy of 27 ± 7 ng/mL against *P. falciparum* NF54 (section 3.3.3, Table 3.10). ^{1}H NMR analysis of fraction 540 revealed it to be too impure to elucidate the structure. Comparatively, the cyclodepsipeptide fraction #3 presented strong antiplasmodial activity of 25 ± 3.5 ng/mL, and its ^{1}H NMR spectrum suggested that there had been a significant improvement in purity.

Generally, removing impurities improves the antiplasmodial activity of the fraction; however, the efficacy displayed by fraction 540 and fraction #3 are comparable. Analysis of the past HRMS data of fraction 540 revealed the presence of both the MCEs and the cyclodepsipeptides (Appendix, Figure 8.11). Due to this it was hypothesised that the MCEs and cyclodepsipeptides interacted in a synergistic manner and further study was conducted to determine if this was true.

A mixture of compounds can interact in three broad ways: additive, synergistic, or antagonistic (van Vuuren and Viljoen, 2011). In terms of antibiotics, an additive effect represents no interaction between the compounds present and any antibiotic activity displayed is merely a summation effect. An antagonistic effect is when the compounds interact to display less than the additive effect. Comparatively, a synergistic effect is when a mixture displays greater than the additive effect. Synergistic effects can occur for several reasons: pharmacodynamic synergism, pharmacokinetic synergism, by overcoming resistance against partner compounds or by reducing the adverse side effects of partner compounds (Caesar and Cech, 2019).

Pharmacodynamic synergism results from the compounds in combination inhibiting multiple targets, which has an overall stronger effect than would be expected from adding the effects of the individual compounds (Hu and Zhang, 2012). Pharmacokinetic synergism occurs when the compounds in combination improve each other's absorption, stability, distribution, or elimination, which increases efficacy (Wagner and Ulrich-Merzenich, 2009).

There is no standardised methodology to determine the relationship between compounds (Matthews *et al.*, 2017). Many models and methods are employed, with the majority based on two definitions of additivity; the Loewe additivity model and the Bliss independence model. The general isobole equation, based on the Loewe additivity model, is the most popular for studying combination effects in many fields, including antimalarial drug research (Fivelman *et al*., 2004; Wagner and Ulrich-Merzenich, 2009; Matthews *et al.*, 2017). In this model, the nature of the interaction between two compounds is determined by the sum of the fraction IC_{50} (ΣFIC), determined using equation 1 and the shape of a plotted isobologram (Fivelman *et al*., 2004; Matthews *et al.*, 2017).

Equation 1: $\Sigma FIC = FIC_A + FIC_B$

$FIC_{50A} = IC_{50}x / IC_{50}A$

Where $IC_{50}A$ is the IC_{50} of the compound alone, and $IC_{50A}x$ is the IC_{50} of the compound in a specific fixed-ratio. If the ΣFIC is equal to 1, then the interaction is deemed as additive, if the interaction is less than 1, it is synergistic and if it is greater than 1, it is antagonistic (van Vuuren and Viljoen, 2011). An isobologram is a graphical representation of combination effects between two samples, where its axes represent the doses of the individual agents and the plotted points represent the combined effect of each combination, i.e. the ΣFIC (van Vuuren and Viljoen, 2011; Caesar and Cech, 2019). When two compounds do not interact, their isobologram plot forms a straight line, which represents additivity. If they are synergistic, the plot will form a concave curve below the additivity line. If they are antagonistic, the plot will result in a convex curve above the line. A generic isobologram showing the three types of interactions is shown in Figure 5.17.

To determine the relationship between the cyclodepsipeptide and MCEs, the fixed-ratio isobologram method (section 5.2.6) was used. Fraction #3, generated by SPE Method #6, (section 5.2.1) and used in previous antiplasmodial efficacy determination, was used to represent the cyclodepsipeptides. Fraction #4, produced by SPE Method #5 (section 3.2.3.5), which was used in the antiplasmodial efficacy determination of the MCEs in Chapter 4, was used to represent the MCEs. The concentrations and ratios used for testing are displayed in Table 5.1.

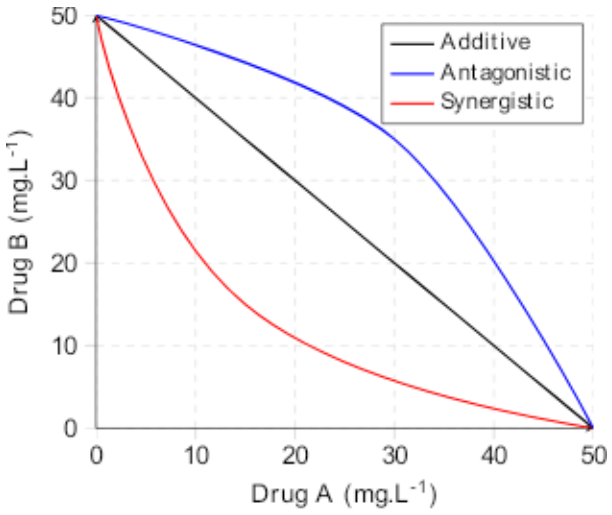

Figure 5.17: Generic isobologram showing the three possible relationships between two active compounds (Part One)**.**

The results of the fixed-ratio method suggested that there is a synergistic relationship between the MCEs and the cyclodepsipeptides. When plotted as an isobologram the FIC_{50}'s of the cyclodepsipeptide fraction and the MCE fraction fall below the additivity line and have a general concave curve suggesting synergy (Figure 5.18).

The ΣFIC of each fixed ratio, was less than 1, which suggested that there is a synergistic relationship between the cyclodepsipeptides and the MCEs (Table 5.13)(Fivelman *et al*., 2004). However, the lack of a standard methodology to determine synergy makes analysis of these results difficult. For example, the ΣFIC cut-off value for each interaction is widely debated, as results can be misinterpreted or biased. Some reviewers believe that the cut-off values for the ΣFIC should be ≤ 0.5 to be classed as synergistic, 0.5–1 for additive, 1.0 to 4.0 for non-interacting and > 4 for antagonistic (van Vuuren and Viljoen, 2011; Caesar and Cech, 2019). Therefore, characterisation of the relationship between the cyclodepsipeptides and MCEs depends on the cut-off values used when interpreting the data presented. Taking this into consideration, when the cyclodepsipeptides and the MCEs are combined in the fixed ratios of 4:1, 3:2 and 1:4, the results suggest that there is an additive, or weak synergistic, effect. The ΣFIC of these fixed-ratios are greater than 0.5, but less than 1. However, when dosed in the fixed ratio of 2:3, both the isobologram and the ΣFIC suggest that there is a definite synergistic relationship between the two neutral ionophores, as the ΣFIC is less than 0.5 and the corresponding point on the isobologram falls much lower than the others. This is highlighted in red in Table 5.13.

Due to the lack of consensus in the scientific community on which method is the best to determine synergy, an additional model based on the work of Chou and Talalay was used to check the results obtained from the fixed-ratio method (Chou and Talalay, 1984). Chou and Talalay argue that synergy is a physiochemical interaction, not a theoretical statistical problem and developed a model which employs the mass-action law principle (Chou and Talalay, 1984; Chou, 2010). The mass-action law principle derives a median-effect equation, which was derived from four existing, well-studied physiochemical equations. These were the Henderson-Hasselbach, Hill, Michaelis-Menten and Scatchard. Additional factors, such as the shape of the inhibition curve are considered, with efficacy, the ΣFIC and shape of the isobologram (Chou and Martin, 2005). The result of the analysis is the combination index (CI) which defines the interaction. Broadly, if a combination generates a CI of 1, this represents additivity and CI values of < 1 and > 1 represent synergy and antagonism, respectively. A detailed description of what each CI represents is displayed in Table 5.14 (Chou and Martin, 2005). Using these

methods, a series of software programmes, such as CompuSyn and CalcuSyn, were developed to allow easy, automated data analysis (Chou and Talalay, 1984; Chou and Martin, 2005)

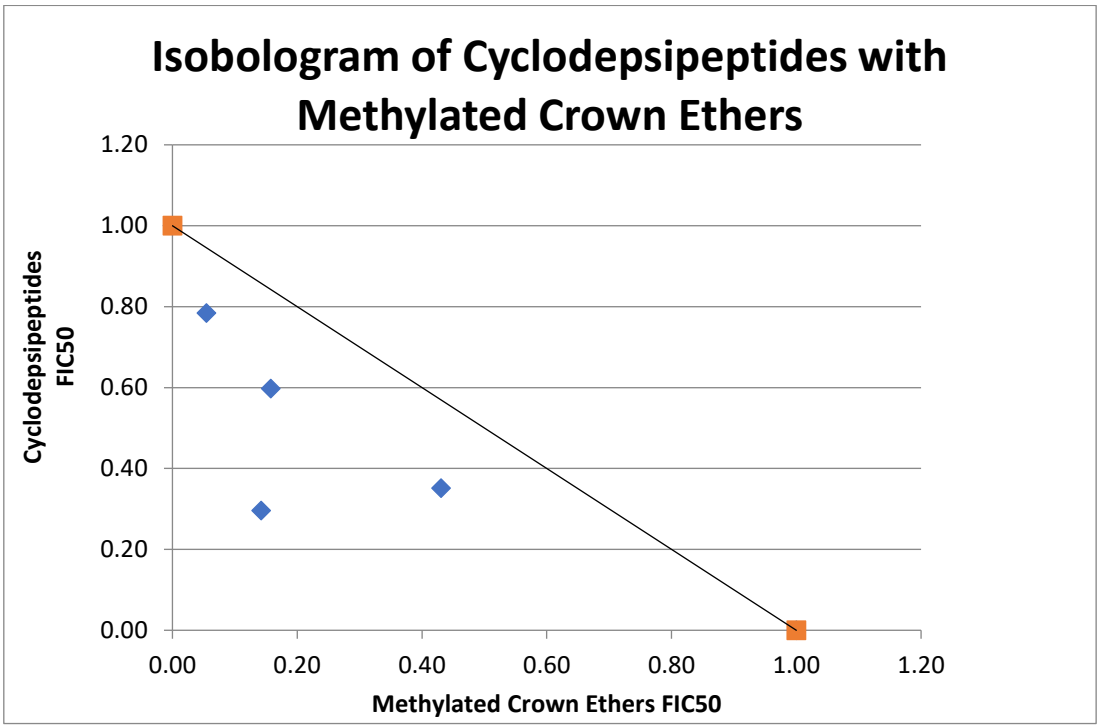

Figure 5.18: Isobologram of the cyclodepsipeptides in combination with the methylated crown ethers.

.

Table 5.13: Mean antiplasmodial activity and fractional IC_{50}s of the cyclodepsipeptides and methylated crown ethers at each fixed-ratio dose and their corresponding sum of the fractional IC_{50}, N=2 biological repeats with 4 technical repeats.

Ratio	Cyclodepsipeptides		Methylated Crown Ethers		Sum of Fractional IC_{50}($\sum FIC_{50}$)
	Antiplasmodial activity against *P. falciparum*, NF54 IC50 (ng/mL)	Fractional IC_{50}(FIC_{50})	Antiplasmodial activity against *P. falciparum*, NF54 IC50 (ng/mL)	Fractional IC_{50}(FIC_{50})	
5:0	23.4 ± 2.3	1.0	N/A	N/A	1.0
4:1	18.3 ± 0.4	0.78	104 ± 31.5	0.05	0.83
3:2	13.9 ± 1.3	0.60	300 ± 7.8	0.16	0.75
2:3	6.9 ± 0.7	0.30	271 ± 47.3	0.14	0.44
1:4	8.2 ± 0.7	0.35	822 ± 69.3	0.43	0.63
0:5	N/A	N/A	1910 ± 42.3	1.0	1.0

Table 5.14: Description of each combination index range (Chou and Martin, 2005).

Combination Index Range (CI)	Description
< 0.1	Very strong synergism
0.1–0.3	Strong synergism
0.3–0.7	Synergism
0.7–0.85	Moderate synergism
0.85–0.90	Slight synergism
0.90–1.10	Nearly additive
1.10–1.20	Slight antagonism
1.20–1.45	Moderate antagonism
1.45–3.3	Antagonism
3.3–10	Strong antagonism
> 10	Very strong antagonism

The raw data produced by the fixed-ratio method was inputted into CompuSyn (section 5.2.7). This allowed a direct comparison to the results generated from the fixed-ratio method and, as CompuSyn analyses the raw data, bias and misinterpretation were removed. The results from CompuSyn corroborate the results obtained from the fixed-ratio method (Table 5.15). The CIs of the fixed-ratios 4:1 and 1:4 suggested a synergistic relationship, while the 3:2 ratio displayed a CI suggesting moderate synergism. The fixed-ratio 2:3 generated a very low CI, suggesting very strong synergism between the cyclodepsipeptides and the MCEs. This is highlighted in red in Table 5.15.

The results obtained from both models suggest that combining the cyclodepsipeptides and MCEs elicits a synergistic response. Both models suggested that the best fixed ratio was 2:3 or a µg/mL combination of 1:40 of cyclodepsipeptides to MCEs. Exactly why this combination is more effective than the others or how the MCEs potentiate the action of the cyclodepsipeptides is unknown. Although the synergistic activity is likely due to their shared ionophore structures, the exact mechanism of action still needs to be elucidated.

These results may also explain why fraction 540 displayed such strong antiplasmodial activity despite being impure, and why other fractions, such as the HPLC-MS purified fraction 870 showed weaker activity. Both fractions contained the MCEs and cyclodepsipeptides, but if the ratios were slightly different it would have had a large impact on the nature of the synergistic

relationship between the two ionophores, which would have impacted antiplasmodial efficacy. The cultivation conditions of *Streptomyces* strain PR3 may also have affected the number of cyclodepsipeptides present in the active fractions, which could explain the activity differences between the ISP-2 and JCM #61derived fractions. It was, unfortunately, not possible to directly compare the HRMS results of fraction 540 and 870 with fraction #3, or with each other because, at this stage of the investigation, no material of fractions 540 and 870 remained. As the conditions were not controlled, comparing past HRMS data from different runs at different times was considered to be too inaccurate.

Table 5.15: Combination index values for each fixed-ratio compound combination calculated by CompuSyn, N=2 biological repeats with 4 technical repeats.

Fraction Ratios	Combination Index (CI)
4:1	0.58
3:2	0.71
2:3	0.01
1:4	0.64

Further study is required to reproduce these results with different synergy models such as the Bliss independence or checkerboard models (Caesar and Cech, 2019). However, these results are intriguing , and future work could focus on determining the viability of using the MCEs in combination therapy with the cyclodepsipeptides and other neutral ionophores. As discussed in Chapter 4, the MCEs showed no toxicity against the CHO and HepG2 cell lines and, no haemotoxicity, suggesting host selectivity. The MCEs' selectivity implies that using them in combination with the more-toxic ionophores, like valinomycin, could reduce the toxic side effects while maintaining antiplasmodial efficacy.

6 Conclusion

6.1 Research Summary

In conclusion, the research objectives set at the beginning of the investigation were met, but more work is required to confirm these observations. Initial screening of the filamentous actinobacteria revealed a high number of hit candidates from a small sample size indicating that that these microorganisms do have the ability to produce potent antiplasmodial agents. This is supported by literature (Gumila *et al.*, 1996; Prudhomme *et al.*, 2008; Bennur *et al.*, 2015; Zin *et al.*, 2017). To determine if these antiplasmodial compounds were novel and suitable for lead drug development, they needed to be identified and elucidated. Therefore, the hit candidates were evaluated for further study and *Streptomyces* strain PR3 was selected as its crude extracts displayed good antiplasmodial efficacy and no cytotoxicity against three mammalian cell lines, CHO, HEPG2, and erythrocytes.

The crude extracts of strain PR3 were studied by bioassay-guided fractionation supported by HRMS and NMR analysis. During the investigation a molecule with mass of 870 Da was associated with antiplasmodial activity. Subsequent purification by reverse and normal phase solid phase extraction (RP+NP SPE) and structural elucidation by HRMS and 2D-NMR revealed the compound to one of several novel methylated crown ethers (MCE). These MCEs were shown to be plastic derivatives specifically, oligomers of polypropylene glycol in the XAD 16-N extraction resin. These oligomers were predicted to cyclize in water to form the MCEs. While these MCEs were found to possess weak antiplasmodial activity, they were non-toxic against the CHO and, HepG2 cell lines, and human erythrocytes, suggesting they could have biomedical applications.

The employment of the Global Natural Products Social (GNPS) molecular networking workflow led to the identification of a series of cyclodepsipeptides in the most active NP SPE fractions, fraction #3 and #4 (SPE Method #6, section 5.2.1). These included valinomycin, montanastatin, and several cyclodepsipeptide analogues. This discovery was supported by HRMS analysis of past samples, ^{1}H NMR analysis, comparison to literature, and genome mining. Further study of these analogues led to the elucidation of two new cyclodepsipeptides, compounds 1054 and 1068 by mass spectrometry and biosynthetic logic. The most active SPE

fraction, fraction #3, was almost wholly comprised of cyclodepsipeptides and displayed good antiplasmodial activity against the drug-sensitive NF54, and multidrug-resistant K1, strains of *P. falciparum*. No cytotoxicity was displayed against the CHO cell line nor haemotoxicity against human erythrocytes. Moderate cytotoxicity was measured against the HepG2 cell line, but the SI suggested that the fraction was selective.

Valinomycin was detected in fraction #3 and the chromatographic methodology developed was unable to separate the cyclodepsipeptide analogues due to their close structural similarities. Therefore, it is a possibility that valinomycin is the cause of the antiplasmodial activity and cytotoxicity detected in fraction #3. Due to the structural similarities of the analogues to valinomycin, it is also possible that the cyclodepsipeptide analogues are contributing to fraction #3's antiplasmodial activity and cytotoxicity. The cyclodepsipeptide analogues may or may not, exhibit greater selectivity than valinomycin as small changes in structure can alter the efficacy and selectivity of neutral ionophores (Pettit *et al.*, 1999; Gokel *et al.*, 2004). Other neutral ionophores such as maduramicin, have been found to exhibit potent and selective activity against multiple stages of the *P. falciparum* lifecycle (Gumila *et al.*, 1996; Maron *et al.*, 2016). Therefore, neutral ionophores such as the cyclodepsipeptides, may make suitable candidates for novel antimalarial compounds and require further study. Finally, through the use of two separate models, it was estimated that combining the cyclodepsipeptides and MCEs elicits a synergistic increase in antiplasmodial activity. This requires further study to determine if the MCEs and cyclodepsipeptides can be used as combination therapies.

6.2 Limitations

Several limitations need to be noted to inform future studies.

During screening, the antiplasmodial efficacy of certain active crude extracts was not replicated. Only the strains selected for further study in this investigation and related ones, were cultured, extracted, and tested multiple times. Before studying the remaining selected hit strains, their antiplasmodial efficacy must be reproduced.

The failure to purify the cyclodepsipeptide analogues from one another impeded the evaluation of their antiplasmodial efficacy, host selectivity, and further description. Subsequent studies must focus of the purification of the cyclodepsipeptides to obtain more information about their

antiplasmodial activity and selectivity. The same issue is faced with the MCEs as a series of MCEs were present in the tested fraction and MCEs of certain ring sizes may be contributing to antiplasmodial activity to a greater or lesser extent.

The combination studies conducted only provide an estimate of synergy between the cyclodepsipeptides and the MCEs. Impure fractions were employed to obtain these results, therefore the ratios of the mixtures are likely inaccurate. The impurity of the fractions makes it impossible to specify exactly which components are interacting. While this limited data analysis, it was still clear that the cyclodepsipeptides and MCEs interact in a synergistic fashion. Once pure samples have been obtained, combination studies should be repeated to obtain a more accurate understanding of the synergistic relationship between the cyclodepsipeptides and MCEs. Additional models such as the Bliss independence and checkerboard models could also be employed to corroborate the synergy predicted by this investigation.

6.3 Future Prospects

The results presented in this investigation and in literature suggest the neutral ionophores could be developed into novel antimalarial compounds. Therefore, in the investigator's opinion, future research should focus on the purification or synthesis of the cyclodepsipeptide analogues for evaluation.

The selected hit candidates that were not investigated warrant further study. Strains such as *Streptomyces* strain PR10 displayed highly active crude extracts which could be due to novel compounds. More intensive screening of the filamentous actinobacteria is also required to fully evaluate their antiplasmodial potential and to isolate novel compounds. This will generate new hit candidates that could be studied. All future studies should utilize the GNPS library and molecular networking functions to aid dereplication and compound identification.

The MCEs also require closer study. As discussed, they may have biomedical applications or present new chemistry. The exact mechanism of cyclization of polypropylene glycol oligomers should be elucidated to improve the purification or allow synthesis of the MCEs. The MCEs synergistic potential is another point of interest and could be useful in future combination therapies.

6.4 Contributions

This investigation is one of the few to study the antiplasmodial potential of the filamentous actinobacteria. While only a small sample size was screened many positive hits were observed suggesting they are suitable source for novel antimalarials.

This study failed to isolate and evaluate a suitable novel antiplasmodial agent, however it did discover a novel class of crown ethers that to the author's knowledge have not been reported in literature.

The work published by Paulo *et al.* (2019) was supported by the results discussed in this investigation and through the same workflow two new cyclodepsipeptides were elucidated. These analogues present new chemistry which may equate to improved host selectivity and antiplasmodial efficacy.

7 References

Abraham, E. P. *et al.* (1941) 'Further Observations on Penicillin', *The Lancet*, 238(6155), pp. 177–189. doi: 10.1016/S0140-6736(00)72122-2.

Achan, J. *et al.* (2011) 'Quinine, an old anti-malarial drug in a modern world: role in the treatment of malaria', *Malaria Journal*, 10(1), p. 144. doi: 10.1186/1475-2875-10-144.

Adnani, N., Michel, C. R. and Bugni, T. S. (2012) 'Universal Quantification of Structurally Diverse Natural Products Using an Evaporative Light Scattering Detector', *Journal of Natural Products*, 75(4), pp. 802–806. doi: 10.1021/np300034c.

Ahmad, S. J. *et al.* (2017) 'Discovery of Antimalarial Drugs from Streptomycetes Metabolites Using a Metabolomic Approach', *Journal of Tropical Medicine*, 2017, pp. 1–7. doi: 10.1155/2017/2189814.

Ajua, A. *et al.* (2015) 'The effect of immunization schedule with the malaria vaccine candidate RTS,S/AS01 on protective efficacy and anti-circumsporozoite protein antibody avidity in African infants', *Malaria journal*, 14(1), p. 72.

Allard, P.-M. *et al.* (2016) 'Integration of Molecular Networking and In-Silico MS/MS Fragmentation for Natural Products Dereplication', *Analytical Chemistry*, 88(6), pp. 3317–3323. doi: 10.1021/acs.analchem.5b04804.

Altenburger, R., Nendza, M. and Schüürmann, G. (2003) 'Mixture Toxicity and Its Modeling by Quantitative Structure Activity Relationships', *Environmental Toxicology and Chemistry*, 22(8), p. 1900. doi: 10.1897/01-386.

Altschul, S. (1997) 'Gapped BLAST and PSI-BLAST: a new generation of protein database search programs', *Nucleic Acids Research*, 25(17), pp. 3389–3402. doi: 10.1093/nar/25.17.3389.

Aly, A. S. I., Vaughan, A. M. and Kappe, S. H. I. (2009) 'Malaria Parasite Development in the Mosquito and Infection of the Mammalian Host', *Annual Review of Microbiology*, 63(1), pp. 195–221. doi: 10.1146/annurev.micro.091208.073403.

Anthony, M. P. *et al.* (2012) 'The global pipeline of new medicines for the control and elimination of malaria', *Malaria journal*, 11, p. 316.

Ara, I. and Kudo, T. (2007) ‘Sphaerosporangium gen. nov., a new member of the family Streptosporangiaceae, with descriptions of three new species as Sphaerosporangium melleum sp. nov., Sphaerosporangium rubeum sp. nov. and Sphaerosporangium cinnabarinum sp. nov., and transfer of Stre’, *Actinomycetologica*, 21(1), pp. 11–21. doi: 10.3209/saj.SAJ210102.

Arenaz, P. *et al.* (1992) ‘Genotoxic potential of crown ethers in mammalian cells: Induction of sister-chromatid exchanges’, *Mutation Research/Genetic Toxicology*, 280(2), pp. 109–115. doi: 10.1016/0165-1218(92)90006-L.

Ariey, F. *et al.* (2013) ‘A molecular marker of artemisinin-resistant Plasmodium falciparum malaria’, *Nature*, 505(7481), pp. 50–55. doi: 10.1038/nature12876.

Aslantürk, Ö. S. (2018) ‘In Vitro Cytotoxicity and Cell Viability Assays: Principles, Advantages, and Disadvantages’, in *Genotoxicity - A Predictable Risk to Our Actual World*. InTech. doi: 10.5772/intechopen.71923.

Atlas, R. (2010) *Handbook of Microbiological Media, Fourth Edition*. Fourth. Edited by L. C. Parks. CRC Press. doi: 10.1201/EBK1439804063.

Baba, M. S. *et al.* (2015) ‘In vivo antimalarial activity of the endophytic actinobacteria, Streptomyces SUK 10’, *Journal of Microbiology*, 53(12), pp. 847–855. doi: 10.1007/s12275-015-5076-6.

Baker, D. D. *et al.* (2007) ‘The value of natural products to future pharmaceutical discovery’, *Natural Product Reports*, 24(6), p. 1225. doi: 10.1039/b602241n.

Barka, E. A. *et al.* (2016) ‘Taxonomy, Physiology, and Natural Products of Actinobacteria’, *Microbiology and Molecular Biology Reviews*, 80(1), pp. 1–43. doi: 10.1128/MMBR.00019-15.

Bartholomew, J. W. and Mittwer, T. (1952) ‘The Gram stain.’, *Bacteriological reviews*, 16(1), pp. 1–29. Available at: http://www.ncbi.nlm.nih.gov/pubmed/14925025.

Basso, L. A. *et al.* (2005) ‘The use of biodiversity as source of new chemical entities against defined molecular targets for treatment of malaria, tuberculosis, and T-cell mediated diseases--a review’, *Memorias do Instituto Oswaldo Cruz*, 100(6), pp. 475–506.

Beck, T. (2006) *Will malaria soon be a thing of the past? The potential of recombinant protein vaccines to control one of the world’s most deadly diseases*. Edited by L. Dean and J. McEntyre. Bethesda, USA. Available at:

https://www.ncbi.nlm.nih.gov/books/NBK5951/figure/malaria_LifeCycle/.

Bennur, T. *et al.* (2015) '*Nocardiopsis* species: a potential source of bioactive compounds', *Journal of Applied Microbiology*, p. n/a-n/a. doi: 10.1111/jam.12950.

Benson, D. A. *et al.* (2012) 'GenBank', *Nucleic Acids Research*, 41(D1), pp. D36–D42. doi: 10.1093/nar/gks1195.

Bérdy, J. (2005) 'Bioactive Microbial Metabolites', *The Journal of Antibiotics*, 58(1), pp. 1–26. doi: 10.1038/ja.2005.1.

Berger, S. and Braun, S. (2004) *200 and More NMR Experiments: A Practical Course*. Wiley. New York.

Bero, J., Frédérich, M. and Quetin-Leclercq, J. (2009) 'Antimalarial compounds isolated from plants used in traditional medicine', *Journal of Pharmacy and Pharmacology*, 61(11), pp. 1401–1433. doi: 10.1211/jpp/61.11.0001.

Berthod, A. *et al.* (2009) 'Countercurrent chromatography in analytical chemistry (IUPAC Technical Report)', *Pure and Applied Chemistry*, 81(2), pp. 355–387. doi: 10.1351/PAC-REP-08-06-05.

Bhal, S. K. (2020) *LogP—Making Sense of the Value*. Toronto, Canada. Available at: www.acdlabs.com.

Bian, G. *et al.* (2013) 'Wolbachia Invades Anopheles stephensi Populations and Induces Refractoriness to Plasmodium Infection', *Science*, 340(6133), pp. 748–751. doi: 10.1126/science.1236192.

Bibb, M. J. (2005) 'Regulation of secondary metabolism in streptomycetes', *Current Opinion in Microbiology*, 8(2), pp. 208–215. doi: 10.1016/j.mib.2005.02.016.

Bingham, E. and Cohrssen, B. (2012) *Patty's Toxicology*. Sixth. Wiley.

Biot, C. *et al.* (2011) 'The antimalarial ferroquine: from bench to clinic', *Parasite*, 18(3), pp. 207–214. doi: 10.1051/parasite/2011183207.

Birkenmeyer, R. D. and Kagan, F. (1970) 'Lincomycin. XI. Synthesis and structure of clindamycin, a potent antibacterial agent', *Journal of Medicinal Chemistry*, 13(4), pp. 616–619. doi: 10.1021/jm00298a007.

Blanco, M. and Villarroya, I. (2002) 'NIR spectroscopy: a rapid-response analytical tool',

TrAC Trends in Analytical Chemistry, 21(4), pp. 240–250. doi: 10.1016/S0165-9936(02)00404-1.

Blaženović, I. *et al.* (2018) 'Software Tools and Approaches for Compound Identification of LC-MS/MS Data in Metabolomics', *Metabolites*, 8(2), p. 31. doi: 10.3390/metabo8020031.

Blin, K. *et al.* (2019) 'antiSMASH 5.0: updates to the secondary metabolite genome mining pipeline', *Nucleic Acids Research*, 47(W1), pp. W81–W87. doi: 10.1093/nar/gkz310.

Boddey, J. A. and Cowman, A. F. (2013) 'Plasmodium Nesting: Remaking the Erythrocyte from the Inside Out', *Annual Review of Microbiology*, 67(1), pp. 243–269. doi: 10.1146/annurev-micro-092412-155730.

Borchardt, J. K. (2002) 'The Beginnings of Drug Therapy: Ancient Mesopotamian Medicine.', *Drug news & perspectives*, 15(3), pp. 187–192. Available at: http://www.ncbi.nlm.nih.gov/pubmed/12677263.

Borner, M. M. *et al.* (1994) 'The detergent Triton X-100 induces a death pattern in human carcinoma cell lines that resembles cytotoxic lymphocyte-induced apoptosis', *FEBS Letters*, 353(2), pp. 129–132. doi: 10.1016/0014-5793(94)01023-4.

Bourdy, G. *et al.* (2008) 'Ethnopharmacology and malaria: New hypothetical leads or old efficient antimalarials?', *International Journal for Parasitology*, 38(1), pp. 33–41. doi: 10.1016/j.ijpara.2007.07.004.

Brohm, D. *et al.* (2002) 'Natural products are biologically validated starting points in structural space for compound library development: solid-phase synthesis of dysidiolide-derived phosphatase inhibitors.', *Angewandte Chemie (International ed. in English)*, 41(2), pp. 307–11. Available at: http://www.ncbi.nlm.nih.gov/pubmed/12491416.

Bruker (2019) *What Is NMR?* Available at: https://www.bruker.com/fileadmin/user_upload/8-PDF-Docs/MagneticResonance/NMR/brochures/what-is-nmr_brochure_0115_T153283.pdf.

Bugelski, P. J. *et al.* (2000) 'A strategy for primary high throughput cytotoxicity screening in pharmaceutical toxicology.', *Pharmaceutical research*, 17(10), pp. 1265–72. doi: 10.1023/a:1026495503939.

Burrows, J. N. *et al.* (2013) 'Designing the next generation of medicines for malaria control and eradication.', *Malaria journal*, 12, p. 187. doi: 10.1186/1475-2875-12-187.

Caesar, L. K. and Cech, N. B. (2019) ‘Synergy and antagonism in natural product extracts: when 1 + 1 does not equal 2’, *Natural Product Reports*, 36(6), pp. 869–888. doi: 10.1039/C9NP00011A.

Campbell, N. *et al.* (2008) *Biology*. Eighth. San Francisco: Pearson.

Carter, G. T. *et al.* (1989) ‘Biosynthetic origin of the carbon skeleton of simaomicin .alpha., a hexacyclic xanthone antibiotic’, *The Journal of Organic Chemistry*, 54(18), pp. 4321–4323. doi: 10.1021/jo00279a018.

Castillo, U. F. *et al.* (2006) ‘Munumbicins E-4 and E-5: novel broad-spectrum antibiotics from Streptomyces NRRL 3052’, *FEMS Microbiology Letters*, 255(2), pp. 296–300. doi: 10.1111/j.1574-6968.2005.00080.x.

Centers for Disease Control and Prevention (2015) ‘Malaria’. Available at: https://www.cdc.gov/malaria/about/disease.html.

Challis, G. L., Ravel, J. and Townsend, C. A. (2000) ‘Predictive, structure-based model of amino acid recognition by nonribosomal peptide synthetase adenylation domains’, *Chemistry & Biology*, 7(3), pp. 211–224. doi: 10.1016/S1074-5521(00)00091-0.

Chambers, M. C. *et al.* (2012) ‘A cross-platform toolkit for mass spectrometry and proteomics’, *Nature Biotechnology*, 30(10), pp. 918–920. doi: 10.1038/nbt.2377.

Chan, K. (1994) ‘The Pharmacology of Chinese Herbs; Kee Chang Huang Published 1993 CRC Press, Inc., Boca Raton, FL 388 pages; ISBN 0 8493 4915 X £100.00’, *Journal of Pharmacy and Pharmacology*, 46(2), pp. 159–160. doi: 10.1111/j.2042-7158.1994.tb03767.x.

Chemicalize (2019) *Drawing Tool*. Available at: https://chemicalize.com/#/.

Chen, N. *et al.* (2014) ‘Fatty acid synthesis and pyruvate metabolism pathways remain active in dihydroartemisinin-induced dormant ring stages of Plasmodium falciparum.’, *Antimicrobial agents and chemotherapy*, 58(8), pp. 4773–81. doi: 10.1128/AAC.02647-14.

Cheng, Y.-Q. (2006) ‘Deciphering the biosynthetic codes for the potent anti-SARS-CoV cyclodepsipeptide valinomycin in Streptomyces tsusimaensis ATCC 15141.’, *Chembiochem : a European journal of chemical biology*, 7(3), pp. 471–7. doi: 10.1002/cbic.200500425.

Chou, T.-C. (2010) ‘Drug combination studies and their synergy quantification using the Chou-Talalay method.’, *Cancer research*, 70(2), pp. 440–6. doi: 10.1158/0008-5472.CAN-09-1947.

Chou, T.-C. and Talalay, P. (1984) 'Quantitative analysis of dose-effect relationships: the combined effects of multiple drugs or enzyme inhibitors', *Advances in Enzyme Regulation*, 22, pp. 27–55. doi: 10.1016/0065-2571(84)90007-4.

Chou, T. and Martin, N. (2005) 'CompuSyn for Drug Combinations: PC Software and User's Guide: A Computer Program for Quantitation of Synergism and Antagonism in Drug Combinations, and the Determination of IC50 and ED50 and LD50 Values'.

Clardy, J. and Walsh, C. (2004) 'Lessons from natural molecules.', *Nature*, 432(7019), pp. 829–37. doi: 10.1038/nature03194.

Coates, A. R. M., Halls, G. and Hu, Y. (2011) 'Novel classes of antibiotics or more of the same?', *British journal of pharmacology*, 163(1), pp. 184–94. doi: 10.1111/j.1476-5381.2011.01250.x.

Combrinck, J. M. *et al.* (2013) 'Insights into the role of heme in the mechanism of action of antimalarials', *ACS chemical biology*, 8(1), pp. 133–137.

Cooke, N. (2003) 'Recent advances in mass spectrometry for drug discovery and development', *Drug Discovery World*. Available at: https://www.ddw-online.com/enabling-technologies/p148395-recent-advances-in-mass-spectrometry-for-drug-discovery-and-development.html.

Coskun, O. (2016) 'Separation Techniques: Chromatography', *Northern Clinics of Istanbul*. doi: 10.14744/nci.2016.32757.

Cowman, A. F. *et al.* (2016) 'Malaria: Biology and Disease', *Cell*. Elsevier Inc., 167(3), pp. 610–624. doi: 10.1016/j.cell.2016.07.055.

Cragg, G. M. and Newman, D. J. (2013) 'Natural products: A continuing source of novel drug leads', *Biochimica et Biophysica Acta (BBA) - General Subjects*, 1830(6), pp. 3670–3695. doi: 10.1016/j.bbagen.2013.02.008.

Craige Trenerry, V. and Rochfort, S. J. (2010) 'Natural Products Research and Metabolomics', in *Comprehensive Natural Products II*. Elsevier, pp. 595–628. doi: 10.1016/B978-008045382-8.00211-2.

D'Alessandro, U. and Buttiens, H. (2001) 'History and importance of antimalarial drug resistance', *Tropical Medicine and International Health*, 6(11), pp. 845–848. doi: 10.1046/j.1365-3156.2001.00819.x.

Davies, J. (2006) ‘Where have All the Antibiotics Gone?’, *The Canadian journal of infectious diseases & medical microbiology = Journal canadien des maladies infectieuses et de la microbiologie medicale,* 17(5), pp. 287–90. doi: 10.1155/2006/707296.

Dayrit, F. M. and Dios, A. C. de (2017) ‘1H and 13C NMR for the Profiling of Natural Product Extracts: Theory and Applications’, in *Spectroscopic Analyses - Developments and Applications*. InTech. doi: 10.5772/intechopen.71040.

Demain, A. L. and Fang, A. (2000) ‘The Natural Functions of Secondary Metabolites’, in, pp. 1–39. doi: 10.1007/3-540-44964-7_1.

Dewick, P. (2002) *Medicinal Natural Products: A Biosynthetic Approach*. 2nd edn, *Journal of Natural Products*. 2nd edn. Edited by J. W. and Sons. doi: 10.1021/np0207217.

Dias, D. A., Urban, S. and Roessner, U. (2012) ‘A Historical Overview of Natural Products in Drug Discovery’, pp. 303–336. doi: 10.3390/metabo2020303.

van Dissel, D., Claessen, D. and van Wezel, G. P. (2014) ‘Morphogenesis of Streptomyces in Submerged Cultures’, in, pp. 1–45. doi: 10.1016/B978-0-12-800259-9.00001-9.

Doi, M. and Asano, A. (2002) ‘Montanastatin, cyclo[–(Val- D -Hyv- D -Val-Lac) 2 –]’, *Acta Crystallographica Section E Structure Reports Online*, 58(8), pp. o935–o936. doi: 10.1107/S1600536802013259.

Dowler, M. G. (1995) ‘Personal Communication’.

van Eijk, A. M. and Terlouw, D. J. (2011) ‘Azithromycin for treating uncomplicated malaria’, *Cochrane Database of Systematic Reviews*. doi: 10.1002/14651858.CD006688.pub2.

Elyashberg, M. (2015) ‘Identification and structure elucidation by NMR spectroscopy’, *Trends in Analytical Chemistry,* 69, pp. 88–97. doi: 10.1016/j.trac.2015.02.014.

Ezra, D. *et al.* (2004) ‘Coronamycins, peptide antibiotics produced by a verticillate Streptomyces sp. (MSU-2110) endophytic on Monstera sp.’, *Microbiology (Reading, England),* 150(Pt 4), pp. 785–93. doi: 10.1099/mic.0.26645-0.

Fan, Y.-L. *et al.* (2018) ‘Antiplasmodial and antimalarial activities of quinolone derivatives: An overview’, *European Journal of Medicinal Chemistry,* 146, pp. 1–14. doi: 10.1016/j.ejmech.2018.01.039.

Farnsworth, N. R. *et al.* (1985) ‘Medicinal plants in therapy.’, *Bulletin of the World Health*

Organization, 63(6), pp. 965–81. Available at: http://www.ncbi.nlm.nih.gov/pubmed/3879679.

Faulkner, D. J. (2000) 'Marine natural products.', *Natural product reports*, 17(1), pp. 7–55. Available at: http://www.ncbi.nlm.nih.gov/pubmed/10714898.

Feachem, R. G. A. *et al.* (2019) 'Malaria eradication within a generation: ambitious, achievable, and necessary', *The Lancet*, 394(10203), pp. 1056–1112. doi: 10.1016/S0140-6736(19)31139-0.

Feling, R. H. *et al.* (2003) 'Salinosporamide A: A Highly Cytotoxic Proteasome Inhibitor from a Novel Microbial Source, a Marine Bacterium of the New Genus Salinospora', *Angewandte Chemie International Edition*, 42(3), pp. 355–357. doi: 10.1002/anie.200390115.

Fidock, D. A. *et al.* (2000) 'Mutations in the P. falciparum digestive vacuole transmembrane protein PfCRT and evidence for their role in chloroquine resistance', *Molecular cell*, 6(4), pp. 861–871.

Fisher Chemicals (2020) *Common Background Contamination Ions in Mass Spectrometry*. Available at: https://beta-static.fishersci.ca/content/dam/fishersci/en_US/documents/programs/scientific/brochures-and-catalogs/posters/fisher-chemical-poster.pdf.

Fivelman, Q. L., Adagu, I. S. and Warhurst, D. C. (2004) 'Modified Fixed-Ratio Isobologram Method for Studying In Vitro Interactions between Atovaquone and Proguanil or Dihydroartemisinin against Drug-Resistant Strains of Plasmodium falciparum', *Antimicrobial Agents and Chemotherapy*, 48(11), pp. 4097–4102. doi: 10.1128/AAC.48.11.4097-4102.2004.

Flannery, E. L., Chatterjee, A. K. and Winzeler, E. A. (2013) 'Antimalarial drug discovery — approaches and progress towards new medicines', *Nature Reviews Microbiology*, 11(12), pp. 849–862. doi: 10.1038/nrmicro3138.

Flärdh, K. and Buttner, M. J. (2009) 'Streptomyces morphogenetics: dissecting differentiation in a filamentous bacterium', *Nature Reviews Microbiology*, 7(1), pp. 36–49. doi: 10.1038/nrmicro1968.

Fleck, W. F. *et al.* (1978) 'Fermentation, isolation, and biological activity of maduramycin: A new antibiotic fromActinomadura rubra', *Zeitschrift für allgemeine Mikrobiologie*, 18(6), pp. 389–398. doi: 10.1002/jobm.3630180602.

Fleming, A. (1929) ‘Classics in infectious diseases: on the antibacterial action of cultures of a penicillium, with special reference to their use in the isolation of B. influenzae by Alexander Fleming, Reprinted from the British Journal of Experimental Pathology 10:226-236’, *Reviews of infectious diseases*, 2(1), pp. 129–39. Available at: http://www.ncbi.nlm.nih.gov/pubmed/6994200.

Flipo, M. *et al.* (2011) ‘Ethionamide Boosters: Synthesis, Biological Activity, and Structure−Activity Relationships of a Series of 1,2,4-Oxadiazole EthR Inhibitors’, *Journal of Medicinal Chemistry*, 54(8), pp. 2994–3010. doi: 10.1021/jm200076a.

Fong, C. W. (2016) ‘Physiology of ionophore transport of potassium and sodium ions across cell membranes: valinomycin and 18-crown-6 ether’, *International Journal of Computational Biology and Drug Design*, 9(3), p. 228. doi: 10.1504/IJCBDD.2016.078284.

Furumai, T. *et al.* (1993) ‘Biosynthesis of the pradimicin family of antibiotics. I. Generation and selection of pradimicin-nonproducing mutants.’, *The Journal of antibiotics*, 46(3), pp. 412–9. Available at: http://www.ncbi.nlm.nih.gov/pubmed/8478259.

Galli, G. *et al.* (1994) ‘Characterization of the surfactin synthetase multi-enzyme complex’, *Biochimica et Biophysica Acta (BBA) - Protein Structure and Molecular Enzymology*, 1205(1), pp. 19–28. doi: 10.1016/0167-4838(94)90087-6.

Gallup, J. L. and Sachs, J. D. (2001) ‘The economic burden of malaria.’, *The American journal of tropical medicine and hygiene*, 64(1-2 Suppl), pp. 85–96. doi: 10.4269/ajtmh.2001.64.85.

Gatton, M. L., Martin, L. B. and Cheng, Q. (2004) ‘Evolution of Resistance to Sulfadoxine-Pyrimethamine in Plasmodium falciparum’, *Antimicrobial Agents and Chemotherapy*, 48(6), pp. 2116–2123. doi: 10.1128/AAC.48.6.2116-2123.2004.

Gaynor, M. and Mankin, A. (2003) ‘Macrolide Antibiotics: Binding Site, Mechanism of Action, Resistance’, *Current Topics in Medicinal Chemistry*, 3(9), pp. 949–960. doi: 10.2174/1568026033452159.

German Culture Collection (2007) *DSMZ #554 Recipe*.

Gibson, M. (2009) *Pharmaceutical Preformulation and Formulation*. Edited by 2nd. CRC Press.

Ginsburg, H. (1994) ‘Transport pathways in the malaria-infected erythrocyte. Their characterization and their use as potential targets for chemotherapy.’, *Biochemical*

pharmacology, 48(10), pp. 1847–56. doi: 10.1016/0006-2952(94)90582-7.

Ginsburg, H. and Deharo, E. (2011) 'A call for using natural compounds in the development of new antimalarial treatments - an introduction.', *Malaria journal*, 10 Suppl 1, p. S1. doi: 10.1186/1475-2875-10-S1-S1.

Gokel, G. W., Leevy, W. M. and Weber, M. E. (2004) 'Crown Ethers: Sensors for Ions and Molecular Scaffolds for Materials and Biological Models', *Chemical Reviews*, 104(5), pp. 2723–2750. doi: 10.1021/cr020080k.

Goshi, K. *et al.* (2002) 'Cloning and Analysis of the Telomere and Terminal Inverted Repeat of the Linear Chromosome of Streptomyces griseus', *Journal of Bacteriology*, 184(12), pp. 3411–3415. doi: 10.1128/JB.184.12.3411-3415.2002.

Greenwood, B. (2010) 'Anti-malarial drugs and the prevention of malaria in the population of malaria endemic areas', *Malaria journal*, 9 Suppl 3, pp. S2-2875-9-S3–S2.

Greenwood, B. and Doumbo, O. K. (2016) 'Implementation of the malaria candidate vaccine RTS,S/AS01', *The Lancet*, 387(10016), pp. 318–319. doi: 10.1016/S0140-6736(15)00807-7.

Greenwood, B. M. *et al.* (2008) 'Malaria: progress, perils, and prospects for eradication', *Journal of Clinical Investigation*, 118(4), pp. 1266–1276. doi: 10.1172/JCI33996.

Grundmann, F. *et al.* (2014) 'Antiparasitic Chaiyaphumines from Entomopathogenic Xenorhabdus sp . PB61.4', *Journal of Natural Products*, 77(4), pp. 779–783. doi: 10.1021/np4007525.

Guantai, E. and Chibale, K. (2011) 'How can natural products serve as a viable source of lead compounds for the development of new/novel anti-malarials?', *Malaria Journal*. BioMed Central Ltd, 10(S1), p. S2. doi: 10.1186/1475-2875-10-S1-S2.

Gumila, C. *et al.* (1996) 'Differential in vitro activities of ionophore compounds against Plasmodium falciparum and mammalian cells.', *Antimicrobial agents and chemotherapy*, 40(3), pp. 602–8. Available at: http://www.ncbi.nlm.nih.gov/pubmed/8851578.

Gumila, C. *et al.* (1997) 'Characterization of the potent in vitro and in vivo antimalarial activities of ionophore compounds.', *Antimicrobial agents and chemotherapy*, 41(3), pp. 523–9. Available at: http://www.ncbi.nlm.nih.gov/pubmed/9055986.

Guo, Z. (2017) 'The modification of natural products for medical use', *Acta Pharmaceutica*

Sinica B, 7(2), pp. 119–136. doi: 10.1016/j.apsb.2016.06.003.

Gurevich, A. *et al.* (2013) 'QUAST: quality assessment tool for genome assemblies', *Bioinformatics*, 29(8), pp. 1072–1075. doi: 10.1093/bioinformatics/btt086.

Hacène, H. and Lefebvre, G. (1995) 'AH17, a new non-polyenic antifungal antibiotic produced by a strain of Spirillospora.', *Microbios*, 83(336), pp. 199–205. Available at: http://www.ncbi.nlm.nih.gov/entrez/query.fcgi?cmd=Retrieve&db=PubMed&dopt=Citation&list_uids=8559083.

Hann, M. M., Leach, A. R. and Harper, G. (2001) 'Molecular complexity and its impact on the probability of finding leads for drug discovery.', *Journal of chemical information and computer sciences*, 41(3), pp. 856–64. Available at: http://www.ncbi.nlm.nih.gov/pubmed/11410068.

Hao, M. *et al.* (2020) 'In vitro Activity of Apramycin Against Carbapenem-Resistant and Hypervirulent Klebsiella pneumoniae Isolates', *Frontiers in Microbiology*, 11. doi: 10.3389/fmicb.2020.00425.

Harmse, R. *et al.* (2015) 'The Case for Development of 11-Azaartemisinins for Malaria', *Current Medicinal Chemistry*, 22, pp. 1–23.

Harvey, A. L., Edrada-Ebel, R. and Quinn, R. J. (2015) 'The re-emergence of natural products for drug discovery in the genomics era', *Nature Reviews Drug Discovery*, 14(2), pp. 111–129. doi: 10.1038/nrd4510.

Hasler, A., Sticher, O. and Meier, B. (1992) 'Identification and determination of the flavonoids from Ginkgo biloba by high-performance liquid chromatography', *Journal of Chromatography A*, 605(1), pp. 41–48. doi: 10.1016/0021-9673(92)85026-P.

Haynes, R. K. *et al.* (2006) 'Artemisone--a highly active antimalarial drug of the artemisinin class', *Angewandte Chemie (International ed.in English)*, 45(13), pp. 2082–2088.

Haynes, R. K. *et al.* (2013) 'Considerations on the mechanism of action of artemisinin antimalarials: part 1--the "carbon radical" and "heme" hypotheses', *Infectious disorders drug targets*, 13(4), pp. 217–277.

Hayter, P. *et al.* (2014) 'Identification of novel haemoglobin-modifying activity in snake venom libraries', *BMG Labtech*.

Hayvalı, Z. *et al.* (2014) 'Novel bis-crown ethers and their sodium complexes as antimicrobial agent: synthesis and spectroscopic characterizations', *Medicinal Chemistry Research*, 23(8), pp. 3652–3661. doi: 10.1007/s00044-014-0937-9.

Hendrixson, R. R. *et al.* (1978) 'Oral toxicity of the cyclic polyethers—12-crown-4, 15-crown-5, and 18-crown-6—in mice', *Toxicology and Applied Pharmacology*, 44(2), pp. 263–268. doi: 10.1016/0041-008X(78)90188-6.

Higgins, D. L. *et al.* (2005) 'Telavancin, a Multifunctional Lipoglycopeptide, Disrupts both Cell Wall Synthesis and Cell Membrane Integrity in Methicillin-Resistant Staphylococcus aureus', *Antimicrobial Agents and Chemotherapy*, 49(3), pp. 1127–1134. doi: 10.1128/AAC.49.3.1127-1134.2005.

Hobbs, C. and Duffy, P. (2011) 'Drugs for malaria: something old, something new, something borrowed', *F1000 Biology Reports*, 3. doi: 10.3410/B3-24.

Hovlid, M. L. and Winzeler, E. A. (2016) 'Phenotypic Screens in Antimalarial Drug Discovery', *Trends in Parasitology*, 32(9), pp. 697–707. doi: 10.1016/j.pt.2016.04.014.

Hu, C.-M. J. and Zhang, L. (2012) 'Nanoparticle-based combination therapy toward overcoming drug resistance in cancer', *Biochemical Pharmacology*, 83(8), pp. 1104–1111. doi: 10.1016/j.bcp.2012.01.008.

Hughes, J. P. *et al.* (2011) 'Principles of early drug discovery.', *British journal of pharmacology*, 162(6), pp. 1239–49. doi: 10.1111/j.1476-5381.2010.01127.x.

Isaka, M. *et al.* (2007) 'Paecilodepsipeptide A, an Antimalarial and Antitumor Cyclohexadepsipeptide from the Insect Pathogenic Fungus Paecilomyces cinnamomeus BCC 9616', *Journal of Natural Products*, 70(4), pp. 675–678. doi: 10.1021/np060602h.

Iwai, Y. and Omura, S. (1982) 'Culture conditions for screening of new antibiotics.', *The Journal of Antibiotics*, 35(2), pp. 123–141. doi: 10.7164/antibiotics.35.123.

Jelić, D. and Antolović, R. (2016) 'From Erythromycin to Azithromycin and New Potential Ribosome-Binding Antimicrobials', *Antibiotics*, 5(3), p. 29. doi: 10.3390/antibiotics5030029.

Jensen, J. B. *et al.* (2002) 'Munumbicins, wide-spectrum antibiotics produced by Streptomyces NRRL 30562, endophytic on Kennedia nigriscans a', *Microbiology*, 148(9), pp. 2675–2685. doi: 10.1099/00221287-148-9-2675.

Jia, C. *et al.* (2006) ‘Sequencing peptides by electrospray ion-trap mass spectrometry: A useful tool in synthesis of Axinastatin 3’, *Open Chemistry*, 4(4). doi: 10.2478/s11532-006-0028-y.

Jilani, K., Qadri, S. M. and Lang, F. (2013) ‘Geldanamycin-Induced Phosphatidylserine Translocation in the Erythrocyte Membrane’, *Cellular Physiology and Biochemistry*, 32(6), pp. 1600–1609. doi: 10.1159/000356596.

Joice, R. *et al.* (2014) ‘Plasmodium falciparum transmission stages accumulate in the human bone marrow’, *Science Translational Medicine*, 6(244), pp. 244re5-244re5. doi: 10.1126/scitranslmed.3008882.

Kang, Q., Shen, Y. and Bai, L. (2012) ‘Biosynthesis of 3,5-AHBA-derived natural products’, *Nat. Prod. Rep.*, 29(2), pp. 243–263. doi: 10.1039/C2NP00019A.

Katsuno, K. *et al.* (2015) ‘Hit and lead criteria in drug discovery for infectious diseases of the developing world’, *Nature Reviews Drug Discovery*, 14(11), pp. 751–758. doi: 10.1038/nrd4683.

Katzung, B. G., Masters, S. B. and Trevor, A. J. (2012) *Basic and Clinical Pharmacology*. 12th edn. London: McGraw-Hill.

Kaufmann, A. and Maden, K. (2005) ‘Determination of 11 Aminoglycosides in Meat and Liver by Liquid Chromatography with Tandem Mass Spectrometry’, *Journal of AOAC INTERNATIONAL*, 88(4), pp. 1118–1125. doi: 10.1093/jaoac/88.4.1118.

Kayser, O., Kiderlen, A. F. and Croft, S. L. (2002) ‘Natural products as potential antiparasitic drugs’, in *Studies in Natural Products Chemistry*, pp. 779–848. doi: 10.1016/S1572-5995(02)80019-9.

Kim, E.-S. *et al.* (2001) ‘Modulation of Actinorhodin Biosynthesis in Streptomyces lividans by Glucose Repression of afsR2 Gene Transcription’, *Journal of Bacteriology*, 183(7), pp. 2198–2203. doi: 10.1128/JB.183.7.2198-2203.2001.

Kind, T. and Fiehn, O. (2007) ‘Seven Golden Rules for heuristic filtering of molecular formulas obtained by accurate mass spectrometry’, *BMC Bioinformatics*, 8(1), p. 105. doi: 10.1186/1471-2105-8-105.

Kind, T. and Fiehn, O. (2010) ‘Advances in structure elucidation of small molecules using mass spectrometry’, *Bioanalytical Reviews*, 2(1–4), pp. 23–60. doi: 10.1007/s12566-010-0015-9.

Kinghorn, A. D. *et al.* (2011) 'The Relevance of Higher Plants in Lead Compound Discovery Programs', *Journal of Natural Products*, 74(6), pp. 1539–1555. doi: 10.1021/np200391c.

Kingston, D. G. and Newman, D. J. (2005) 'Natural products as drug leads: an old process or the new hope for drug discovery?', *IDrugs : the investigational drugs journal*, 8(12), pp. 990–2. Available at: http://www.ncbi.nlm.nih.gov/pubmed/16320131.

Kitagaki, J. *et al.* (2015) 'Cyclic depsipeptides as potential cancer therapeutics', *Anti-Cancer Drugs*, 26(3), pp. 259–271. doi: 10.1097/CAD.0000000000000183.

Kola, I. and Landis, J. (2004) 'Can the pharmaceutical industry reduce attrition rates?', *Nature Reviews Drug Discovery*, 3(8), pp. 711–716. doi: 10.1038/nrd1470.

Kotra, L. P., Haddad, J. and Mobashery, S. (2000) 'Aminoglycosides: Perspectives on Mechanisms of Action and Resistance and Strategies to Counter Resistance', *Antimicrobial Agents and Chemotherapy*, 44(12), pp. 3249–3256. doi: 10.1128/AAC.44.12.3249-3256.2000.

Krause, K. M. *et al.* (2016) 'Aminoglycosides: An Overview', *Cold Spring Harbor Perspectives in Medicine*, 6(6), p. a027029. doi: 10.1101/cshperspect.a027029.

Kremsner, P. G. (1990) 'Clindamycin in malaria treatment', *Journal of Antimicrobial Chemotherapy*, 25(1), pp. 9–14. doi: 10.1093/jac/25.1.9.

Krishna, S., Uhlemann, a and Haynes, R. (2004) 'Artemisinins: mechanisms of action and potential for resistance', *Drug Resistance Updates*, 7(4–5), pp. 233–244. doi: 10.1016/j.drup.2004.07.001.

Krugliak, M., Waldman, Z. and Ginsburg, H. (1987) 'Gentamicin and amikacin repress the growth of Plasmodium falciparum in culture, probably by inhibiting a parasite acid phospolipase', *Life Sciences*, 40(13), pp. 1253–1257. doi: 10.1016/0024-3205(87)90581-9.

Lai, T., Yang, Y. and Ng, S. (2013) 'Advances in Mammalian Cell Line Development Technologies for Recombinant Protein Production', *Pharmaceuticals*, 6(5), pp. 579–603. doi: 10.3390/ph6050579.

Lazzarini, A. *et al.* (2000) 'Rare genera of actinomycetes as potential producers of new antibiotics.', *Antonie van Leeuwenhoek*, 78(3–4), pp. 399–405. Available at: http://www.ncbi.nlm.nih.gov/pubmed/11386363.

Lechevalier, H. and Lechevalier, M. (1965) 'Classification des actinomycètes aérobies basée

sur leur morphologie et leur composition chimique', *Annales de l' Institut Pasteur*, 108(5), pp. 662–73.

Lengeler, C. (2004) 'Insecticide-treated bed nets and curtains for preventing malaria', *Cochrane Database of Systematic Reviews*, (2). doi: 10.1002/14651858.CD000363.pub2.

Levine, D. P. (2006) 'Vancomycin: A History', *Clinical Infectious Diseases*, 42(Supplement_1), pp. S5–S12. doi: 10.1086/491709.

Li, J. W.-H. and Vederas, J. C. (2009) 'Drug Discovery and Natural Products: End of an Era or an Endless Frontier?', *Science*, 325(5937), pp. 161–165. doi: 10.1126/science.1168243.

de Lima Procópio, R. E. *et al.* (2012) 'Antibiotics produced by Streptomyces', *The Brazilian Journal of Infectious Diseases*. Elsevier Editora Ltda, 16(5), pp. 466–471. doi: 10.1016/j.bjid.2012.08.014.

Lipinski, C. a. (2000) 'Drug-like properties and the causes of poor solubility and poor permeability', *Journal of Pharmacological and Toxicological Methods*, 44(2000), pp. 235–249. doi: 10.1016/S1056-8719(00)00107-6.

Lipinski, C. A. (2004) 'Lead- and drug-like compounds: the rule-of-five revolution', *Drug Discovery Today: Technologies*, 1(4), pp. 337–341. doi: 10.1016/j.ddtec.2004.11.007.

Liras, P. (1999) 'Biosynthesis and molecular genetics of cephamycins. Cephamycins produced by actinomycetes.', *Antonie van Leeuwenhoek*, 75(1–2), pp. 109–24. Available at: http://www.ncbi.nlm.nih.gov/pubmed/10422584.

Liu, G. *et al.* (2013) 'Molecular Regulation of Antibiotic Biosynthesis in Streptomyces', *Microbiology and Molecular Biology Reviews*, 77(1), pp. 112–143. doi: 10.1128/MMBR.00054-12.

Liu, R., Li, X. and Lam, K. S. (2017) 'Combinatorial chemistry in drug discovery', *Current Opinion in Chemical Biology*, 38, pp. 117–126. doi: 10.1016/j.cbpa.2017.03.017.

Liu, W.-T. *et al.* (2009) 'Interpretation of Tandem Mass Spectra Obtained from Cyclic Nonribosomal Peptides', *Analytical Chemistry*, 81(11), pp. 4200–4209. doi: 10.1021/ac900114t.

Liu, Z., Nalluri, S. K. M. and Stoddart, J. F. (2017) 'Surveying macrocyclic chemistry: from flexible crown ethers to rigid cyclophanes', *Chemical Society Reviews*, 46(9), pp. 2459–2478.

doi: 10.1039/C7CS00185A.

Ma, Y. *et al.* (2014) 'MS2Analyzer: A Software for Small Molecule Substructure Annotations from Accurate Tandem Mass Spectra', *Analytical Chemistry*, 86(21), pp. 10724–10731. doi: 10.1021/ac502818e.

Magill, A. J. *et al.* (2011) 'Doxycycline for Malaria Chemoprophylaxis and Treatment: Report from the CDC Expert Meeting on Malaria Chemoprophylaxis', *The American Journal of Tropical Medicine and Hygiene*, 84(4), pp. 517–531. doi: 10.4269/ajtmh.2011.10-0285.

Mahmoudi, S. and Keshavarz, H. (2017) 'Efficacy of phase 3 trial of RTS, S/AS01 malaria vaccine: The need for an alternative development plan', *Human Vaccines & Immunotherapeutics*, 13(9), pp. 2098–2101. doi: 10.1080/21645515.2017.1295906.

Makler, M. T. *et al.* (1993) 'Parasite lactate dehydrogenase as an assay for Plasmodium falciparum drug sensitivity', *The American Journal of Tropical Medicine and Hygiene*, 48(6), pp. 739–741.

Der Marderosian, A. and Beutler, J. A. (2014) *The Review of Natural Products*. 8th edn, *Journal of Consumer Health On the Internet*. 8th edn. Edited by T. Tarver. doi: 10.1080/15398285.2014.932189.

Maron, M. I. *et al.* (2016) 'Maduramicin Rapidly Eliminates Malaria Parasites and Potentiates the Gametocytocidal Activity of the Pyrazoleamide PA21A050', *Antimicrobial Agents and Chemotherapy*, 60(3), pp. 1492–1499. doi: 10.1128/AAC.01928-15.

Martin, J. F. and Demain, A. L. (1980) 'Control of antibiotic biosynthesis.', *Microbiological reviews*, 44(2), pp. 230–51. Available at: http://www.ncbi.nlm.nih.gov/pubmed/6991900.

Maskey, R. P. *et al.* (2004) 'Anti-cancer and Antibacterial Trioxacarcins with High Anti-malaria Activity from a Marine Streptomycete and their Absolute Stereochemistry', *The Journal of Antibiotics*, 57(12), pp. 771–779. doi: 10.7164/antibiotics.57.771.

MassBank (2016) *Apramycin MS/MS Spectrum*. Available at: https://metabolomics-usi.ucsd.edu/spectrum/?usi=mzspec:MASSBANK:KO002240.

Mathur, S. and Hoskins, C. (2017) 'Drug development: Lessons from nature', *Biomedical Reports*, 6(6), pp. 612–614. doi: 10.3892/br.2017.909.

Matsuo, T., Matsuda, H. and Katakuse, I. (1979) 'Use of field desorption mass spectra of

polystyrene and polypropylene glycol as mass references up to mass 10000', *Analytical Chemistry*, 51(8), pp. 1329–1331. doi: 10.1021/ac50044a050.

Matt, T. *et al.* (2012) 'Dissociation of antibacterial activity and aminoglycoside ototoxicity in the 4-monosubstituted 2-deoxystreptamine apramycin', *Proceedings of the National Academy of Sciences*, 109(27), pp. 10984–10989. doi: 10.1073/pnas.1204073109.

Matter, A. M. *et al.* (2009) 'Valinomycin Biosynthetic Gene Cluster in Streptomyces: Conservation, Ecology and Evolution', *PLoS ONE*. Edited by M. Thattai, 4(9), p. e7194. doi: 10.1371/journal.pone.0007194.

Matthews, H. *et al.* (2017) 'Investigating antimalarial drug interactions of emetine dihydrochloride hydrate using CalcuSyn-based interactivity calculations', *PLOS ONE*. Edited by M. Bogyo, 12(3), p. e0173303. doi: 10.1371/journal.pone.0173303.

McClure, W. F. (2003) '204 Years of near Infrared Technology: 1800–2003', *Journal of Near Infrared Spectroscopy*, 11(6), pp. 487–518. doi: 10.1255/jnirs.399.

Medema, M. H. *et al.* (2011) 'antiSMASH: rapid identification, annotation and analysis of secondary metabolite biosynthesis gene clusters in bacterial and fungal genome sequences', *Nucleic Acids Research*, 39(suppl_2), pp. W339–W346. doi: 10.1093/nar/gkr466.

Meyers, P. R. *et al.* (2003) 'Streptomyces speibonae sp . nov ., a novel streptomycete with blue substrate mycelium isolated from South African soil', 53(May), pp. 801–805. doi: 10.1099/ijs.0.02341-0.

Michigan State University (no date) *Drug Discovery Project Pipeline*. Available at: https://drugdiscovery.msu.edu/project-pipeline/.

Miguélez, E. M., Hardisson, C. and Manzanal, M. B. (1999) 'Hyphal Death during Colony Development in Streptomyces antibioticus : Morphological Evidence for the Existence of a Process of Cell Deletion in a Multicellular Prokaryote', *The Journal of Cell Biology*, 145(3), pp. 515–525. doi: 10.1083/jcb.145.3.515.

Mingeot-Leclercq, M. P., Glupczynski, Y. and Tulkens, P. M. (1999) 'Aminoglycosides: activity and resistance.', *Antimicrobial agents and chemotherapy*, 43(4), pp. 727–37. Available at: http://www.ncbi.nlm.nih.gov/pubmed/10103173.

Miret, S., De Groene, E. M. and Klaffke, W. (2006) 'Comparison of In Vitro Assays of Cellular Toxicity in the Human Hepatic Cell Line HepG2', *Journal of Biomolecular Screening*, 11(2),

pp. 184–193. doi: 10.1177/1087057105283787.

Mok, S. *et al.* (2011) 'Artemisinin resistance in Plasmodium falciparum is associated with an altered temporal pattern of transcription.', *BMC genomics*, 12, p. 391. doi: 10.1186/1471-2164-12-391.

Mootz, H. D., Schwarzer, D. and Marahiel, M. A. (2002) 'Ways of Assembling Complex Natural Products on Modular Nonribosomal Peptide Synthetases A list of abbreviations can be found at the end of the text.', *ChemBioChem*, 3(6), p. 490. doi: 10.1002/1439-7633(20020603)3:6<490::AID-CBIC490>3.0.CO;2-N.

Mosha, D. *et al.* (2014) 'Effectiveness of intermittent preventive treatment with sulfadoxine-pyrimethamine during pregnancy on placental malaria, maternal anaemia and birthweight in areas with high and low malaria transmission intensity in Tanzania', *Tropical medicine & international health : TM & IH*, 19(9), pp. 1048–1056.

Mosmann, T. (1983) 'Rapid colorimetric assay for cellular growth and survival: application to proliferation and cytotoxicity assays', *Journal of immunological methods*, 65(1–2), pp. 55–63.

Muller, I. B. and Hyde, J. E. (2010) 'Antimalarial drugs: modes of action and mechanisms of parasite resistance', *Future microbiology*, 5(12), pp. 1857–1873.

Myers, O. D. *et al.* (2017) 'One Step Forward for Reducing False Positive and False Negative Compound Identifications from Mass Spectrometry Metabolomics Data: New Algorithms for Constructing Extracted Ion Chromatograms and Detecting Chromatographic Peaks', *Analytical Chemistry*, 89(17), pp. 8696–8703. doi: 10.1021/acs.analchem.7b00947.

Nájera, J. A., González-Silva, M. and Alonso, P. L. (2011) 'Some Lessons for the Future from the Global Malaria Eradication Programme (1955–1969)', *PLoS Medicine*, 8(1), p. e1000412. doi: 10.1371/journal.pmed.1000412.

National Center for Biotechnology Information (2019) *PubChem Database CID 5259460, CID=5259460*. Available at: https://pubchem.ncbi.nlm.nih.gov/compound/5259460 (Accessed: 7 December 2019).

National Center for Biotechnology Information (2020) *PubChem Database. Ethyl acetate, CID=8857*. Available at: https://pubchem.ncbi.nlm.nih.gov/compound/Ethyl-acetate (Accessed: 12 June 2020).

Newman, D. J., Cragg, G. M. and Snader, K. M. (2003) 'Natural Products as Sources of New

Drugs over the Period 1981−2002', *Journal of Natural Products*, 66(7), pp. 1022–1037. doi: 10.1021/np030096l.

Nichols, D. *et al.* (2010) 'Use of Ichip for High-Throughput In Situ Cultivation of " Uncultivable " Microbial Species □', 76(8), pp. 2445–2450. doi: 10.1128/AEM.01754-09.

Nikolic, V. *et al.* (2011) 'Paclitaxel as an anticancer agent: isolation, activity, synthesis and stability', *Open Medicine*, 6(5). doi: 10.2478/s11536-011-0074-5.

Noedl, H. *et al.* (2008) 'Evidence of artemisinin-resistant malaria in western Cambodia', *The New England journal of medicine*, 359(24), pp. 2619–2620.

Nzila, A. M. *et al.* (2000) 'Molecular Evidence of Greater Selective Pressure for Drug Resistance Exerted by the Long-Acting Antifolate Pyrimethamine/Sulfadoxine Compared with the Shorter-Acting Chlorproguanil/Dapsone on Kenyan Plasmodium falciparum', *The Journal of Infectious Diseases*, 181(6), pp. 2023–2028. doi: 10.1086/315520.

OChemPal (no date) *Crown Ether*. Available at: http://www.ochempal.org/index.php/alphabetical/c-d/crown-ether/.

Ohnishi, Y. *et al.* (2008) 'Genome Sequence of the Streptomycin-Producing Microorganism Streptomyces griseus IFO 13350', *Journal of Bacteriology*, 190(11), pp. 4050–4060. doi: 10.1128/JB.00204-08.

Okami, Y. and Hotta, K. (1988) 'Search and discovery of new antibiotics', in Goodfellow, M., Williams, S. T., and Mordarski, M. (eds) *Actinomycetes in Biotechnology*. San Diego: Academic Press, Inc, pp. 33–67. doi: 10.1016/B978-0-12-289673-6.50007-5.

Oudhoff, K. A., Schoenmakers, P. J. and Kok, W. T. (2003) 'Characterization of polyethylene glycols and polypropylene glycols by capillary zone electrophoresis and micellar electrokinetic chromatography', *Journal of Chromatography A*, 985(1–2), pp. 479–491. doi: 10.1016/S0021-9673(02)01469-3.

Ovchinnikov, Y. (1979) 'Physico-chemical Basis of Ion Transport through Biological Membranes: Ionophores and Ion Channels', *European Journal of Biochemistry*, 94(2), pp. 321–336. doi: 10.1111/j.1432-1033.1979.tb12898.x.

Paananen, A. *et al.* (2005) 'Valinomycin-induced apoptosis of human NK cells is predominantly caspase independent.', *Toxicology*, 212(1), pp. 37–45. doi: 10.1016/j.tox.2005.04.003.

Park, C. N. *et al.* (2008) 'Antifungal activity of valinomycin, a peptide antibiotic produced by Streptomyces sp. Strain M10 antagonistic to Botrytis cinerea.', *Journal of microbiology and biotechnology*, 18(5), pp. 880–4. Available at: http://www.ncbi.nlm.nih.gov/pubmed/18633285.

Part One (no date) *Drug Interactions*. Available at: http://www.partone.lifeinthefastlane.com/drug_interactions.html (Accessed: 18 November 2019).

Paulo, B. S. *et al.* (2019) 'New Cyclodepsipeptide Derivatives Revealed by Genome Mining and Molecular Networking', *ChemistrySelect*, 4(27), pp. 7785–7790. doi: 10.1002/slct.201900922.

Pedersen, C. J. (1967) 'Cyclic polyethers and their complexes with metal salts', *Journal of the American Chemical Society*, 89(26), pp. 7017–7036. doi: 10.1021/ja01002a035.

Pérez-Moreno, G. *et al.* (2016) 'Discovery of New Compounds Active against Plasmodium falciparum by High Throughput Screening of Microbial Natural Products', *PLOS ONE*. Edited by S. McGowan, 11(1), p. e0145812. doi: 10.1371/journal.pone.0145812.

Peternel, L. *et al.* (2009) 'Comparison of 3 Cytotoxicity Screening Assays and Their Application to the Selection of Novel Antibacterial Hits', *Journal of Biomolecular Screening*, 14(2), pp. 142–150. doi: 10.1177/1087057108329452.

Pettit, G. R. *et al.* (1999) 'Antineoplastic agents. Part 409: Isolation and structure of montanastatin from a terrestrial actinomycete.', *Bioorganic & medicinal chemistry*, 7(5), pp. 895–9. doi: 10.1016/s0968-0896(99)00024-3.

Phan Trong Giao *et al.* (2001) 'Artemisinin for treatment of uncomplicated falciparum malaria: Is there a place for monotherapy?', *American Journal of Tropical Medicine and Hygiene*, 65(6), pp. 690–695.

Phenomenex (2013) *PHREE Phospholipid Removal Solutions*. Available at: https://www.phenomenex.com/Products/HPLCDetail/phree.

Pink, R. *et al.* (2005) 'Opportunities and Challenges in Antiparasitic Drug Discovery', 4(September), pp. 727–741. doi: 10.1038/nrd1824.

Pluskal, T. *et al.* (2010) 'MZmine 2: Modular framework for processing, visualizing, and analyzing mass spectrometry-based molecular profile data', *BMC Bioinformatics*, 11(1), p.

395. doi: 10.1186/1471-2105-11-395.

Prudhomme, J. *et al.* (2008) 'Marine Actinomycetes: A New Source of Compounds against the Human Malaria Parasite', *PLoS ONE*. Edited by A. Gregson, 3(6), p. e2335. doi: 10.1371/journal.pone.0002335.

Rafieenia, R. (2013) 'Effect of nutrients and culture conditions on antibiotic synthesis in Streptomycetes', *Asian Journal of Pharmaceutical and Health Sciences*.

Raghavendra, K. *et al.* (2011) 'Malaria vector control: from past to future', *Parasitology Research*, 108(4), pp. 757–779. doi: 10.1007/s00436-010-2232-0.

Ranson, H. and Lissenden, N. (2016) 'Insecticide Resistance in African Anopheles Mosquitoes: A Worsening Situation that Needs Urgent Action to Maintain Malaria Control', *Trends in Parasitology*, 32(3), pp. 187–196. doi: 10.1016/j.pt.2015.11.010.

Reed, K. W. and Yalkowsky, S. H. (1985) 'Lysis of human red blood cells in the presence of various cosolvents.', *Journal of parenteral science and technology : a publication of the Parenteral Drug Association*, 39(2), pp. 64–9. Available at: http://www.ncbi.nlm.nih.gov/pubmed/3989614.

Renner, M. K. *et al.* (1999) 'Cyclomarins A−C, New Antiinflammatory Cyclic Peptides Produced by a Marine Bacterium (Streptomyces sp.)', *Journal of the American Chemical Society*, 121(49), pp. 11273–11276. doi: 10.1021/ja992482o.

Reponen, T. A. *et al.* (1998) 'Characteristics of airborne actinomycete spores.', *Applied and environmental microbiology*, 64(10), pp. 3807–12. Available at: http://www.ncbi.nlm.nih.gov/pubmed/9758803.

Rindelaub, J. D. *et al.* (2019) 'Identifying extractable profiles from 3D printed medical devices', *PLOS ONE*. Edited by Z. Gao, 14(5), p. e0217137. doi: 10.1371/journal.pone.0217137.

Roberts, L. (2017) 'Drug-resistant malaria advances in Mekong', *Science*, 358(6360), pp. 155–156. doi: 10.1126/science.358.6360.155.

Rodriguez, E. and Wrangham, R. (1993) 'Zoopharmacognosy: The Use of Medicinal Plants by Animals', in *Phytochemical Potential of Tropical Plants*. Boston, MA: Springer US, pp. 89–105. doi: 10.1007/978-1-4899-1783-6_4.

Rowinsky, E. K. and Donehower, R. C. (1995) ‘Paclitaxel (Taxol)’, *New England Journal of Medicine*. Edited by A. J. J. Wood, 332(15), pp. 1004–1014. doi: 10.1056/NEJM199504133321507.

Ryden, R. and Moore, B. J. (1977) ‘The in vitro activity of apramycin, a new aminocyditol antibiotic’, *Journal of Antimicrobial Chemotherapy*, 3(6), pp. 609–613. doi: 10.1093/jac/3.6.609.

Ryoo, I.-J. *et al.* (2006) ‘Selective cytotoxic activity of valinomycin against HT-29 Human colon carcinoma cells via down-regulation of GRP78.’, *Biological & pharmaceutical bulletin*, 29(4), pp. 817–20. doi: 10.1248/bpb.29.817.

Sacramento, D. R. *et al.* (2004) ‘Antimicrobial and antiviral activities of an actinomycete (Streptomyces sp.) isolated from a Brazilian tropical forest soil’, *World Journal of Microbiology and Biotechnology*, 20(3), pp. 225–229. doi: 10.1023/B:WIBI.0000023824.20673.2f.

Sánchez, S. *et al.* (2010) ‘Carbon source regulation of antibiotic production’, *The Journal of Antibiotics*, 63(8), pp. 442–459. doi: 10.1038/ja.2010.78.

Sandell, L. S. (1970) *Hydrodynamic and Volumetric Behaviour Of Polypropylene Glycol Oligomers in Solution*. McGill.

Saravolatz, L. D., Stein, G. E. and Johnson, L. B. (2009) ‘Telavancin: A Novel Lipoglycopeptide’, *Clinical Infectious Diseases*, 49(12), pp. 1908–1914. doi: 10.1086/648438.

Sarker, D., Latif, Z. and Gray., A. I. (2006) *Methods in Biotechnology. Natural Products Isolation*. 2nd edn, *Journal of Medicinal Chemistry*. 2nd edn. Edited by S. H. Press. doi: 10.1021/jm0680068.

Sarmah, N. P. *et al.* (2017) ‘Antifolate drug resistance: Novel mutations and haplotype distribution in dhps and dhfr from Northeast India.’, *Journal of biosciences*, 42(4), pp. 531–535. Available at: http://www.ncbi.nlm.nih.gov/pubmed/29229871.

Scherf, A. *et al.* (1998) ‘Antigenic variation in malaria: in situ switching, relaxed and mutually exclusive transcription of var genes during intra-erythrocytic development in Plasmodium falciparum’, *The EMBO Journal*, 17(18), pp. 5418–5426. doi: 10.1093/emboj/17.18.5418.

Sciex (2017) *Information Dependent Acquisition (IDA) Scanning*. Available at: https://sciex.com/community/application-

discussions/technology/qtof/fundamentals/information-dependent-acquisition-ida-scanning.

Shannon, P. *et al.* (2003) 'Cytoscape: a software environment for integrated models of biomolecular interaction networks.', *Genome research*, 13(11), pp. 2498–504. doi: 10.1101/gr.1239303.

Sherrard-Smith, E. *et al.* (2018) 'Systematic review of indoor residual spray efficacy and effectiveness against Plasmodium falciparum in Africa.', *Nature communications*, 9(1), p. 4982. doi: 10.1038/s41467-018-07357-w.

Shirling, E. B. and Gottlieb, D. (1966) 'Methods for characterization of Streptomyces species', *International Journal of Systematic Bacteriology*, 16(3), pp. 313–340. doi: 10.1099/00207713-16-3-313.

Sigma (1998) 'XAD-16 N Product Information', pp. 1–3.

Silverstein, R., Webster, F. and Kiemle, D. (2005) *Spectrometric Identification of Organic Compounds*. 7th edn. New York: John Wiley and Sons.

Singh, V. P. *et al.* (2019) 'Isolation of depsipeptides and optimization for enhanced production of valinomycin from the North-Western Himalayan cold desert strain Streptomyces lavendulae', *The Journal of Antibiotics*, 72(8), pp. 617–624. doi: 10.1038/s41429-019-0183-y.

Slater, K. (2001) 'Cytotoxicity tests for high-throughput drug discovery', *Current Opinion in Biotechnology*, 12(1), pp. 70–74. doi: 10.1016/S0958-1669(00)00177-4.

Smith, J. D. *et al.* (1995) 'Switches in expression of plasmodium falciparum var genes correlate with changes in antigenic and cytoadherent phenotypes of infected erythrocytes', *Cell*, 82(1), pp. 101–110. doi: 10.1016/0092-8674(95)90056-X.

Sohlenkamp, C. and Geiger, O. (2016) 'Bacterial membrane lipids: diversity in structures and pathways', *FEMS Microbiology Reviews*. Edited by F. Narberhaus, 40(1), pp. 133–159. doi: 10.1093/femsre/fuv008.

Sousa, C. da S., Soares, A. C. F. and Garrido, M. da S. (2008) 'Characterization of streptomycetes with potential to promote plant growth and biocontrol', *Scientia Agricola*, 65(1), pp. 50–55. doi: 10.1590/S0103-90162008000100007.

Stone, V., Johnston, H. and Schins, R. P. F. (2009) 'Development of in vitro systems for nanotoxicology: methodological considerations', *Critical Reviews in Toxicology*, 39(7), pp.

613–626. doi: 10.1080/10408440903120975.

Sturm, A. (2006) ‘Manipulation of Host Hepatocytes by the Malaria Parasite for Delivery into Liver Sinusoids’, *Science*, 313(5791), pp. 1287–1290. doi: 10.1126/science.1129720.

Subramani, R. and Aalbersberg, W. (2012) ‘Marine actinomycetes: An ongoing source of novel bioactive metabolites’, *Microbiological Research*, 167(10), pp. 571–580. doi: 10.1016/j.micres.2012.06.005.

Sun, W. *et al.* (2015) ‘Chemical signatures and new drug targets for gametocytocidal drug development’, *Scientific Reports*, 4(1), p. 3743. doi: 10.1038/srep03743.

Supong, K. *et al.* (2018) ‘Antimicrobial substances from the rare actinomycete Nonomuraea rhodomycinica NR4-ASC07 T’, *Natural Product Research*. Taylor & Francis, 6419, pp. 1–7. doi: 10.1080/14786419.2018.1440223.

Swinney, D. C. (2013) ‘Phenotypic vs. target-based drug discovery for first-in-class medicines.’, *Clinical pharmacology and therapeutics*, 93(4), pp. 299–301. doi: 10.1038/clpt.2012.236.

Tavassoly, I., Goldfarb, J. and Iyengar, R. (2018) ‘Systems biology primer: the basic methods and approaches’, *Essays in Biochemistry*. Edited by W. Kolch, D. Fey, and C. J. Ryan, 62(4), pp. 487–500. doi: 10.1042/EBC20180003.

Tawfike, A. F., Viegelmann, C. and Edrada-Ebel, R. (2013) ‘Metabolomics and Dereplication Strategies in Natural Products’, in, pp. 227–244. doi: 10.1007/978-1-62703-577-4_17.

Teklehaimanot and Paola Mejia, A. (2008) ‘Malaria and Poverty’, *Annals of the New York Academy of Sciences*, 1136(1), pp. 32–37. doi: 10.1196/annals.1425.037.

Thaithong, S., Beale, G. H. and Chutmongkonkul, M. (1983) ‘Susceptibility of Plasmodium falciparum to five drugs: an in vitro study of isolates mainly from Thailand’, *Transactions of the Royal Society of Tropical Medicine and Hygiene*, 77(2), pp. 228–231. doi: 10.1016/0035-9203(83)90080-9.

Tietz, J. and Mitchell, D. (2016) ‘Using Genomics for Natural Product Structure Elucidation’, *Current Topics in Medicinal Chemistry*, 16(15), pp. 1645–1694. doi: 10.2174/1568026616666151012111439.

Tiwari, K. and Gupta, R. K. (2012) ‘Rare actinomycetes: a potential storehouse for novel

antibiotics', *Critical Reviews in Biotechnology*, 32(2), pp. 108–132. doi: 10.3109/07388551.2011.562482.

Trager, W. and Jensen, J. (1976) 'Human malaria parasites in continuous culture', *Science*, 193(4254), pp. 673–675. doi: 10.1126/science.781840.

Trivella, D. B. B. and de Felicio, R. (2018) 'The Tripod for Bacterial Natural Product Discovery: Genome Mining, Silent Pathway Induction, and Mass Spectrometry-Based Molecular Networking', *mSystems*, 3(2). doi: 10.1128/mSystems.00160-17.

Tse, E. G., Korsik, M. and Todd, M. H. (2019) 'The past, present and future of anti-malarial medicines', *Malaria Journal*, 18(1), p. 93. doi: 10.1186/s12936-019-2724-z.

Ui, H. *et al.* (2007) 'Selective and Potent In Vitro Antimalarial Activities Found in Four Microbial Metabolites', *The Journal of Antibiotics*, 60(3), pp. 220–222. doi: 10.1038/ja.2007.27.

Umezawa, H. *et al.* (1965) 'Kasugamycin, a new antibiotic.', *Antimicrobial agents and chemotherapy*, 5, pp. 753–7. Available at: http://www.ncbi.nlm.nih.gov/pubmed/5883494.

UNICEF/WHO (2015) 'Achieving the Malaria MDG Target: Reversing the Incidence of Malaria 2000–2015', *WHO Global Malaria Programme*, pp. 1–40. Available at: http://apps.who.int/iris/bitstream/10665/184521/1/9789241509442_eng.pdf?ua=1.

Vaidya, A. B. *et al.* (2014) 'Pyrazoleamide compounds are potent antimalarials that target Na+ homeostasis in intraerythrocytic Plasmodium falciparum', *Nature Communications*, 5(1), p. 5521. doi: 10.1038/ncomms6521.

Vakulenko, S. B. and Mobashery, S. (2003) 'Versatility of Aminoglycosides and Prospects for Their Future', *Clinical Microbiology Reviews*, 16(3), pp. 430–450. doi: 10.1128/CMR.16.3.430-450.2003.

Vinet, L. and Zhedanov, A. (2010) 'A "missing" family of classical orthogonal polynomials', p. 238. doi: 10.1088/1751-8113/44/8/085201.

van Vuuren, S. and Viljoen, A. (2011) 'Plant-Based Antimicrobial Studies – Methods and Approaches to Study the Interaction between Natural Products', *Planta Medica*, 77(11), pp. 1168–1182. doi: 10.1055/s-0030-1250736.

Wagenaar, M. (2008) 'Pre-fractionated Microbial Samples – The Second Generation Natural

Products Library at Wyeth', *Molecules*, 13(6), pp. 1406–1426. doi: 10.3390/molecules13061406.

Wagner, H. and Ulrich-Merzenich, G. (2009) 'Synergy research: Approaching a new generation of phytopharmaceuticals', *Phytomedicine*, 16(2–3), pp. 97–110. doi: 10.1016/j.phymed.2008.12.018.

Waitz, J. A. *et al.* (1981) 'Kijanimicin (Sch 25663), a novel antibiotic produced by Actionmadura kijaniata SCC 1256. Fermentation, isolation, characterization and biological properties.', *The Journal of Antibiotics*, 34(9), pp. 1101–1106. doi: 10.7164/antibiotics.34.1101.

Waksman, S. A. (1947) 'What Is an Antibiotic or an Antibiotic Substance?', *Mycologia*, 39(5), p. 565. doi: 10.2307/3755196.

Waksman, S. A., Reilly, H. C. and Johnstone, D. B. (1946) 'Isolation of Streptomycin-producing Strains of Streptomyces griseus.', *Journal of bacteriology*, 52(3), pp. 393–7. Available at: http://www.ncbi.nlm.nih.gov/pubmed/16561191.

Waksman, S. A. and Woodruff, H. B. (1942) 'Streptothricin, a New Selective Bacteriostatic and Bactericidal Agent, Particularly Active Against Gram-Negative Bacteria.', *Experimental Biology and Medicine*, 49(2), pp. 207–210. doi: 10.3181/00379727-49-13515.

Wallace, M. S. (2006) 'Ziconotide: a new nonopioid intrathecal analgesic for the treatment of chronic pain.', *Expert review of neurotherapeutics*, 6(10), pp. 1423–8. doi: 10.1586/14737175.6.10.1423.

Walton, J. R. (1978) 'Apramycin, a new aminocyclitol antibiotic', *Journal of Antimicrobial Chemotherapy*, 4(4), pp. 309–313. doi: 10.1093/jac/4.4.309.

Wang, M. *et al.* (2016) 'Sharing and community curation of mass spectrometry data with Global Natural Products Social Molecular Networking', *Nature Biotechnology*, 34(8), pp. 828–837. doi: 10.1038/nbt.3597.

Wehrli, F. and Wirthlin, T. (1976) *Interpretation of Carbon-13 NMR Spectra*. New York: Heyden.

Weller, M. G. (2012) 'A Unifying Review of Bioassay-Guided Fractionation, Effect-Directed Analysis and Related Techniques', *Sensors*, 12(7), pp. 9181–9209. doi: 10.3390/s120709181.

Wells, T. N. (2011) ‘Natural products as starting points for future anti-malarial therapies: going back to our roots?’, *Malaria Journal*, 10(S1), p. S3. doi: 10.1186/1475-2875-10-S1-S3.

Wildermuth, H. (1970) ‘Development and Organization of the Aerial Mycelium in Streptomyces coelicolor’, *Journal of General Microbiology*, 60(1), pp. 43–50. doi: 10.1099/00221287-60-1-43.

Wolfender, J.-L. (2009) ‘HPLC in Natural Product Analysis: The Detection Issue’, *Planta Medica*, 75(07), pp. 719–734. doi: 10.1055/s-0028-1088393.

Wood, S. A. *et al.* (2007) ‘PCR screening reveals unexpected antibiotic biosynthetic potential in Amycolatopsis sp. strain UM16’, *Journal of Applied Microbiology*, 102(1), pp. 245–253. doi: 10.1111/j.1365-2672.2006.03043.x.

World Health Organization (2018) *World Malaria Report 2018*. Available at: www.who.int/malaria.

World Health Organization (2019) *World Malaria Report 2019*.

Wu, C.-Y. *et al.* (2004) ‘Small molecules targeting severe acute respiratory syndrome human coronavirus.’, *Proceedings of the National Academy of Sciences of the United States of America*, 101(27), pp. 10012–7. doi: 10.1073/pnas.0403596101.

Xie, L. H. *et al.* (2009) ‘Pharmacokinetics, tissue distribution and mass balance of radiolabeled dihydroartemisinin in male rats’, *Malaria journal*, 8, p. 112.

Yapar, E. and Ýnal, Ö. (2013) ‘Poly(ethylene oxide)–Poly(propylene oxide)-Based Copolymers for Transdermal Drug Delivery: An Overview’, *Tropical Journal of Pharmaceutical Research*, 11(5). doi: 10.4314/tjpr.v11i5.20.

Yeates, C. (2003) ‘DB-289 Immtech International.’, *IDrugs : the investigational drugs journal*, 6(11), pp. 1086–93. Available at: http://www.ncbi.nlm.nih.gov/pubmed/14600842.

Yoshida, K. *et al.* (1982) ‘Studies on new vasodilators, WS-1228 A and B. I. Discovery, taxonomy, isolation and characterization.’, *The Journal of Antibiotics*, 35(2), pp. 151–156. doi: 10.7164/antibiotics.35.151.

Zeuthen, T. *et al.* (2006) ‘Ammonia permeability of the aquaglyceroporins from Plasmodium falciparum, Toxoplasma gondii and Trypansoma brucei’, *Molecular Microbiology*, 61(6), pp. 1598–1608. doi: 10.1111/j.1365-2958.2006.05325.x.

Zhang, Q.-W., Lin, L.-G. and Ye, W.-C. (2018) ‘Techniques for extraction and isolation of natural products: a comprehensive review’, *Chinese Medicine*, 13(1), p. 20. doi: 10.1186/s13020-018-0177-x.

Ziedan, N. I. *et al.* (2010) ‘Design, synthesis and pro-apoptotic antitumour properties of indole-based 3,5-disubstituted oxadiazoles’, *European Journal of Medicinal Chemistry*, 45(10), pp. 4523–4530. doi: 10.1016/j.ejmech.2010.07.012.

Ziegler, H. L. *et al.* (2002) ‘Possible Artefacts in the in vitro Determination of Antimalarial Activity of Natural Products that Incorporate into Lipid Bilayer: Apparent Antiplasmodial Activity of Dehydroabietinol, a Constituent of Hyptis suaveolens’, *Planta Medica*, 68(6), pp. 547–549. doi: 10.1055/s-2002-32548.

Zin, N. M. *et al.* (2017) ‘Gancidin W, a potential low-toxicity antimalarial agent isolated from an endophytic Streptomyces SUK10’, *Drug Design, Development and Therapy*, 11, pp. 351–363. doi: 10.2147/DDDT.S121283.

8. Appendix

Table 8.1: Raw efficacy data for each positive control, chloroquine and artesunate, for all filamentous actinobacteria screening results displayed in Tables 2.1 and 2.2.

Assay Number	Antiplasmodial activity against *P. falciparum*, NF54 IC_{50} (ng/mL)	
	Chloroquine	Artesunate
#1	3,5	3,6
#2	4,6	2,1
#3	6,2	2,9
#4	2,2	4,0
#5	6,8	4,9
#6	3,4	4,2
#7	4,4	5,9
#8	7,1	3,5
#9	5,8	1,9
#10	4,0	5,9
#11	7,8	5,6
#12	7,2	2,1
#13	5,3	3,8
#14	6,1	5,9
#15	5,3	4,4
#16	5,3	5,6
#17	5,5	4,5
#18	7,2	3,8

Table 8.2: Mean antiplasmodial activity of ethyl acetate and methanol blanks, N=2 biological repeats with 4 technical repeats.

Sample	Antiplasmodial activity against *P. falciparum*, NF54 IC_{50}
Ethyl Acetate Blank	> 0.25 % (*v/v*)
Methanol Blank	> 0.25 % (*v/v*)
Chloroquine	6.2 ± 1.4 ng/mL
Artesunate	3.4 ± 0.8 ng/mL

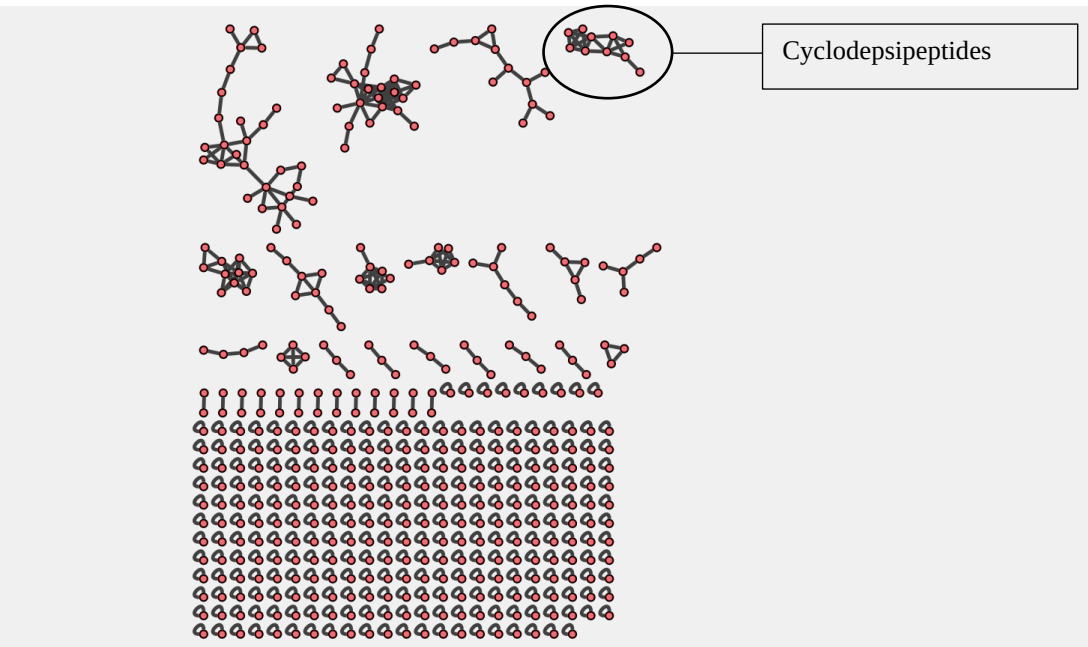

Figure 8.1: Molecular network of fraction #3 produced though RP + NP SPE Methods #3 and #6, and visualised through Cytoscape (Shannon *et al.*, 2003)**.** Each red node is a MS/MS spectrum and each black edge connects similar spectra. The cluster representing the cyclodepsipeptides is labelled.

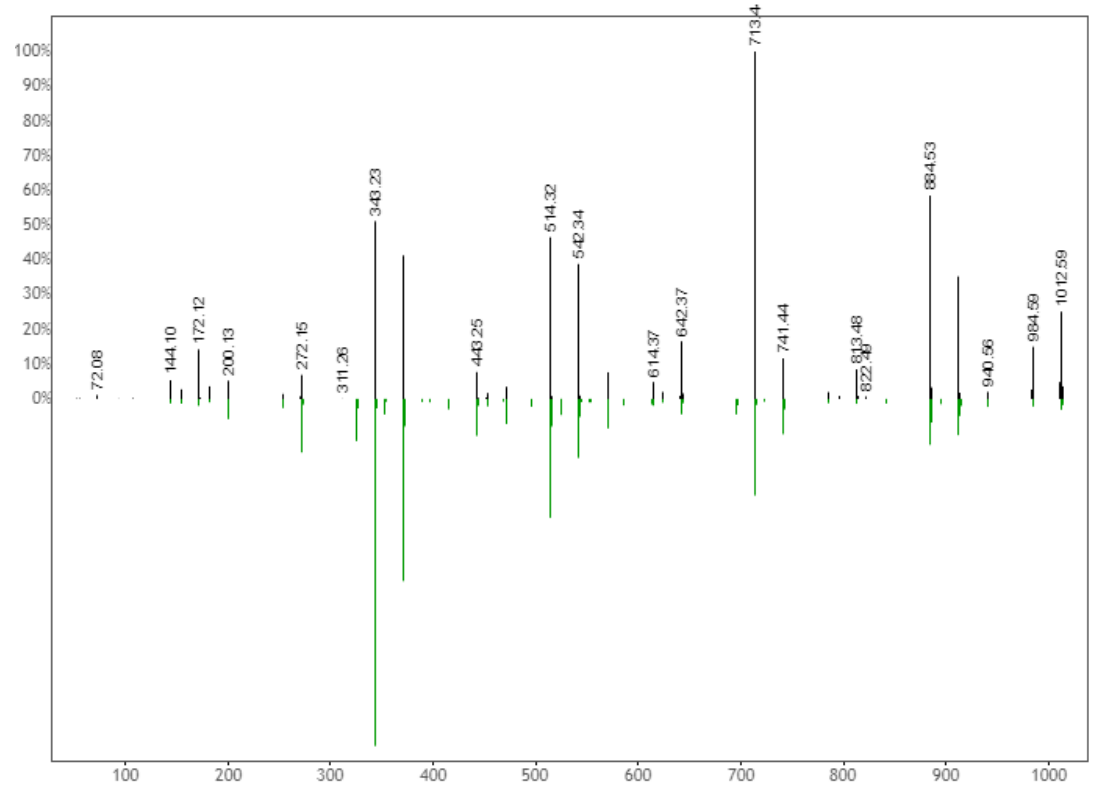

Figure 8.2: Valinomycin MS/MS spectral overlay of experimental spectrum (green) vs GNPS library spectrum (black) from fraction #4 NP SPE. Note how it is identical to Figure 5.6.

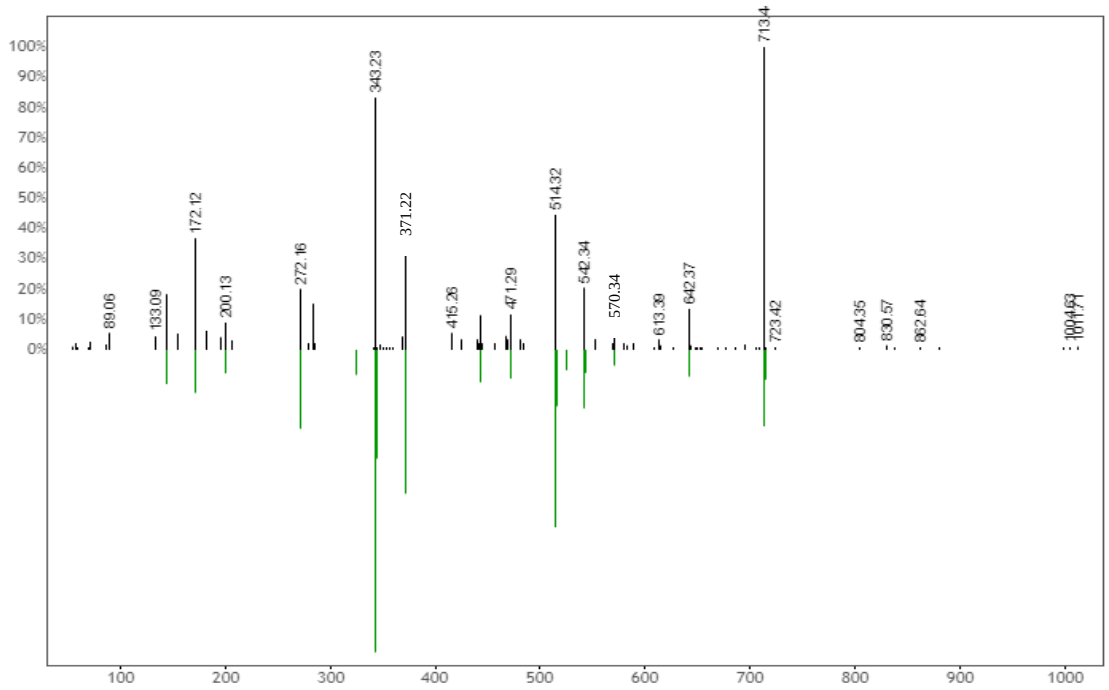

Figure 8.3: Montanastatin MS/MS spectral overlay of experimental spectrum (green) v GNPS library spectrum (black) from fraction #4 NP SPE. Note how it is identical to Figure 5.7

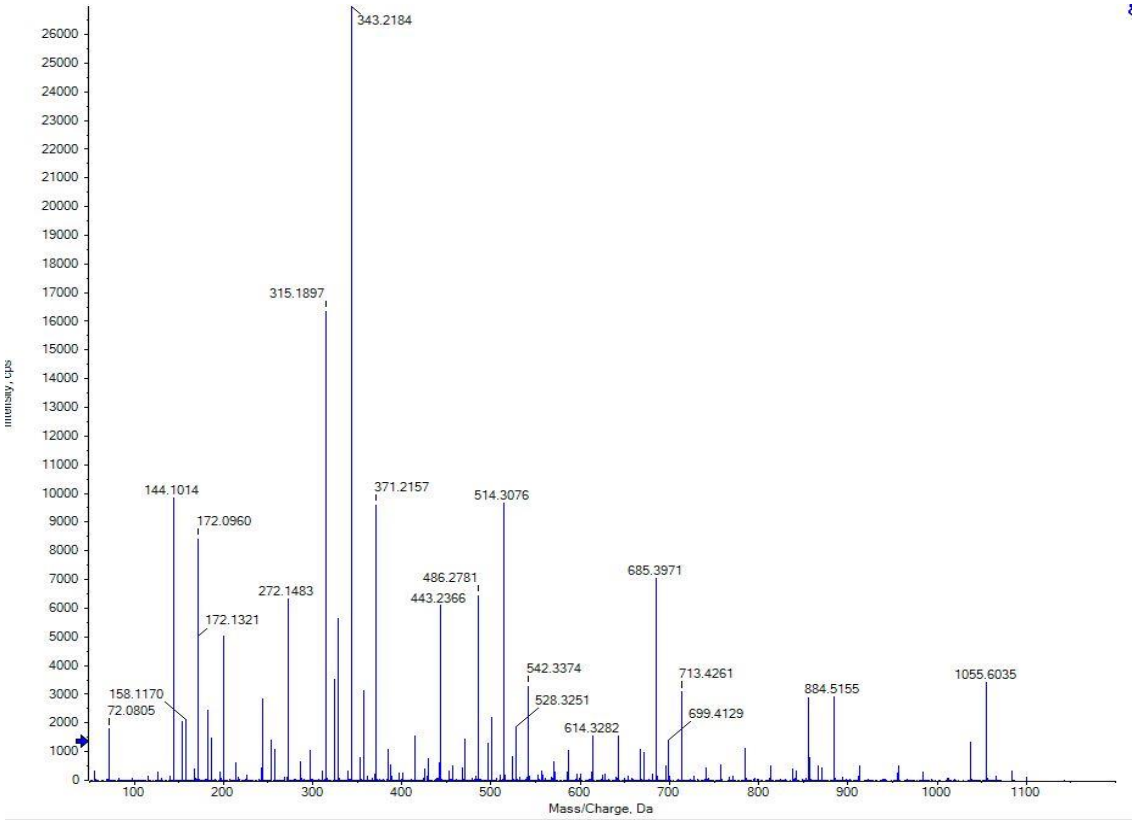

Figure 8.4: Cyclodepsipeptide 1100's MS/MS spectrum.

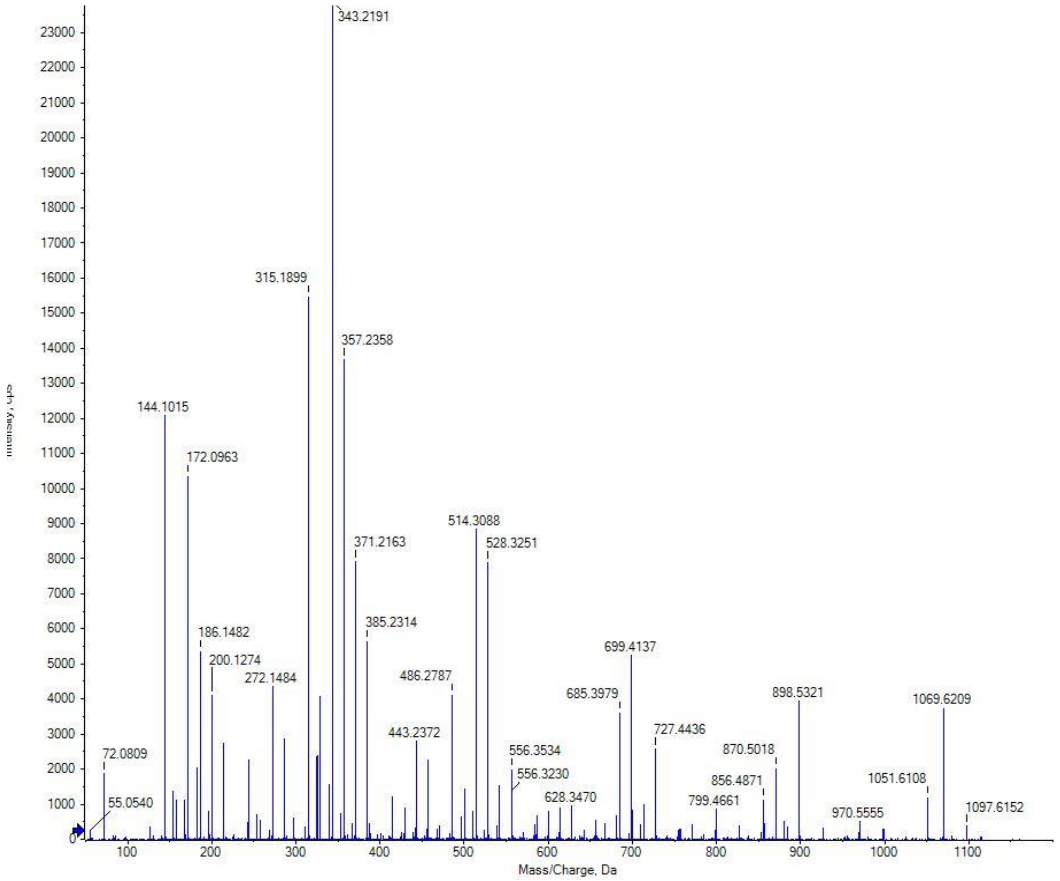

Figure 8.5: Cyclodepsipeptide 1114's MS/MS spectrum.

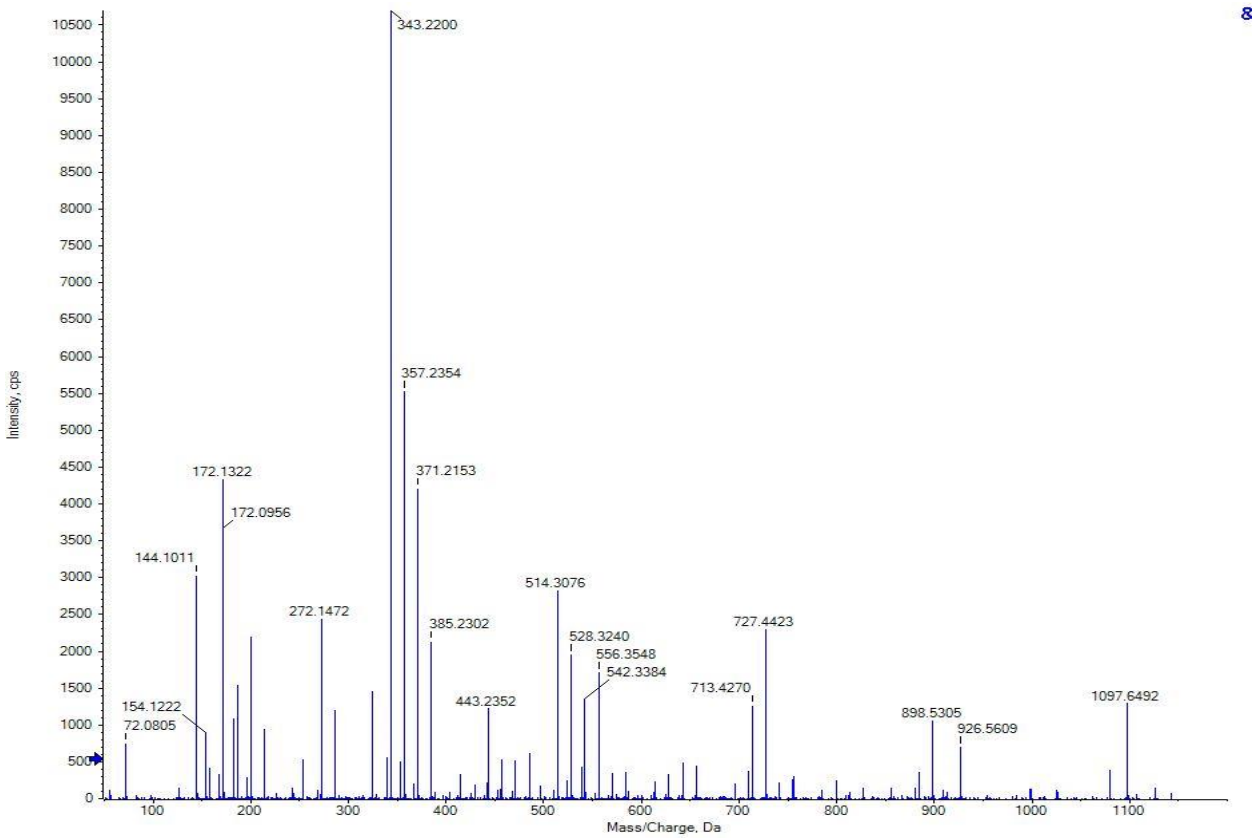

Figure 8.6: Cyclodepsipeptide 1142's MS/MS spectrum.

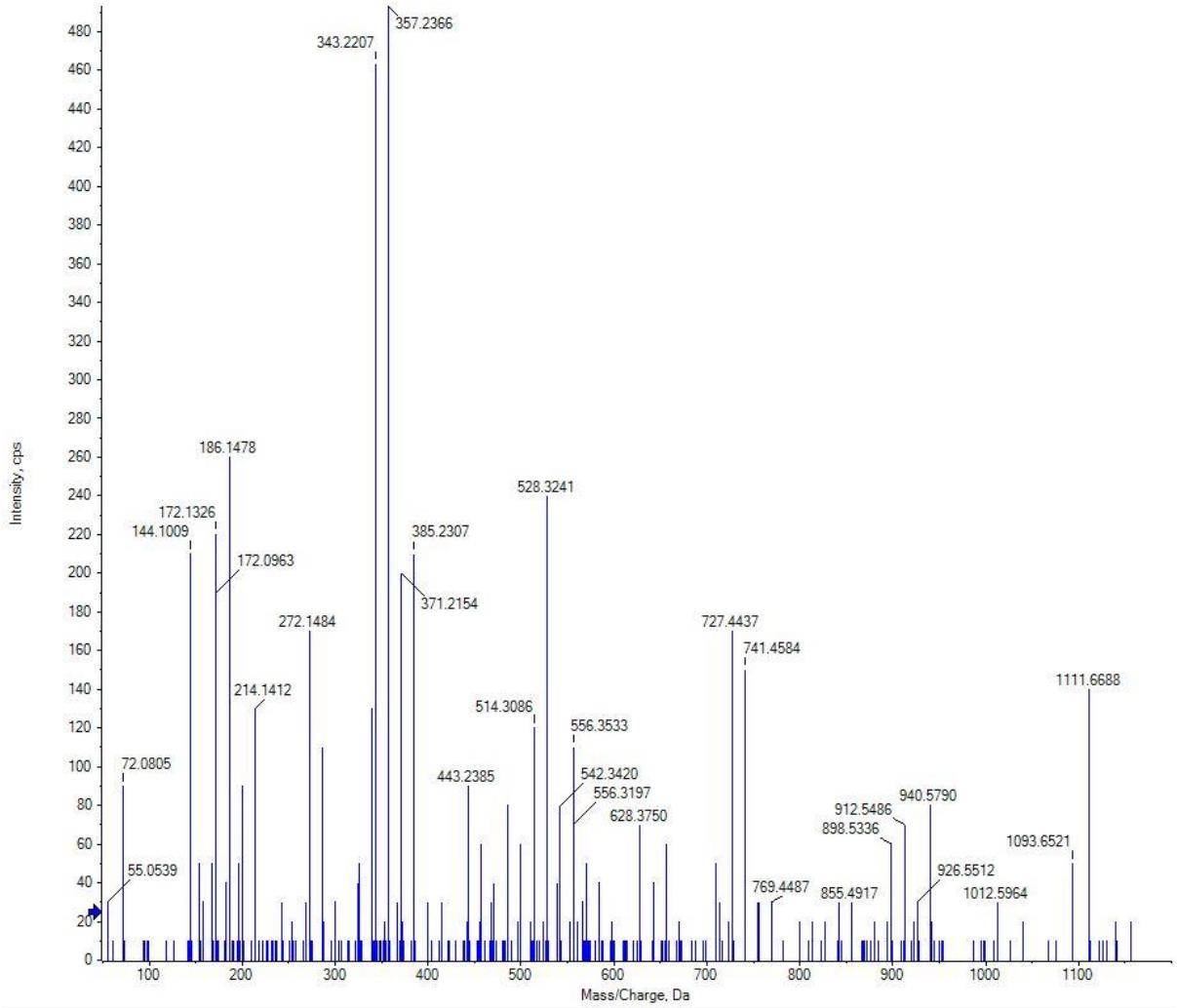

Figure 8.7: Cyclodepsipeptide 1156's MS/MS spectrum.

ID	Average		Identity	Comment	Peak shape	Glass Blank and 150 Active-R150 Crude.mzXML		
	m/z	RT				Status	Height	Area
13171	1128.6705	10.69	Valinomycin				1.5E6	5.6E6
8184	758.5682	10.31	Montanastatin				4.8E3	1.0E4
12930	1086.6223	10.34	Compound 1068				1.0E4	3.0E4
12841	1072.6078	10.22	Compound 1054				3.3E4	8.5E4
13382	1156.7001	10.94	1156				3.8E3	1.3E4
13263	1142.6852	10.81	1142				2.2E5	7.6E5
13089	1114.6548	10.56	1114				1.6E5	4.8E5
13013	1100.6385	10.46	1100				1.5E5	4.4E5
10850	888.6046	9.01	[150]crown-15				1.4E4	4.9E4

Figure 8.8: Table displaying the LC-MS data of the cyclodepsipeptides and [150]crown-15 in a crude extract sample (section 3.2.2.2).

ID	Average		Identity	Comment	Peak shape	Glass Blank and 150 Active-R150.3.mzXML		
	m/z	RT				Status	Height	Area
5572	1128.6722	10.71	Valinomycin				1.9E6	7.6E6
3002	758.5078	9.14	Montanastatin				1.9E3	1.0E4
5491	1086.6263	10.35	Compound 1068				1.6E4	4.5E4
5469	1072.6100	10.24	Compound 1054				3.6E4	1.1E5
5655	1156.7090	10.95	1156				7.2E3	3.0E4
5601	1142.6877	10.82	1142				3.1E5	1.0E6
5544	1114.6562	10.58	1114				2.4E5	6.6E5
5516	1100.6404	10.48	1100				2.0E5	5.7E5
4462	888.6029	9.03	[150]crown-15				2.7E3	1.2E4

Figure 8.9: Table displaying the LC-MS data of the cyclodepsipeptides and [150]crown-15 in a RP SPE MeOH fraction (section 3.2.3.3).

ID	Average		Identity	Comment	Peak shape	Active Samples_5July19_DJW-125 EtAc.mzXML		
	m/z	RT				Status	Height	Area
2386	1128.6660	10.45	Valinomycin				2.0E6	1.2E7
2039	758.4552	9.94	Montanastatin				8.3E3	3.0E4
2345	1086.6180	10.08	Compound 1068				4.1E5	1.7E6
2339	1072.6013	9.95	Compound 1054				1.0E6	4.2E6
2405	1156.6974	10.67	1156				1.3E4	5.6E4
2396	1142.6818	10.57	1142				5.0E5	2.2E6
2377	1114.6492	10.33	1114				1.1E6	4.3E6
2368	1100.6318	10.21	1100				1.8E6	9.0E6
2230	888.6614	9.73	[150]-crown15				1.5E4	6.1E4

Figure 8.10: Table displaying the LC-MS data of the cyclodepsipeptides and [150]crown-15 in a PHREE SPE fraction (section 3.2.3.4)

ID	Average		Identity	Comment	Peak shape	Active Samples_5July19_DJW-Huntdomycin A ...		
	m/z	RT				Status	Height	Area
9135	1128.6638	10.42	Valinomycin				1.9E6	8.1E6
8227	758.4420	9.90	Montanastatin				1.8E3	3.5E3
9029	1086.6171	10.07	Compound 1068				6.9E5	2.6E6
9023	1072.6014	9.97	Compound 1054				4.4E5	1.6E6
9227	1156.6964	10.67	1156				2.3E4	9.1E4
9216	1142.6804	10.57	1142				6.1E4	2.1E5
9130	1114.6486	10.32	1114				6.2E4	2.1E5
9116	1100.6332	10.22	1100				7.9E3	2.4E4
8755	888.6620	9.89	[150]crown-15				1.0E4	7.4E4

Figure 8.11: Table displaying the LC-MS data of the cyclodepsipeptides and [150]crown-15 in fraction 540 (section 3.3.5.4).

ID	Average		Identity	Comment	Peak shape	Active Samples_5July19_DJW-Hundtomycin B....		
	m/z	RT				Status	Height	Area
9160	1128.6642	10.45	Valinomycin				5.8E4	2.1E5
8182	758.5652	10.16	Montanastatin				2.9E3	9.4E3
9054	1086.6179	10.07	Compound 1068				4.1E4	1.4E5
9040	1072.6031	10.40	Compound 1054				4.8E3	4.1E4
9173	1156.6960	10.70	1156				2.8E3	8.5E3
9167	1142.6796	10.86	1142				1.7E3	4.5E3
9158	1114.6508	10.33	1114				4.5E3	1.3E4
9146	1100.6334	10.21	1100				1.7E4	5.3E4
8732	888.6613	9.77	[150]crown-15				7.9E5	3.7E6

Figure 8.12: Table displaying the the LC-MS data of the cyclodepsipeptides and [150]crown-15 in fraction 870 (section 3.3.5.4).

ID	Average		Identity	Comment	Peak shape	Glass Blank and 150 Active-R150.7.mzXML		
	m/z	RT				Status	Height	Area
1466	1128.6717	10.72	Valinomycin				2.0E6	1.5E7
1003	758.4591	10.21	Montanastatin				2.0E4	5.6E4
1440	1086.6245	10.33	Compound 1068				9.6E3	2.8E4
1438	1072.6086	10.23	Compound 1054				4.9E3	1.2E4
1487	1156.7035	10.95	1156				4.9E4	2.9E5
1478	1142.6866	10.82	1142				1.7E6	7.6E6
1458	1114.6550	10.56	1114				1.1E6	3.7E6
1445	1100.6405	10.46	1100				7.6E5	2.0E6

Figure 8.13: Table displaying the LC-MS data of the cyclodepsipeptides in NP SPE fraction #3 (section 3.2.3.5).

ID	Average		Identity	Comment	Peak shape	.8.mzXML		
	m/z	RT				Status	Height	Area
1820	1128.6719	10.67	Valinomycin				2.0E6	1.4E7
1383	758.4588	10.22	Montanastatin				1.5E5	4.1E5
1803	1086.6243	10.35	Compound 1068				1.6E5	4.7E5
1800	1072.6088	10.24	Compound 1054				1.3E5	3.9E5
1841	1156.7049	10.88	1156				5.3E3	2.2E4
1834	1142.6868	10.82	1142				5.7E5	2.4E6
1812	1114.6539	10.58	1114				1.7E6	6.3E6
1806	1100.6396	10.48	1100				1.7E6	6.1E6

Figure 8.14: Table displaying the LC-MS data of the cyclodepsipeptides in NP SPE fraction #4 (section 3.2.3.5).

ID	Average		Identity	Comment	Peak shape	.9.mzXML		
	m/z	RT				Status	Height	Area
1679	1128.6721	10.69	Valinomycin				1.9E6	9.3E6
1315	758.4597	10.22	Montanastatin				9.5E4	2.6E5
1663	1086.6243	10.35	Compound 1068				3.4E5	1.2E6
1659	1072.6091	10.24	Compound 1054				9.9E5	2.9E6
1685	1142.6881	10.81	1142				1.4E5	5.4E5
1673	1114.6553	10.57	1114				1.2E6	3.6E6
1667	1100.6396	10.46	1100				1.3E6	4.6E6

Figure 8.15: Table displaying the LC-MS data of the cyclodepsipeptides in NP SPE fraction #5 (section 3.2.3.5).